

15139

MANUFACTURE OF SODIUM DITHIONITE FROM SODIUM-
MERCURY AMALGAM AND AQUEOUS SOLUTION
OF SULFUR DIOXIDE

by

RAMAN NAYAR

B. Tech. (Hon.), I.I.T., Kharagpur, 1967

A THESIS SUBMITTED IN PARTIAL FULFILMENT OF
THE REQUIREMENTS FOR THE DEGREE OF
DOCTOR OF PHILOSOPHY

in the Department

of

CHEMICAL ENGINEERING

We accept this thesis as conforming to the
required standard

THE UNIVERSITY OF BRITISH COLUMBIA

November, 1972

In presenting this thesis in partial fulfillment of the requirements for an advanced degree at the University of British Columbia, I agree that the Library shall make it freely available for reference and study. I further agree that permission for extensive copying of this thesis for scholarly purposes may be granted by the Head of my Department or by his representatives. It is understood that publication, in part or in whole, or the copying of this thesis for financial gain shall not be allowed without my written permission.

RAMAN NAYAR

Department of Chemical Engineering

The University of British Columbia
Vancouver 8, Canada

Date March 20' 1973

ABSTRACT

A relatively dilute (approximately 1 to 2%) water solution of sodium dithionite was produced from sodium-mercury amalgam and aqueous solution of sulfur dioxide in a simple "once through" reactor [proposed process]. The reactor could be run in conjunction with the Castner-Kellner type cell. The manufactured solution could then be used directly for the brightening of groundwood pulp.

The bench scale experiments were carried out in a continuous-flow-stirred-tank reactor where the aqueous and amalgam phases formed an interface. The effects of important process variables on the steady-state concentration of sodium dithionite in the reactor and yields of sodium dithionite on sulfur dioxide in the aqueous feed and on sodium consumed in a single pass were determined. The above-mentioned yields are important in assessing the economic feasibility of the proposed process. The steady-state yield of sodium dithionite on sodium in the amalgam entering the reactor and conversion of sodium to different products in the reactor were also determined.

The present investigation showed that the process variables can be controlled to give approximately 2.3% sodium

dithionite solution with steady-state $\text{Na}_2\text{S}_2\text{O}_4$ yields of about 21% on sulfur dioxide in the aqueous feed and about 67% on sodium consumed. The yields obtained depend on the levels of process variables such as:

1. the concentration of sodium in the amalgam entering the reactor,
2. the concentration of total sulfur dioxide in the aqueous feed solution,
3. the agitation in the aqueous phase,
4. the agitation in the amalgam phase,
5. the residence time in the aqueous phase,
6. the residence time in the amalgam phase,
7. the interfacial-area/aqueous-volume ratio,
8. the temperature of the aqueous phase, and
9. the pH of the aqueous phase.

This experimental study indicates that it may be economically feasible for a pulp mill to change from zinc dithionite produced *in situ* to sodium dithionite produced *in situ* by the proposed process. Further, the proposed process compared to the manufacture of zinc dithionite *in situ* avoids the discharge of zinc ions which act as biocidal agents when discharged into the effluent receiving waters.

The models suggested by Ketelaar (44) and Gerritsen (30) were found inadequate to explain the processes occurring

in the reacting system sodium-mercury amalgam and aqueous sulfur dioxide. A qualitative model has been suggested on the basis of the experimental work and the information available in the literature.

This work also sheds some light on the type of reactor which would be suitable for the proposed process.

ACKNOWLEDGEMENT

The author wishes to express his thanks to the faculty and staff of the Chemical Engineering Department, The University of British Columbia. Special thanks are extended to Dr. F.E. Murray, who suggested the project and under whose guidance this work was undertaken.

The author is indebted to the Chemical Engineering Workshop personnel for their assistance in assembling the experimental equipment. The author wishes to thank Mr. E. Rudischer, in particular, for his assistance and cooperation.

Financial support for this research was most gratefully received from the National Research Council of Canada and from the British Columbia Research Council.

The author is also indebted to his wife Jane for her invaluable help throughout this work.

TABLE OF CONTENTS

CHAPTER	PAGE
I. INTRODUCTION	1
II. REVIEW OF PERTINENT PRIOR WORK	7
A. Manufacturing Processes for Sodium Dithionite	7
1. Zinc dust: sodium carbonate process	7
2. Electrolytic or cathodic reduction process	9
3. Sodium formate process	9
4. Sodium borohydride process	10
5. Sodium amalgam process	11
(a) Advantages of the sodium amalgam process	11
(b) Types of the sodium amalgam process	12
(i) Sodium amalgam: SO ₂ -organic solvent process	12
(ii) Sodium amalgam: gaseous SO ₂ process and sodium amalgam: liquid SO ₂ process	13
(iii) Sodium amalgam: SO ₂ -NaHSO ₃ /Na ₂ SO ₃ buffer process	13
B. Recommended Conditions for Improving the Yield of Sodium Dithionite in the Sodium Amalgam: SO ₂ -NaHSO ₃ /Na ₂ SO ₃ Buffer Process	15
C. Mercury Contamination of Sodium Dithionite Produced by the Sodium Amalgam: SO ₂ -NaHSO ₃ / Na ₂ SO ₃ Buffer Process	17

D. Lignin Preserving Bleaching of Ground- wood Pulp by Sodium Dithionite	19
1. Definition of the terms "brightening" and "bleaching"	19
2. Characteristics of the groundwood bleach- ing process	20
3. Effects of groundwood brightening	21
4. Conditions for groundwood brightening by sodium dithionite	21
E. Sodium-mercury Amalgam	24
1. Molecular structure of sodium-mercury amalgam	24
2. Surface tension of sodium-mercury amalgam	25
3. Sensitivity to oxidation of sodium- mercury amalgam	25
4. Density of sodium-mercury amalgam	26
F. Sulfur Dioxide Solution in Water	26
1. Principal equilibria	26
2. Diffusion of sulfur dioxide in water	32
G. Important Reactions in the Proposed Process	33
1. The Sodium dithionite formation reaction	35
2. The water reaction	39
3. The sodium dithionite decomposition reactions	43
(a) Homogeneous decomposition of sodium dithionite	43
(b) Heterogeneous decomposition of sodium dithionite	46

CHAPTER

PAGE

4. The sodium dithionite oxidation reaction	48
III. THEORETICAL MODELS	50
IV. EXPERIMENTAL	54
A. Experimental Materials	54
1. Sodium-mercury amalgam	54
2. Aqueous sulfur dioxide solution	54
B. Experimental Apparatus	55
1. Reactor	55
2. pH measurement of the aqueous phase	64
3. Temperature measurement of different streams	65
4. Insulation of the equipment	67
5. Electrical wiring diagram	67
C. Calibration Curves	67
D. An Experimental Run	69
E. Analytical Procedures and Errors	71
1. Sodium-mercury amalgam	71
(a) Analysis of sodium-mercury amalgam	71
(b) Accuracy and precision of the analytical procedure	72
2. Aqueous sulfur dioxide solution	75
(a) Analysis of aqueous sulfur dioxide solution	75
(b) Accuracy and precision of the analytical procedure	76
3. Aqueous sodium dithionite solution	77

CHAPTER	PAGE
(a) Analysis of sodium dithionite in the product stream	77
(b) Accuracy and precision of the analytical procedures	79
V. EXPERIMENTAL RESULTS	82
A. Batch Experiments	82
B. Introduction to Experiments in the CFSTR	87
C. Definitions of Some Important Quantities which are used for the Interpretation of Data	90
D. Reproducibility of Experimental Runs in the CFSTR	94
E. Data from CFSTR Experiments	101
1. Concentration of sodium in fresh amalgam	101
2. Concentration of "total" sulfur dioxide in the aqueous feed solution	121
3. Agitation in the aqueous phase	133
4. Flow rate of aqueous sulfur dioxide solution, i.e. residence time in the aqueous phase	144
5. Interfacial-area/aqueous-volume ratio	153
6. Temperature of the aqueous phase	164
7. pH of the aqueous phase	168
8. Flow rate of fresh amalgam, i.e. residence time in the amalgam phase	168
VI. DISCUSSION	170
A. Model for the Reacting System in the Proposed Process	170

CHAPTER	PAGE
1. Development of the model	170
2. The model.	185
B. Conditions for Improving the Yields of Sodium Dithionite in the Proposed Process	188
C. Economic Feasibility of the Proposed Process	194
D. Reactor for the Proposed Process	198
VII. CONCLUSIONS	199
VIII. RECOMMENDATIONS FOR FURTHER WORK	203
IX. NOMENCLATURE	205
BIBLIOGRAPHY	208
 APPENDIX	
A. EQUIPMENT SPECIFICATION	A-1
1. pH measurement	A-1
2. Digital temperature recording	A-1
3. Calibration curves	A-2
B. STATISTICAL EVALUATION OF ACCURACY AND PRECISION	B-1
1. Error of a measurement process	B-1
2. Evaluation of accuracy	B-3
3. Evaluation of precision (or imprecision).	B-4
4. Propagation of random error	B-8
C. SODIUM-MERCURY AMALGAM	C-1
1. Purity of the chemicals in preparing amalgam	C-1
2. Problems encountered in preparation of amalgam	C-2

APPENDIX	PAGE
3. Calculation of sodium content in an amalgam sample	C-3
4. Estimation of the precision of the analytical procedure	C-4
D. AQUEOUS SOLUTION OF SULFUR DIOXIDE	D-1
1. Purity of the chemicals in preparing aqueous sulfur dioxide solution	D-1
2. Calculation of the total sulfur dioxide concentration in an aqueous solution sample	D-2
3. Estimation of the precision of the analytical procedure	D-3
E. SODIUM DITHIONITE IN THE PRODUCT STREAM	E-1
1. Details of the analytical procedures and sample calculations	E-1
(a) The iodine-formaldehyde method	E-1
(b) The Rubine-R method	E-8
2. Estimation of the precision of the Rubine-R method	E-16
F. DATA PROCESSING	F-1
1. Mathematical expressions for calculating $C_{S_2O_4}$, Y_{SO_2} , Y_{Na} , CONNA, X_{Na} and Na/SO ₂ , rate of sodium consumption, and sample calculations	F-1
2. The 95 per cent confidence limits of the steady-state $C_{S_2O_4}$, Y_{SO_2} , Y_{Na} , CONNA, X_{Na} , Na/SO ₂ and rate of sodium consumption for an experimental run	F-7
3. Experimental data and results	F-12

LIST OF FIGURES

Figure	Page
1. Concentrations of free sulfur dioxide, bisulfite ions and sulfite ions versus pH in a 0.399 molar sulfur dioxide solution in water at 25°C	31
2. Effective diffusion coefficients for sulfur dioxide in aqueous $(\text{NH}_4)_2\text{SO}_3$. 'Total' sulfur dioxide concentration = 1 gm mole/liter	34
3. Schematic flow-sheet of the experimental apparatus	56
4. Reactor assembly	61
5. Digital temperature measurement (schematic).	66
6. Electrical wiring diagram (schematic).	68
7. Reproducibility of the experimental runs in the CFSTR	97
8. Reproducibility of the experimental runs in the CFSTR	100
9. Steady-state values of sodium dithionite concentration and various yields versus Na/SO ₂ ratios entering the CFSTR for the experimental set: 65-77	103
10. Steady-state values of sodium dithionite concentration and various yields versus concentrations of sodium in amalgam entering the CFSTR for the experimental set: 65-77	104
11. Rates of sodium consumption versus Na/SO ₂ ratios entering the CFSTR for the experimental set: 65-77	107
12. Rates of sodium consumption versus concentrations of sodium in amalgam entering the CFSTR for the experimental set: 65-77	108

Figure		Page
13.	Rates of sodium consumption versus concentrations of sodium in amalgam entering the CFSTR for the experimental sets: 95-105, 23-28, 65-77 and 42-46	111
14.	Concentrations of sodium dithionite in the product stream versus time for runs in the experimental set: 42-46	115
15.	Concentrations of sodium in amalgam leaving the CFSTR versus time for runs in the experimental set: 42-46	116
16.	Concentrations of sodium dithionite in the product stream versus time for runs in the experimental set: 23-28	117
17.	Concentrations of sodium in amalgam leaving the CFSTR versus time for runs in the experimental set: 23-28	118
18.	Concentrations of sodium dithionite in the product stream versus time for runs in the experimental set: 65-77	119
19.	Concentrations of sodium in amalgam leaving the CFSTR versus time for runs in the experimental set: 65-77	120
20.	Steady-state values of sodium dithionite concentration and various yields versus Na/SO ₂ ratio entering the CFSTR for the experimental set: 23-28	123
21.	Steady-state values of sodium dithionite concentration and various yields versus Na/SO ₂ ratio entering the CFSTR for the experimental set: 42-46	124
22.	Steady-state sodium dithionite concentrations versus Na/SO ₂ ratios entering the CFSTR at different concentrations of sulfur dioxide in the aqueous feed	125
23.	Steady-state sodium dithionite concentrations versus concentrations of sodium in amalgam entering the CFSTR at different concentrations of sulfur dioxide in the aqueous feed . . .	127

Figure	Page
24. Critical concentrations of sodium in amalgam entering the CFSTR versus molarity of sulfur dioxide in the aqueous solutions entering the CFSTR	128
25. Steady-state yields of sodium dithionite on sulfur dioxide in the aqueous feed versus Na/SO ₂ ratios entering the CFSTR at different concentrations of sulfur dioxide in the aqueous feed	129
26. Steady-state yields of sodium dithionite on sodium in the amalgam entering the CFSTR versus Na/SO ₂ ratios entering the CFSTR at different concentrations of sulfur dioxide in the aqueous feed	130
27. Steady-state yields of sodium dithionite on sodium consumed in the CFSTR versus Na/SO ₂ ratios entering the CFSTR at different concentrations of sulfur dioxide in the aqueous feed	131
28. Steady-state conversions of sodium to different products in the CFSTR versus Na/SO ₂ ratios entering the CFSTR at different concentrations of sulfur dioxide in the aqueous feed	132
29. Steady-state values of sodium dithionite concentration and various yields versus Na/SO ₂ ratios entering the CFSTR for the experimental set: 86-90	137
30. Steady-state sodium dithionite concentrations versus Na/SO ₂ ratios entering the CFSTR at different levels of agitation in the aqueous feed	139
31. Steady-state yields of sodium dithionite on sulfur dioxide in the aqueous feed versus Na/SO ₂ ratios entering the CFSTR at different levels of agitation in the aqueous feed	140
32. Steady-state yields of sodium dithionite on sodium in the amalgam entering the CFSTR versus Na/SO ₂ ratios entering the CFSTR at different levels of agitation in the aqueous feed	141

Figure		Page
33.	Steady-state yields of sodium dithionite on sodium consumed in the CFSTR versus Na/SO ₂ ratios entering the CFSTR at different levels of agitation in the aqueous feed	142
34.	Steady-state conversions of sodium to different products in the CFSTR versus Na/SO ₂ ratios entering the CFSTR at different levels of agitation in the aqueous feed	143
35.	Steady-state values of sodium dithionite concentration and various yields versus Na/SO ₂ ratios entering the CFSTR for the experimental set: 94-104	145
36.	Steady-state values of sodium dithionite concentration and various yields versus Na/SO ₂ ratios entering the CFSTR for the experimental set: 95-105	146
37.	Steady-state sodium dithionite concentrations versus Na/SO ₂ ratios entering the CFSTR at different flow rates of the aqueous feed . .	147
38.	Steady-state yields of sodium dithionite on sulfur dioxide in the aqueous feed versus Na/SO ₂ ratios entering the CFSTR at different flow rates of the aqueous feed	148
39.	Steady-state yields of sodium dithionite on sodium in the amalgam entering the CFSTR versus Na/SO ₂ ratios entering the CFSTR at different flow rates of the aqueous feed . .	149
40.	Steady-state yields of sodium dithionite on sodium consumed in the CFSTR versus Na/SO ₂ ratios entering the CFSTR at different flow rates of the aqueous feed	150
41.	Steady-state conversions of sodium to different products in the CFSTR versus Na/SO ₂ ratios entering the CFSTR at different flow rates of the aqueous feed . .	151

Figure	Page
42. Steady-state values of sodium dithionite concentration and various yields versus Na/SO ₂ ratios entering the CFSTR for the experimental set: 122-134	156
43. Steady-state values of sodium dithionite concentration and various yields versus Na/SO ₂ ratios entering the CFSTR for the experimental set: 123-135	157
44. Steady-state sodium dithionite concentrations versus Na/SO ₂ ratios entering the CFSTR at different values of interfacial-area/aqueous-volume ratio	158
45. Steady-state yields of sodium dithionite on sulfur dioxide in the aqueous feed versus Na/SO ₂ ratios entering the CFSTR at different values of interfacial-area/aqueous volume ratio	159
46. Steady-state yields of sodium dithionite on sodium in the amalgam entering the CFSTR versus Na/SO ₂ ratios entering the CFSTR at different values of interfacial-area/aqueous-volume ratio	160
47. Steady-state yields of sodium dithionite on sodium consumed in the CFSTR versus Na/SO ₂ ratios entering the CFSTR at different values of interfacial-area/aqueous-volume ratio	161
48. Steady-state conversions of sodium to different products in the CFSTR versus Na/SO ₂ ratios entering the CFSTR at different values of interfacial-area/aqueous-volume ratio	162
49. Steady-state values of sodium dithionite concentration and yield of sodium dithionite on sulfur dioxide in the aqueous feed versus interfacial-area/aqueous-volume ratios at different Na/SO ₂ ratios entering the CFSTR	163
50. Steady-state yields of sodium dithionite on sulfur dioxide in the aqueous feed versus Na/SO ₂ ratios entering the CFSTR at different steady-state temperatures of the aqueous phase	166

Figure		Page
51.	Steady-state yields of sodium dithionite on sodium consumed in the CFSTR versus Na/SO ₂ ratios entering the CFSTR at different steady-state temperatures of the aqueous phase	167
A-I.	Flow rate of mercury pumped by Moyno pump versus micrometer setting on Graham transmission	A-3
A-II.	Flow rate of aqueous sulfur dioxide versus reading on the rotameter scale	A-4
A-III.	Flow rate of cooling water versus reading on the rotameter scale	A-5
A-IV.	Millivolt output of iron-constantan thermocouples versus temperature °C	A-6
A-V.	RPM of the propeller versus micrometer setting on the thyatron controller for the variable speed drive (Heller motor)	A-7

LIST OF TABLES

TABLE	PAGE
1. Conditions for Brightening Groundwood by $\text{Na}_2\text{S}_2\text{O}_4$	23
2. Precision of the Amalgam Analytical Procedure	74
3. Precision of the Sulfur Dioxide Analytical Procedure	76
4. Process Variables and Their Units	93
5. Levels of the Process Variables in Set: 47-57	96
6. Levels of the Process Variables in Set: 65-77	96
7. Levels of the Process Variables in Set: 66-76	99
8. Levels of the Process Variables in Set: 62-63	99
9. Levels of the Process Variables in Set: 87-91	99
10. Levels of the Process Variables in Set: 95-105	110
11. Levels of the Process Variables in Set: 23-28	110
12. Levels of the Process Variables in Set: 42-46	110
13. Levels of the Process Variables in Set: 86-90	136
14. Levels of the Process Variables in Set: 94-104	136
15. Levels of the Process Variables in Set: 122-134	155

TABLE	PAGE
16. Levels of the Process Variables in Set: 123-135	155
17. Levels of the Process Variables in Set: 106-118	165
18. Levels of the Process Variables in Set: 110-113	165
19. Levels of the Process Variables for the Run 44	195
C-I. Measured Values, Range of Random Errors and Variances of different measured quantities (amalgam analytical procedure)	C-7
F-I. Steady-State Data and Results for Experimental Set: 47-57	F-14
F-II. Steady-State Data and Results for Experimental Set: 65-77	F-15
F-III. Steady-State Data and Results for Experimental Set: 66-76	F-16
F-IV. Steady-State Data and Results for Experimental Set: 62-63	F-17
F-V. Steady-State Data and Results for Experimental Set: 87-91	F-18
F-VI. Steady-State Data and Results for Experimental Set: 95-105	F-19
F-VII. Steady-State Data and Results for Experimental Set: 23-28	F-20
F-VIII. Steady-State Data and Results for Experimental Set: 42-46	F-21
F-IX. Steady-State Data and Results for Experimental Set: 86-90	F-22
F-X. Steady-State Data and Results for Experimental Set: 94-104	F-23

TABLE

PAGE

F-XI.	Steady-State Data and Results for Experimental Set: 122-134	F-24
F-XII.	Steady-State Data and Results for Experimental Set: 123-135	F-25
F-XIII.	Steady-State Data and Results for Experimental Set: 106-118	F-26
F-XIV.	Steady-State Data and Results for Experimental Set: 110-113	F-27
F-XV.	Unsteady-State Results for Experimental Run 42	F-28
F-XVI.	Unsteady-State Results for Experimental Run 43	F-28
F-XVII.	Unsteady-State Results for Experimental Run 44	F-29
F-XVIII.	Unsteady-State Results for Experimental Run 45	F-29
F-XIX.	Unsteady-State Results for Experimental Run 46	F-30
F-XX.	Unsteady-State Results for Experimental Run 23	F-30
F-XXI.	Unsteady-State Results for Experimental Run 24	F-31
F-XXII.	Unsteady-State Results for Experimental Run 25	F-31
F-XXIII.	Unsteady-State Results for Experimental Run 26	F-32
F-XXIV.	Unsteady-State Results for Experimental Run 27	F-32
F-XXV.	Unsteady-State Results for Experimental Run 28	F-33
F-XXVI.	Unsteady-State Results for Experimental Run 65	F-33

TABLE		PAGE
F-XXVII.	Unsteady-State Results for Experimental Run 67	F-34
F-XXVIII.	Unsteady-State Results for Experimental Run 69	F-34
F-XXIX.	Unsteady-State Results for Experimental Run 71	F-35
F-XXX.	Unsteady-State Results for Experimental Run 73	F-35
F-XXXI.	Unsteady-State Results for Experimental Run 75	F-36
F-XXXII.	Unsteady-State Results for Experimental Run 77	F-36

CHAPTER I

INTRODUCTION

Groundwood pulps, especially those obtained from western softwood species, are dark in colour and must be brightened for use in newsprint manufacture. Brightening is done usually with a solution of zinc dithionite (ZnS_2O_4), manufactured on the mill site from zinc dust and aqueous sulfur dioxide solution, according to the reaction:



This process is economical and efficient but suffers from one serious drawback. That is, the zinc ion which remains in the spent bleach solution must be discharged to the available effluent receiving waters. Since zinc ion is an active biocidal agent (46, 37), this is very objectionable from the standpoint of water pollution control. Already the use of zinc dithionite is prohibited in some areas and in others, pressure is developing to prohibit its use.

For a mill which can not use zinc dithionite, the available alternative is to purchase manufactured sodium

dithionite ($\text{Na}_2\text{S}_2\text{O}_4$). Sodium dithionite is available in the market as the anhydrous crystalline salt. It is quite unstable in aqueous solution or when it carries water of crystallization ($\text{Na}_2\text{S}_2\text{O}_4 \cdot 2\text{H}_2\text{O}$). The cost of ZnS_2O_4 produced in pulp mills (62) is approximately 16¢/lb of $\text{S}_2\text{O}_4^{=}$ ion. The cost of crystalline $\text{Na}_2\text{S}_2\text{O}_4$ bought in the market (65) is approximately 39¢/lb of $\text{S}_2\text{O}_4^{=}$ ion. Preferred application of sodium dithionite for the brightening of ground-wood pulp is 0.2 - 1.5% of the fibre weight (62, 106). For the following example, it was assumed that in the bleaching plant, the concentration of sodium dithionite is 1% of the fibre weight. For a mill producing 500 tons per day of groundwood pulp, forced to change from ZnS_2O_4 produced *in situ* to crystalline $\text{Na}_2\text{S}_2\text{O}_4$ bought in the market, the extra cost involved would be about one million dollars per year.

A good part of the cost in purchased crystalline sodium dithionite is incurred in the crystallization and subsequent drying steps. It would be possible to reduce substantially the cost of sodium dithionite for mill use if it could be manufactured *in situ* in a simple "once through" reactor and the solution fed directly to the groundwood bleaching plant.

One possible means of doing this would be by the sodium-mercury amalgam route (Chapter II). In this process, a solution of sulfur dioxide (or sodium bisulfite) in water is allowed to react with sodium dissolved in mercury to produce a solution of sodium dithionite. This approach may

be of a special interest to pulp mills where chlorine and caustic soda are manufactured in mercury cells. Considering the fact that $\text{Na}_2\text{S}_2\text{O}_4$ ($\approx 39\text{¢}/\text{lb}$ of $\text{S}_2\text{O}_4^{=}$ ion in the anhydrous crystalline salt) is a more valuable product than NaOH [$\approx 2.75\text{¢}/\text{lb}(65)$], sodium-mercury amalgam produced in the brine electrolysis unit could be used as a relatively inexpensive source of sodium to produce sodium dithionite. In other words, it might be advantageous to divert a part of the sodium-mercury amalgam to the proposed sodium dithionite manufacturing unit. The rest of the amalgam could go to the conventional "decomposer" to produce caustic soda. The sodium-depleted amalgam from the decomposer and the sodium dithionite manufacturing unit could be sent back to the brine electrolysis unit.

The sodium amalgam process for making sodium dithionite has been investigated quite extensively. A summary of the literature search is given in Chapter II. Although a good deal of information has been developed on this process, it is directed primarily at producing concentrated solutions of sodium dithionite for easy recovery of the solid salt. The reason behind this was probably to compete with the existing zinc dust: sodium carbonate method (Chapter II), which has been used industrially to manufacture anhydrous sodium dithionite crystals.

For the proposed sodium amalgam process, solutions obtained could be as dilute as 1 to 2% $\text{Na}_2\text{S}_2\text{O}_4$. It can be

shown from a mass-balance that if an approximately 1% solution of sodium dithionite is manufactured, it would not change appreciably the pulp consistency which is employed in the normal groundwood brightening process (62, 106).

Based on the above discussion the problem for the present research was defined. It was decided to investigate the effect of different process variables on the yields of sodium dithionite produced as a relatively dilute (approximately 1-2%) water solution from sodium-mercury amalgam and sulfur dioxide in a simple "once through" reactor. The manufactured aqueous solution would be used directly for the brightening of groundwood pulp. It was also hoped that the investigation would lead to a better understanding of the sodium amalgam process and might yield sufficient information for the design of a semi-commercial or a commercial plant.

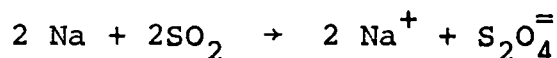
Since it was decided to have no recycle of sulfur dioxide in this investigation, yields of sodium dithionite on sulfur dioxide entering † and on sodium consumed* in a single pass must be economical.

† Yield of sodium dithionite on total sulfur dioxide entering the reactor (%),

$$Y_{SO_2} = \frac{(\text{gm molar conc. of Na}_2\text{S}_2\text{O}_4 \text{ in product}) \times 2 \times 100}{(\text{gm molar conc. of total SO}_2 \text{ in aqueous feed})}$$

A rough economic assessment of a sodium amalgam process to produce sodium dithionite solution *in situ* can be made. In the manufacture of chlorine and caustic soda using mercury cells, the cost of production may be apportioned to these two products on a weight basis (57). Thus, the cost of chlorine gas and caustic soda is almost equal. The market value of caustic soda can be taken as approximately 2.75¢/lb (65). An evaluation of the sodium in the amalgam would be approximately 5¢ (40/23 x 2.75 ≈ 5) per pound. The cost of crude sulfur varies depending on the market conditions but may be taken as 1.8¢/lb (65). The cost of sulfur dioxide gas produced by oxidation of this sulfur would be about 0.9¢ plus processing cost for a total of about 1.5¢/lb.

The reaction between sodium and sulfur dioxide is given stoichiometrically by the equation:



*Yield of sodium dithionite on sodium consumed in the reactor (%),

$$\text{CONNA} = \frac{(\text{gm moles of Na}_2\text{S}_2\text{O}_4 \text{ in product/min}) \times 2 \times 100}{\left(\begin{array}{l} \text{gm moles of Na entering with fresh amalgam/min} \\ - \text{gm moles of Na leaving with spent amalgam/min} \end{array} \right)}$$

If it is assumed that a 100% yield of sodium dithionite on sodium consumed is obtained and the yield of sodium dithionite on sulfur dioxide entering is 100%, then the cost of sodium dithionite (chemical cost only) would be about 3.3¢/lb of $S_2O_4^{=}$ ion.

This cost can be compared with the cost of anhydrous sodium dithionite crystals bought in the market ($\approx 39\text{¢}/\text{lb}$ of $S_2O_4^{=}$ ion) as well as the cost of zinc dithionite produced *in situ* ($\approx 16\text{¢}/\text{lb}$ of $S_2O_4^{=}$ ion). If reasonably high yields of sodium dithionite on sulfur dioxide entering and on sodium consumed could be obtained by the proposed sodium amalgam process, it seems possible to decrease the cost of sodium dithionite substantially for mill use. It is also possible that the cost of dithionite ions produced by the proposed sodium amalgam process may not be very different from the cost of dithionite ions in the zinc dithionite produced *in situ*.

CHAPTER II

REVIEW OF PERTINENT PRIOR WORK

A. Manufacturing Processes for Sodium Dithionite

A number of methods are available in the literature describing preparation of sodium dithionite. All of them are based on the reduction of sulfur dioxide (or sodium bisulfite). The ones which could be used commercially are:

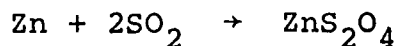
1. Zinc dust: sodium carbonate process
2. Electrolytic or cathodic reduction process
3. Sodium formate process
4. Sodium borohydride process
5. Sodium amalgam process.

Brief outlines of these processes are given below. Special emphasis has been put on the sodium amalgam process because of its similarity to the proposed process.

1. Zinc dust: sodium carbonate process

Sodium dithionite is manufactured by reacting an aqueous solution of sulfur dioxide with a stirred suspension of zinc dust in water and then converting the zinc salt into the sodium salt by the addition of sodium carbonate (8-10,

17, 19, 30, 73, 76, 78, 94, 98, 148). The chemical reactions involved are:



After the removal of the zinc carbonate by filtration, $\text{Na}_2\text{S}_2\text{O}_4 \cdot 2\text{H}_2\text{O}$ is salted out by the addition of NaCl . Dehydration and drying steps follow to make the anhydrous salt, $\text{Na}_2\text{S}_2\text{O}_4$.

Badischen Anilin - und Sodafabrik (Germany) used this method industrially (9, 10). A 20% solution of sodium dithionite was crystallized, dehydrated, then dried. This German firm obtained a yield of 65-75% based on sulfur dioxide feed and about 70% on zinc. Virginia Chemical Inc. of the U.S.A. has also been reported to use this method industrially.

Some of the disadvantages of the zinc dust:sodium carbonate process to produce sodium dithionite are:

- (a) The market for zinc oxide, which is a by-product, is contracting. Zinc dust is quite expensive, and the initial cost incurred in the raw material is not compensated by revenue from the sale of zinc oxide.
- (b) The process is discontinuous and involves the extra steps (compared to the other processes) of precipitating zinc carbonate and calcining the precipitated carbonate to obtain zinc oxide.

- (c) Zinc is always present as an impurity in the $\text{Na}_2\text{S}_2\text{O}_4$ and zinc ions, as mentioned earlier, are a pollution hazard if released with mill effluent.
- (d) Dehydration and drying steps to make stable anhydrous $\text{Na}_2\text{S}_2\text{O}_4$ are complicated and expensive.

2. Electrolytic or cathodic reduction process

In this method dithionite ion is produced cathodically (8, 10, 21, 39, 40, 61, 71, 75, 131, 132, 135, 136, 139, 142-144, 147) according to the reaction:

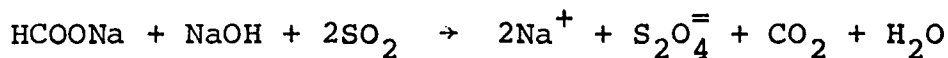


Although the cathodic reduction of sulfur dioxide (or bisulfite) solution in water has been studied repeatedly since 1904, this method has never been used industrially. The process is reported to give low yields of sodium dithionite on sulfur dioxide and low current efficiencies. However, in a recently published investigation based on laboratory experiments, Oloman (67, 68) claims that $\text{Na}_2\text{S}_2\text{O}_4$ produced by this method could compete with ZnS_2O_4 produced *in situ*.

3. Sodium formate process

This process was invented by Kinzlberger & Co. (122, 123). In this process sulfur dioxide is dissolved in a solu-

tion of sodium hydroxide in methanol. The sulfur dioxide is reduced in turn, by a suspension of sodium formate in aqueous methanol at a temperature of about 70°C according to the reaction:

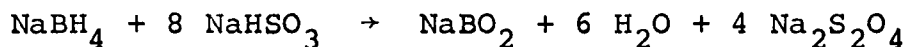


The product is filtered, washed with methanol and then dried to give anhydrous sodium dithionite.

According to Gerritsen (30) this process was commercially used in the past, but it was dropped because the product was a very finely divided powder and therefore not very stable to oxidation. Recently some investigators (128, 141, 146, 151, 152), on the basis of laboratory experiments, have reported high yields of sodium dithionite on sulfur dioxide ($\approx 80\%$) and high purity of the product ($\approx 90\%$) from the formate process.

4. Sodium borohydride process

In this process an aqueous solution of sulfur dioxide (or sodium bisulfite) is reduced by sodium borohydride (140, 150) according to the reaction:



So far this method has not been used industrially.

5. Sodium amalgam process

In this process sodium metal dissolved in mercury is used to reduce sulfur dioxide to give sodium dithionite. The overall reaction can be written as follows:



The standard oxidation potential of pure sodium metal is greater than that of sodium in sodium-mercury amalgam (35, 36, 57). The overvoltage of hydrogen gas on sodium-mercury amalgam is high (57). Thus it is possible to bring about a controlled reaction between sodium in mercury solution and various other reactive compounds in aqueous solution, with little loss due to reaction of the sodium with water.

(a) Advantages of the sodium amalgam process

(i) Compared to the zinc dust: sodium carbonate process, which is used industrially, extra steps are avoided such as separation of zinc carbonate and calcining the precipitated carbonate to obtain zinc oxide.

(ii) Sodium dithionite obtained by this process is not contaminated by the zinc ions as is the dithionite obtained by the zinc dust: sodium carbonate method.

(iii) The reactor could work as the decomposer in conjunction with mercury cells which may be used for chlorine manufacture at a mill site.

(iv) As the reducing agent is a solution, continuous reduction can be easily carried out.

(v) Sodium-mercury amalgam is an inexpensive source of sodium metal, particularly if the sodium is produced in a mercury chlor-alkali cell.

(b) Types of the sodium amalgam process

Sulfur dioxide in a number of forms may be reacted with sodium-mercury amalgam to produce sodium dithionite.

Some of these forms are:

- (i) Sulfur dioxide dissolved in organic solvents
- (ii) Gaseous or liquid sulfur dioxide
- (iii) Sulfur dioxide introduced into aqueous buffer containing NaHSO_3 and Na_2SO_3 .

(i) Sulfur dioxide dissolved in organic solvents (sodium amalgam: SO_2 - organic solvent process)

A number of investigators (49, 83, 117, 126) have prepared sodium dithionite from sodium-mercury amalgam and sulfur dioxide dissolved in non-aqueous media such as hydrocarbons, ethers, amides, alcohol and kerosene. They have claimed high

yields of the anhydrous product which is obtained directly. According to the information available, this process has never been used industrially.

- (ii) Gaseous or liquid sulfur dioxide (sodium amalgam: gaseous SO_2 process and sodium amalgam: liquid SO_2 process)

Rougeot (89) reported finding $\text{Na}_2\text{S}_2\text{O}_4$ in the reaction mass when SO_2 was bubbled through sodium-mercury amalgam for 7 to 8 hours, or when liquid sulfur dioxide was in contact with sodium amalgam for 2 to 3 hours at room temperature. According to the information available, this method has never been used industrially.

- (iii) Sulfur dioxide introduced into aqueous buffer containing NaHSO_3 and Na_2SO_3 (Sodium amalgam: SO_2 - $\text{NaHSO}_3/\text{Na}_2\text{SO}_3$ buffer process)

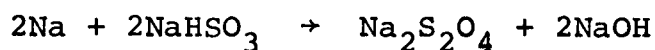
This method has been a subject of interest for many investigators (10, 18, 19, 26, 56, 64, 69, 120, 121, 124, 129, 130, 132-134, 137, 145). In this process sodium metal dissolved in mercury reduces the sulfur dioxide added to an aqueous buffer solution of NaHSO_3 and Na_2SO_3 , at a pH of about 5 to 6 and at a temperature of about 15 to 30°C, to give a concentrated solution of sodium dithionite. Hydrated sodium dithionite crystals ($\text{Na}_2\text{S}_2\text{O}_4 \cdot 2\text{H}_2\text{O}$) are salted out by the addition of sodium chloride and the slurry is taken to a

filtration unit where the crystals are removed and the mother liquor is sent back to the reactor. These hydrated crystals are then dehydrated by heating them rapidly to a temperature of about 60 to 65°C, after which they are filtered, washed with alcohol and dried under vacuum. High yields of sodium dithionite and high purity of the product have been reported.

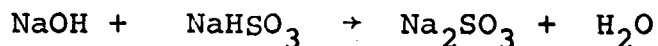
Some other investigators (74, 125, 138, 149) have recommended that a certain percentage of water-miscible alcohol should be added to the aqueous buffer solution to improve the recovery of anhydrous sodium dithionite.

The steps in the reaction for this process are as follows:

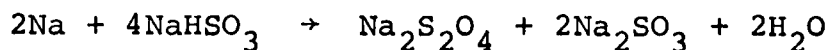
Formation reaction



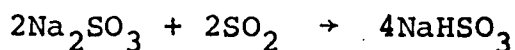
Neutralization reaction



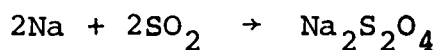
Overall formation and neutralization reaction



Regeneration reaction



Overall reaction



This method of preparation of sodium dithionite was used industrially (30 to 40 tons $\text{Na}_2\text{S}_2\text{O}_4$ /month) from 1923 to 1930 by Farbenfabriken Bayer in Leverkusen (9) but it was plagued by poor yields and formation of unwanted by-products. As late as the early 1940's they had concluded that the zinc dust: sodium carbonate process was the most economical route to sodium dithionite unless the price of zinc were unusually high and provided that the by-product zinc oxide could be sold (26). J. Olmstead (66) reported that R.B. MacMullin Associates of Niagara Falls, N.Y. had built a sodium dithionite plant some years ago, using the sodium-mercury amalgam route, for the Marathon Paper Company, but that this operation was discontinued for some unknown reason.

B. Recommended Conditions for Improving the Yield of Sodium Dithionite in the Sodium Amalgam: SO_2 - NaHSO_3 / Na_2SO_3 Buffer Process

A brief description of this process has been given on pp. 13-15. Although the objective of the proposed investigation (study of the sodium-mercury amalgam process for the manufacture

of a relatively dilute water solution of sodium dithionite) is quite different from the aim of most of the previous investigations (manufacture of a solution of sodium dithionite, generally 15-25% solution, for efficient recovery of the solid salt), it was felt important to consider the recommended levels of process variables for the latter case as they might yield some useful information for the proposed investigation.

A number of investigators (10, 18, 19, 26, 56, 64, 69) have spelled out conditions for increasing the yield* of sodium dithionite by the sodium amalgam: $\text{SO}_2 - \text{NaHSO}_3/\text{Na}_2\text{SO}_3$ buffer process. Their conclusions are given below.

It was generally recognized that conditions of extreme acidity and high temperatures in the reactor increase the rate of decomposition of sodium dithionite. Therefore, to obtain reasonable yields of sodium dithionite, it was found necessary to maintain the reactor pH between 5 and 6 and the reactor temperature in the range 15 to 30°C. It was also found that sodium dithionite is rapidly oxidized by atmospheric oxygen; therefore, an inert atmosphere of nitrogen (or carbon dioxide) was provided in the entire apparatus. The concentration of sodium in the inlet-sodium amalgam was kept in the range .01% to .05% (by weight) and sulfur dioxide was introduced in stoichiometric proportions to the sodium fed from the amalgam. The residence time of the aqueous solution

*The word "yield" has not been defined very carefully in the available literature. In most cases it appears that the authors considered the yield of sodium dithionite on sodium consumed.

in the reactor was kept as short as possible to avoid the decomposition of sodium dithionite formed. The aqueous solution was well agitated in the reactor in order to disperse the sulfur dioxide and to renew the solution at the interface.

Some other investigators (74, 125, 138, 149) modified the process by using a 20-30% ethanol solution in water rather than water alone as the solvent for NaHSO_3 - Na_2SO_3 buffer. The presence of ethanol helped in the recovery of better crystals of sodium dithionite.

Most of the information mentioned above has been obtained from the patent literature and different investigators used varied experimental devices and contacting methods for amalgam and aqueous phases. Unfortunately, very little effort has been made to improve understanding of the sodium amalgam process in general.

For the proposed "once through" process, recommendations such as the addition of 20 to 30% ethanol to the buffer solution were considered uneconomical. Some other recommendations provided guide lines for the proposed investigation.

C. Mercury Contamination of Sodium Dithionite Produced by the Sodium Amalgam: SO_2 - $\text{NaHSO}_3/\text{NaSO}_3$ buffer process

At least two investigators (10, 19) have reported that sodium dithionite obtained by the sodium amalgam: SO_2 -

$\text{NaHSO}_3/\text{Na}_2\text{SO}_3$ buffer process was contaminated with small amounts of mercury. However, it is not indicated whether the mercury was entrained in the product stream or some chemical compounds of mercury were present.

Farbenfabriken Bayer (10) manufactured sodium dithionite industrially in a reactor where sodium-mercury amalgam was thoroughly mixed with the sulfur dioxide solution in the presence of a buffer solution of NaHSO_3 and Na_2SO_3 (pH 5-7). Sodium dithionite produced by their process was contaminated with mercury, but they reported that it was possible to prepare a product with not more than 20 ppm mercury. At that time the mercury content of their product was not considered objectionable in the bleaching of groundwood pulp.

Dijs, Hoogland and Waterman (19) manufactured a 15% solution of sodium dithionite in a packed bed (column packed with glass rods). Sodium-mercury amalgam entered the reactor at the top of the column, divided into fine droplets which, after interaction with sulfur dioxide in the presence of a 5% NaHSO_3 and Na_2SO_3 buffer (pH 5-5.5), gathered at the bottom of the column. The buffer solution flowed up the column, counter current to the amalgam, and the product stream was recycled to the bottom of the reactor. The operation was made continuous by introducing an aqueous solution of sulfur dioxide to the feed and bleeding off an equal volume of the product stream. According to Dijs *et al.* the product stream was sometimes contaminated with mercury.

Removal of small amounts of mercury from the product stream is relatively easy. Dijs *et al.* recommended a solution of Na_2S to precipitate small amounts of mercury as HgS , which might be removed by filtration. Recently, Imperial Chemical Industries, England, has patented (127) a process to remove mercury from the waste brine of mercury cells. Generally, the waste brine contains 3 to 4 ppm of Hg and this mercury can be removed by treating the brine with a solution of NaHS and subsequently filtering the suspension to remove HgS . The same principle can also be used to remove mercury from the sodium dithionite solution.

D. Lignin Preserving Bleaching of Groundwood Pulp by Sodium Dithionite(62, 106)

1. Definition of the terms "brightening" and "bleaching"

When referring to groundwood, the term "brightening" is generally used to describe the whitening action of reducing agents such as the sulfites and dithionites. The term "bleaching" generally refers to the action of oxidizing agents, such as peroxides, which modify the coloured substances of the wood pulp for a longer period of time. However, the term "bleaching" is sometimes used to describe the action of both dithionites and peroxides.

2. Characteristics of the groundwood bleaching process

The essence of the groundwood bleaching process can be summarized as follows:

(a) A major requirement in groundwood bleaching, in contrast to chemical pulp bleaching, is that lignin must be retained.

(b) Unlike chemical pulp brightness, unbleached groundwood brightness varies widely with wood species and, for each species, varies with the condition of the wood being ground. Therefore, a great deal of care in cleaning and selecting wood must be taken so that all groundwood produced can be raised to the desired brightness by the available processes at an acceptable cost.

(c) The brightness of groundwood after bleaching is much more unstable than that of bleached chemical pulps. The brightness reversion rate is greater after the reducing treatment by dithionites than after the oxidizing action of peroxides. This is understandable, considering that the oxygen of the air will tend to reverse the reducing action of the dithionites. For papers of limited use, like newsprint, groundwood brightening with dithionite gives just adequate brightness gains [10-12 G.E. brightness points with 1-2% (by weight) dithionite on fibre]. Since peroxide bleaching costs are between 5 and 10 times as high as for dithionite brightening, the latter has gained wide acceptance in the production of newsprint.

3. Effects of groundwood brightening

The action of dithionite on groundwood pulps has two major effects:

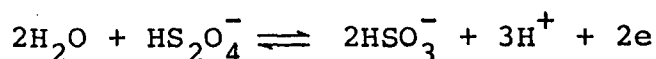
(a) The sheet reflects more light, and hence it becomes brighter.

(b) The colour of the sheet shifts appreciably from yellow-pink towards a bluer shade, and so it becomes whiter.

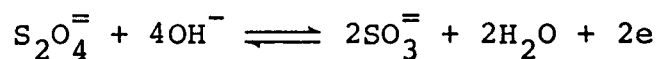
This is because dithionite treatment affects particularly the substances which absorb strongly the blue components of light and are responsible for the yellow-pink appearance of unbleached pulps.

4. Conditions for groundwood brightening by sodium dithionite

In the chemical action of dithionite during groundwood brightening, the oxidation state of the sulfur atom changes from S^{3+} to S^{4+} , that is, from dithionite to sulfite or bisulfite (62). Depending on pH, the reaction can be written in two ways. In acid solution, dithionite reacts as follows:



The standard oxidation potential of this reaction at 25°C on the hydrogen scale is $E^\circ = + .08$ volts (51). In strongly alkaline solution the reaction is:



The standard oxidation potential of this reaction at 25°C on the hydrogen scale is $E^\circ = + 1.12$ volts. Thus, dithionite is a far stronger reducing agent in alkaline than in acidic solution.

However, high alkalinity causes degradation and discolouration of wood lignin; so, in practice, it is necessary to carry out the dithionite treatment at pH levels 1 to 2 units below neutrality. The instability of dithionite solutions to acids, oxygen and high temperature has been mentioned earlier and will be discussed in detail in section II. G. The mixing of the groundwood pulp with dithionite should be rapid, intimate and uniform; and the pulp should be as free of air as possible.

Ranges for permissible and preferred conditions (62) for brightening groundwood from most species are shown in Table 1.

TABLE 1
CONDITIONS FOR BRIGHTENING GROUNDWOOD BY $\text{Na}_2\text{S}_2\text{O}_4$

Process Variable	Permissible Conditions	Preferred Conditions
Temperature	32 to 82°C	50 to 74°C
Reaction Time	1/2 to 8 hrs	1 to 2 hrs
pH	5 to 7.5	5 to 5.6
Consistency	3 to 18%	3 to 6%
Dithionite Treatment % (by weight) of Fibre	.2 to 2%	.2 to 1.5%

E. Sodium-mercury Amalgam

For the proposed continuous manufacture of sodium dithionite, it would be necessary to use liquid sodium-mercury amalgam. It has been reported in the literature (35, 36) that the solubility of sodium in mercury, at 25°C, is about 0.6% by weight. If the sodium dithionite manufacturing unit was to work in conjunction with a mercury cell, sodium in mercury would be available at a certain composition, and that would, without the use of some special equipment, put an upper limit on the concentration that could be used. Normally, the maximum concentration of sodium in the amalgam produced in the mercury cell is about .05 to .15% by weight (2, 28). In the proposed process, the maximum concentration of sodium in the inlet-amalgam would be about 0.15% by weight. The following information available in the literature on some of the important properties of liquid sodium-mercury amalgam is pertinent.

1. Molecular structure of sodium-mercury amalgam

According to Vanstone (107-109) and Schüller (92), the discontinuities in the freezing point diagram and in the specific volume versus weight per cent curve, as well as the micrographic study of mixtures of sodium and mercury, indicate that there are six compounds of the two elements

in solid sodium-mercury amalgam. However, the molecular structure of liquid sodium-mercury amalgam remains uncertain. Vanstone (107, 109) and Bent (7) determined the specific volume, electrical conductivity, oxidation potential, depression of freezing point, lowering of vapour pressure and heat of formation of liquid sodium-mercury amalgams. On the basis of their results, it can be assumed that liquid sodium-mercury amalgams are monoatomic, true solutions of sodium in mercury.

2. Surface tension of sodium-mercury amalgam

The surface tension of pure mercury has been determined against air and vacuum at different temperatures (16). Schmidt (90) determined the surface tension of mercury against air at 20°C and reported a value of 435.5 dynes/cm. According to Hohn (35) the surface tension of mercury is lowered when sodium is dissolved in it.

3. Sensitivity to oxidation of sodium-mercury amalgam

Liquid sodium mercury amalgam is highly sensitive to oxidation by atmospheric oxygen. According to Hohn (35), when the liquid sodium amalgam is exposed to air it is immediately coated with a grey film of oxide. A thin layer of paraffin oil has been recommended to avoid oxidation.

4. Density of sodium-mercury amalgam

Copious data on the specific volume of sodium-mercury amalgam, in liquid as well as solid state, has been reported in the literature (4, 58, 79, 107-109, 112). Maey's (58) data can be used to plot density of the liquid amalgam at a temperature of 17°C against weight per cent of sodium in the amalgam upto a concentration of 0.3% sodium. A regression fit on his data gives the following expression.

Density of sodium amalgam at 17°C

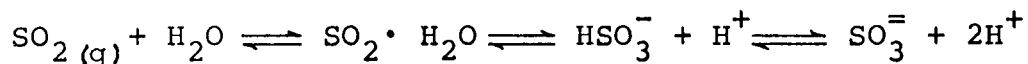
$$= 13.55 - .9986 \times \text{weight per cent of sodium in amalgam}$$

It can be seen from this expression that the density of liquid sodium-mercury amalgam decreases with increasing concentration of sodium in the above-mentioned range.

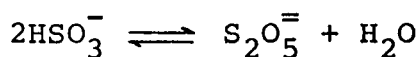
F. Sulfur Dioxide Solution in Water

1. Principal equilibria

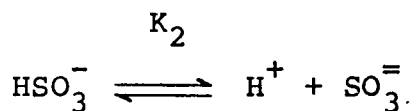
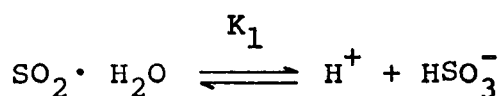
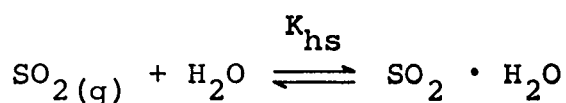
On the basis of numerous investigations (5, 24, 25, 29, 31, 42, 96, 99-101, 115) it can be concluded that when sulfur dioxide is dissolved in water, the following equilibria exist.



It is interesting to note that at very low pH's, an aqueous solution of sulfur dioxide does not contain H_2SO_3 molecules; sulfur dioxide exists in the molecular state. Simon and Waldmann (100), working with Raman spectra and aqueous solutions of sulfur dioxide of concentration greater than 1 molar, detected lines attributed to $\text{S}_2\text{O}_5^{=}$, suggesting that another ionic equilibrium exists in the system, namely



Not much is known about this equilibrium, hence, the presence of $\text{S}_2\text{O}_5^{=}$ ions has been ignored in the present investigation. Thus, the principal equilibria may be written as follows:



where,

K_{hs} = Thermodynamic equilibrium constant for $\text{SO}_2\text{-H}_2\text{O}$ system

$$K_{hs} = \frac{a_{\text{SO}_2 \cdot \text{H}_2\text{O}}}{a_{\text{SO}_2} \times a_{\text{H}_2\text{O}}} = \frac{[\text{SO}_2 \cdot \text{H}_2\text{O}]}{P_{\text{SO}_2}} \cdot f_{\text{SO}_2 \cdot \text{H}_2\text{O}} \dots (1)$$

K_1 = Thermodynamic ionization constant for the first dissociation of $\text{SO}_2 \cdot \text{H}_2\text{O}$

$$= \frac{a_{\text{H}^+} \times a_{\text{HSO}_3^-}}{a_{\text{SO}_2 \cdot \text{H}_2\text{O}}} = \frac{[\text{H}^+][\text{HSO}_3^-]}{[\text{SO}_2 \cdot \text{H}_2\text{O}]} \cdot \frac{f_{\text{H}^+} \times f_{\text{HSO}_3^-}}{f_{\text{SO}_2 \cdot \text{H}_2\text{O}}} \dots (2)$$

K_2 = Thermodynamic ionization constant for the second dissociation of $\text{SO}_2 \cdot \text{H}_2\text{O}$

$$= \frac{a_{\text{H}^+} \times a_{\text{SO}_3^{2-}}}{a_{\text{HSO}_3^-}} = \frac{[\text{H}^+][\text{SO}_3^{2-}]}{[\text{HSO}_3^-]} \cdot \frac{f_{\text{H}^+} \times f_{\text{SO}_3^{2-}}}{f_{\text{HSO}_3^-}} \dots (3)$$

In the equations (1), (2) and (3) 'a' is the activity of the indicated species. [] is the concentration in gram ions or gram moles per liter of the enclosed species.

'f' is the activity coefficient of the indicated species.

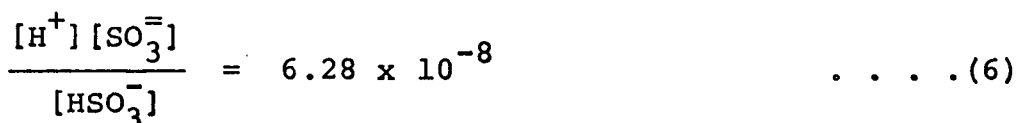
P_{SO_2} is the pressure of sulfur dioxide gas in atm.

The values of K_1 , K_2 and K_{hs} have been reported by several investigators (93, 111, 118). According to Scott

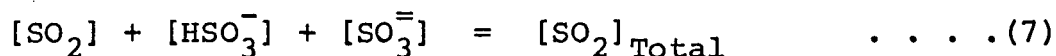
(93), at 25°C, $K_1 = .0127$; $K_2 = 6.28 \times 10^{-8}$; and $K_{hs} = 1.233$ gm moles/liter atm.

In the proposed investigation the concentration of total sulfur dioxide ($SO_2 + HSO_3^- + SO_3^{=}$) in the aqueous solutions used was in the range 0.4 molar to 1.3 molar. No data is available to-date on the molar activity coefficients of the sulfur dioxide molecules dissolved in water and mean molar activity coefficients of hydrogen and sulfite ions. Mean molar activity coefficients of hydrogen and bisulfite ions have been reported (34, 77) for very dilute solutions of sulfur dioxide in water (3.27×10^{-3} to 12.6×10^{-3} molar).

In the absence of any reasonable data, for the purposes of this investigation, the activity coefficients were assumed to be unity. Hence, the principal equilibria, at 25°C, could be written as follows:



The concentration of total sulfur dioxide in the aqueous solution could be written as follows:



If the concentration of total sulfur dioxide in the aqueous solution and the pH were known, the concentrations of all the ionic species and the dissolved sulfur dioxide in molecular state could be calculated using the equations (5), (6) and (7). A computer program was written using these equations and for a typical $[\text{SO}_2]_{\text{Total}} = .399$ molar, the concentrations of different species of sulfur dioxide in the aqueous solution were calculated. These concentrations are plotted against pH (.1 to 9) in Figure 1. It can be observed from this figure that at very low pH (pH \approx 1), most of the sulfur dioxide in the aqueous solution is available as molecular sulfur dioxide; the remainder is present as bisulfite ions. As the pH increases, the proportion of bisulfite ions increases and reaches a maximum at a pH of about 4.5. With further increase in the pH the concentration of sulfite ions starts building up and above a pH of 9, most of the sulfur dioxide is available as sulfite ions.

The conclusions arrived at by the author, agree with the following comments made by Eriksen (22), despite the latter's usage of slightly different ionization constants

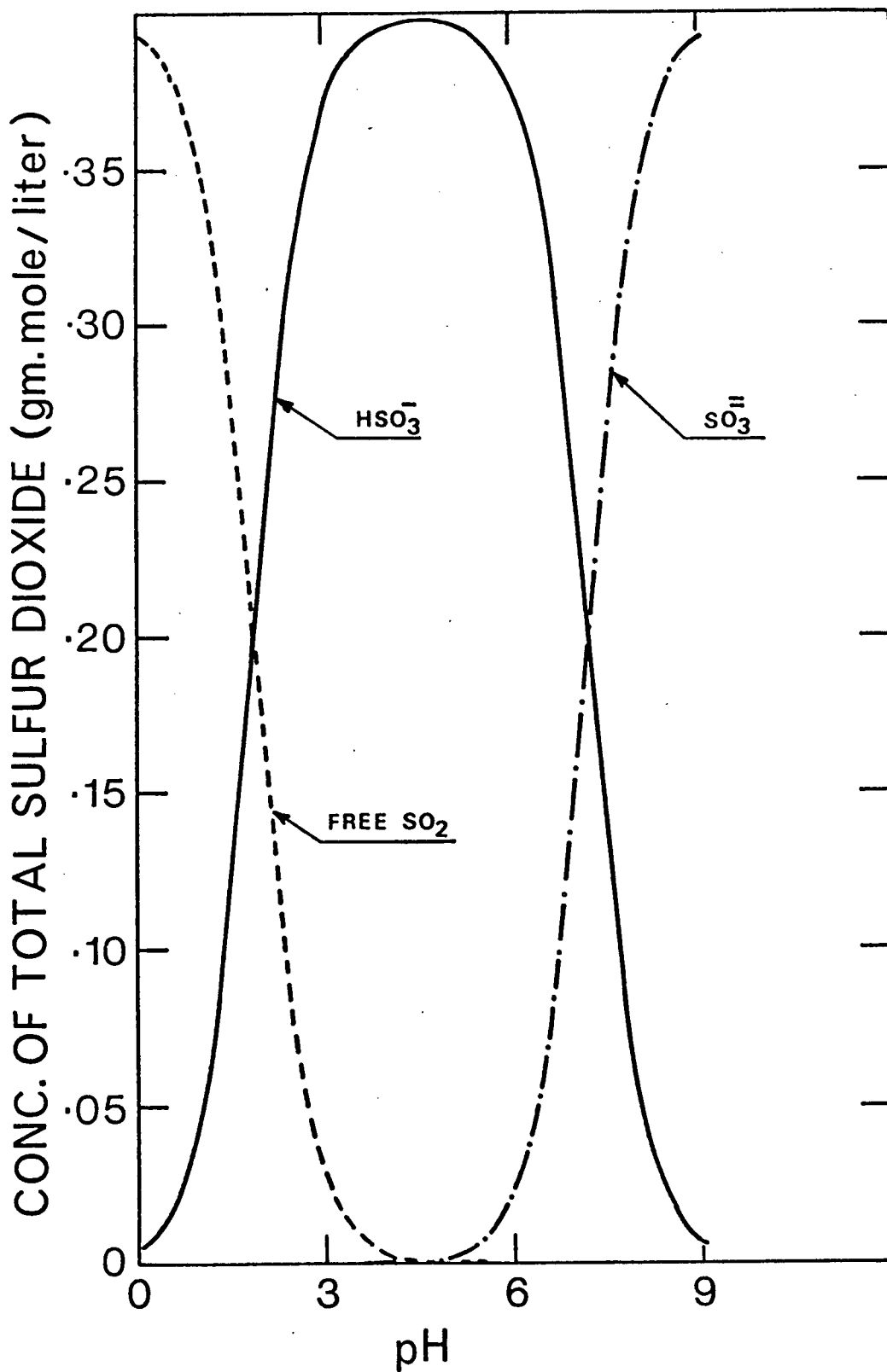


Figure 1 Concentrations of free sulfur dioxide, bisulfite ions and sulfite ions versus pH in a 0.399 molar sulfur dioxide solution in water at 25°C

($K_1 = 1.54 \times 10^{-2}$; $K_2 = 6.9 \times 10^{-7}$). "More than 97 per cent of the sulfur atoms in the solutions were contained as sulfur dioxide molecules in a solution of pH 0.3 and more than 99 per cent as bisulfite ions at pH 4.5 and as sulfite ions at pH 9.0. This selection of different pH values seems to be the closest one could come to achieving pure solutions of these molecules or ions."

2. Diffusion of sulfur dioxide in water

Eriksen (22, 23) investigated the self-diffusion of sulfur dioxide in aqueous solutions using ^{35}S as a tracer. He used Anderson and Saddington's (1) assumption that there was no interaction between the three diffusing species, namely, SO_2 , HSO_3^- and SO_3^{2-} . He calculated the composition of a saturated solution of sulfur dioxide in water at 20°C and atmospheric pressure, finding 1.6 molar SO_2 and 0.15 molar HSO_3^- , i.e. about 11 per cent was ionized. Therefore, he concluded that the diffusion coefficient of sulfur dioxide in water could not be ascribed to any one diffusing species but might be treated as an "effective diffusion coefficient." He reported the integral concentration weighted (effective) diffusion coefficient of sulfur dioxide in a saturated aqueous solution at 20°C to be 1.45×10^{-5} cm^2/sec . This value of effective diffusivity is comparable to the values obtained by several other investigators (33, 48, 55, 72, 105, 113).

According to Eriksen the diffusivities of the different species of sulfur dioxide in water are unequal, and the relative amounts of molecular SO_2 , HSO_3^- and $\text{SO}_3^{=}$ will vary with pH for a fixed concentration of total sulfur dioxide in the system. Hence, the "effective diffusion coefficient" will be a variable with pH. The effective diffusion coefficient for sulfur dioxide, in aqueous $(\text{NH}_4)_2\text{SO}_3$, as a function of pH is shown in Figure 2 (22). It can be seen from Figure 2 that the effective diffusivity of sulfur dioxide decreases with increasing pH of the solution.

The effect of temperature, total ionic concentration and type of cations on the effective diffusion coefficient of sulfur dioxide in aqueous solutions were also investigated by Eriksen.

G. Important Reactions in the Proposed Process

After carefully studying different manufacturing processes for sodium dithionite (including the patent literature), it was possible to outline some of the major reactions that may take place if a dilute aqueous solution of sodium dithionite were to be produced by contacting sodium-mercury amalgam and a solution of sulfur dioxide in water (proposed process). These reactions are:

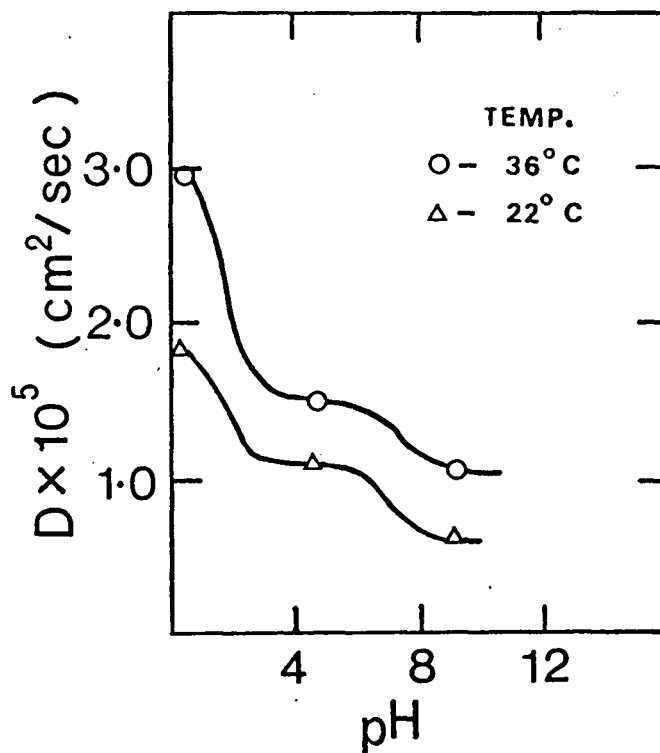


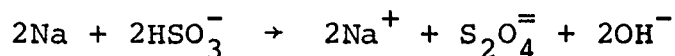
Figure 2 Effective diffusion coefficients for sulfur dioxide in aqueous $(\text{NH}_4)_2\text{SO}_3$. 'Total' sulfur dioxide concentration = 1 gm mole/liter

1. The sodium dithionite formation reaction
2. The water reaction
3. The sodium dithionite decomposition reactions
4. The sodium dithionite oxidation reaction.

Unfortunately, very little information has been reported about the kinetics and mechanisms of these reactions. The available information is as follows:

1. The sodium dithionite formation reaction

Although the mechanism of dithionite formation on sodium-mercury amalgam is not exactly known, it can be postulated (44) that the atomic sodium in the amalgam reduces bisulfite ion to give sodium dithionite according to the reaction:



The mechanism of the formation reaction has been investigated by several workers (32, 44, 48) using polarographic techniques. They studied the reduction of sulfur dioxide in aqueous solutions at a dropping mercury electrode. None of the investigators found reduction waves at dropping mercury electrodes with neutral or alkaline sulfite solutions, but well-defined waves were observed in acid medium. In other words, aqueous solutions of sulfur dioxide were reduced

in strong as well as weakly acidic media.

In strongly acidic medium (pH 0 to 2), the reduction of aqueous sulfur dioxide to dithionite takes place in one step at a half-wave potential, $E_{1/2} = -0.37$ volts (reduction potential, at pH = 1 and temperature = 25°C, measured against a saturated calomel electrode) (32, 48). The reaction could be written as follows:



In weakly acidic medium (pH 6), the polarograph shows two waves (32, 44, 48), one at $E_{1/2} = -0.67$ volt and the other at $E_{1/2} = -1.23$ volts (reduction potentials, at pH = 6 and temperature = 25°C, measured against a saturated calomel electrode). According to Ketelaar (44), at both of these half-wave potentials, dithionite is formed exclusively. This is contradictory to the explanation of Kolthoff and Miller (48), who reported that the step at -1.23 volt is connected with the formation of thiosulfate according to the empirical equation:

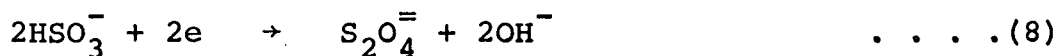


or

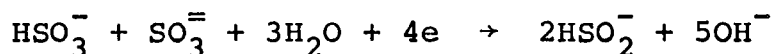


Ketelaar concluded that thiosulfate is formed at still more

negative potentials, and hydrogen is liberated at the same time ($E_{1/2} = -1.4$ volts). At more negative potentials, further reductions occur, which lead to the formation of sulfide ions and other products. The sulfite ions are not reducible at these potentials. Ketelaar postulated that the reduction reaction at $E_{1/2} = -0.67$ volt may be written as:



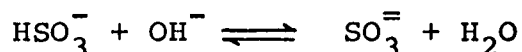
However, the reaction based on the step at $E_{1/2} = -1.23$ volt is uncertain. According to Ketelaar, this reaction could be written as follows:



The total reduction at $E_{1/2} = -1.23$ volts could be written:



When the formation reaction (9) is combined with the equilibrium between HSO_3^- and SO_3^{2-} ions in the aqueous medium,



the resultant formation reaction is equivalent to equation (8).

Previous investigators (30, 44) assumed that when sodium-mercury amalgam is brought in contact with an aqueous solution of sulfur dioxide, the dithionite formation probably takes place at the interface of the two phases. The author has attempted to explain this assumption as follows:

According to information available in the literature, sodium cannot exist in aqueous solutions in atomic form. Sodium, from the amalgam gets ionized at the interface to give an electron:



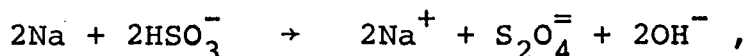
Free electrons or hydrated electrons (95) have not been known to exist in aqueous solutions for any measurable length of time. They would react with bisulfite ions and hydrogen ions rapidly. This may be taken as a justification of the assumption that the reduction by sodium-mercury amalgam probably does not take place inside the aqueous medium.

No data has been reported on the solubility of aqueous sulfur dioxide in sodium-mercury amalgam or pure mercury. It is believed that the aqueous solution of sulfur dioxide is insoluble in the amalgam. Hence, the reduction reactions would not take place inside the amalgam phase.

Having accepted the assumption that the dithionite

formation takes place at the interface of the two phases, attention was directed to determine if the reaction is reversible or irreversible.

The equilibrium constant for the reaction



at 25°C, was calculated by using the standard free energy of formation values (51) of different atomic and ionic species for the reaction at 25°C. The value of the equilibrium constant, at that temperature was approximately 10^{67} . Such a high value of the equilibrium constant implies that the reaction can be considered an irreversible reaction at 25°C.

No data is available in the literature on the rate of the sodium dithionite formation reaction. However, it has been suggested by previous investigators (30, 44) that the rate of the dithionite formation on the amalgam surface is exclusively dependent on the mass-transfer rate of bisulfite ions on the aqueous side and the supply of sodium from the amalgam to the interface. This implies that compared to the mass-transfer rate in the two phases, the chemical reaction rate is infinitely fast.

2. The water reaction

Avedikian (125), in 1956, was granted a patent for the manufacture of sodium dithionite by the sodium amalgam

process. He reported that, in his process when the concentration of sodium in the amalgam was greater than .04% (by weight), some of the sodium was consumed in what he called the water reaction. This is an unproductive reaction compared to dithionite formation, and produces sodium hydroxide and gaseous hydrogen thus lowering the yield of sodium dithionite. According to him the water reaction may be written as follows:



The evolution of hydrogen has also been reported by Ketelaar (44) in his investigations.

It was felt necessary to investigate this reaction at different pH values, for it would compete with the sodium dithionite formation reaction. The reactions of sodium-mercury amalgam with different acids, buffer solutions, water and sodium hydroxide have been studied by several investigators (12, 20, 45). Unfortunately, none of the investigators studied the rate of the water reaction from the point of view of the modern approach to mass-transfer with chemical reaction as outlined by Astarita (3). Different investigators experimented under entirely different conditions, hence, it is difficult from the information available in the literature, to formulate a mathematical model which would predict the rate of the water reaction under a given set of conditions.

The most reliable work has been done by Dunning and Kilpatrick (20) and their conclusions are as follows:

The rate of the water reaction is proportional to the square root of concentration of sodium in the amalgam, independent of hydrogen ion concentration in the range 10^{-4} to 10^{-10} moles/liter, and proportional to the area of the interface. Thus, the empirical equation could be written as follows:

$$-\frac{dC_{\text{Na}}}{dt} = k_{\text{water}} A \sqrt{C_{\text{Na}}} \quad \dots (10)$$

where,

C_{Na} = Concentration of sodium in the amalgam, gm moles/liter

A = Surface area of the sodium-mercury amalgam in contact with water, cm^2

k_{water} = Reaction rate constant

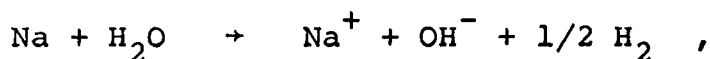
$\frac{dC_{\text{Na}}}{dt}$ = Rate of dissolution of sodium from the amalgam into water, gm moles/liter sec

Presence of certain electrolytes in the aqueous phase also affects the rate of the water reaction; however, no quantitative relationship has been proposed.

Dunning and Kilpatrick (20) and Fletcher and Kilpatrick (27) also showed that the rate of dissolution of sodium (or lithium) from the amalgam into water increased very sharply when the concentration of hydrogen ions increased above 10^{-4} moles/liter.

The nature of the empirical rate equation (10) implies that, in the pH range 4 to 10, the rate of the water reaction is not controlled by the mass-transfer rate of sodium to the interface. Dunning and Kilpatrick suggested that the rate is probably controlled by the rate of chemical reaction at the interface.

Like the sodium dithionite formation reaction, the water reaction probably also takes place at the interface of the amalgam and aqueous phases. The equilibrium constant for the water reaction,



at 25°C, was calculated by using the standard free energy of formation values (51) of the different atomic and ionic species in the reaction. The equilibrium constant, for the water reaction, at 25°C is approximately 10^{32} . This high value of the equilibrium constant indicates that the water reaction is essentially irreversible.

3. The sodium dithionite decomposition reactions

Two types of decomposition reactions should be considered. The homogeneous decomposition reaction takes place in all parts of the aqueous phase. Heterogeneous decomposition takes place at the interface of the amalgam and aqueous phases where dithionite is reduced by sodium of the amalgam.

(a) Homogeneous decomposition of sodium dithionite

Studies (40, 43, 53, 54, 59, 60, 70, 82, 116) of the decomposition of sodium dithionite in various aqueous solutions, in the absence of oxygen, have shown that at a pH of about 7, the main overall reaction is:

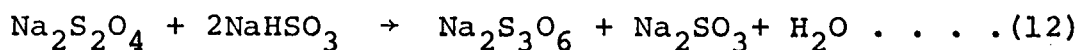
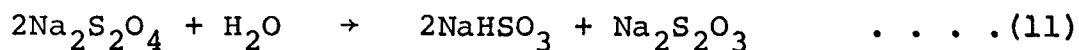


Several side reactions occur, however, and there has been little agreement on their importance or products. The kinetics have been in dispute and different mechanisms have been suggested.

Spencer (102), in 1967, reviewed most of the previous work and pointed out that the kinetic studies by earlier workers had been in dispute because the rate of decomposition is a function of solution pH and the concentrations of bisulfite, thiosulfate and dithionite ions; all of which change during the decomposition reaction. By the use of buffered

solutions containing high bisulfite concentrations, he avoided the kinetic irregularities of the earlier work. He was also able to elucidate some features of the decomposition reaction mechanism.

Sodium dithionite decomposition was followed in standard solutions over a range of concentrations (.015 to .20 moles/liter) and temperature (15 to 40°C). In most of his experiments, the pH of the aqueous buffer containing NaHSO₃ and Na₂SO₃ was about 5.2. According to Spencer, two sets of stable products, (Na₂S₂O₃ + NaHSO₃) and Na₂S₃O₆ are obtained. It was also found that about 10% of the overall decomposition reaction gives trithionite ions, even when the concentrations of NaHSO₃ and Na₂SO₃ are low. Ketelaar (113) also reported the formation of trithionite ions in the homogeneous decomposition reaction. According to Spencer, the decomposition reactions could be written as follows:



He also postulated that the initial, rate-determining steps are common to both reactions (11) and (12), with the final product distribution being determined by subsequent alternative routes. The mechanism of the rate determining step was also suggested.

It was found that the rate of decomposition is first order in $[S_2O_4^{=}]$ and, of various solution components, bisulfite ion has the strongest influence on the decomposition rate. The effects of pH, $[HSO_3^-]$ and $[SO_3^{=}]$ can not be separated rigorously, but it seems probable that the decomposition rate is first order in $[HSO_3^-]$, variable fractional order in $[H^+]$ and zero order in $[SO_3^{=}]$. The presence of $S_2O_3^{=}$ ions accelerates the rate of decomposition.

In most of the investigations (24, 121-129) on the rate of decomposition of sodium dithionite in aqueous solutions, it was found that an increase in temperature increases the rate of decomposition. Thus, the rate of decomposition of sodium dithionite in aqueous solutions can be given by the following expression.

$$r_{\text{homo}} = k_c [S_2O_4^{=}]^1 [HSO_3^-]^1 [SO_3^{=}]^0 [H^+]^x [S_2O_3^{=}]^y \quad \dots (13)$$

where,

k_c = Reaction rate constant; increases with an increase in the temperature. No data has been reported on its value by Spencer.

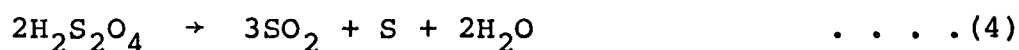
x = Variable.

y = Not determined by Spencer

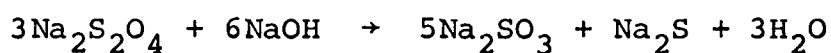
Some idea about the rate of decomposition may be obtained from Spencer's experiments. In concentrated buffer solutions of bisulfite and sulfite (2.38 moles $NaHSO_3$ /liter;

0.25 moles Na_2SO_3 /liter) at a pH of 5.2 and a temperature of 20°C , sodium dithionite decomposed from a concentration of 0.135 to .02 moles/liter in approximately 350 minutes.

Decomposition of sodium dithionite in the solutions at very low pH levels was investigated by Scholder and Denk (91). According to them, auto-decomposition of sodium dithionite is very rapid in strongly acidic solutions and eventually elemental sulfur is precipitated. The reaction can be written as follows:



Decomposition of sodium dithionite in highly alkaline aqueous solutions has also been investigated (10, 60). It was suggested that the reaction can be written as follows:



Hence, for a sodium dithionite manufacturing process, the conditions of extreme acidity or alkalinity and high temperatures must be avoided to obtain reasonable yields of the desired product.

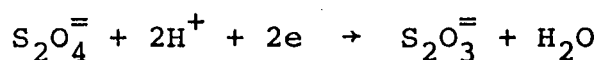
(b) Heterogeneous decomposition of sodium dithionite

Chassain and Ostertag (14) reported that when sodium dithionite was prepared by bubbling gaseous sulfur dioxide

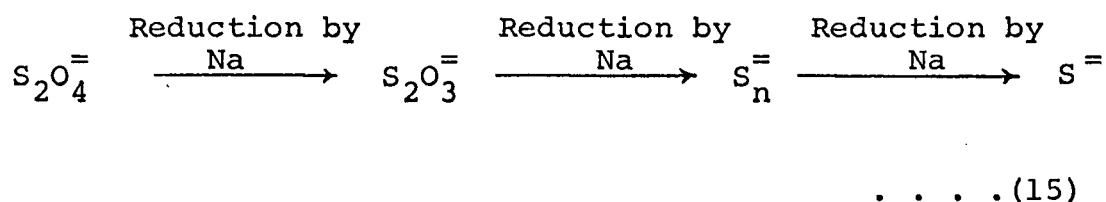
through sodium-mercury amalgam in the presence of traces of water, some of the dithionite was further reduced by sodium dissolved in mercury according to the following reaction:



Kolthoff and Miller (48) and Ketelaar (44), from the polarographic investigation of aqueous sulfur dioxide solutions, also concluded that the dithionite ions can be further reduced according to the equation:



Ketelaar also observed that at stronger reduction potentials, $\text{S}_2\text{O}_4^{=}$ ion in the aqueous solution was reduced to $\text{S}^{=}$ ion. Thus, when sodium-mercury amalgam is contacted with an aqueous solution of sulfur dioxide, the heterogeneous decomposition of the dithionite ions formed at the interface can be written schematically as follows:



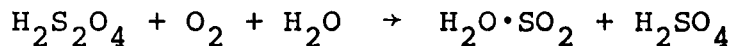
No data has been reported, in the literature, on the rates or mechanisms of these reactions. Like the sodium dithionite formation and the water reaction, the heterogeneous

decomposition reaction probably also take place at the interface of the amalgam and aqueous phases.

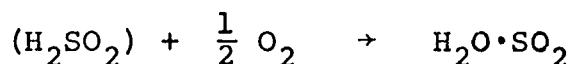
4. The sodium dithionite oxidation reaction

Since sodium dithionite is a strong reducing agent, it is rapidly attacked in solution and more slowly as a hydrated solid, by common oxidants such as atmospheric oxygen (13, 30, 38, 83).

Many investigations (6, 43, 54, 63, 80, 81) have been done on the kinetics and mechanism of air oxidation of the dithionite ions in aqueous solutions. According to Jouan (43), the oxidation of sodium dithionite by oxygen in aqueous solutions involves two reactions, and sulfite and sulfate ions are the products exclusively. The first reaction is very rapid and involves 82.4 per cent of the dithionite in solution:



Simultaneously, the remaining 17.6 per cent of the dithionite is converted into an unidentified compound of similar reducing power, presumably sulfoxylic acid, which then oxidizes more slowly to sulfite:



According to Rinker et al. (81), the rate of oxidation of sodium dithionite in aqueous solutions by atmospheric oxygen under the conditions where diffusion of air was not the rate controlling step, could be given by the following expression:

$$r_{\text{oxidation}} = k_o [S_2O_4^{=}]^{1/2} [O_2]$$

A correlation of the rate constants with temperature was made by use of the Arrhenius equation. A value of 9.3 Kcal/mole was obtained for the activation energy and the frequency factor was found to be 7.2×10^5 (moles/liter)^{-1/2} (sec)⁻¹.

In view of the information mentioned above, an inert atmosphere should be provided in an apparatus which is used to manufacture sodium dithionite.

CHAPTER III

THEORETICAL MODELS

As outlined in the Section II.G., when sodium-mercury amalgam is contacted with an aqueous solution of sulfur dioxide to produce sodium dithionite, the following reactions should be considered:

- A. The Sodium Dithionite Formation Reaction
- B. The Water Reaction
- C. The Heterogeneous Decomposition of Sodium Dithionite
- D. The Homogeneous Decomposition of Sodium Dithionite
- E. The Oxidation of Sodium Dithionite.

The literature cited in the Section II.A.5.b.iii. shows that, although several investigators have tried to develop the sodium amalgam: $\text{SO}_2 - \text{NaHSO}_3/\text{Na}_2\text{SO}_3$ buffer process from the point of view of obtaining good yields of the solid salt, none considered all of the reactions mentioned above. In most of the studies only the sodium dithionite formation reaction, the homogeneous decomposition reaction and the oxidation reaction were considered. Even for such a simplified case, in the absence of kinetic data on the reactions considered, no mathematical models have been suggested which would predict the yields of sodium dithionite

on sulfur dioxide and on sodium consumed as a function of the process variables.

Ketelaar (44) suggested a mathematical model for the rate of sodium dithionite formation reaction on the basis of the diffusion rates of the reactants in the amalgam and the aqueous phases. He also discussed the importance of homogeneous decomposition of the dithionite briefly.

Gerritsen (30) attempted to correlate some process variables to the yield of sodium dithionite on sodium consumed for a theoretically ideal reactor (the amalgam and aqueous phases perfectly mixed separately). He assumed no loss of dithionite due to oxidation and considered, primarily, the sodium dithionite formation reaction and the homogeneous decomposition of dithionite along with the mass-transfer of the reactants in the two phases. In the absence of mass-transfer coefficients and kinetic data, he arrived at the following general conclusions. According to Gerritsen, yields of sodium dithionite on sodium consumed could be improved by using large interfacial-area/aqueous-volume ratios, large mass-transfer rates of sulfur dioxide, high concentrations of sulfur dioxide in the aqueous phase and low rates of homogeneous decomposition of the dithionite.

For the present investigation, where dilute aqueous solutions of sodium dithionite were produced, mass-transfer of the different reacting species in the amalgam and aqueous

phases along with all of the major reactions mentioned above should be considered to formulate a theoretical model. The oxidation of sodium dithionite in the aqueous solution could be avoided by providing an inert atmosphere of nitrogen in the entire apparatus used to manufacture sodium dithionite and by using fresh, oxygen-free distilled water to prepare the sulfur dioxide solution. Already, a lot of information has been developed on the homogeneous decomposition of sodium dithionite in acidic, aqueous solution, and a quantitative relationship may be obtained by studying this reaction in the samples taken from the experimental reactor. Although some information (II.G.2.) is available on the rate of the water reaction, it is not known how this rate is quantitatively affected by the electrolytes present in the experimental reactor. It would be very difficult to isolate the water reaction, the sodium dithionite formation reaction and the heterogeneous decomposition of dithionite for kinetic investigation separately because they are parallel-series reactions.

Other than lack of reliable kinetic data on the major reactions, the formulation of a theoretical model is further complicated by the following:

1. The diffusion of ionic species in the aqueous phase (50) may not be treated as molecular diffusion.

2. The mass-transfer of sodium in the amalgam may increase due to the Marangoni effect.
3. Some products may get adsorbed at the mercury surface.

Thus, it was difficult to suggest a theoretical model for the proposed process from the information available. However, a qualitative model has been postulated on the basis of the information in the literature and the experiments carried out by the author. This model will be discussed in Chapter VI.

CHAPTER IV

EXPERIMENTAL

A. Experimental Materials

1. Sodium-mercury amalgam

A known quantity of distilled mercury was taken in a stainless-steel container and covered with a thin layer of paraffin oil. Sodium metal was cut under paraffin oil and cleaned to remove the layer of oxide formed on its surface. The desired amount of clean sodium metal was slowly added to the mercury with constant agitation, and was allowed to amalgamate. (The layer of paraffin oil prevents oxidation of the sodium amalgam by the atmospheric oxygen).

The purity of the chemicals and some problems involved in the preparation of amalgam are presented in Appendix C.

2. Aqueous sulfur dioxide solution

Solutions of sulfur dioxide gas in freshly distilled water were made by using an absorption column (2 1/2" x 30") filled with 1/2" Raschig Rings. This solution was always kept under an atmosphere of nitrogen to avoid oxidation. The absorption column could prepare solutions up to 1.4 molar sulfur dioxide in water.

When pH of the SO₂ solution required adjustment, a concentrated aqueous solution of sodium hydroxide was added.

The purity of chemicals used in the preparation of aqueous sulfur dioxide solutions is given in Appendix D.

B. Experimental Apparatus

The experimental apparatus used in this study is described schematically in Figure 3. Legend for Figure 3 has been enclosed in the following pages. For the sake of clarity, the types of valves used in the apparatus have not been described in the flow-sheet or the legend. For precise control of flow rate (e.g. the flow rate of the aqueous sulfur dioxide solution), a needle valve made of stainless-steel-316 was used. For less accurate control of flow rates, vee valves made of stainless-steel-316 were utilized. When an on-off control of flow rates was required, toggle-operated valves made of stainless-steel-316 were employed. Some important features of the experimental apparatus are presented below.

1. Reactor

To obtain the desired information, a continuous-flow-stirred-tank reactor (CFSTR) was designed with aqueous and

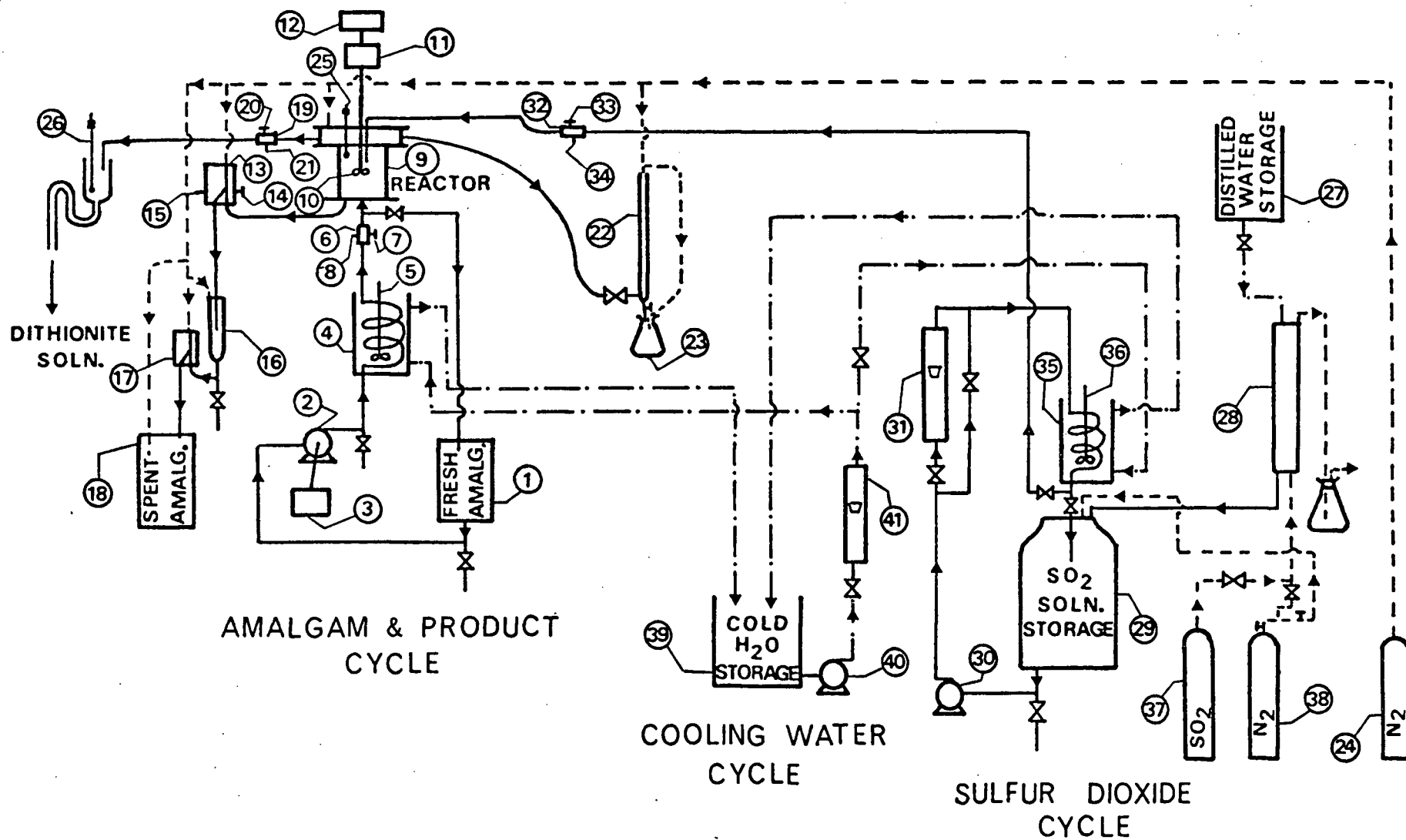


Figure 3 Schematic flow-sheet of the experimental apparatus

LEGEND FOR FIGURE 3

A. Amalgam and Product Cycle:

1. Fresh amalgam storage, 8 liter polyethylene bottle
2. Moyno pump (Type 3M1, SSQ). Positive displacement pump for pumping amalgam to the reactor (0-730 ml/min)
3. Graham transmission; variable speed drive for Moyno pump (0-450 rpm)
4. Amalgam cooling heat-exchanger
5. Variable speed stirrer in the amalgam heat-exchanger (200-1400 rpm)
6. Plexiglass connector
7. Fresh amalgam sampling place
8. Stainless-steel-sheathed iron-constantan thermocouple
9. Pyrex CFSTR
10. Propeller mixer (1 1/2" dia) mounted on 5/16" stainless-steel shaft
11. Heller motor; variable speed drive (0-3000 rpm)
12. Thyatron controller for Heller motor
13. Plexiglass level controller for amalgam layer in the reactor
14. Spent amalgam sampling place
15. Stainless-steel-sheathed iron-constantan thermocouple
16. Spent amalgam reservoir (1" x 12" glass)
17. Plexiglass level controller for spent amalgam in the reservoir

Legend for Figure 3 (continued)

18. Spent amalgam storage, 8 liter polyethylene bottle
19. Plexiglass connector
20. Product sampling place
21. Stainless-steel-sheathed iron-Constantan thermocouple
22. Burette filled with the product
23. Erlenmeyer flask with Rubine-R solution
24. N₂ gas cylinder
25. Combination pH electrode
26. Thermocompensator

B. SO₂ Cycle:

27. Distilled water storage tank, 10 gallon polyethylene bottle
28. Absorption column (2.1/2" x 30") packed with Raschig Rings
29. SO₂ solution storage tank, 20 gallon polyethylene bottle
30. Centrifugal pump; Eastern type D-11
31. Rotameter (0-400 ml/min)
32. Plexiglass connector
33. SO₂ solution sampling place
34. Stainless-steel-sheathed iron-Constantan thermocouple
35. SO₂ solution cooling heat-exchanger
36. Variable speed stirrer in SO₂ solution heat-exchanger (200-1400 rpm)
37. SO₂ gas cylinder

Legend for Figure 3 (continued)

38. N₂ gas cylinder

C. Cooling Water Cycle

39. Cooling water storage tank, 10 gallon enamelled
container

40. Centrifugal pump, Eastern type E-1

41. Rotameter (0-3920 ml/min)

amalgam phases forming an interface. This was selected rather than a packed, spray or a tubular reactor because all of the variables could be investigated independently and conveniently. This reactor might not be the ideal commercial reactor, but it was convenient to provide information on the proposed process. One of the requirements for the present investigation was to design a CFSTR that could be scaled-up, if necessary, for a future semi-commercial or full-scale plant.

The reactor consisted of a 4" x 6" Pyrex pipe section. The amalgam/aqueous solution interface was about 4 inches in diameter. The reactor assembly is shown in Figure 4 along with the applicable legend. The major parts of the reactor are described in the following paragraphs.

Initially it was planned to stir the two phases in the reactor perfectly but independently. This would have required separate stirrers and baffles for each phase. To simplify the reactor design for the present investigation, no stirrer or baffles were provided in the amalgam phase. Mixing in the amalgam phase was due to flow of the amalgam.

The part of the reactor which contained the aqueous phase was designed for perfect mixing using the recommended dimensions given by Sterbacek and Tausk (103).

It was decided to use a centrally-located marine propeller (Part 2), fixed to a rotating vertical shaft (Part 3) and driven by a variable speed drive (Heller

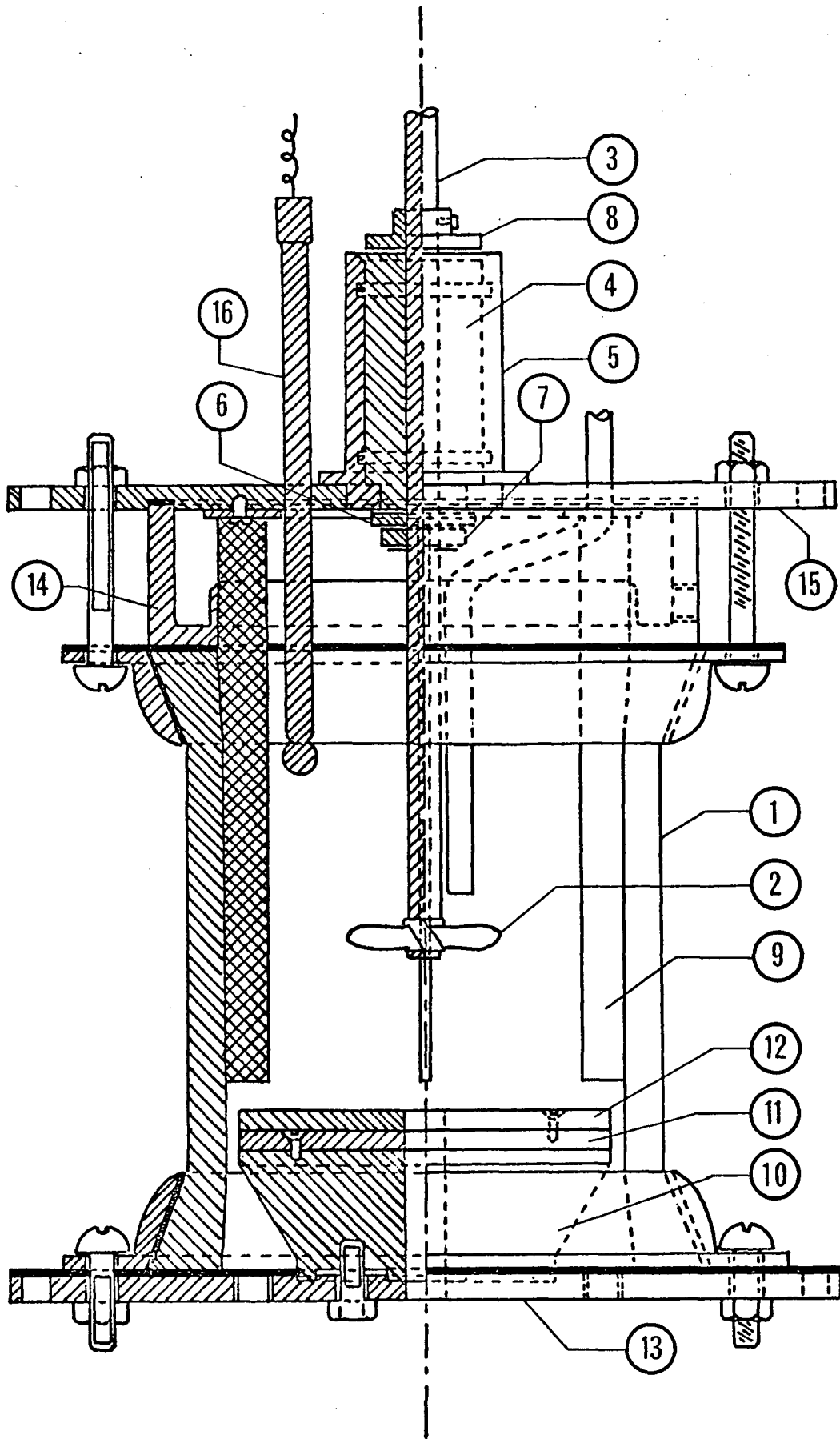


Figure 4 Reactor assembly

LEGEND FOR FIGURE 4

Part No.

- 1 4" x 6" Pyrex pipe section
- 2 1 1/2" diameter 3 blade stainless-steel marine propeller; angle of tilt = 42° from verticle
- 3 5/16" stainless-steel shaft
- 4 nylon bushing
- 5 stainless-steel packing gland
- 6 teflon washer
- 7 stainless-steel collar for the teflon washer
- 8 stainless collar
- 9 four baffles (stainless-steel)
- 10 stainless-steel slab
- 11 1/5" thick stainless-steel disc mounted on part 10
- 12 1/5" thick stainless-steel disc mounted on part 11
- 13 stainless-steel bottom flange
- 14 polyethylene weir
- 15 stainless-steel top flange
- 16 combination pH electrode

motor), in the aqueous phase. The advantages of the propeller mixer were its high speed, axial flow pattern and great pumping effect, which permits short mixing times. The aqueous sulfur dioxide solution was introduced just above the propeller. The flow patterns were such that the solution was forced to the interface primarily by axial flow, and then mixed with the rest of the aqueous medium by radial flow, axial flow and tangential flow.

The shaft of the propeller entered the reactor through a nylon bushing (Part 4) in a stainless-steel packing gland (Part 5). The lower end of the bushing was sealed by a teflon washer (Part 6), held in place by a stainless-steel collar (Part 7) which, in turn, rested on a circlip. Another stainless-steel collar (Part 8) was mounted on the propeller shaft above the bushing, such that the distance between its lower face and the top end of the bushing was approximately 1/16". Distilled water was injected into this gap periodically to lubricate the shaft in the bushing. This collar also restricted any movement of the bushing in the packing gland.

Four baffles (Part 9) were provided in the aqueous phase to promote perfect mixing conditions. To ensure that stirring in the aqueous phase did not agitate the amalgam phase significantly, the baffles in the aqueous phase extended only to the interface.

The sodium-mercury amalgam entered at the bottom of the reactor centrally and then it flowed outward radially over a stainless-steel slab (Part 10). The hold-up of the amalgam in the reactor could be changed, without changing the interfacial area, by using 1/5 inch thick stainless-steel discs (Parts 11 and 12).

The surface area of the interface could be changed by opening the bottom flange (Part 13) of the reactor and introducing thin stainless-steel discs with annular holes of various diameters. These discs were pressed against the bottom of the baffles.

The product stream containing sodium dithionite flowed over a polyethylene weir (Part 14), thus fixing the height of the aqueous medium. The weir rested on top of the Pyrex pipe section and it was kept in its position by the top flange (Part 15) made of stainless-steel.

Holes were provided in the top flange for inserting a pH electrode, the sulfur dioxide inlet tube, and the nitrogen inlet and outlet tubes. Holes were provided in the bottom flange for introducing fresh sodium-mercury amalgam and removing the spent amalgam.

2. pH measurement of the aqueous phase

The combination pH electrode was located in the reactor and the thermocompensator placed in the product stream. The pH output was recorded continuously. The

specifications of the instruments used are presented in Appendix A.

When the combination pH electrode was placed in the reactor, it became contaminated repeatedly. This was probably caused by entry of the aqueous solution resulting from the greater pressure exerted on the reference-electrode liquid junction by the aqueous phase in the reactor than the hydrostatic pressure of KCl-solution inside the reference electrode. However, the combination pH electrode worked satisfactorily when the reference electrode was pressurized by about 15 psig N_2 through the refill aperture.

3. Temperature measurement of different streams

The temperatures of the inlet sulfur dioxide solution, product stream, fresh amalgam and spent amalgam were measured by stainless-steel-sheathed iron-constantan thermocouples. These temperatures were recorded digitally with the aid of electronic instruments including a digital clock, digital millivolt meter, scanner, multiplexer and a printer system (printer and printer controller). The system used to measure the temperatures digitally is outlined schematically in Figure 5. The specifications of the different temperature measuring instruments used are given in Appendix A.

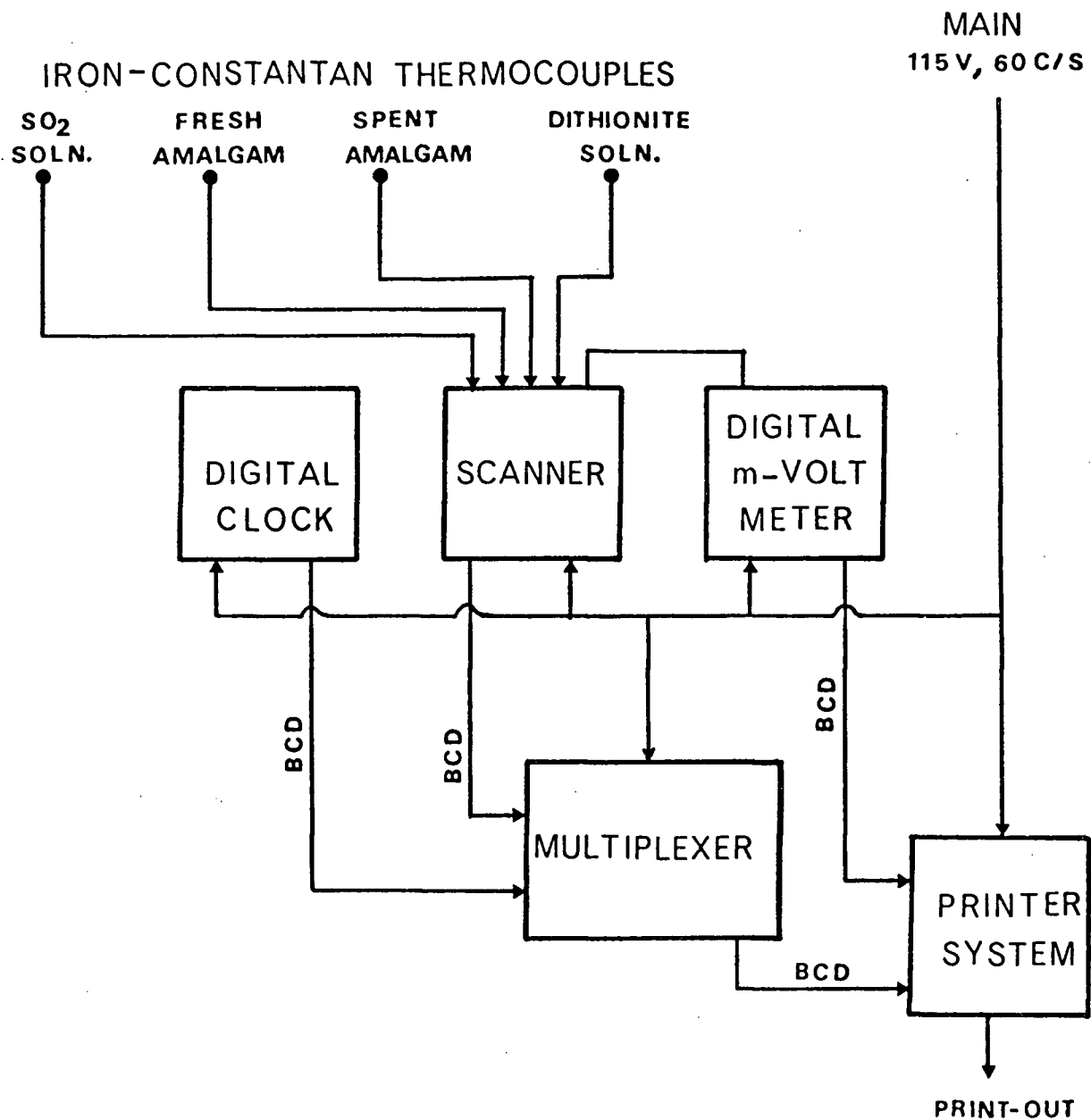


Figure 5 Digital temperature measurement (schematic)

4. Insulation of the equipment

The heat of formation of the sodium dithionite at 25°C was calculated. A value of $\Delta H^\circ = -88.29$ Kcal/gm mole implies that the dithionite formation reaction is highly exothermic. To maintain low temperatures in the reactor, the inlet streams were cooled and most of the equipment was insulated with glass-wool.

5. Electrical wiring diagram

A schematic wiring diagram for the experimental apparatus is shown in Figure 6.

C. Calibration Curves

The following calibrations were done and the calibration curves have been attached in Appendix A:

1. Flow rate of mercury pumped by the Moyno pump against micrometer setting on the Graham transmission.
2. Flow rate of aqueous sulfur dioxide against reading on the rotameter scale.
3. Flow rate of cooling water against reading on the rotameter.

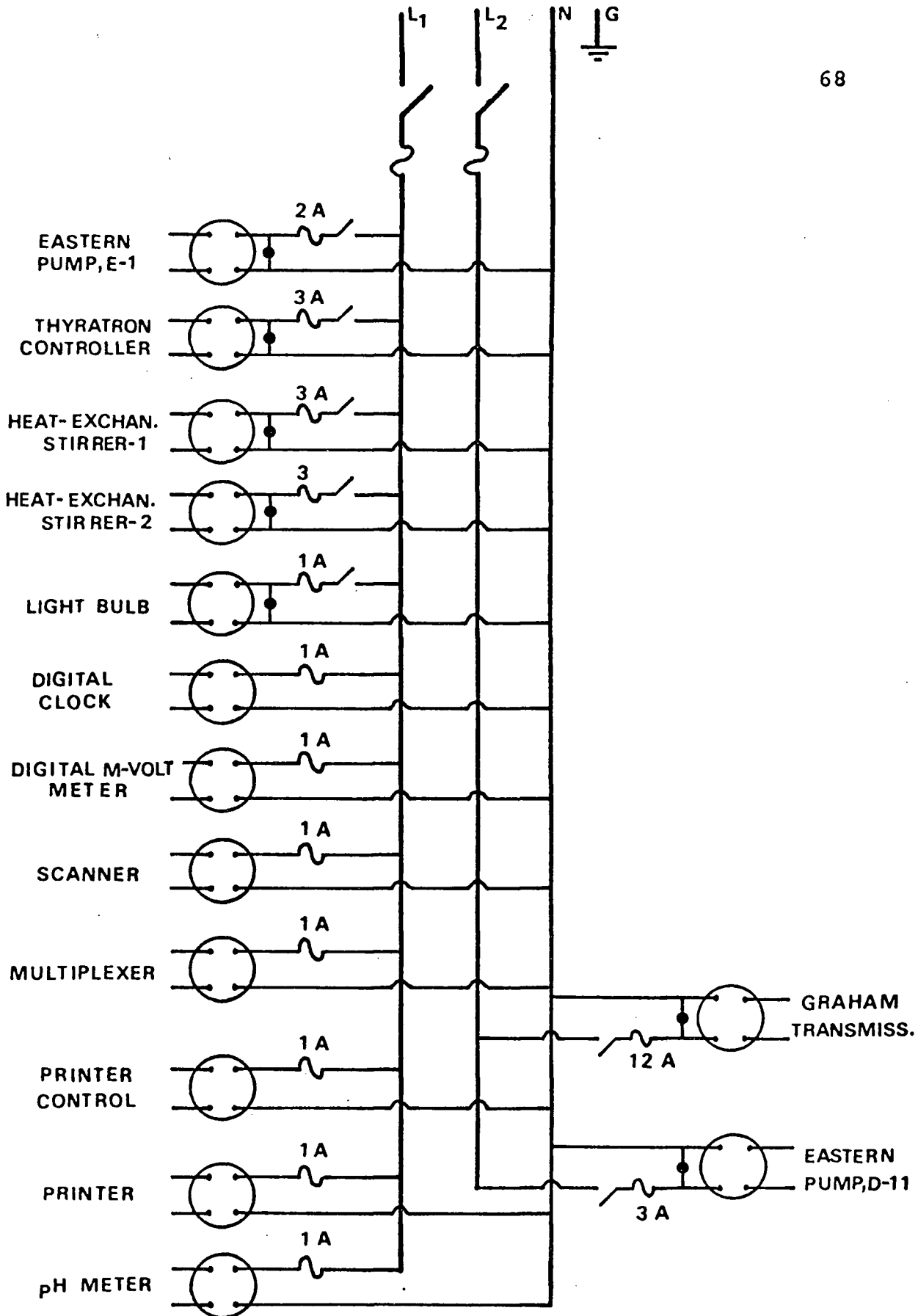


Figure 6 Electrical wiring diagram (schematic)

4. Millivolt output of iron-constantan thermocouples against temperature ($^{\circ}\text{C}$).
5. RPM of the propeller against micrometer setting on the thyatron controller for the variable speed drive (Heller motor).

D. An Experimental Run

Sodium-mercury amalgam, the sodium content of which was known approximately, was prepared and stored in the fresh amalgam storage bottle under a thin layer of paraffin oil. A concentrated aqueous solution of sulfur dioxide was prepared in the absorption column and stored, under N_2 , in the sulfur dioxide storage bottle. The concentration of total sulfur dioxide in the solution was determined and then it was diluted with distilled water, so that it was slightly above the desired concentration. The pH of this solution was adjusted in the desired range, by the addition of concentrated sodium hydroxide solution.

The amalgam and sulfur dioxide solution streams were then circulated through the heat-exchangers (closing the inlets to the reactor) and cooled by water. Samples were taken from the amalgam and sulfur dioxide-solution streams for analysis and their concentrations were determined.

The reactor was flushed with N_2 and kept under a slight pressure of nitrogen gas. The cooled amalgam was sent through the heat-exchanger to the reactor and the height of the amalgam layer in the reactor (slightly above the bottom of the baffles) was adjusted by the mechanical level controller. The flow rate of the amalgam was adjusted by the micrometer screw on the Graham transmission which was driving the Moyno pump. The propeller in the reactor, driven by the variable speed drive (Heller motor), was started and its rpm was fixed at the desired level with the help of a thyatron controller. The combination pH electrode was then introduced into the reactor and the pH meter was kept in the "standby" position. The cooled sulfur dioxide solution entered the reactor at a very high flow rate until the reactor was filled and then the flow rate was reduced and adjusted to the desired level, using a needle valve and a rotameter. Generally, the amalgam level controller had to be re-adjusted so that the amalgam just touched the bottom of the baffles. The pH meter was turned on and pH of the aqueous phase in the reactor was recorded continuously.

The desired temperature of the aqueous phase in the reactor was obtained by controlling the temperatures of the reactant streams. The temperatures of the reactant streams were controlled by the flow rate of the cooling water. The temperatures of the fresh amalgam, spent amalgam, inlet sulfur dioxide solution and the product stream were recorded periodically.

Outlet amalgam samples were taken periodically during the run from a sample point on the level controller. From time to time, the product stream was taken from the top of the reactor to the burette (under a N_2 atmosphere) and titrated against Rubine-R dye for its dithionite content.

The experimental run was continued until the process attained steady-state. A steady-state was attained when successive titrations with Rubine-R dye gave the same concentration of sodium dithionite in the product stream.

E. Analytical Procedures and Errors

1. Sodium-mercury amalgam

(a) Analysis of sodium-mercury amalgam

The analytical procedure used was similar to that employed by Rinker and Lynn (83). The sodium-mercury amalgam sample was taken using a hypodermic syringe and injected under distilled water (to avoid oxidation by air) in an Erlenmeyer flask. A known volume of standard H_2SO_4 was pipetted into it and the Erlenmeyer flask was agitated thoroughly. The sodium dissolved in mercury completely reacted with H_2SO_4 to give H_2 provided there was an excess of H_2SO_4 . Excess of H_2SO_4 was back-titrated with a standard solution of NaOH

using phenolphthalein as an indicator. A sample calculation to determine the concentration of sodium in amalgam is presented in Appendix C.

(b) Accuracy and precision of the analytical procedure

The theory behind the estimation of uncertainty in the results obtained by an analytical method is discussed in Appendix B.

The most efficient way to test the accuracy and precision of the proposed analytical method in our laboratory, would have been to make an amalgam of known sodium concentration and check its sodium content several times by the analytical method.

Unfortunately, it was found difficult to prepare an amalgam of known sodium concentration starting with known quantities of mercury and sodium metal (Appendix C). Hence, it was not possible to calculate the accuracy of the analytical method by the above-mentioned approach. However, it was evident from the information available in the literature (52, 97, 104, 110) that the chemical reactions involved in the analytical procedure were irreversible and went to completion in a very short time. Precautions were taken to avoid any systematic errors in various steps of the procedure. Based on the above arguments, it was assumed that the analytical procedure, as applied in the present

investigation, provided accurate estimates of sodium content in the amalgam.

The precision of the analytical procedure was estimated by the method of "propagation of random error" (Appendix B). In short, the precision of measurement of directly measured quantities, in various steps of the analytical procedure, was known. From this knowledge, the 95 per cent confidence limits (precision of the analytical procedure) of the weight per cent of sodium in the amalgam were estimated (Appendix C).

In the instances where fairly dilute ($\approx 0.1N$) standard solutions of H_2SO_4 and $NaOH$ were used and sufficiently large samples (≈ 30 gms) of the amalgam were taken, the analytical procedure was precise enough for the present investigation. To illustrate this, three amalgams of different sodium content were analysed by the proposed analytical method. The sodium concentrations of these amalgams, covered the range of sodium content in the amalgams used in the present work. The precision of the method, at 95 per cent confidence level, for determining the concentration of sodium in these three amalgams was estimated (Appendix C) and the results are given in Table 2.

TABLE 2

PRECISION OF THE AMALGAM ANALYTICAL PROCEDURE

Amalgam Sample No.	gm of Na/ 100 gm of Amalgam	Precision (95% Confi- dence limits)	Percentage Precision
I	.0015	$\pm .0005$	$\approx \pm 33$
II	.0383	$\pm .0005$	$\approx \pm 1.3$
III	.1533	$\pm .0005$	$\approx \pm .33$

It has been shown in Appendix F that the large imprecision in determining very small concentrations of sodium in the amalgam (e.g. amalgam no. I) did not cause appreciable error in the desired yields and conversions.

To verify the estimated precision mentioned above, several samples of spent amalgam were taken from the reactor after steady-state had been attained during an experimental run. These samples were analyzed for their sodium content by the analytical method used. The scatter in the data was caused by:

- (i) random errors involved in various steps of the analytical procedure, and
- (ii) the change of sodium content in the spent amalgam depending on the reactor dynamics.

The variance was estimated from the experimental data using the equation (B-2).

In almost all of the experimental runs, it could be said with 95 per cent confidence that there was no significant difference between the experimentally estimated variance and the variance estimated by the method of propagation of random error. The variances were compared by the 'F' test. This conclusion also implied that the fluctuations of sodium content in the spent amalgam caused by reactor dynamics were insignificant compared to the imprecision caused by the analytical method.

2. Aqueous sulfur dioxide solution

(a) Analysis of aqueous sulfur dioxide solution

The total sulfur dioxide ($\text{SO}_2 + \text{HSO}_3^- + \text{SO}_3^{=}$) in aqueous solution was determined by iodometric analysis as outlined by Vogel (110) and Kolthoff and Belcher (47).

A liquid sample of the aqueous sulfur dioxide solution was injected, using a hypodermic syringe, into an excess of standard iodine solution. The excess of iodine in the solution was back-titrated with a standard solution of sodium thiosulfate using a starch-solution as an indicator.

The method used to calculate the concentration of total sulfur dioxide in water is presented in Appendix D.

(b) Accuracy and precision of the analytical procedure

The iodometric method to determine total sulfur dioxide in aqueous solution is a standard text-book method (47, 110) and is considered to give accurate results by several investigators (22, 93).

Three different concentrations of sulfur dioxide in aqueous solutions were used in the present investigation; 0.40 molar, 0.655 molar and 1.30 molar. The method used to estimate the precision of the analytical procedure, at 95 per cent confidence level, in determining the concentration of total sulfur dioxide in these three solutions has been outlined in Appendix D. The results are presented in Table 3.

TABLE 3

PRECISION OF THE SULFUR DIOXIDE ANALYTICAL PROCEDURE

Aqueous sulfur dioxide solution No.	Moles of Total sulfur dioxide/liter	Precision (95% Confidence limits)	Percentage Precision
I	0.400	± 0.002	$\approx \pm 0.5$
II	0.655	± 0.004	$\approx \pm 0.6$
III	1.300	± 0.007	$\approx \pm 0.5$

3. Aqueous sodium dithionite solution

When air oxidation was avoided, the product stream from the CFSTR contained mainly $S_2O_4^{=}$, $S_2O_3^{=}$ and $HSO_3^{=}$ (or $SO_3^{=}$ or SO_2 depending on pH) ions.

(a) Analysis of sodium dithionite in the product stream

The assay of sodium dithionite has been thoroughly studied by a committee and their findings have been published (114). In its attempt to determine the most suitable method for sodium dithionite analysis, the committee reviewed about fourteen different methods. This committee concluded that it is possible to obtain precise and comparable results by faithful application of the following three methods.

- (i) The iodine-formaldehyde method
- (ii) The Rubine-R method
- (iii) The ammonical-copper method.

The iodine-formaldehyde (47) and the Rubine-R (114, 119) methods were modified and then used in the present investigation. A detailed description of these analytical procedures along with sample calculations are presented in Appendix E.

The general principle of the iodine-formaldehyde method is as follows. The dithionite ions are oxidized quantitatively to sulfate ions by iodine according to the

following reaction:



However, the direct titration is of no practical value since sulfite ions (or bisulfite ions), which are always present with the dithionite ions, also react. This interference can be eliminated by the addition of an excess of formaldehyde which reacts with the dithionite to form formaldehyde-bisulfite and formaldehyde-sulfoxylate according to the reaction:



Formaldehyde-bisulfite is inert to iodine, whereas the sulfoxylate reacts readily according to:



Rubine-R is a bright red dye. A solution of Rubine-R is reduced instantaneously by the dithionite ions, to an amber coloured liquid. Although, HSO_3^- and $\text{S}_2\text{O}_3^{\bar{=}}$ ions also reduce Rubine-R, the rate of reaction is very slow and it takes them weeks to reduce a small quantity of the dye solution. Thus, Rubine-R can be considered specific for determination of dithionite ions.

In the present investigation, the iodine-formaldehyde and the Rubine-R methods gave comparable results. The Rubine-R

method was used most of the time because of its simplicity and better precision. The disadvantage of the Rubine-R method was that it gave only $S_2O_4^{=}$ in the product stream while $S_2O_4^{=}$, $S_2O_3^{=}$ and HSO_3^- (or $SO_3^{=}$) could be determined by the iodine-formaldehyde method.

(b) Accuracy and precision of the analytical procedures

The most efficient way to test the accuracy and precision of the two analytical methods used in the present investigation would have been to make aqueous sodium dithionite solution of a known concentration and check its sodium dithionite content several times by both methods.

It was found impractical to prepare a solution of known $Na_2S_2O_4$ content as a primary standard because reagent grade sodium dithionite purchased from the market contains an unknown amount of $Na_2S_2O_4$. Fresh stock obtained from the market may contain as high as 90% $Na_2S_2O_4$ while old stock may have less than 60% $Na_2S_2O_4$ due to the decomposition of $Na_2S_2O_4$ to $NaHSO_3$ and $Na_2S_2O_3$.

As mentioned in the last section, the iodine-formaldehyde and the Rubine-R methods have been accepted as the most accurate and precise methods for determining the concentration of $Na_2S_2O_4$ in a solution. After steady-state conditions had been obtained in an experimental run, samples of the product stream were taken from the reactor, and were analyzed by both methods. The mean concentration

(gm $\text{Na}_2\text{S}_2\text{O}_4$ /100 ml) of $\text{Na}_2\text{S}_2\text{O}_4$, determined by the Rubine-R method, was about 5 per cent higher than the mean concentration determined by the iodine-formaldehyde method.

The scatter in the data for an analytical method was caused by:

- (i) random errors involved in various steps of the analytical procedure, and
- (ii) the change of $\text{Na}_2\text{S}_2\text{O}_4$ content in the product stream depending on the reactor dynamics.

From the experimental data, the precision of the two analytical methods at the 95 per cent confidence level, for determining the concentration of $\text{Na}_2\text{S}_2\text{O}_4$ in the product stream was estimated.

In most of the cases, the precision of the Rubine-R method derived from experimental data was within $\pm 1\%$ and the precision of the iodine-formaldehyde method was about $\pm 5\%$.

The precision of the Rubine-R method was also estimated by the method of propagation of random error. Various steps involved in the Rubine-R method for precision calculations have been outlined in Appendix E. Using this approach, the estimated precision of the Rubine-R method was also found to be within approximately $\pm 1\%$ for the concentrations of sodium dithionite analyzed in the present investigation.

The observation that, at 95 per cent confidence interval, there was no significant difference between the experimentally estimated precision and the precision estimated by the method of propagation of random error, implied that the fluctuations of $\text{Na}_2\text{S}_2\text{O}_4$ concentration in the product stream caused by the reactor dynamics were insignificant compared to the imprecision caused by the analytical method.

CHAPTER V

EXPERIMENTAL RESULTS

A. Batch Experiments

On the basis of information available in the literature, five possible reactions were outlined in Section II. G that may take place in the proposed process. Some batch experiments showed that, under the experimental conditions of the present investigation, almost all of these reactions would take place.

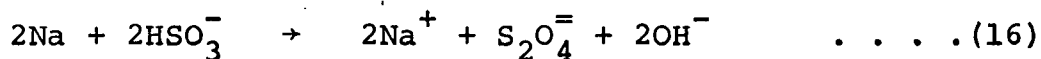
1. Presence of the sodium dithionite formation reaction

Four 50 ml samples of an approximately 0.22% sodium-mercury amalgam (0.22 gms Na/100 gms of amalgam) were taken in four separate beakers. An approximately 2.2 molar solution of sodium bisulfite in water was prepared and the solution was divided into four parts. The pH of the four portions of the NaHSO_3 solution was adjusted to 0.8, 1.7, 4.0 and 9.0 respectively by the addition of concentrated H_2SO_4 or NaOH. Four 50 ml samples of the NaHSO_3 solutions at the different pH's were added to the four amalgam samples respectively and the contents in the beaker were stirred with a glass rod. An approximately 1 ml solution of dilute

Rubine-R dye was added to each of the beakers.

The bright red colour of the Rubine-R dye disappeared almost immediately in the beakers where NaHSO_3 solutions at pH's 0.8, 1.7 and 4.0 were added. In all of the three cases, immediately after the Rubine-R was discoloured, the pH of the aqueous phase was below 7. In the fourth beaker, where the pH of the NaHSO_3 solution sample was 9, the Rubine-R dye was not discoloured.

These experiments demonstrated that when sodium-mercury amalgam is brought in contact with an aqueous solution of sodium bisulfite, sodium dithionite is produced at a rapid rate. The results also agree with the literature information presented in section II.G.1 that the sodium dithionite formation reaction can take place only when the pH of the aqueous solution is in the acidic range. This reaction can be written as follows:



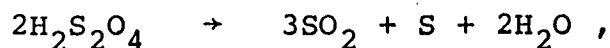
2. Presence of homogeneous decomposition of sodium dithionite in an acidic solution

Approximately 20 gms of the anhydrous sodium dithionite (reagent grade salt) was dissolved in a liter of oxygen-free distilled water (this is the maximum concentration of $\text{Na}_2\text{S}_2\text{O}_4$ expected in the present investigation) and the solu-

tion was stored under an inert atmosphere of N_2 gas. The concentration of sodium dithionite in the solution was determined by the Rubine-R method. The solution was then divided into three parts and their pH was adjusted to 0.8, 1.7 and 5.5 respectively. All these solutions were kept at room temperature ($20^\circ C$) and under a N_2 blanket to avoid oxidation of sodium dithionite.

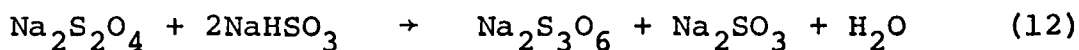
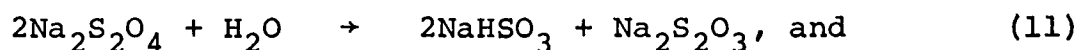
By taking samples from these solutions at different intervals of time and analyzing them for their sodium dithionite content by the Rubine-R method, it was concluded that the rate of homogeneous decomposition of sodium dithionite increased with decreasing pH. By varying the temperature of a sodium dithionite solution at a fixed pH, it was observed that the rate of homogeneous decomposition of sodium dithionite increased with increasing temperature. These conclusions agree with the information available in the literature (Section II.G.3.a). These experiments were not exhaustive enough to determine a quantitative expression for the rate of decomposition.

The following observation of some special significance was obtained from the above-mentioned experiments. No elemental sulfur was observed in any of the sodium dithionite solutions kept at $20^\circ C$ and pH's of 0.8, 1.7 and 5.5 even after 48 hours. This implies that the rate of auto-decomposition of sodium dithionite according to the equation,



in the pH range 0.8 to 5.5 is negligibly small.

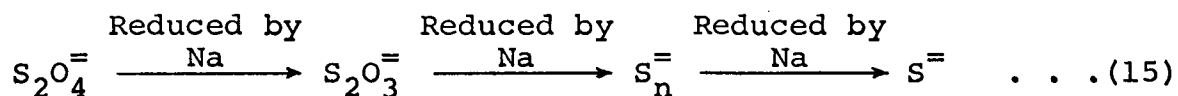
It was thought that, in the proposed investigation, the pH of the aqueous medium would not be less than 0.8 and the residence time of the product in the aqueous medium would not be more than an hour, hence, the auto-decomposition of dithionite could be neglected. Thus, only the following homogeneous decomposition reactions, outlined by Spencer (102), were considered to occur.



3. Presence of the heterogeneous decomposition of sodium dithionite

Approximately 50 ml of a 0.22% sodium-mercury amalgam was taken in a beaker. An approximately 5 ml sample of a 1% sodium dithionite solution in water was added to the amalgam sample and the contents in the beaker were stirred with a glass rod. After a short time H_2S gas was detected as one of the products by its distinctive smell. The gas was confirmed to be H_2S when it turned lead acetate paper black. The experiment was repeated with approximately 1 ml

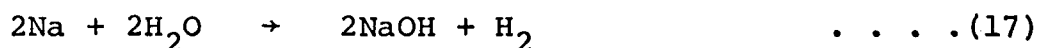
of the 0.22% amalgam and a large excess (approximately 200 ml) of the 1% $\text{Na}_2\text{S}_2\text{O}_4$ solution; no H_2S was detected. These results qualitatively agree with the reported (Section II.G.3.b) heterogeneous decomposition of sodium dithionite by sodium-mercury amalgam:



When the $\text{Na}/\text{Na}_2\text{S}_2\text{O}_4$ ratio was very high, the reduction of $\text{S}_2\text{O}_4^{\equiv}$ took place progressively and eventually S^{\equiv} ions were obtained which reacted with the H^+ ions present in the aqueous medium to give H_2S . On the other hand, when the $\text{Na}/\text{Na}_2\text{S}_2\text{O}_4$ ratio was very small, the reduction probably stopped after the first or the second step and, therefore, no S^{\equiv} ions were formed to produce H_2S .

4. Presence of the water reaction

In the batch experiments, at low Na/NaHSO_3 ratios and low pH's of the solution (pH 0.8 and 1.7), a gas evolving from the interface could be seen. This gas was not H_2S . Most probably it was hydrogen generated due to the water reaction (Section II.G.2)



At high Na/NaHSO₃ ratios, the water reaction probably also takes place.

5. Presence of the sodium dithionite oxidation reaction in an aqueous solution

Approximately 10 gms of reagent grade sodium dithionite salt was dissolved in 1 liter of oxygen-free distilled water and the solution was neutralized by sodium hydroxide to avoid acidic decomposition. This solution was stored under N₂ gas at 20°C. The Na₂S₂O₄ content of this solution was accurately determined by the Rubine-R method. A sample of the standard solution was taken in a beaker; the beaker was exposed to air and its contents were stirred with a glass rod. The concentration of Na₂S₂O₄ in the sample decreased with increasing time as has been reported in the literature (Section II.G.4).

B. Introduction to Experiments in the CFSTR

Nine process variables were identified for consideration. They were:

1. the concentration of sodium in the fresh amalgam,
2. the concentration of total sulfur dioxide in the aqueous feed solution,

3. the agitation in the aqueous phase,
4. the agitation in the amalgam phase,
5. the flow rate of the aqueous sulfur dioxide solution (residence time in the aqueous phase),
6. the flow rate of the sodium-mercury amalgam (residence time in the amalgam phase),
7. the interfacial-area/aqueous-volume ratio,
8. the temperature of the aqueous phase, and
9. the pH of the aqueous phase.

The effect of different process variables and their interactions on yields of sodium dithionite, based on total sulfur dioxide entering the reactor and on sodium consumed in the reactor could possibly be determined if a factorial design of experiments were done at least at five levels of each variable. This would amount to doing $(5)^9 = 1953125$ experimental runs. Since considerable time was required for preparing reagents and analyzing products for an experimental run, it was difficult to do more than four to five experimental runs a week. Doing all possible experiments would have taken an exceptionally long time, and many would not have produced reasonable dithionite yields or dithionite concentrations from the point of view of economics and use respectively. Therefore, the effects of process variables considered of primary importance and their interactions on the yields of sodium dithionite were investigated.

For all the experimental runs the depth of the

amalgam and the volume of the aqueous layer in the CFSTR were kept fixed. As a result of this arrangement, for the reactor of a specified geometry (Section IV.B.1), the volume of the aqueous layer was approximately 980 ml and the volume of the amalgam layer was about 96 ml.

It was mentioned in Section II.G. that probably none of the process reactions take place inside the amalgam phase. The sodium metal dissolved in mercury is transferred to the mercury/aqueous interface where the sodium dithionite formation reaction, the water reaction and the heterogeneous decomposition of sodium dithionite take place. A critical look at the list of the process variables showed that the effect of variables (4), (6) and (1) should have a similar effect on the rate of mass-transfer of sodium in the amalgam. In other words, an increase in the level of agitation in the amalgam phase by introducing a mechanical stirrer and baffles in that phase, at a fixed concentration of sodium in the fresh amalgam entering the reactor, should increase the rate of mass-transfer of sodium to the interface. Similarly, an increase in the volumetric flow rate of the fresh amalgam at a fixed concentration of sodium in fresh amalgam or an increase in the concentration of sodium in fresh amalgam at a fixed flow rate of fresh amalgam should also increase the rate of mass-transfer of sodium to the interface. Therefore, an increase in the level of any of these three variables should affect the yields of sodium dithionite in the same manner.

In the present investigation, the effect of the rate of mass-transfer of sodium to the interface on the yields of sodium dithionite was investigated primarily by changing the concentration of sodium in fresh amalgam and keeping the volumetric flow rate of the amalgam fixed. As mentioned in Section IV.B.1, to simplify the reactor design, no stirrer or baffles were provided in the amalgam phase. Due to a limited supply of mercury available for the experiments, the volumetric flow rate of the amalgam could not be changed significantly. In any case, it was hoped that by a systematic investigation of the other process variables, one could predict the effect of a variation in the level of agitation in the amalgam phase or the volumetric flow rate of the amalgam.

The effects of the remaining process variables on the yields of sodium dithionite are discussed in the following sections.

C. Definitions of Some Important Quantities which are Used for the Interpretation of Data

These quantities have been defined below. The mathematical expressions to calculate them and sample calculations have been presented in Appendix F.

1. Concentration of sodium dithionite in the product stream,

$$C_{S_2O_4} = \frac{(\text{gms of sodium dithionite})}{(100 \text{ ml of the product stream})}$$

2. Yield of sodium dithionite on total sulfur dioxide entering the reactor (%),

$$Y_{SO_2} = \frac{(\text{gm molar conc. of Na}_2\text{S}_2\text{O}_4 \text{ in product}) \times 2 \times 100}{(\text{gm molar conc. of total SO}_2 \text{ in aqueous feed})}$$

3. Yield of sodium dithionite on sodium entering the reactor with the fresh amalgam (%),

$$Y_{Na} = \frac{(\text{gm moles of Na}_2\text{S}_2\text{O}_4 \text{ in product/min}) \times 2 \times 100}{(\text{gm moles of Na entering with fresh amalgam/min})}$$

4. Yield of sodium dithionite on sodium consumed in the reactor (%),

$$CONNA = \frac{(\text{gm moles of Na}_2\text{S}_2\text{O}_4 \text{ in product/min}) \times 2 \times 100}{\left(\begin{array}{l} \text{gm moles of Na entering with fresh amalgam/min} \\ - \text{gm moles of Na leaving with spent amalgam/min} \end{array} \right)}$$

5. Conversion of sodium from the amalgam to different products in the reactor (%),

$$X_{\text{Na}} = \frac{\left(\begin{array}{l} \text{gm moles of Na entering with fresh amalgam/min} \\ - \text{gm moles of Na leaving with spent amalgam/min} \end{array} \right) \times 100}{\text{gm moles of Na entering with fresh amalgam/min}}$$

6. Na/SO₂ ratio entering the reactor,

$$= \frac{\text{gm moles of Na entering with fresh amalgam/min}}{\text{gm moles of total SO}_2 \text{ entering with aqueous feed/min}}$$

7. Rate of sodium consumption in the reactor,

$$= \begin{array}{l} \text{gm moles of Na entering with fresh amalgam/min} \\ - \text{gm moles of Na leaving with spent amalgam/min} \end{array}$$

For brevity, symbols were used for the different process variables in the following sections. These symbols along with their units have been described in Table 4.

TABLE 4
PROCESS VARIABLES AND THEIR UNITS

SYMBOLS	DESCRIPTION	UNITS
CHGF	Concentration of sodium in the fresh amalgam	gm of Na/100 gm of the fresh amalgam
STSO ₂	Concentration of total sulfur dioxide in the aqueous feed solution	gm mole/liter
(RPM) _{Aq}	Speed of the marine propeller in aqueous phase	revolutions/min
FLSO ₂	Flow rate of the aqueous sulfur dioxide solution	liter/min
FLHG	Flow rate of the sodium-mercury amalgam	ml/min
(A/V) _{Aq}	The interfacial-area/aqueous-volume ratio	cm ² /cm ³
TEMP	Temperature of the aqueous phase	degree centigrade
pH	pH of the aqueous phase	$-\log \left(\frac{\text{gm ions of H}^+}{\text{liter}} \right)$

D. Reproducibility of Experimental Runs in the CFSTR

Before a detailed experimental investigation could be started, it was decided to check the reproducibility of the experimental runs in the CFSTR. Unfortunately, the following problems made the task somewhat difficult.

The sodium-mercury amalgam for the experimental runs was prepared in a batch. It is explained in Appendix C why it was difficult to make an amalgam of a specified sodium-concentration starting with known quantities of mercury and sodium.

Generally, it took over an hour to obtain steady-state conditions during an experimental run. The supply of mercury was limited (≈ 7.5 liters), therefore, it was not convenient to do more than two experimental runs, at the flow rate of the fresh amalgam considered, under identical amalgam concentrations. The results obtained from only two experimental runs under identical levels of different process variables would not offer a very powerful statistical test for reproducibility. Hence, the following scheme was used.

A set of seven experimental runs (set: 47-57, expts. 47, 50, 52, 53, 54, 55 and 57) was performed under almost identical levels of different process variables except the concentration of sodium in the fresh amalgam which was varied in the range .0403% to .0932%. The experimental conditions for the set: 47-57 have been presented in Table 5.

From the observations made, the steady-state $C_{S_2O_4}$, Y_{SO_2} , Y_{Na} , CONNA and X_{Na} and their 95 per cent confidence limits were calculated for each experimental run. Sample calculations for these quantities in the experimental run 54 are shown in Appendix F.

For all the experimental runs in the set: 47-57, the steady-state $C_{S_2O_4}$, Y_{SO_2} , Y_{Na} , CONNA and X_{Na} were plotted against the Na/SO₂ ratio entering the reactor in each run. Thus, five smooth curves were drawn as shown in Figure 7. The 95 per cent confidence limits are not shown on the graphs. It is important to point out that the nature of the curves obtained by plotting steady-state $C_{S_2O_4}$, Y_{SO_2} , Y_{Na} , CONNA and X_{Na} against the concentrations of sodium in fresh amalgam would be similar because the molarity of the sulfur dioxide solution entering the reactor, STSO₂, during all of the experimental runs in this set was approximately the same. However, plotting these quantities against Na/SO₂ ratios offered certain advantages in the interpretation of data as discussed in later sections.

At a later date, another set of seven experimental runs (set: 65-77, expts. 65, 67, 69, 71, 73, 75 and 77) was performed using different batches of reagents for the analytical work. The levels of the process variables were nearly the same as for the set: 47-57, except that the concentration of sodium in fresh amalgam was varied in the range .0392 % to .1010 %. The experimental conditions for the set: 65-77 have

TABLE 5

LEVELS OF THE PROCESS VARIABLES IN SET: 47 - 57

Range of the Changed Variable	VALUES OF THE FIXED VARIABLES						
	STSO ₂	(RPM) _{Aq}	FLSO ₂	FLHG	(A/V) _{Aq}	TEMP	pH
.0403 - .0932	.639 -.656	673	.096	47.5	.0784	17	5.6 - 6.0

TABLE 6

LEVELS OF THE PROCESS VARIABLES IN SET: 65 - 77

Range of the Changed Variable	VALUES OF THE FIXED VARIABLES						
	STSO ₂	(RPM) _{Aq}	FLSO ₂	FLHG	(A/V) _{Aq}	TEMP	pH
.0392 - .1010	.650 -.658	673	.096	47.5	.0784	17	5.4 - 6.0

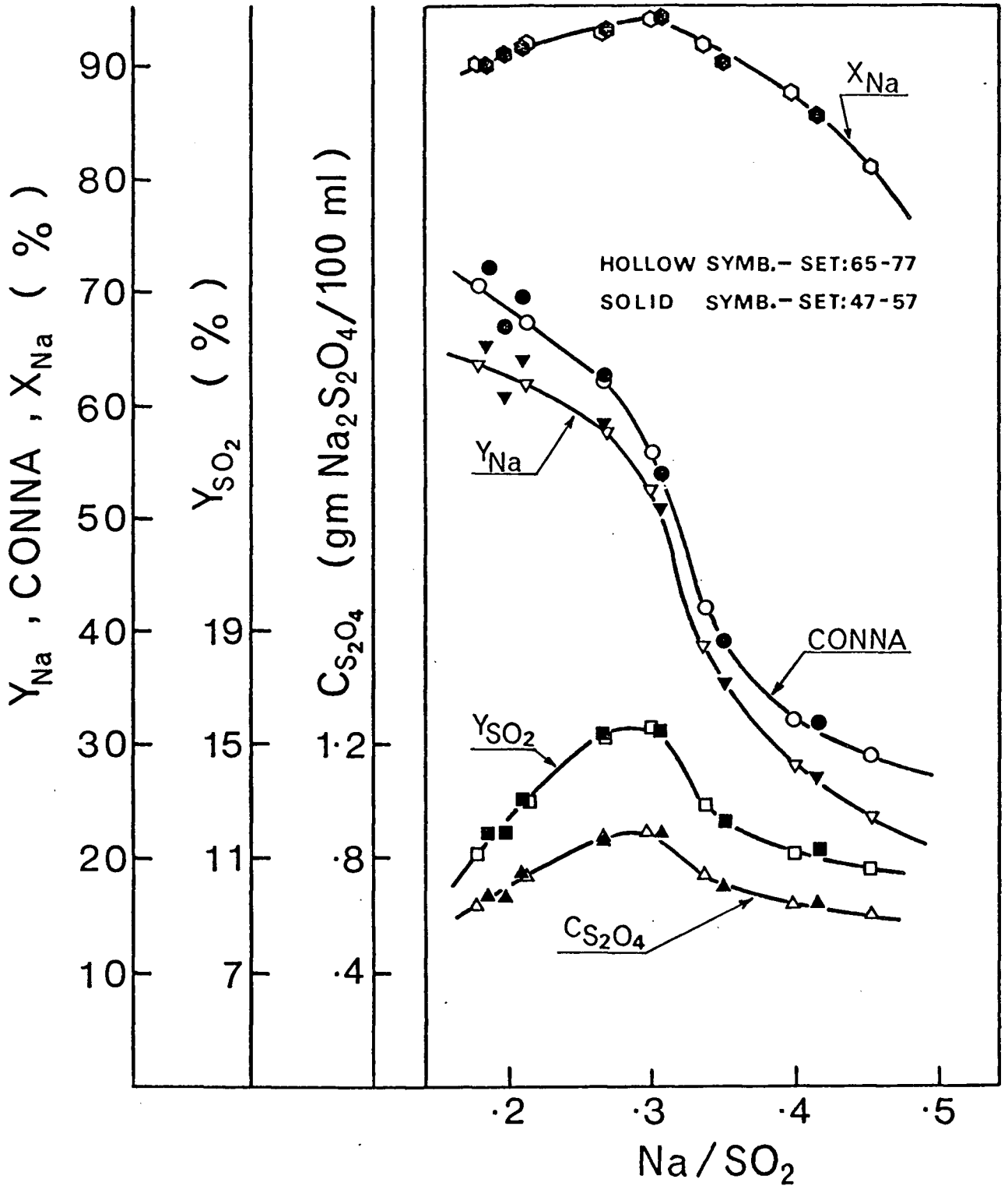


Figure 7 Reproducibility of the experimental runs in the CFSTR. See Tables 5 and 6 for the levels of the process variables

been presented in Table 6. Once again, the steady-state $C_{S_2O_4}$, Y_{SO_2} , Y_{Na} , CONNA and X_{Na} , calculated from the observations made for each experimental run, were plotted against their respective Na/SO₂ ratios and are shown in Figure 7.

Figure 7 shows that, within the 95 per cent confidence limits there is no significant difference between the steady-state $C_{S_2O_4}$, Y_{SO_2} , Y_{Na} , CONNA and X_{Na} curves for the two sets: 47-57 and 65-77. Furthermore, for two experimental runs, run 55 and 73, which were performed under almost identical conditions, it can be said with 95 per cent confidence that there is no significant difference between their respective steady-state $C_{S_2O_4}$, Y_{SO_2} , Y_{Na} , CONNA and X_{Na} values.

Further confirmation of the reproducibility of the experimental runs was provided by the results obtained from the set: 66-76 (expts. 66, 68, 70, 72, 74 and 76), set: 62-63 (expts. 62 and 63) and set: 87-91 (expts. 87, 89 and 91). These sets used different batches of the reagents for the analytical work but they basically differed from the sets: 47-57 and 65-77 in that the rpm of the propeller in the aqueous phase was decreased from 673 to 225. The experimental conditions for the sets: 66-76, 62-63 and 87-91 are presented in the Tables 7, 8 and 9 respectively and the results are shown in Figure 8.

TABLE 7

LEVELS OF THE PROCESS VARIABLES IN SET: 66 - 76

Range of the Changed Variable	VALUES OF THE FIXED VARIABLES						
	STSO ₂	(RPM) _{Aq}	FLSO ₂	FLHG	(A/V) _{Aq}	TEMP	pH
.0392 - .0892	.650 -.658	225	.096	47.5	.0784	17	5.35-5.95

TABLE 8

LEVELS OF THE PROCESS VARIABLES IN SET: 62 - 63

Range of the Changed Variable	VALUES OF THE FIXED VARIABLES						
	STSO ₂	(RPM) _{Aq}	FLSO ₂	FLHG	(A/V) _{Aq}	TEMP	pH
.0635 - .1012	.639 -.646	225	.096	47.5	.0784	17	5.7-6.15

TABLE 9

LEVELS OF THE PROCESS VARIABLES IN SET: 87 - 91

Range of the Changed Variable	VALUES OF THE FIXED VARIABLES						
	STSO ₂	(RPM) _{Aq}	FLSO ₂	FLHG	(A/V) _{Aq}	TEMP	pH
.0372 - .0986	.655 -.658	225	.096	47.5	.0784	17	5.35-5.85

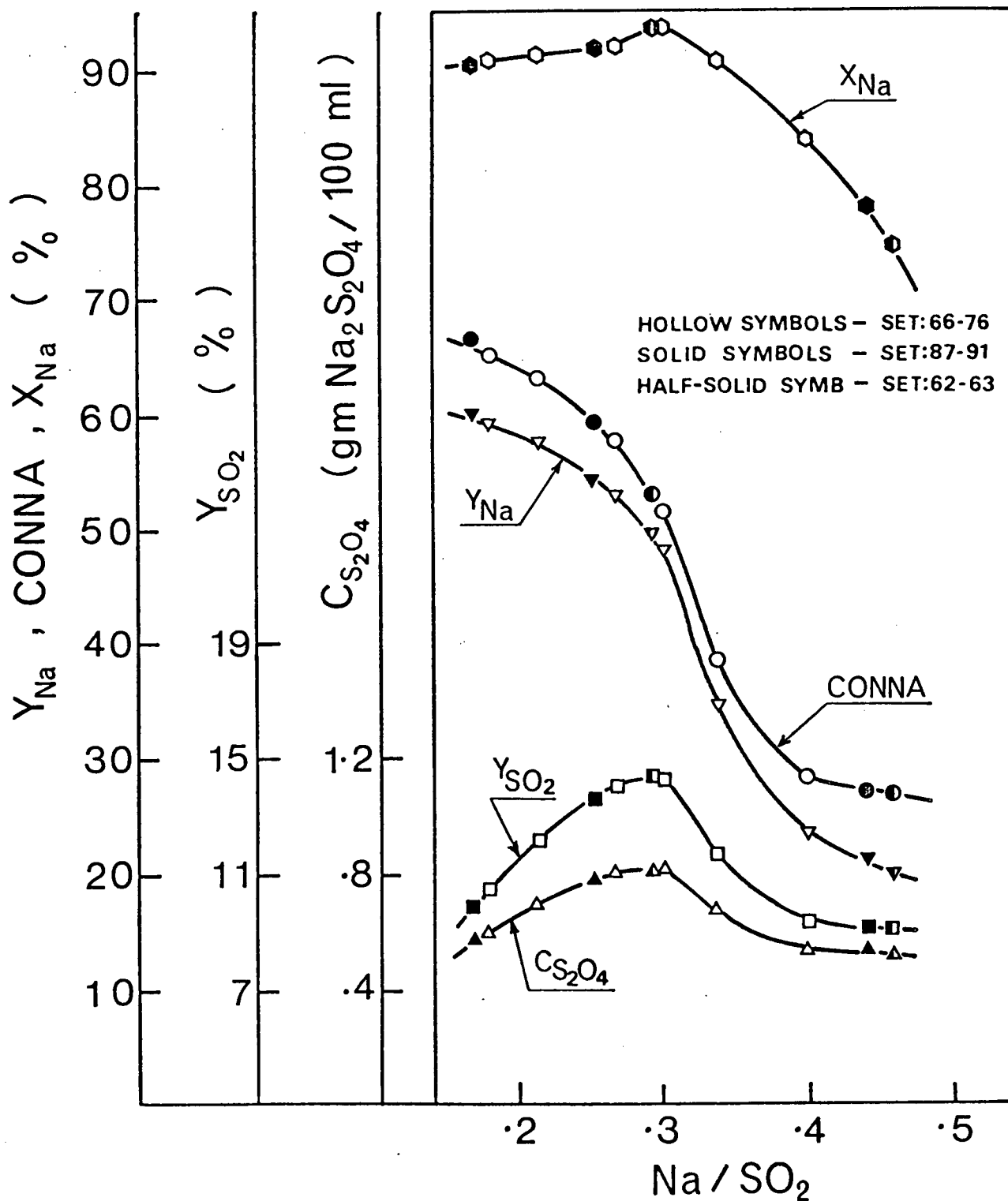


Figure 8 Reproducibility of the experimental runs in the CFSTR. See Tables 7, 8 and 9 for the levels of the process variables

E. Data from CFSTR Experiments

1. Concentration of sodium in fresh amalgam

The general plan of the work involved a set of experimental runs at various concentrations of sodium in fresh amalgam, and at chosen fixed levels of the other process variables. The effects of the concentration of sodium in fresh amalgam on the steady-state values of $C_{S_2O_4}$, Y_{SO_2} , Y_{Na} , CONNA and X_{Na} were determined at different levels of each variable. Generally, these calculated quantities were plotted against the Na/SO₂ ratios entering the reactor. These quantities were also plotted against the concentration of sodium in the fresh amalgam to obtain additional information. The nature of the curves obtained by plotting the steady-state $C_{S_2O_4}$, Y_{SO_2} , Y_{Na} , CONNA and X_{Na} against the Na/SO₂ ratios (or the concentration of sodium in the fresh amalgam) was found to be similar for different sets of the experimental runs.

During an experimental run, the unsteady-state concentration profiles of sodium dithionite in the product stream and sodium in the spent amalgam, as well as the pH of the aqueous phase, were also investigated. The effect of varying the concentration of sodium in fresh amalgam on the nature of these unsteady-state curves was also determined.

- (a) The variation of steady-state values of $C_{S_2O_4}$, Y_{SO_2} , Y_{Na} , CONNA and X_{Na} with change in the Na/SO₂ ratios entering the reactor

The experimental set: 65-77 may be considered a typical set of experimental runs where, as mentioned in Section V.D., the concentration of sodium in fresh amalgam was varied in the range .0392 % to .1010 %. The experimental conditions for this set are presented in Table 6.

Steady-state values of $C_{S_2O_4}$, Y_{SO_2} , Y_{Na} , CONNA and X_{Na} were plotted against Na/SO₂ ratios in Figure 9 and against the concentration of sodium in fresh amalgam in Figure 10. The curves in Figure 9 and 10 were similar because the molarity of sulfur dioxide solution entering the reactor during all of the experimental runs in this set was approximately the same.

- (i) The variation of steady-state sodium dithionite concentration in the product stream, $C_{S_2O_4}$, with change in Na/SO₂ ratios entering the reactor

Steady-state concentrations of sodium dithionite in the product stream are of considerable importance if this product stream is to be used for groundwood brightening. Figure 9 shows the effect on values of steady-state $C_{S_2O_4}$ caused by changing Na/SO₂ ratios. The concentration of sodium dithionite in the product stream increases with increasing Na/SO₂ ratios to a value of Na/SO₂ equal to 0.29.

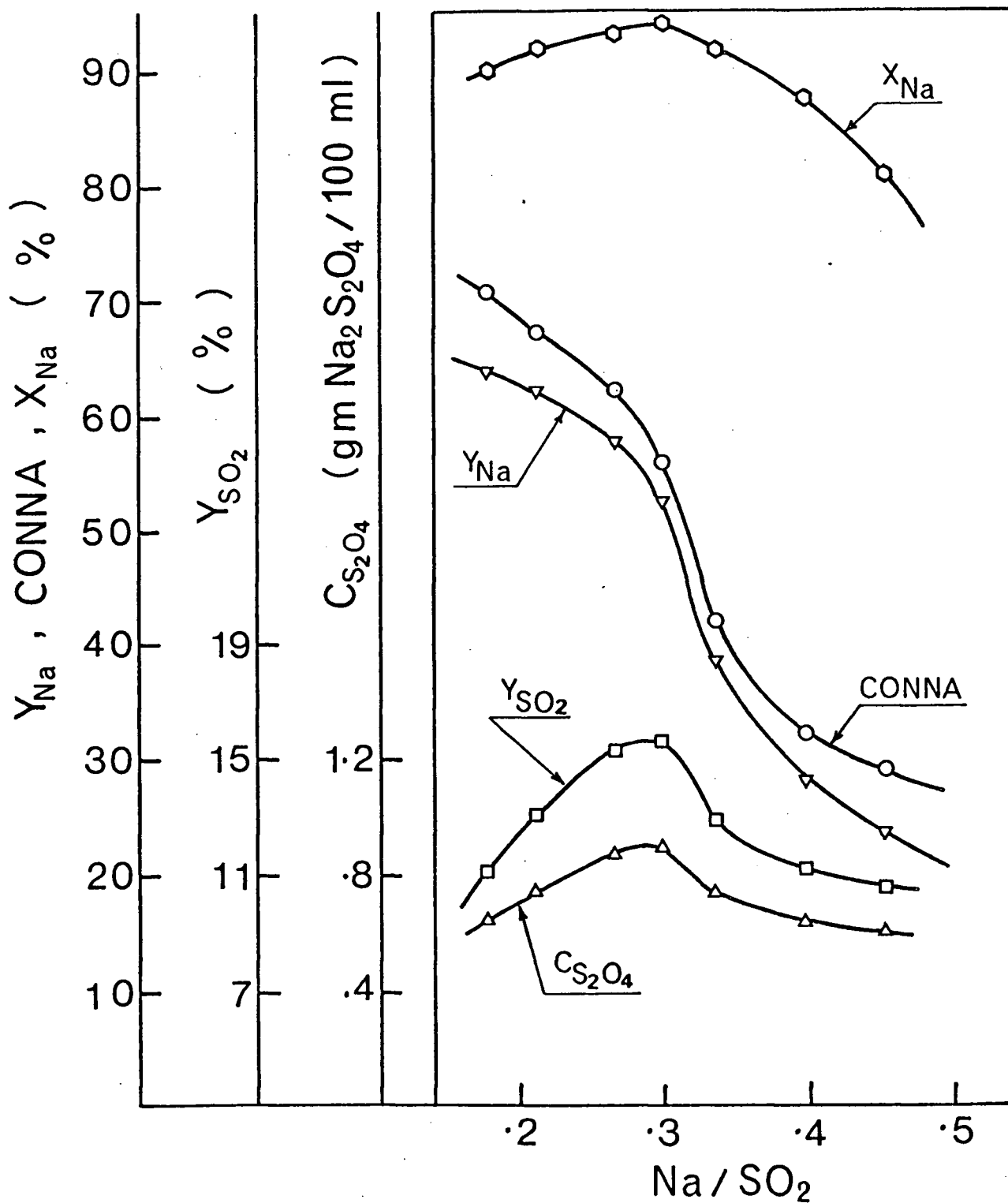


Figure 9 Steady-state values of sodium dithionite concentration and various yields versus Na/SO₂ ratios entering the CFSTR for the experimental set: 65-77. See Table 6 for the levels of the process variables

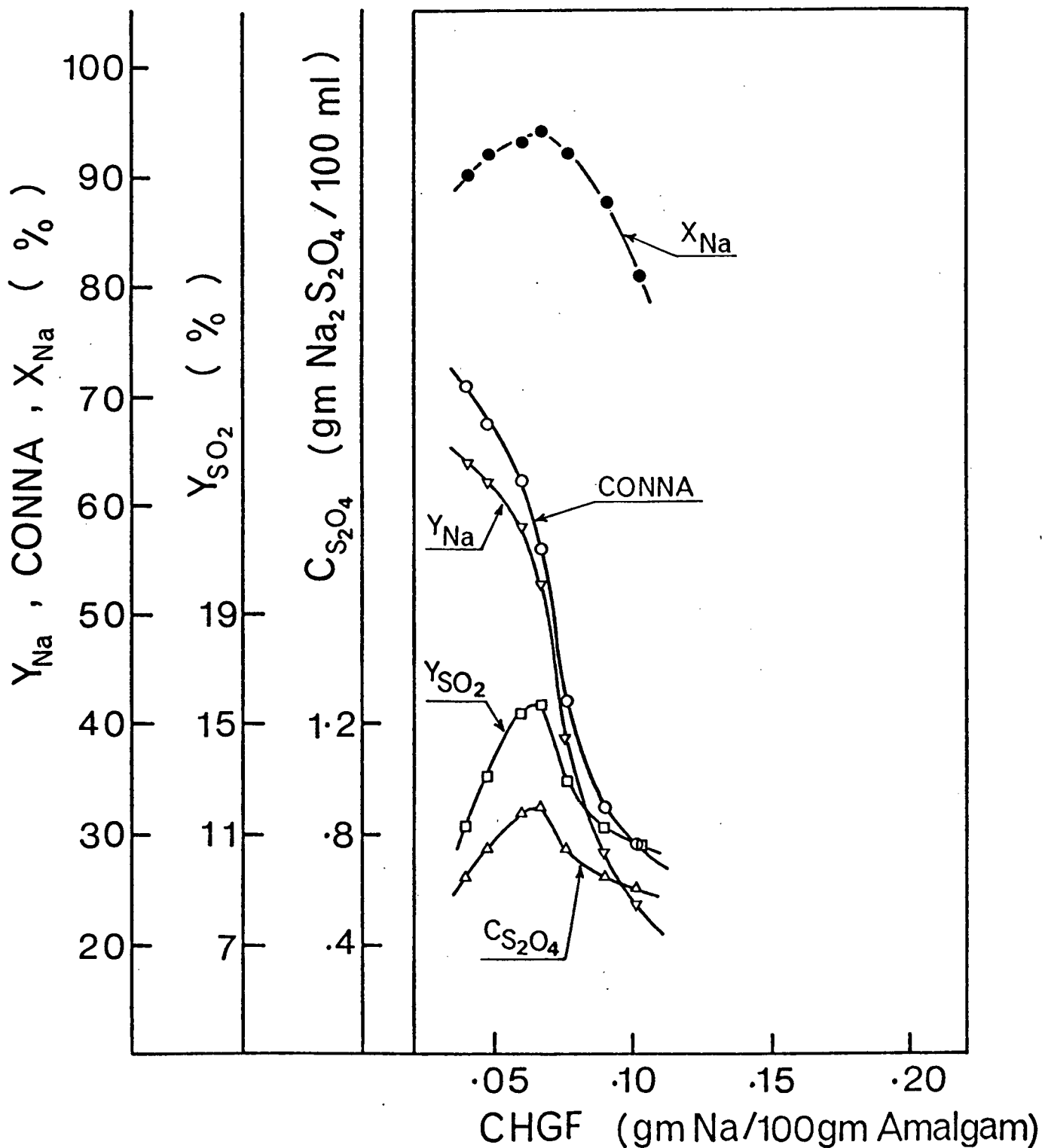


Figure 10 Steady-state values of sodium dithionite concentration and various yields versus concentrations of sodium in amalgam entering the CFSTR for the experimental set: 65-77. See Table 6 for the levels of the process variables

At this point, steady-state $C_{S_2O_4}$ reaches its maximum value of 0.9%. At values of the Na/SO₂ ratio greater than 0.29, the concentration of dithionite drops sharply; then levels off to decrease slowly with further increase in the Na/SO₂ ratio.

For the set: 65-77, a Na/SO₂ ratio of about 0.29 corresponds to a sodium concentration in fresh amalgam of .064% (molarity of sulfur dioxide in the aqueous solution was fixed at about 0.65 molar).

(ii) The variation of steady-state yield of sodium dithionite on total sulfur dioxide entering the reactor, Y_{SO_2} , with change in Na/SO₂ ratios entering the reactor

Figure 9 shows the effect of Na/SO₂ ratios on the yield of sodium dithionite calculated on sulfur dioxide. The values of steady-state Y_{SO_2} respond in a way similar to the steady-state concentration of sodium dithionite when the Na/SO₂ ratio is changed. Yield on sulfur dioxide reaches a maximum of 15.6% at the Na/SO₂ ratio of 0.29.

(iii) The variation of steady-state conversion of sodium (from the amalgam) to different products in the reactor, X_{Na} , with change in Na/SO₂ ratios entering the reactor

As shown in Figure 9, when the steady-state values of X_{Na} are plotted against the Na/SO₂ ratios entering the

reactor, a curve is obtained showing a maximum. A maximum conversion of 94% is obtained at a Na/SO₂ ratio of 0.29.

For the set: 65-77, the rate of sodium consumption by the aqueous phase (gm moles of sodium entering the reactor with fresh amalgam minus gm moles of sodium leaving the reactor with spent amalgam per minute) is plotted against the Na/SO₂ ratios in Figure 11 and against the concentration of sodium in fresh amalgam in Figure 12. These curves demonstrate that when the Na/SO₂ ratio entering the reactor or the concentration of sodium in fresh amalgam is increased, keeping the levels of all of the other process variables fixed, the rate of sodium removal from the amalgam phase increases. Figures 11 and 12 also show that at Na/SO₂ ratios below 0.29 corresponding to sodium concentration in fresh amalgam of less than .064%, the rate of sodium consumption is linearly related to the Na/SO₂ ratio entering the reactor or the concentration of sodium in fresh amalgam. However, at Na/SO₂ ratios above 0.29 the rate of sodium consumption is not linearly proportional to the Na/SO₂ ratios entering the reactor (Figure 11). A similar result is obtained at CHGF above .064% when the rate of sodium consumption is plotted against the concentration of sodium in fresh amalgam (Figure 12).

In Figure 12, when the curve is extrapolated to zero rate of sodium consumption, the line does not go through the origin. For the set: 65-77, it appears that upto

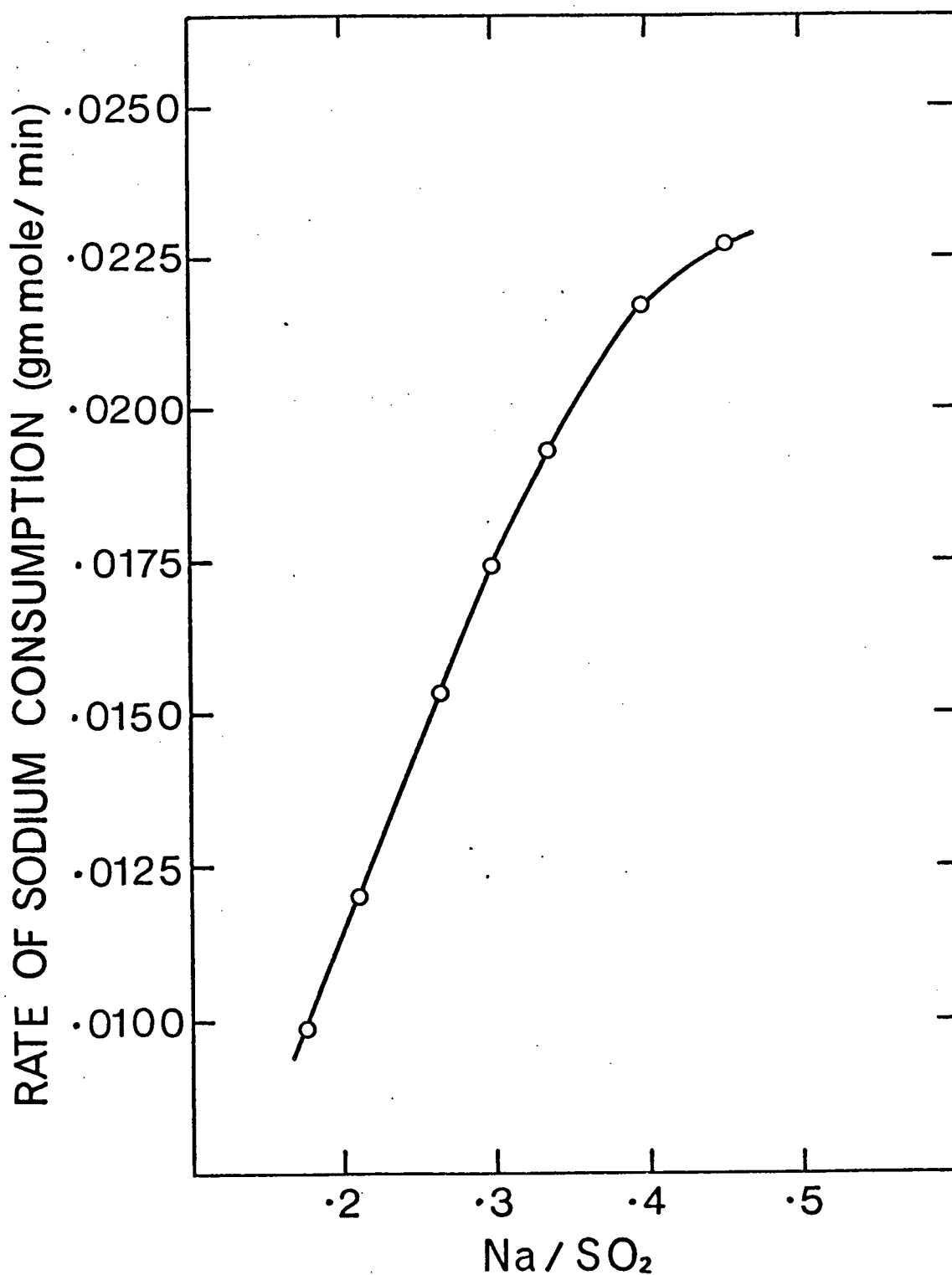


Figure 11 Rates of sodium consumption versus Na/SO₂ ratios entering the CFSTR for the experimental set: 65-77. See Table 6 for the levels of the process variables

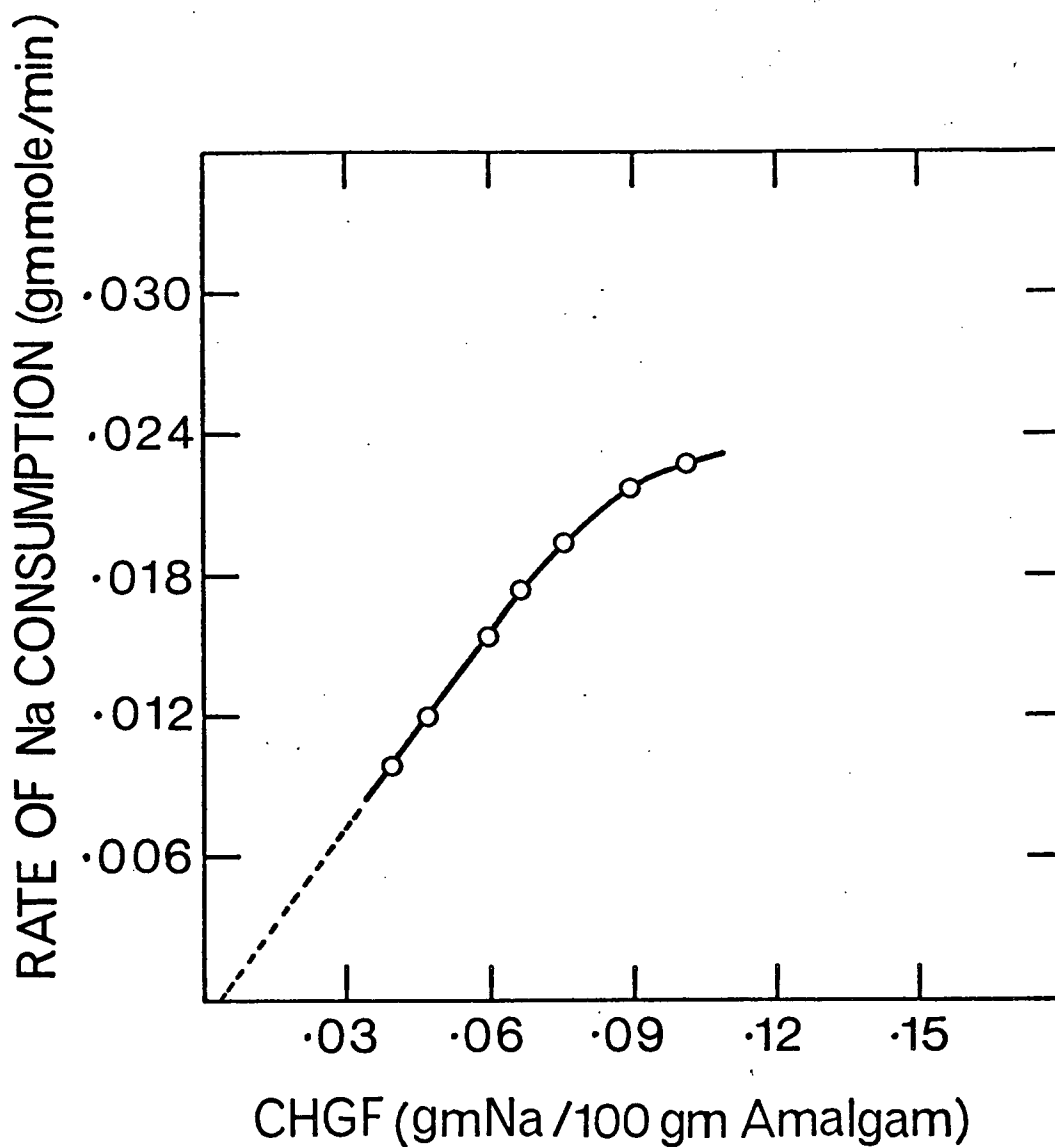


Figure 12 Rates of sodium consumption versus concentrations of sodium in amalgam entering the CFSTR for the experimental set: 65-77. See Table 6 for the levels of the process variables

approximately 0.0035% sodium in fresh amalgam, no sodium is consumed by any reaction. A few statistical calculations (95 per cent confidence limits) show that this deviation from the origin can be attributed neither to the errors in the analytical method nor to the calculation technique.

To further verify the above-mentioned phenomena, the rate of sodium consumption is plotted against the concentration of sodium in fresh amalgam for different sets of the experimental runs. For the sets: 95-105 (expts. 95,97,99,103 and 105), 23-28 (expts. 23,24,25,26,27 and 28), 65-77 (expts. 65,67,69,71,73,75 and 77) and 42-46 (expts. 42,43,44,45 and 46), the plots are shown in Figure 13 and the experimental conditions have been presented in Tables 10,11,6 and 12 respectively. Figure 13 shows that for each experimental set at values of CHGF below the steady-state sodium dithionite concentration maximum, the rate of sodium consumption is linearly related to the concentration of sodium in the fresh amalgam (CHGF). But at values of CHGF above the steady-state $\text{Na}_2\text{S}_2\text{O}_4$ concentration maximum, the rate of sodium consumption is not linearly proportional to the values of CHGF. Further, for none of the sets does the extrapolated line pass through the origin.

(iv) The variation of steady-state yield of sodium dithionite on sodium consumed in the reactor, CONNA, with change in Na/SO_2 ratios entering the reactor

TABLE 10

LEVELS OF THE PROCESS VARIABLES IN SET: 95-105

Range of the Changed Variable	VALUES OF THE FIXED VARIABLES						
	STSO ₂	(RPM) _{Aq}	FLSO ₂	FLHG	(A/V) _{Aq}	TEMP	pH
.0439 - .0912	.653 -.660	673	.198	47.5	.0784	17	5.20 - 5.65

TABLE 11

LEVELS OF THE PROCESS VARIABLES IN SET: 23-28

Range of the Changed Variable	VALUES OF THE FIXED VARIABLES						
	STSO ₂	(RPM) _{Aq}	FLSO ₂	FLHG	(A/V) _{Aq}	TEMP	pH
.0173 - .0544	.397 -.403	673	.096	47.5	.0784	17	5.2 - 5.9

TABLE 12

LEVELS OF THE PROCESS VARIABLES IN SET: 42-46

Range of the Changed Variable	VALUES OF THE FIXED VARIABLES						
	STSO ₂	(RPM) _{Aq}	FLSO ₂	FLHG	(A/V) _{Aq}	TEMP	pH
.0656 - .2127	1.270 -1.310	673	.096	47.5	.0784	17	5.0 - 5.75

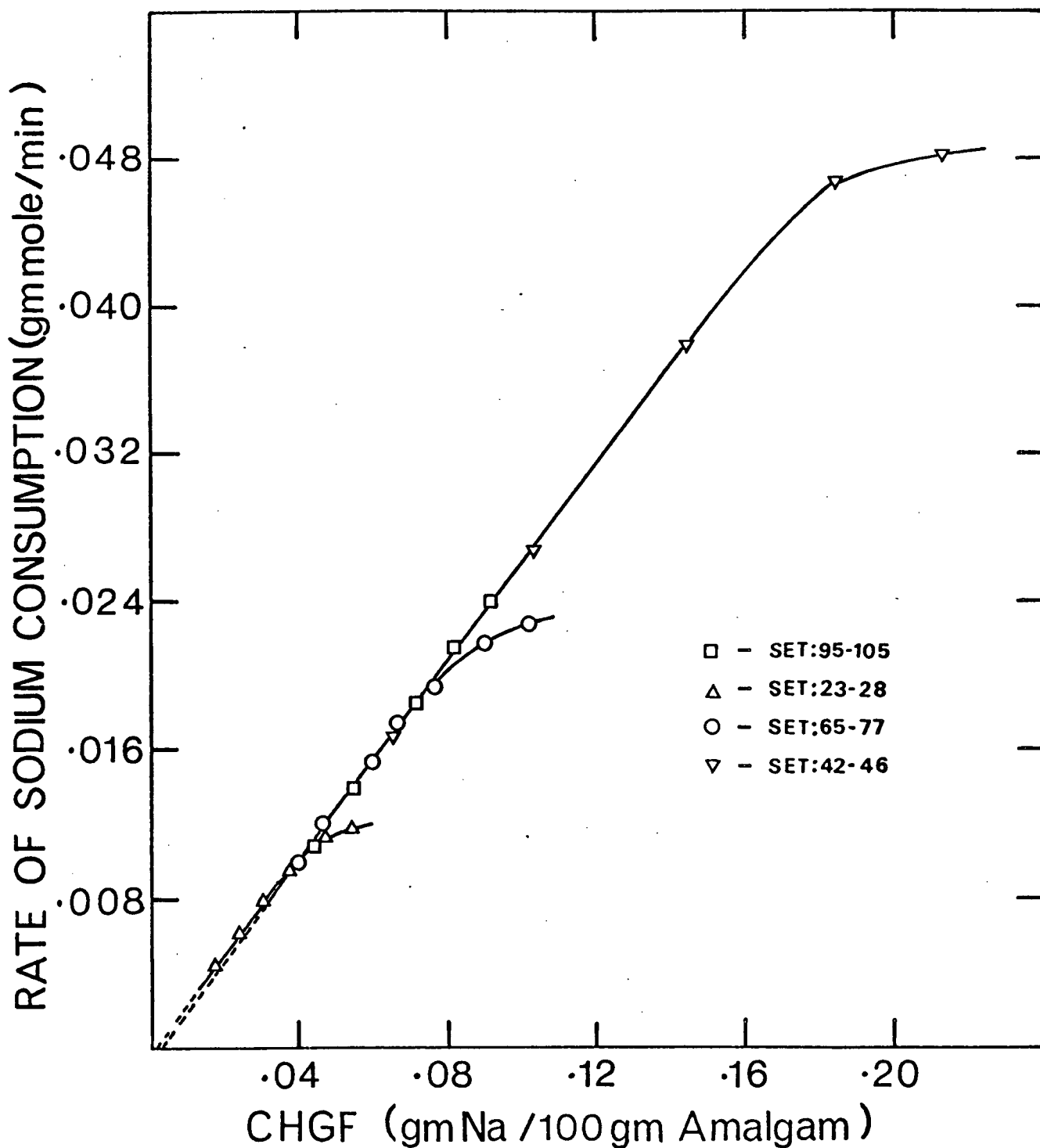


Figure 13 Rates of sodium consumption versus concentrations of sodium in amalgam entering the CFSTR for the experimental sets: 95-105, 23-28, 65-77 and 42-46. See Tables 6, 10, 11 and 12 for the levels of the process variables

When the steady-state CONNA values were plotted against the Na/SO_2 ratios for the set: 65-77, the curve shown in Figure 9 was obtained. This curve shows no maximum. The steady-state yield of sodium dithionite on sodium consumed in the reactor is about 71% at a Na/SO_2 ratio of .176 (smallest Na/SO_2 ratio for the experimental set: 65-77). The steady-state value of CONNA decreases gradually with increasing Na/SO_2 ratios to a value of Na/SO_2 equal to 0.29. At values of the Na/SO_2 ratio greater than 0.29, the yield of sodium dithionite on sodium consumed in the reactor drops sharply then levels off to decrease slowly with further increase in the Na/SO_2 ratio.

(v) The variation of steady-state yield of sodium dithionite on sodium entering the reactor with the fresh amalgam, Y_{Na} , with change in Na/SO_2 ratios entering the reactor

Figure 9 shows that the form of the curves obtained by plotting steady-state Y_{Na} versus Na/SO_2 ratios and steady-state CONNA versus Na/SO_2 ratios is similar; the latter having been discussed in the last section. However, at a fixed Na/SO_2 ratio entering the reactor the steady-state yield of sodium dithionite on sodium consumed in the reactor (CONNA) is always greater than the steady-state yield of sodium dithionite on sodium entering the reactor with fresh amalgam, Y_{Na} .

(b) The variation of unsteady-state concentration profiles with change in Na/SO_2 ratios entering the reactor

(i) Concentration of H^+ ions in the aqueous phase

For an experimental run, starting with sulfur dioxide in water at $\text{pH} = 3$ to 3.5 and the system in unsteady-state, the pH of the aqueous phase in the CFSTR increases and then attains a steady-state value in the range 5 to 6 .

Starting with an aqueous sulfur dioxide solution of a fixed concentration and pH , when the Na/SO_2 ratio entering the reactor is increased (or the concentration of sodium in fresh amalgam is increased), the steady-state pH of the aqueous phase in the reactor also increases.

(ii) Concentration of sodium dithionite in the product stream and concentration of sodium in spent amalgam

For the following presentation 'M' has been defined as the Na/SO_2 ratio, for a set of experimental runs, at which maximum steady-state concentration of sodium dithionite is obtained in the product stream.

The concentration of sodium dithionite in the product stream versus time curves for two typical sets, sets: 42-46 and 23-28, at various Na/SO_2 ratios entering the reactor are shown in Figures 14 and 16 respectively. The concentration of sodium in spent amalgam versus time curves for

these sets are shown in Figures 15 and 17 respectively. The levels of the different process variables, under steady-state conditions, for these sets (42-46, 23-28) have been presented in Tables 12 and 11 respectively.

At Na/SO_2 ratios less than M , for the experimental runs in various sets including the sets: 42-46 and 23-28 (Figures 14 and 16), the concentration of sodium dithionite in the product stream from the reactor increases with time and then attains a steady-state value. Figures 15 and 17 show that the concentration of sodium in the spent amalgam decreases and also attains a steady-state value. At Na/SO_2 ratios above M , as can be seen from Figures 14 to 17, transient maxima (for sodium dithionite) and minima (for sodium in spent amalgam) are observed in the unsteady-state concentration profiles. However, no such maximum in pH is observed on the pH versus time curves in this region.

A better understanding of this phenomenon is obtained by examining the curve for concentration of sodium dithionite in the product stream versus time (Figure 18) and the concentration of sodium in spent amalgam versus time curve (Figure 19) for the experimental runs in the set: 65-77. The steady-state experimental conditions for this set have been presented in Table 6. As mentioned earlier, for this set, $M = 0.29$.

The experimental run 69 was done at a Na/SO_2 ratio < 0.29 . The pH of the aqueous phase increased from 3.35 to 5.65 and as

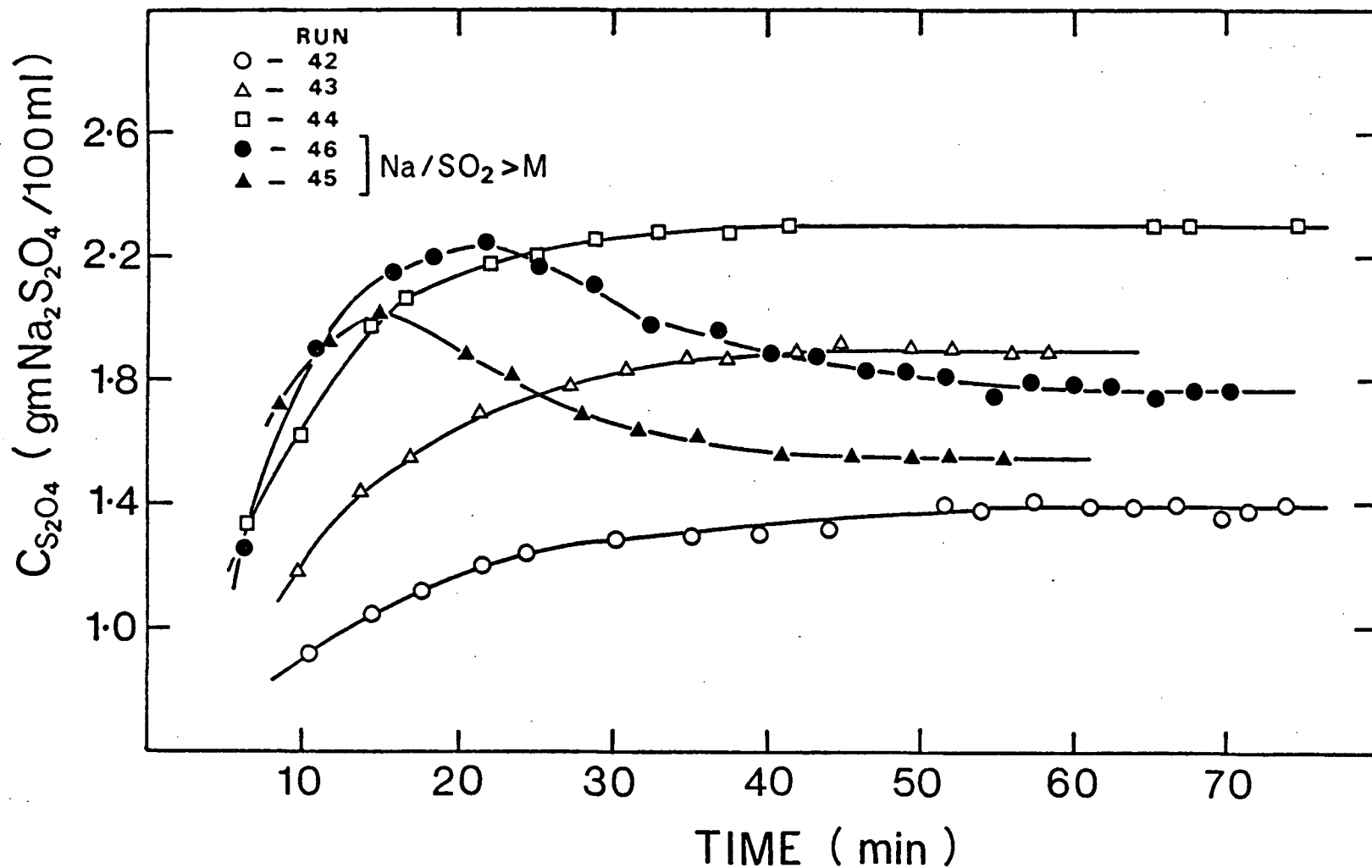


Figure 14 Concentrations of sodium dithionite in the product stream versus time for runs in the experimental set: 42-46. See Table 12 for the steady-state levels of the process variables. See Tables F-XV to F-XIX for the unsteady-state results

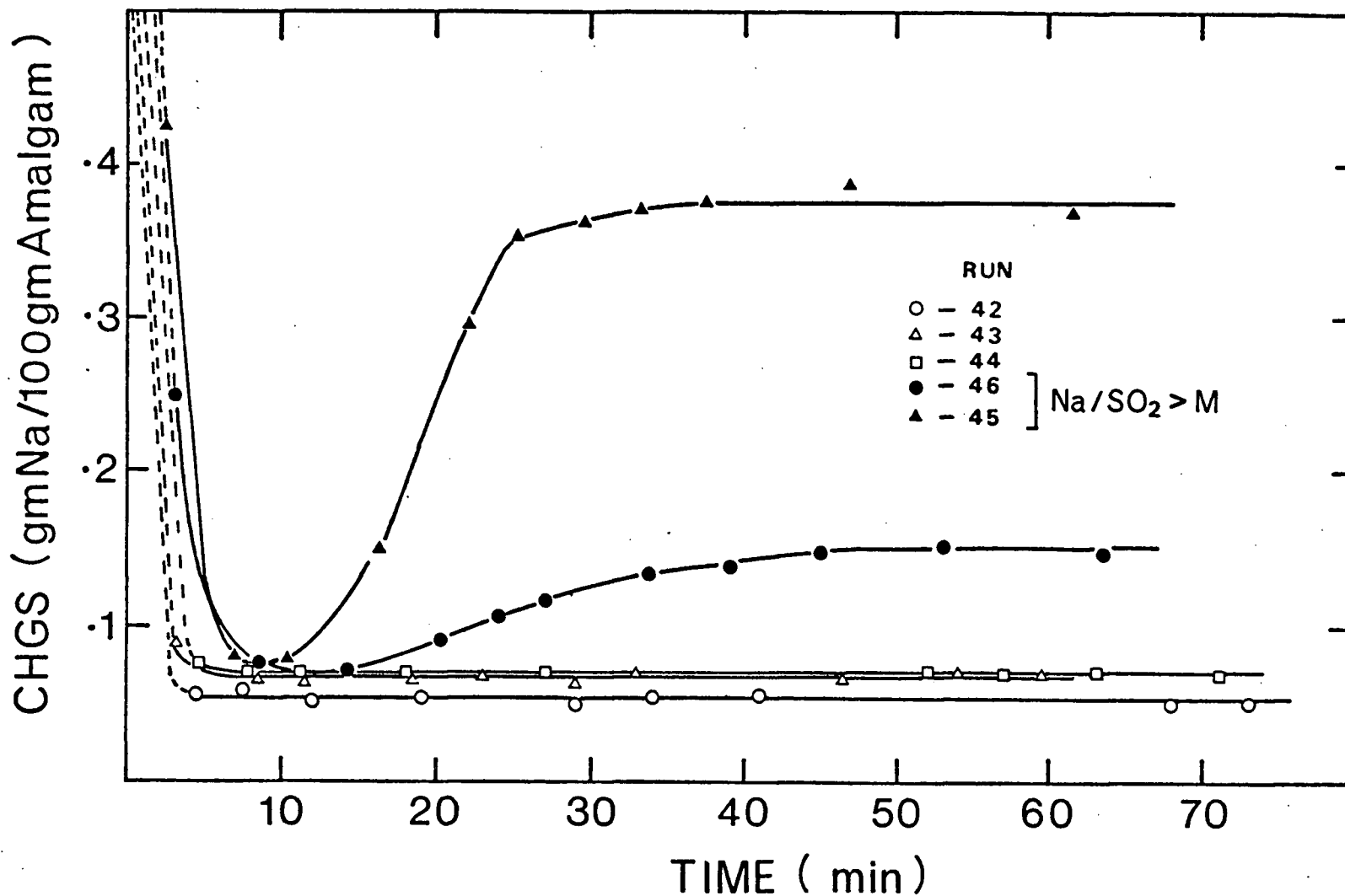


Figure 15 Concentrations of sodium in amalgam leaving the CFSTR versus time for runs in the experimental set: 42-46. See Table 12 for the steady-state levels of the process variables. See Tables F-XV to F-XIX for the unsteady-state results

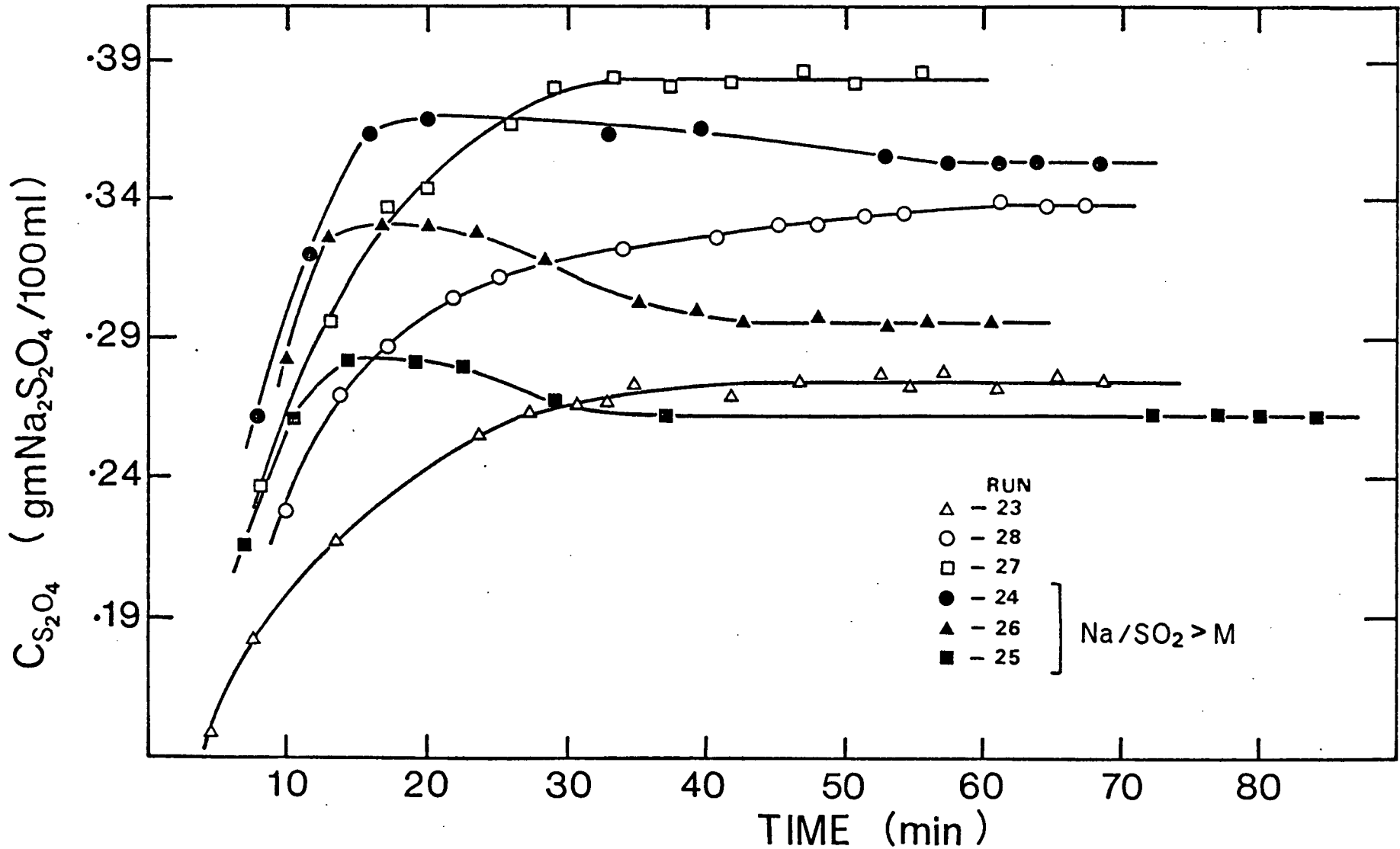


Figure 16 Concentrations of sodium dithionite in the product stream versus time for runs in the experimental set: 23-28. See Table 11 for the steady-state levels of the process variables. See Tables F-XX to F-XXV for the unsteady-state results

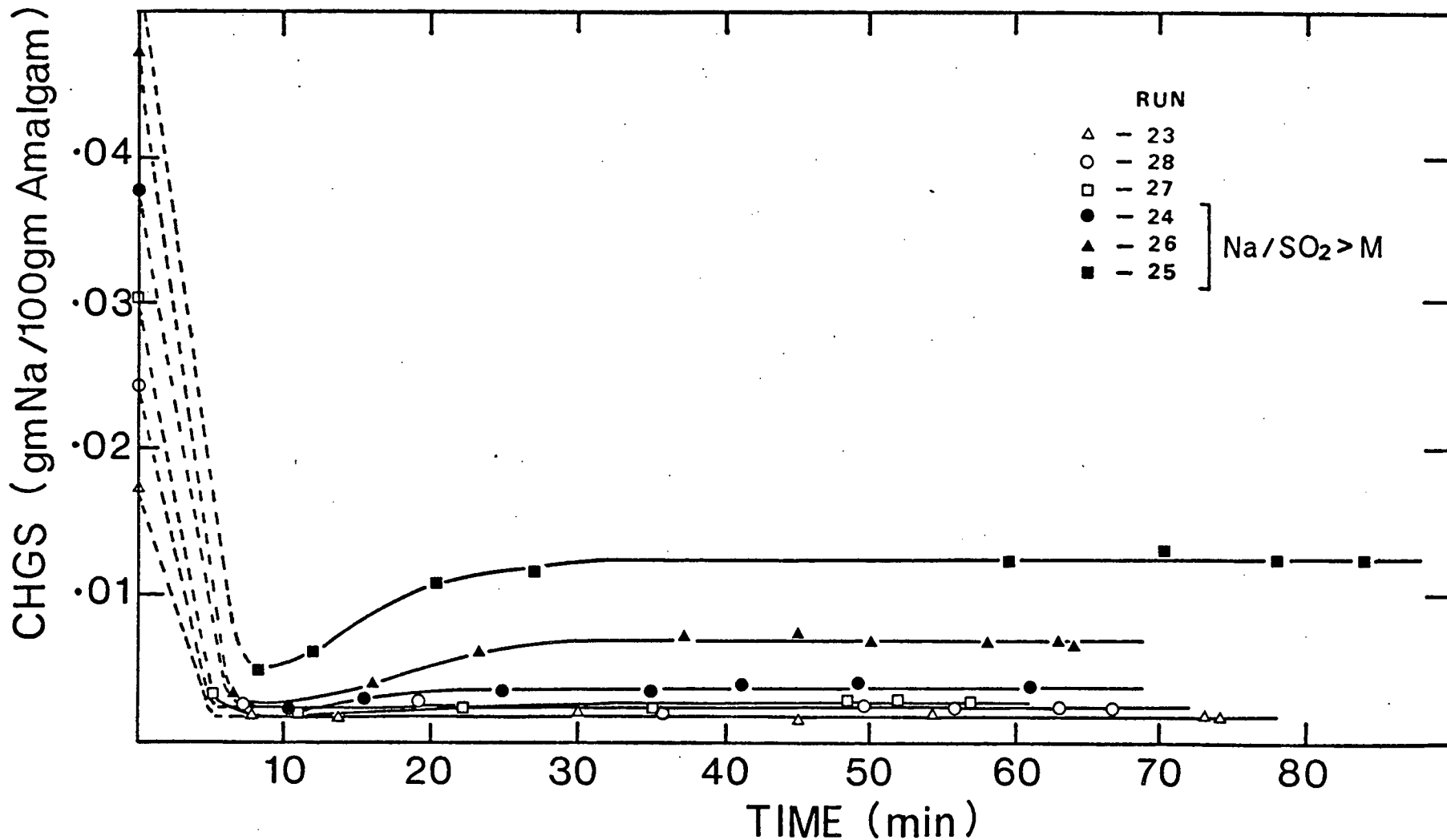


Figure 17 Concentrations of sodium in amalgam leaving the CFSTR versus time for runs in the experimental set: 23-28. See Table 11 for the steady-state levels of the process variables. See Tables F-XX to F-XXV for the unsteady-state results

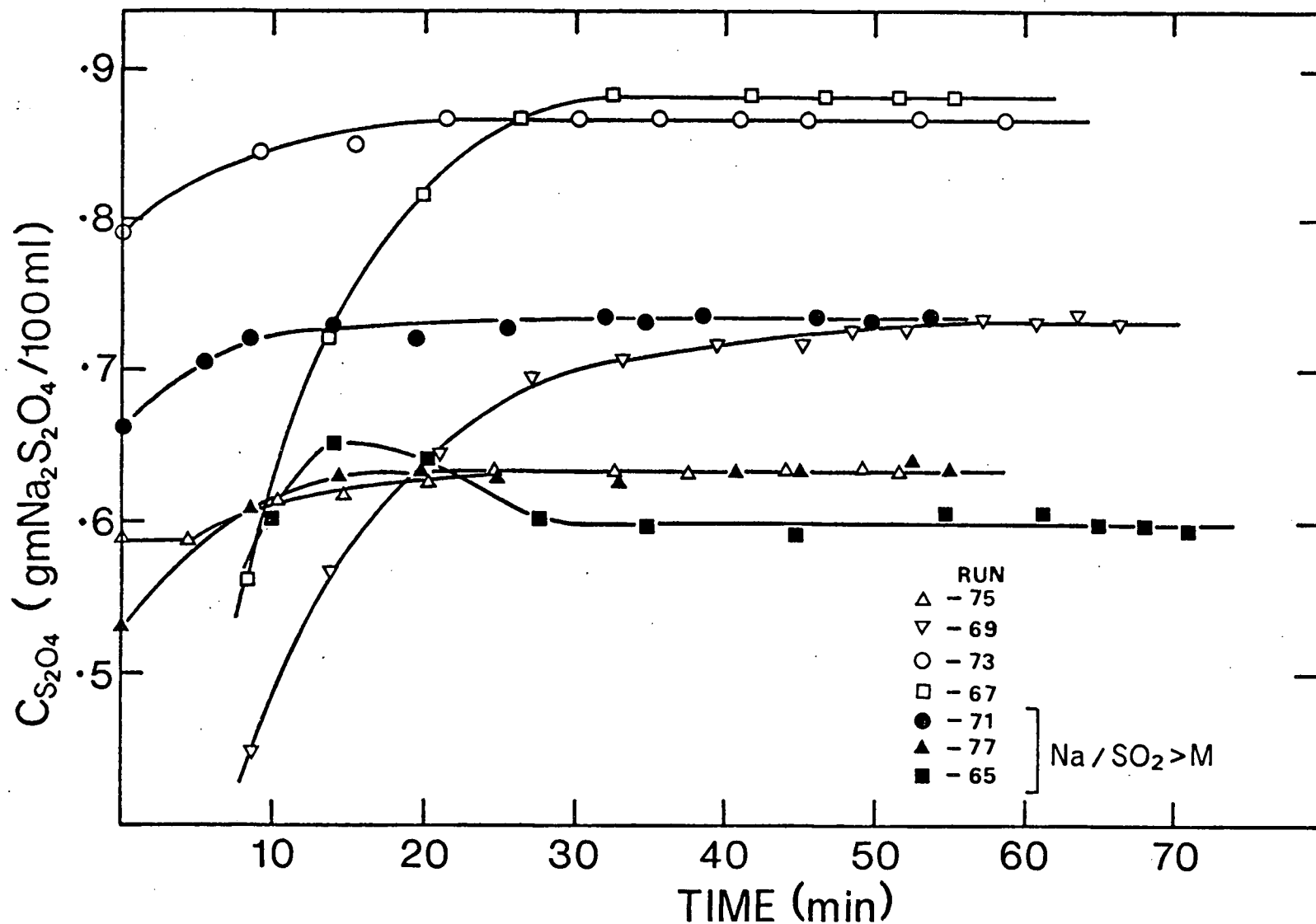


Figure 18 Concentrations of sodium dithionite in the product stream versus time for runs in the experimental set: 65-77. See Table 6 for the steady-state levels of the process variables. See Tables F-XXVI to F-XXXII for the unsteady-state results

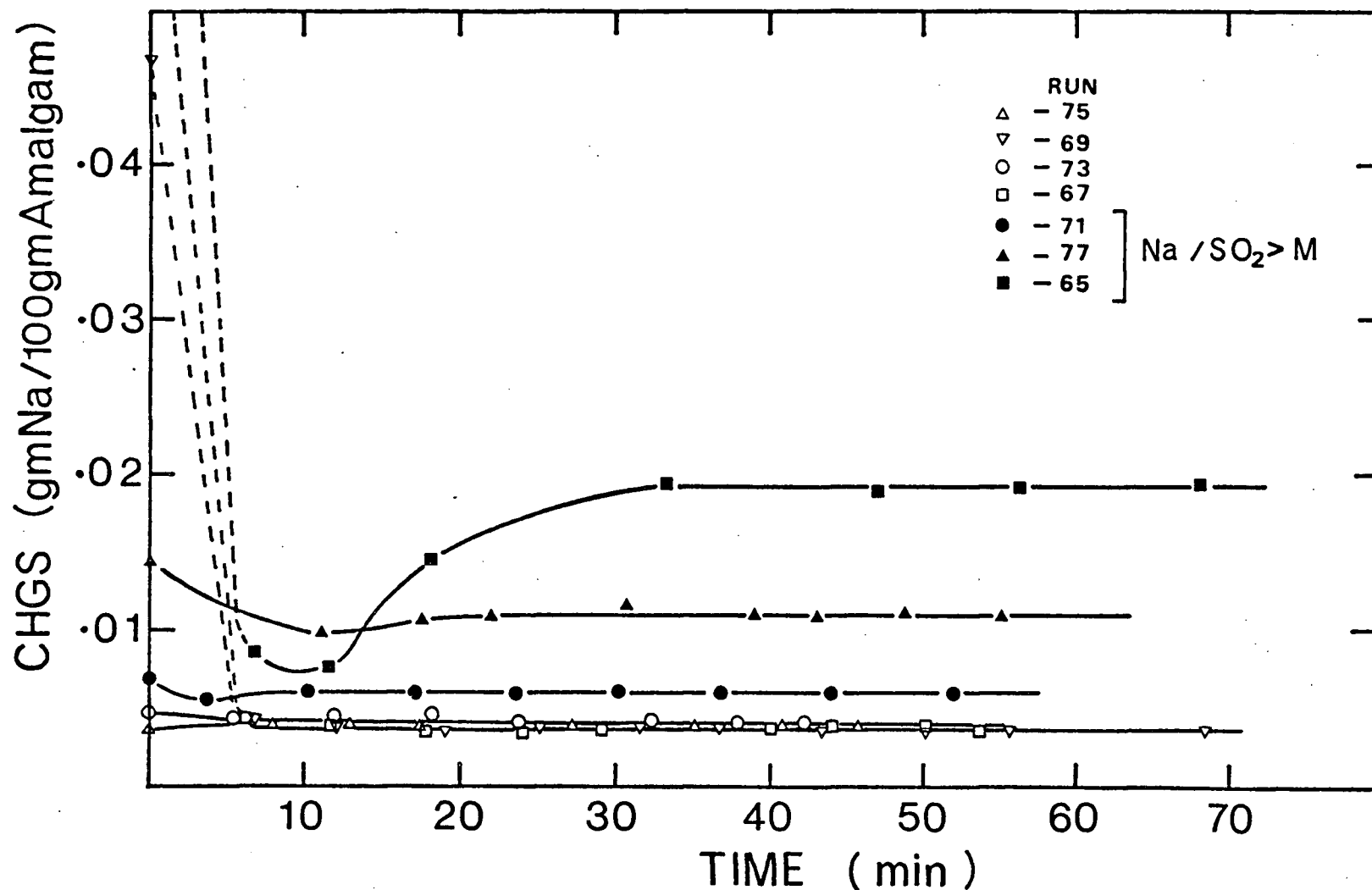


Figure 19 Concentrations of sodium in amalgam leaving the CFSTR versus time for runs in the experimental set: 65-77. See Table 6 for the steady-state levels of the process variables. See Tables F-XXVI to F-XXXII for the unsteady-state results

shown in Figures 18 and 19 no maximum nor minimum is observed in the unsteady-state curves. The experimental run 73 was also done at a Na/SO₂ ratio <0.29, however, the pH of the aqueous phase was fixed at about 5.8 during the unsteady-state as well as the steady-state periods. Again, no maximum nor minimum is observed in the unsteady-state concentration profiles (Figures 18 and 19).

The experimental run 65 was done at a Na/SO₂ ratio >0.29 and the pH of the aqueous phase increased from 3.53 to 6.0 at the steady-state. Figures 18 and 19 show that for this experimental run maximum and minimum are observed in the unsteady-state curves. The experimental runs 71 and 77 were also done at Na/SO₂ ratios >0.29, however, the pH of the aqueous phase was fixed at about 5.9 under the unsteady-state and the steady-state conditions. In these experimental runs, no maxima nor minima are observed in the unsteady-state concentration profiles (Figures 18 and 19).

2. Concentration of "total" sulfur dioxide in the aqueous feed solution

To investigate the effect of variation in the concentration of total sulfur dioxide in the aqueous feed solution on the steady-state $C_{S_2O_4}$, Y_{SO_2} , Y_{Na} , CONNA and X_{Na} at different Na/SO₂ ratios entering the reactor, sets: 23-28, 65-77 and 42-46 were performed. The concentration of total

sulfur dioxide in these sets was about 0.4 molar, 0.65 molar and 1.30 molar respectively. The levels of the other process variables for these sets, under steady-state conditions, are presented in Tables 11, 6 and 12 respectively. The steady-state $C_{S_2O_4}$, Y_{SO_2} , Y_{Na} , CONNA and X_{Na} , for the sets: 23-28, 65-77 and 42-46, are plotted against the Na/SO₂ ratios entering the reactor in Figures 20, 9 and 21 respectively.

(a) The variation of steady-state sodium dithionite concentration in the product stream, $C_{S_2O_4}$, with change in the concentration of sulfur dioxide in the aqueous feed solution

Figure 22 shows that the nature of the curves obtained by plotting the steady-state concentration of sodium dithionite in the product stream against the Na/SO₂ ratios entering the reactor for sets: 23-28 and 42-46 was the same as for the set: 65-77, which has been discussed in Section V.E.1.a.i.

Figure 22 also shows that at a fixed Na/SO₂ ratio, when all of the other process variables are kept constant, an increase in the concentration of total sulfur dioxide in the aqueous feed solution increases the steady-state concentration of sodium dithionite in the product stream.

As the concentration of sulfur dioxide in the aqueous feed for all of the experimental runs in each set was fixed, the steady-state $C_{S_2O_4}$ is plotted against the concentration of sodium in fresh amalgam, CHGF, for the sets: 23-28, 65-77

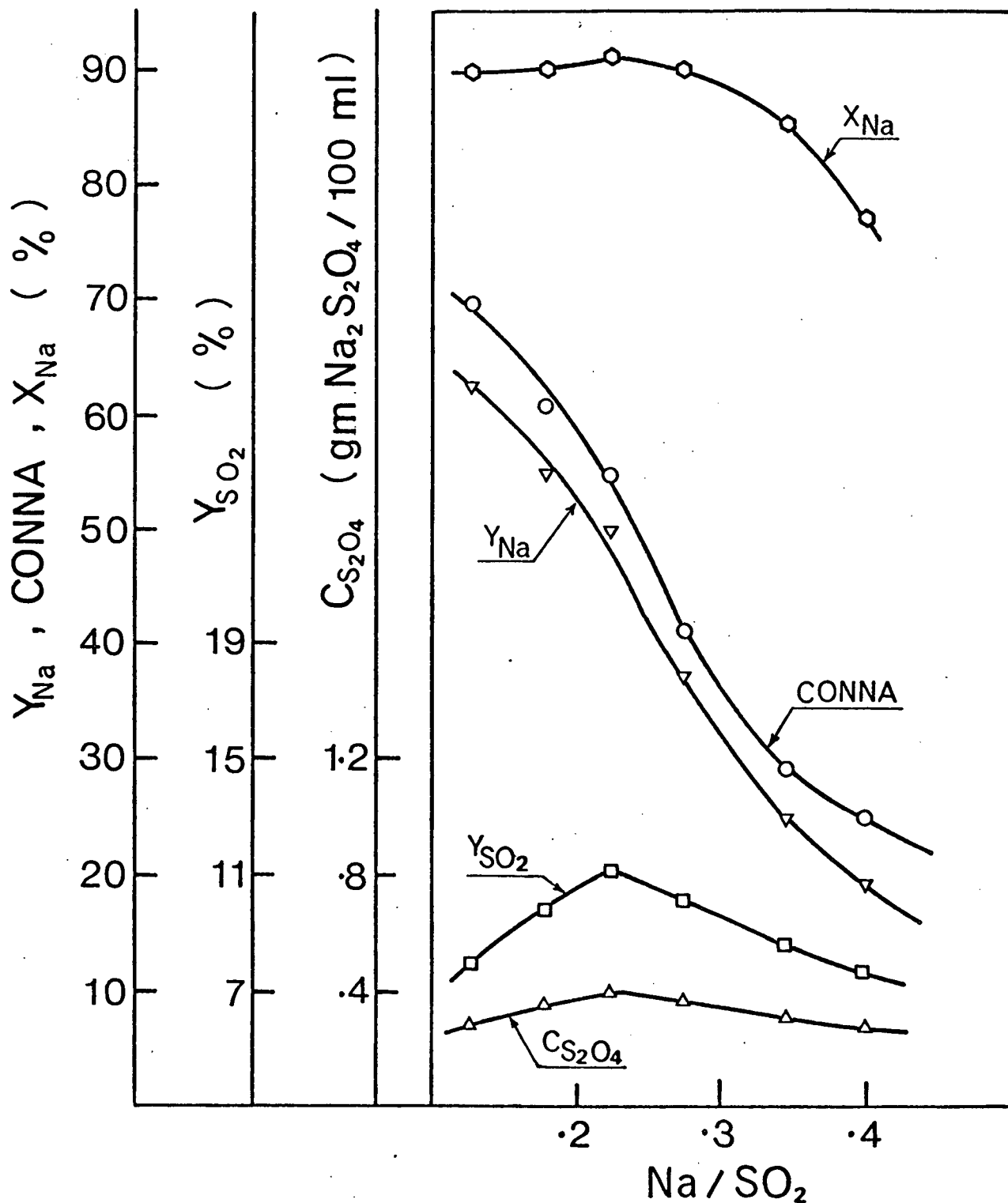


Figure 20 Steady-state values of sodium dithionite concentration and various yields versus Na/SO₂ ratio entering the CFSTR for the experimental set: 23-28. See Table 11 for the levels of the process variables

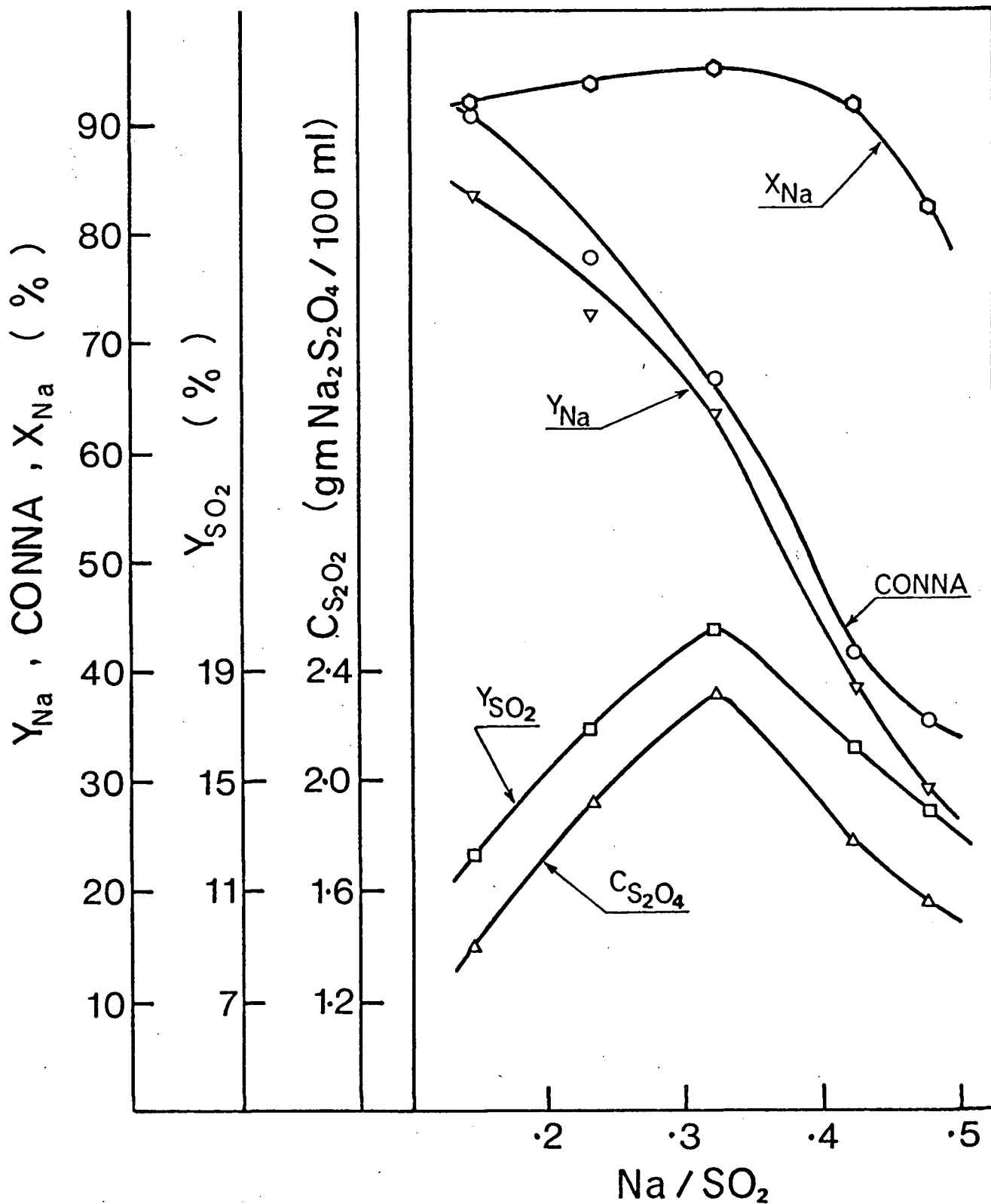


Figure 21 Steady-state values of sodium dithionite concentration and various yields versus Na/SO₂ ratio entering the CFSTR for the experimental set: 42-46. See Table 12 for the levels of the process variables

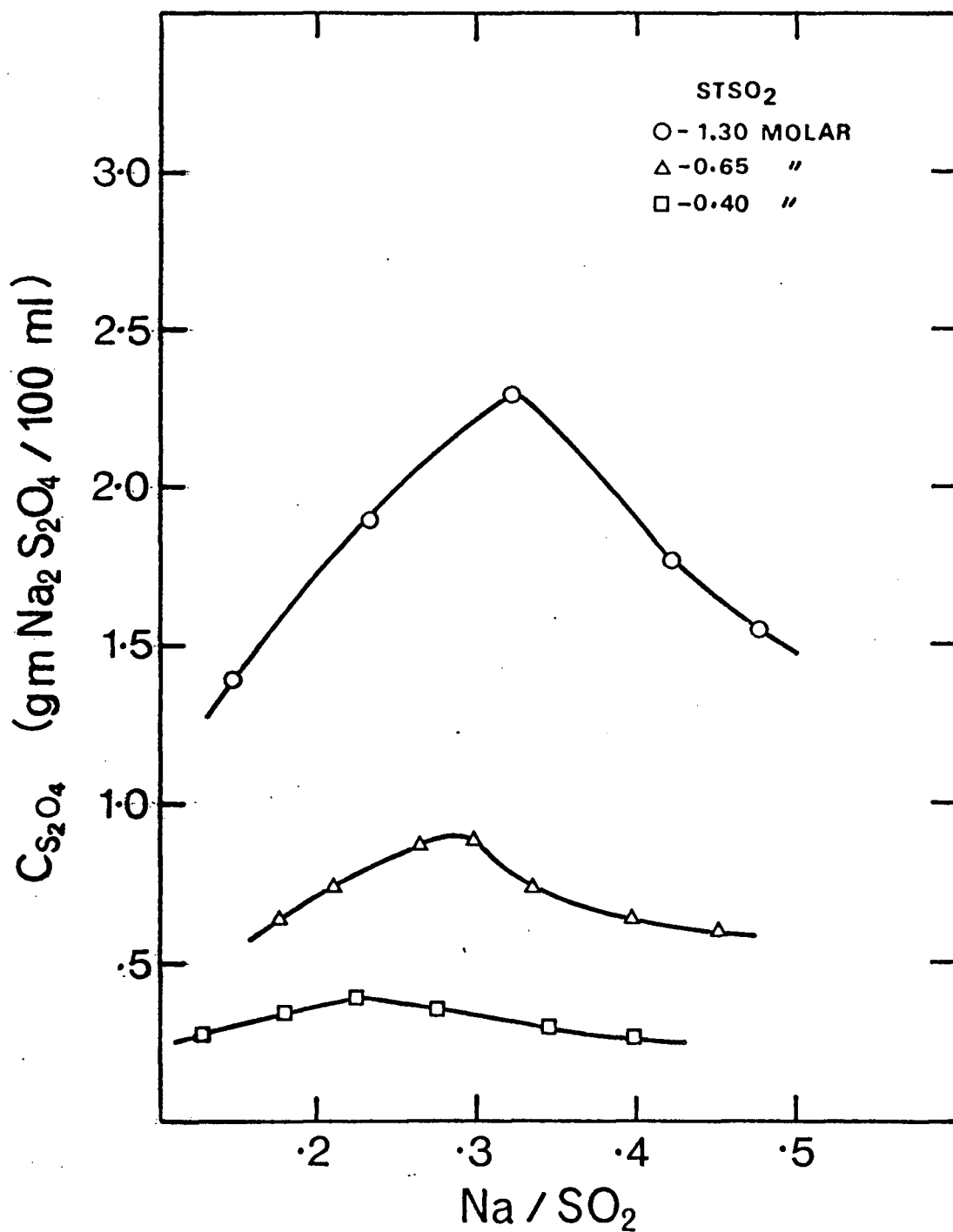


Figure 22 Steady-state sodium dithionite concentrations versus Na/SO₂ ratios entering the CFSTR at different concentrations of sulfur dioxide in the aqueous feed. See Tables 6, 11 and 12 for the levels of the process variables

and 42-46. These curves are shown in Figure 23. For the sets: 23-28, 65-77 and 42-46, the maximum steady-state concentration of sodium dithionite in the product stream is 0.385%, 0.89% and 2.3% at the CHGF values of 0.0303%, 0.064% and 0.1439% respectively. For the following presentation, the concentration of sodium in fresh amalgam at which the maximum steady-state concentration of sodium dithionite was produced for a set of experimental runs, is called $\text{CHGF}_{\text{critical}}$. Therefore, the $\text{CHGF}_{\text{critical}}$ for the sets: 23-28, 65-77 and 42-46 are 0.0303%, 0.064% and 0.1439% respectively.

The $\text{CHGF}_{\text{critical}}$ is found to be linearly related to the molarity of sulfur dioxide in the aqueous feed as shown in Figure 24. The correlation shown in Figure 24 could be very useful from the practical point of view. If the concentration of sulfur dioxide in the aqueous feed solution is known, the concentration of sodium in the fresh amalgam at which the maximum concentration of sodium dithionite would be obtained, can be determined.

(b) The variation of steady-state values of Y_{SO_2} , Y_{Na} , CONNA and X_{Na} with change in the concentration of sulfur dioxide in the aqueous feed solution

The trend of the steady-state Y_{SO_2} versus Na/SO_2 , Y_{Na} versus Na/SO_2 , CONNA versus Na/SO_2 and X_{Na} versus Na/SO_2 curves for the sets: 23-28 and 42-46 is the same as that of the corresponding curves for the set: 65-77. These

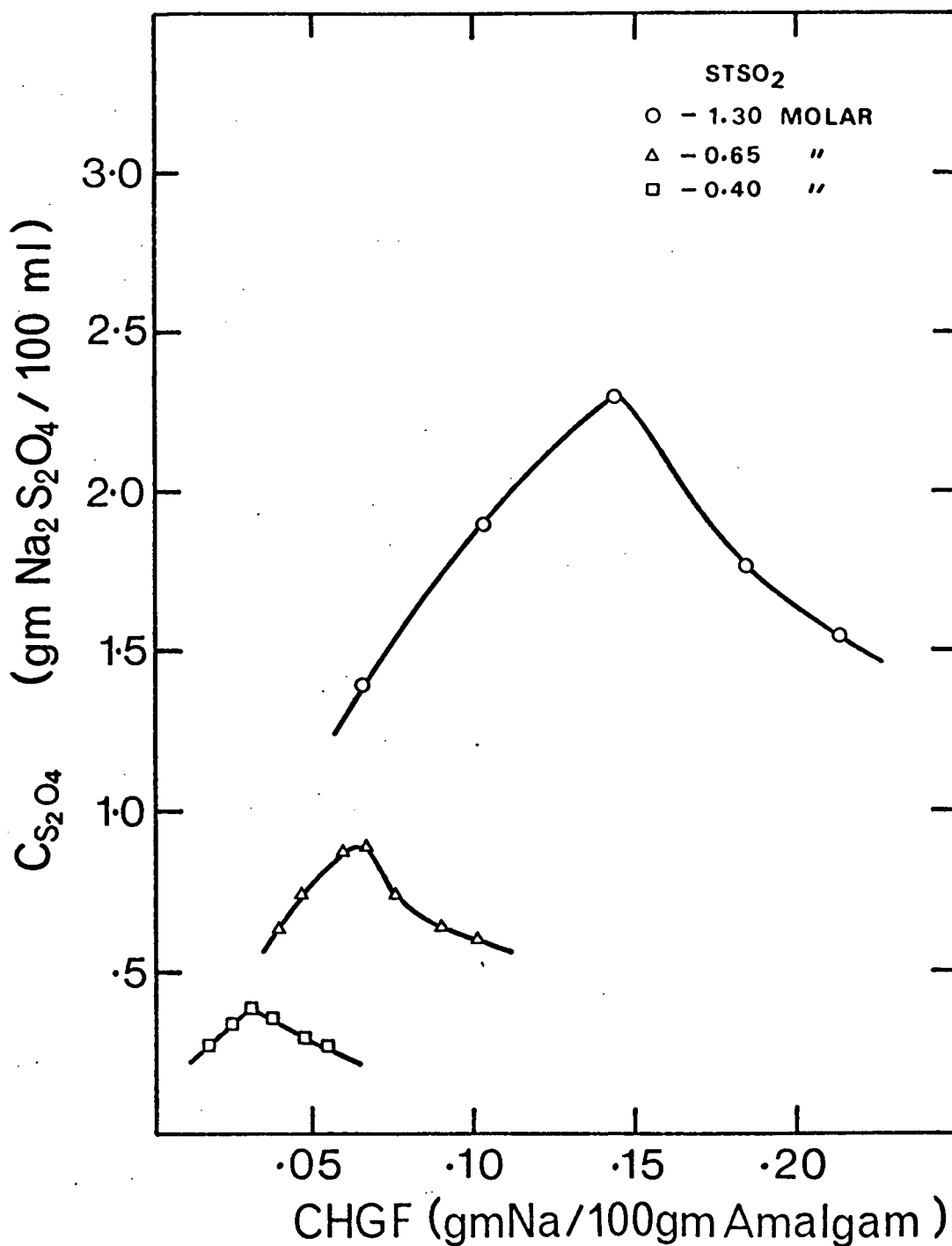


Figure 23 Steady-state sodium dithionite concentrations versus concentrations of sodium in amalgam entering the CFSTR at different concentrations of sulfur dioxide in the aqueous feed. See Tables 6, 11 and 12 for the levels of the process variables

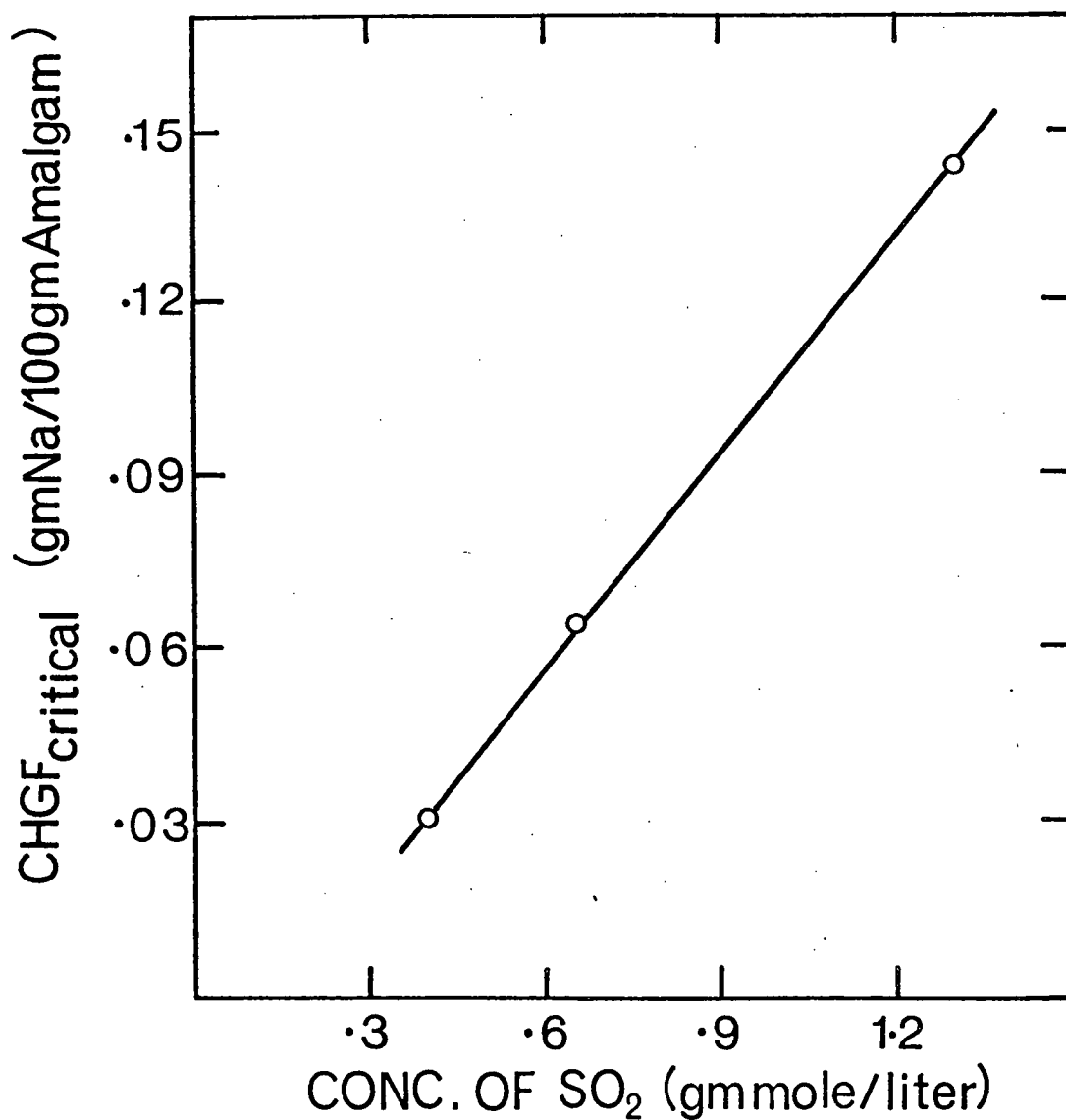


Figure 24 Critical concentrations of sodium in amalgam entering the CFSTR versus molarity of sulfur dioxide in the aqueous solutions entering the CFSTR. See Tables 6, 11 and 12 for the levels of the process variables

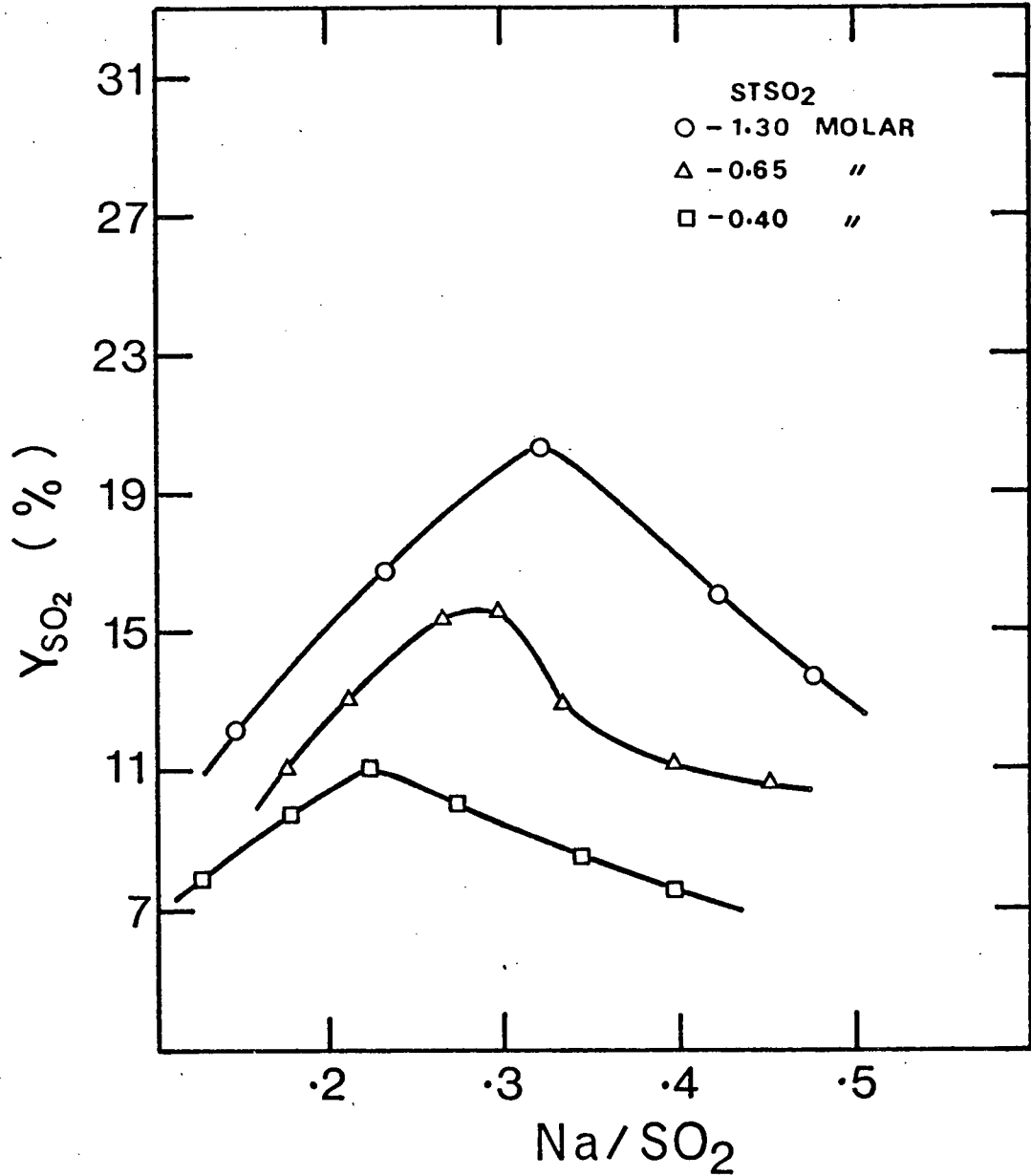


Figure 25 Steady-state yields of sodium dithionite on sulfur dioxide in the aqueous feed versus Na/SO_2 ratios entering the CFSTR at different concentrations of sulfur dioxide in the aqueous feed. See Tables 6, 11 and 12 for the levels of the process variables

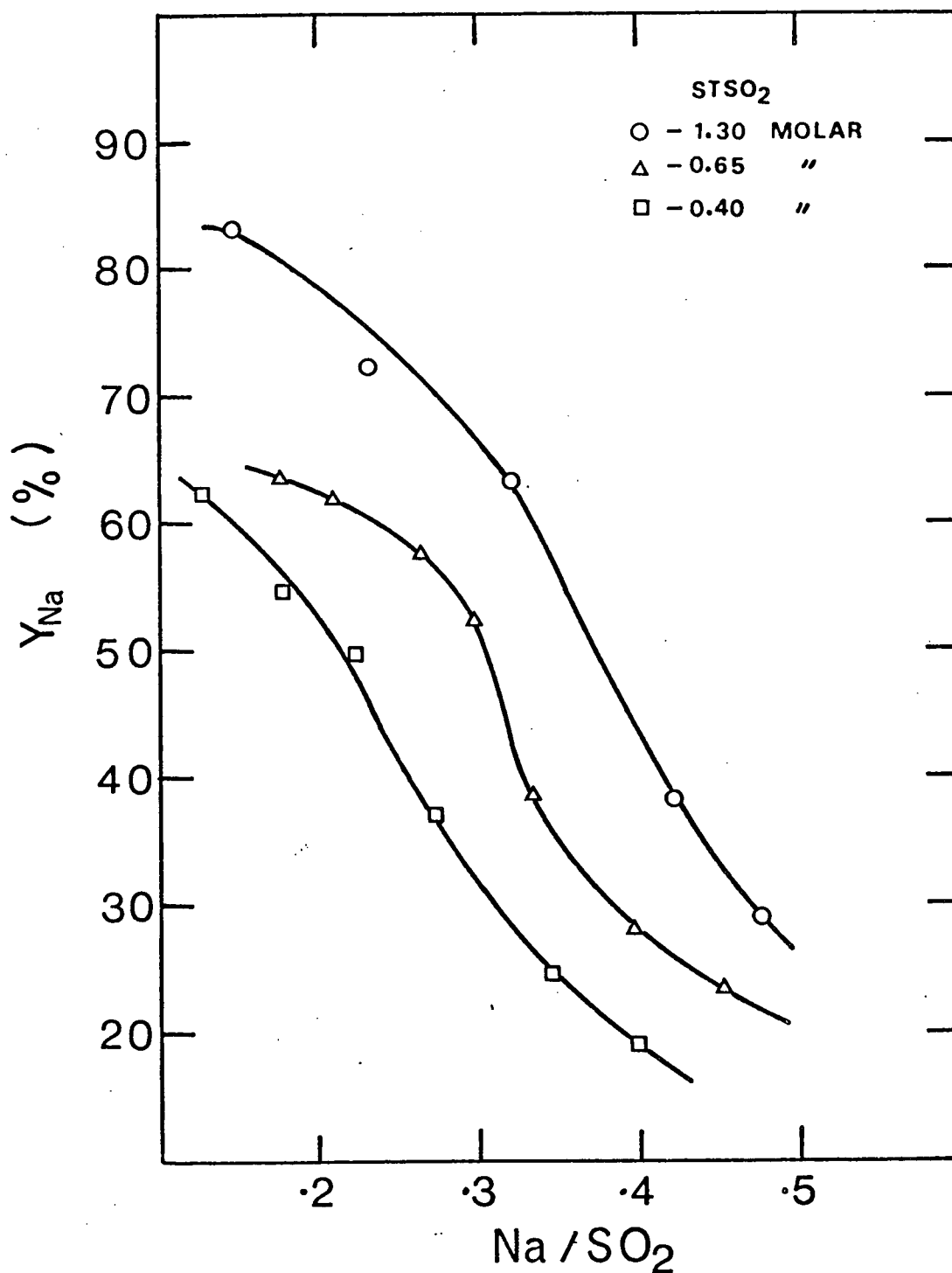


Figure 26 Steady-state yields of sodium dithionite on sodium in the amalgam entering the CFSTR versus Na/SO_2 ratios entering the CFSTR at different concentrations of sulfur dioxide in the aqueous feed. See Tables 6, 11 and 12 for the levels of the process variables

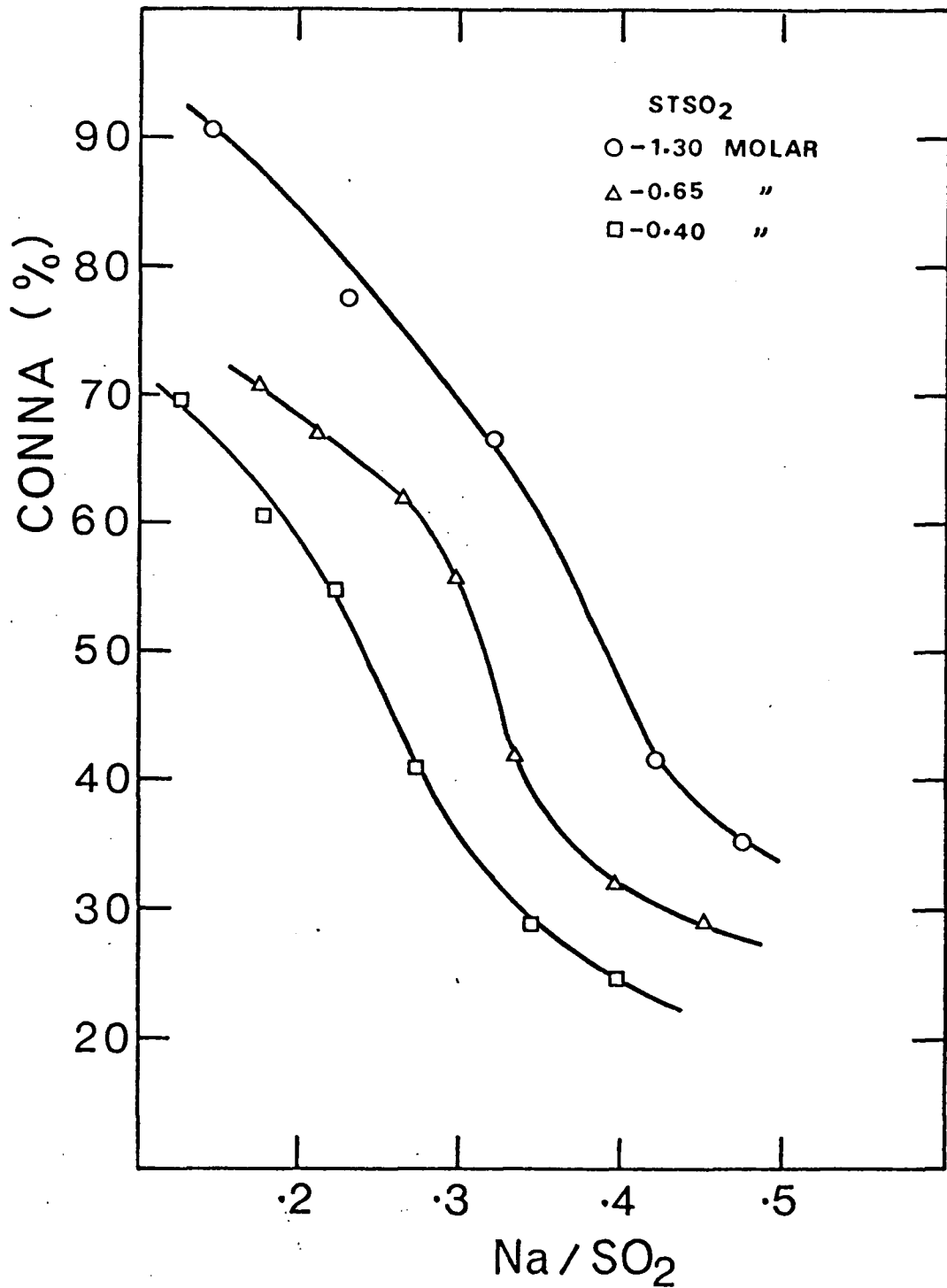


Figure 27 Steady-state yields of sodium dithionite on sodium consumed in the CFSTR versus Na/SO₂ ratios entering the CFSTR at different concentrations of sulfur dioxide in the aqueous feed. See Tables 6, 11 and 12 for the levels of the process variables

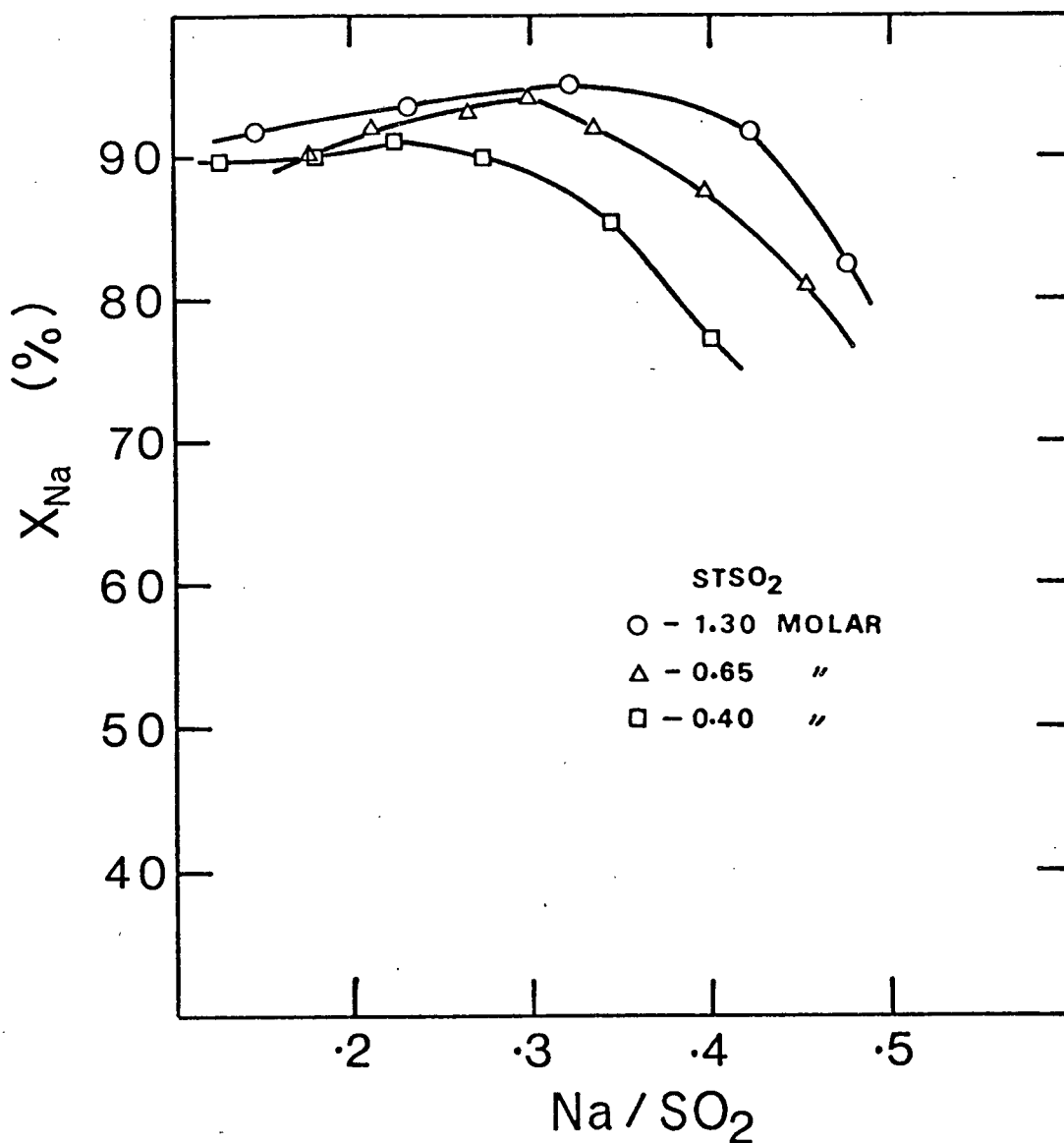


Figure 28 Steady-state conversions of sodium to different products in the CFSTR versus Na/SO₂ ratios entering the CFSTR at different concentrations of sulfur dioxide in the aqueous feed. See Tables 6, 11 and 12 for the levels of the process variables

curves for the sets under consideration are shown in Figures 25 to 28 respectively.

Figures 25 to 27 show that at a fixed Na/SO₂ ratio entering the reactor, when all of the other process variables are kept constant, an increase in the concentration of sulfur dioxide in the feed solution increased the steady-state yield of sodium dithionite on total sulfur dioxide entering the reactor (Y_{SO_2}), the steady-state yield of sodium dithionite on sodium entering the reactor with fresh amalgam (Y_{Na}) and the steady-state yield of sodium dithionite on sodium consumed in the reactor (CONNA).

Figure 28 shows that at relatively low values of Na/SO₂ ratio entering the reactor, an increase in the concentration of sulfur dioxide in the feed solution does not affect the steady-state conversion of sodium to different products in the reactor, X_{Na} , appreciably (considering the 95% error limits). However, at relatively high values of Na/SO₂ ratio entering the reactor, an increase in the concentration of sulfur dioxide in the feed solution increases the steady-state values of X_{Na} significantly.

3. Agitation in the aqueous phase

Before describing the experimental work in detail it should be pointed out that there were some difficulties which influenced the choice of lower and upper limits on

degree of agitation in the aqueous phase. Below a stirrer Reynolds No.= 10,000 (corresponding to the propeller rpm of 376), the results obtained from the laboratory investigation could not be used in making estimations using scale-up methods (84-88, 103). On the other hand when the rpm of the propeller was well above 700, a substantial agitation was imparted to the amalgam phase causing ripples.

Some preliminary experiments were performed to assess the effects of agitation but they did not yield any useful information. A short account of these experiments follows. The reactor was filled up to the lower end of the baffles with an amalgam of a known sodium concentration. Then, known volumes of a sulfur dioxide solution of a known concentration and a Rubine-R solution of a known normality were added to the reactor and the agitation in the aqueous phase was started. The rpm of the propeller was varied through the range of 110 to 700 for the different experiments and the times taken for the Rubine-R colour to disappear were compared. These experiments did not provide very useful data, since even for large volumes of Rubine-R (the dye solution available was very dilute), the colour disappeared almost immediately.

Informative results were obtained when the effect of agitation in the aqueous phase of the CFSTR, on the steady-state $C_{S_2O_4}$, Y_{SO_2} , Y_{Na} , CONNA and X_{Na} was investigated.

During the sets: 65-77 and 47-57, the rpm of the propeller in the aqueous phase was kept fixed at 673. The levels of the other process variables, under steady-state conditions, are presented in Tables 6 and 5 respectively and the steady-state $C_{S_2O_4}$ versus Na/SO_2 , Y_{SO_2} versus Na/SO_2 , Y_{Na} versus Na/SO_2 , CONNA versus Na/SO_2 and X_{Na} versus Na/SO_2 curves are shown in Figure 7. The experimental sets: 66-76, 62-63 and 87-91 were performed at an rpm of 225 and the steady-state $C_{S_2O_4}$ versus Na/SO_2 , Y_{SO_2} versus Na/SO_2 , Y_{Na} versus Na/SO_2 , CONNA versus Na/SO_2 and X_{Na} versus Na/SO_2 curves are shown in Figure 8. For these sets, the levels of all of the other process variables were the same as for the sets: 65-77 and 45-57 as shown in Table 7 to 9. Similarly, the experimental set: 86-90 (expts. 86, 88 and 90) was performed at an rpm of 110. The steady-state $C_{S_2O_4}$, Y_{SO_2} , Y_{Na} , CONNA and X_{Na} were calculated at the three Na/SO_2 ratios and the results are shown in Figure 29. As there were only three points for each calculated quantity, only broken line curves are drawn. The levels of the process variables, under the steady-state conditions for the set: 86-90 are presented in Table 13.

Prior to presenting the results, it should be mentioned that a few experiments were carried out in the experimental

TABLE 13

LEVELS OF THE PROCESS VARIABLES IN SET: 86-90

Range of the Changed Variable	VALUES OF THE FIXED VARIABLES						
CHGF	STSO ₂	(RPM) _{Aq}	FLSO ₂	FLHG	(A/V) _{Aq}	TEMP	pH
.0372 - .0986	.655 -.658	110	.096	47.5	.0784	17	5.35 - 5.8

TABLE 14

LEVELS OF THE PROCESS VARIABLES IN SET: 94-104

Range of the Changed Variable	VALUES OF THE FIXED VARIABLES						
CHGF	STSO ₂	(RPM) _{Aq}	FLSO ₂	FLHG	(A/V) _{Aq}	TEMP	pH
.0280 - .0912	.652 -.660	673	.066	47.5	.0784	17	5.75 - 6.1

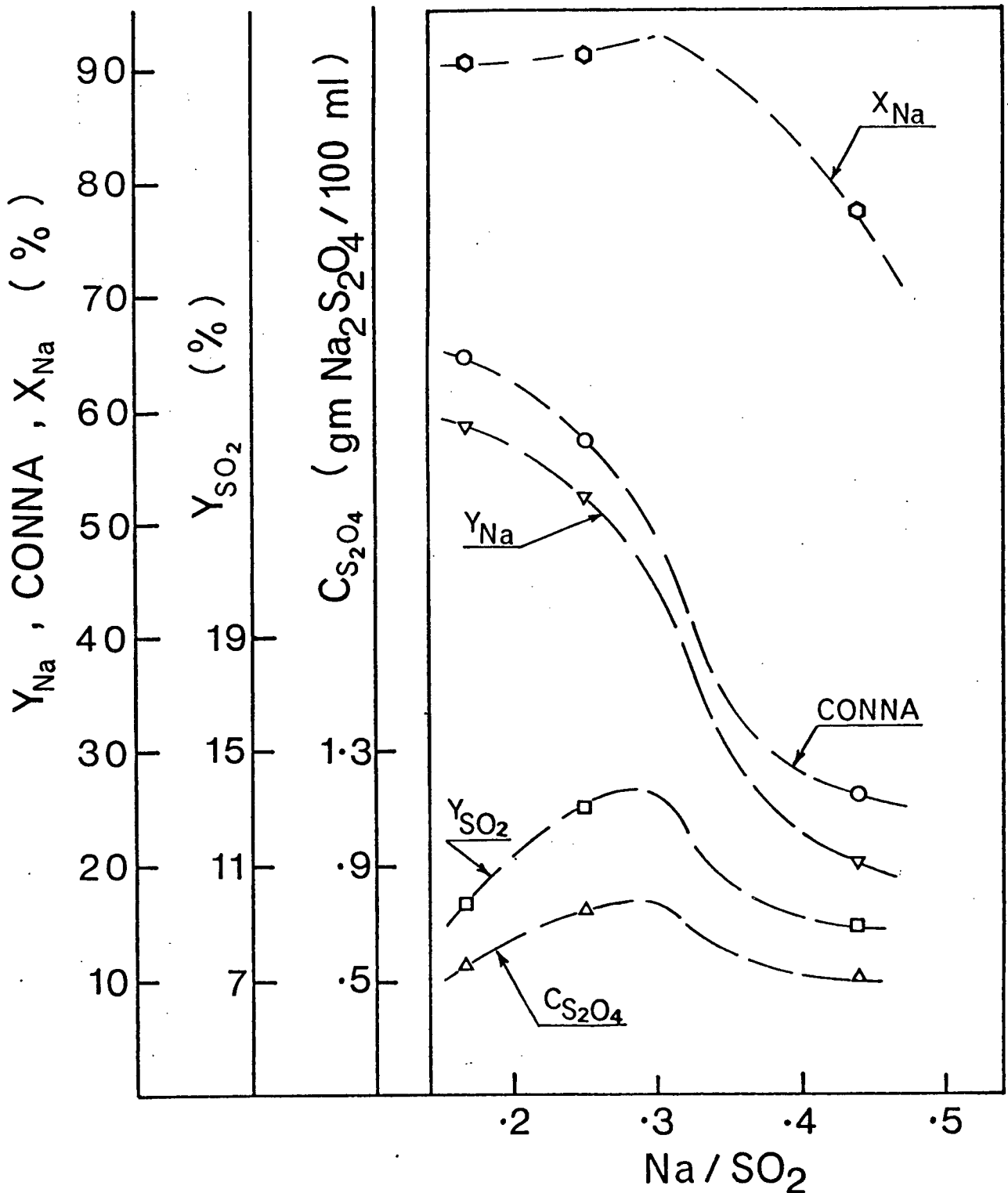


Figure 29 Steady-state values of sodium dithionite concentration and various yields versus Na/SO₂ ratios entering the CFSTR for the experimental set: 86-90. See Table 13 for the levels of the process variables

reactor to ensure that the conditions of perfect mixing existed at the different levels of agitation. Johnson (41) carried out tracer studies in the experimental reactor under the conditions used in the present investigation. Using the Cholette and Cloutier model (15) for the CFSTR his results showed that, under the specified experimental conditions, perfect mixing occurred in the reactor.

The curves obtained by plotting the steady-state $C_{S_2O_4}$ versus Na/SO_2 , Y_{SO_2} versus Na/SO_2 , Y_{Na} versus Na/SO_2 , CONNA versus Na/SO_2 and X_{Na} versus Na/SO_2 at three different levels of agitation in the aqueous phase are shown Figures 30 to 34 respectively. Figures 30 to 33 show that at a fixed Na/SO_2 ratio entering the reactor, when the level of agitation in the aqueous phase was increased, the steady-state concentration of sodium dithionite in the product stream ($C_{S_2O_4}$), the yield of sodium dithionite on total sulfur dioxide entering the reactor (Y_{SO_2}), the yield of sodium dithionite on sodium entering the reactor with the fresh amalgam (Y_{Na}) and the yield of sodium dithionite on sodium consumed in the reactor (CONNA) also increased. However, the percentage increase in the steady-state $C_{S_2O_4}$, Y_{SO_2} , Y_{Na} and CONNA at values of Na/SO_2 ratio below the steady-state $Na_2S_2O_4$ concentration maximum (i.e. at the Na/SO_2 ratios <0.29) is less than the percentage increase in these values at Na/SO_2 ratio above the steady-state sodium dithionite concentration maximum (i.e., at the Na/SO_2 ratios >0.29). Figure 34 shows that at

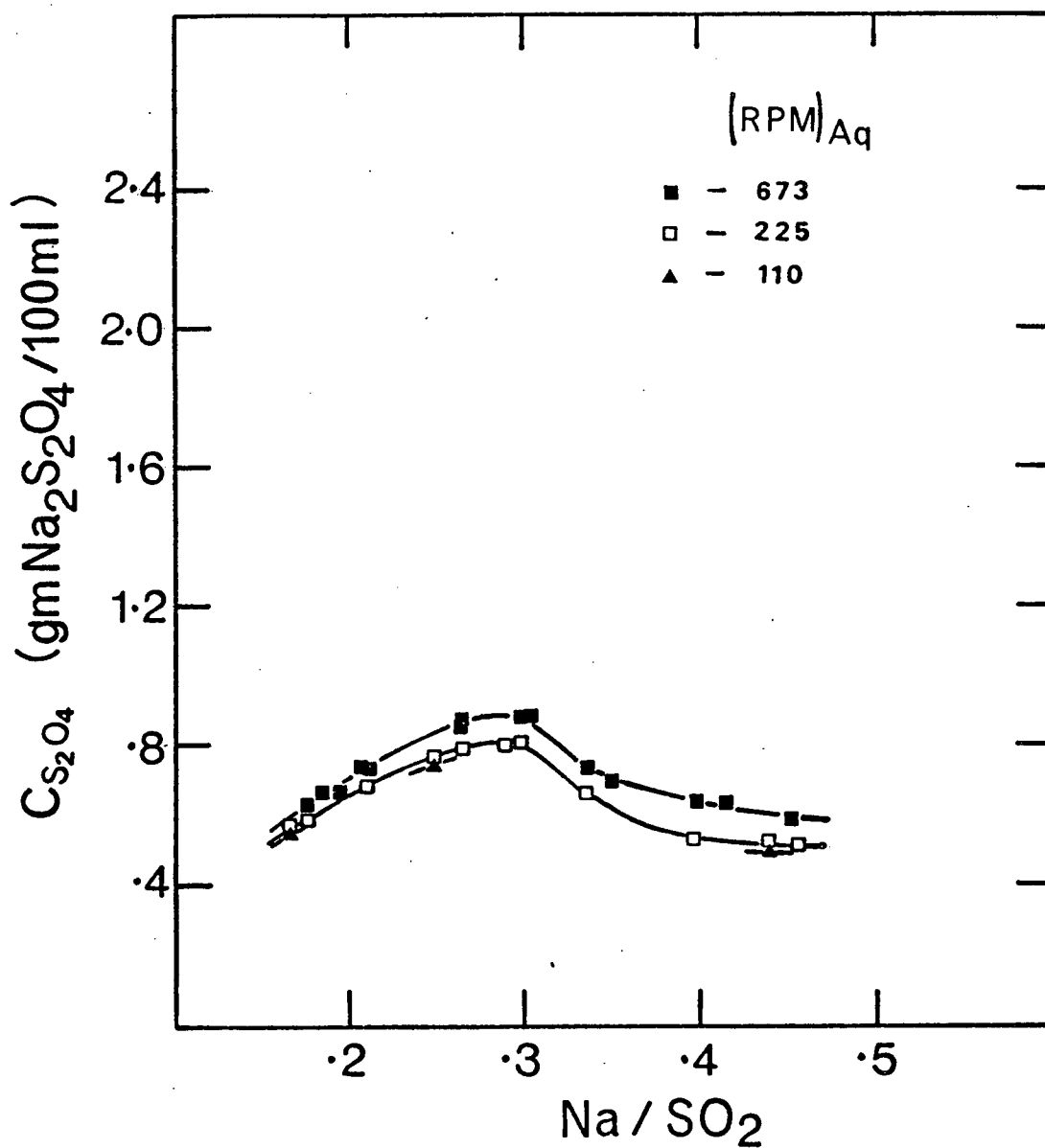


Figure 30 Steady-state sodium dithionite concentrations versus Na/SO_2 ratios entering the CFSTR at different levels of agitation in the aqueous feed. See Tables 5-9 and 13 for the levels of the process variables.

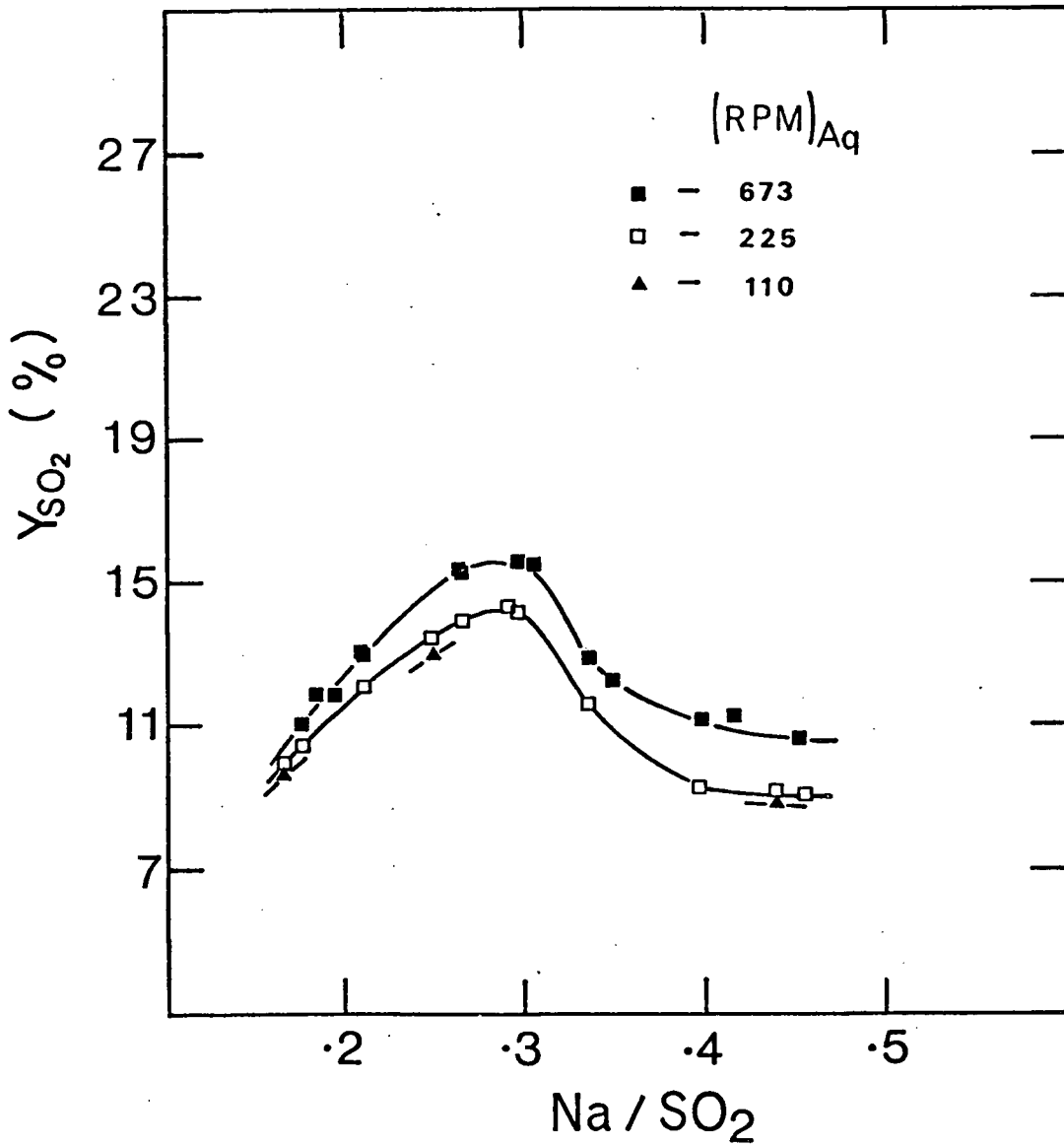


Figure 31 Steady-state yields of sodium dithionite on sulfur dioxide in the aqueous feed versus Na/SO_2 ratios entering the CFSTR at different levels of agitation in the aqueous feed. See Tables 5-9 and 13 for the levels of the process variables

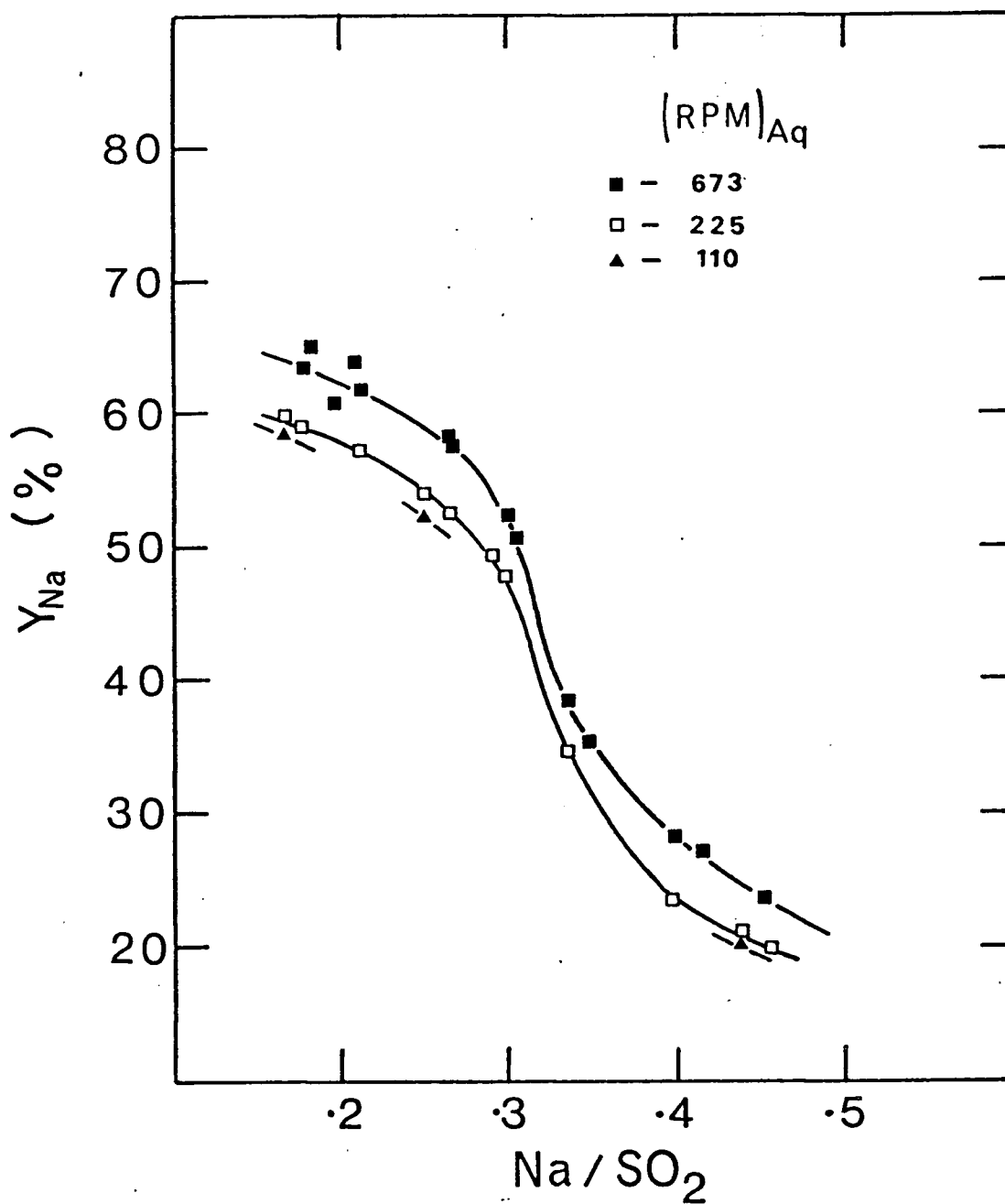


Figure 32 Steady-state yields of sodium dithionite on sodium in the amalgam entering the CFSTR versus Na/SO_2 ratios entering the CFSTR at different levels of agitation in the aqueous feed. See Tables 5-9 and 13 for the levels of the process variables

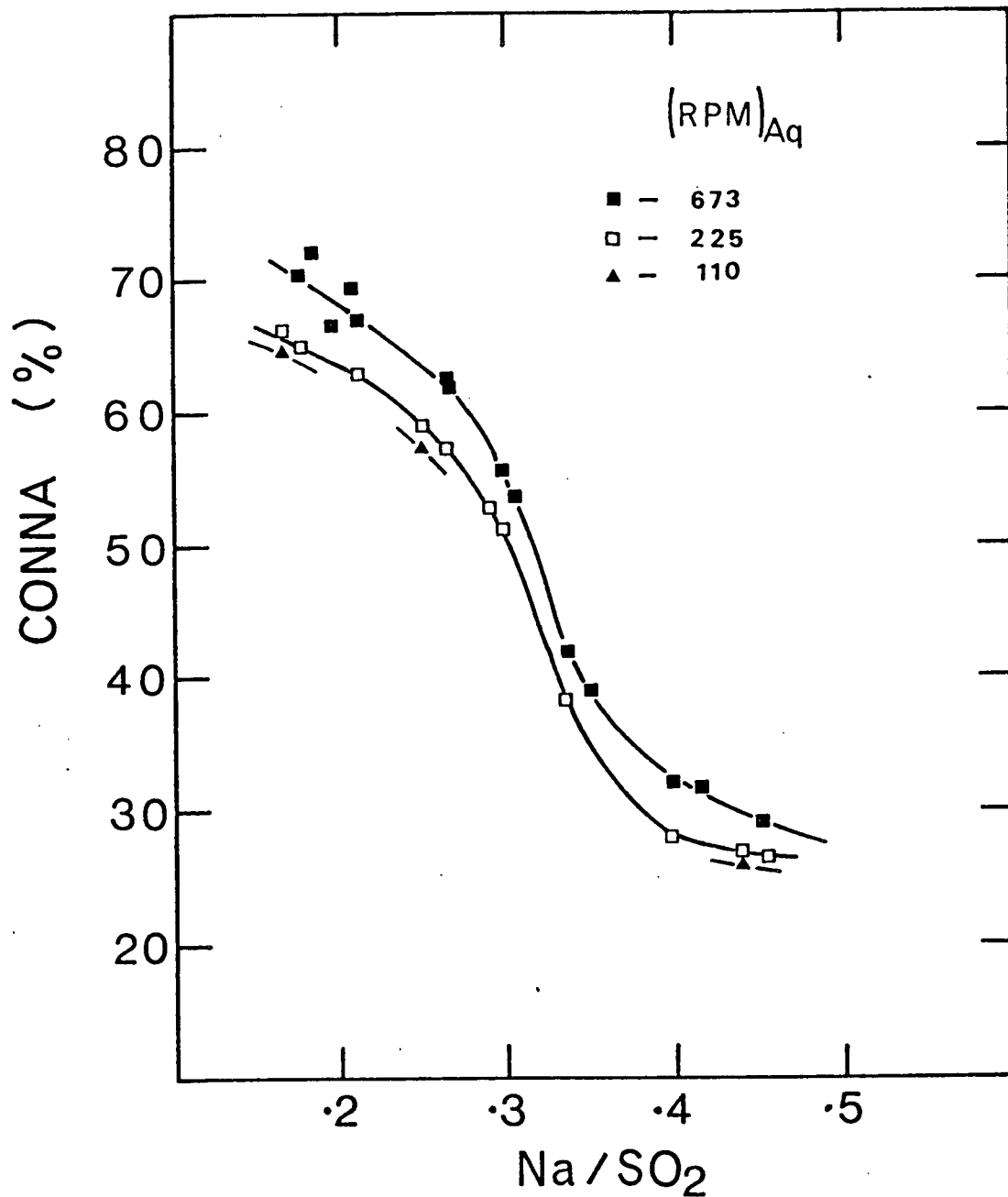


Figure 33 Steady-state yields of sodium dithionite on sodium consumed in the CFSTR versus Na/SO_2 ratios entering the CFSTR at different levels of agitation in the aqueous feed. See Tables 5-9 and 13 for the levels of the process variables

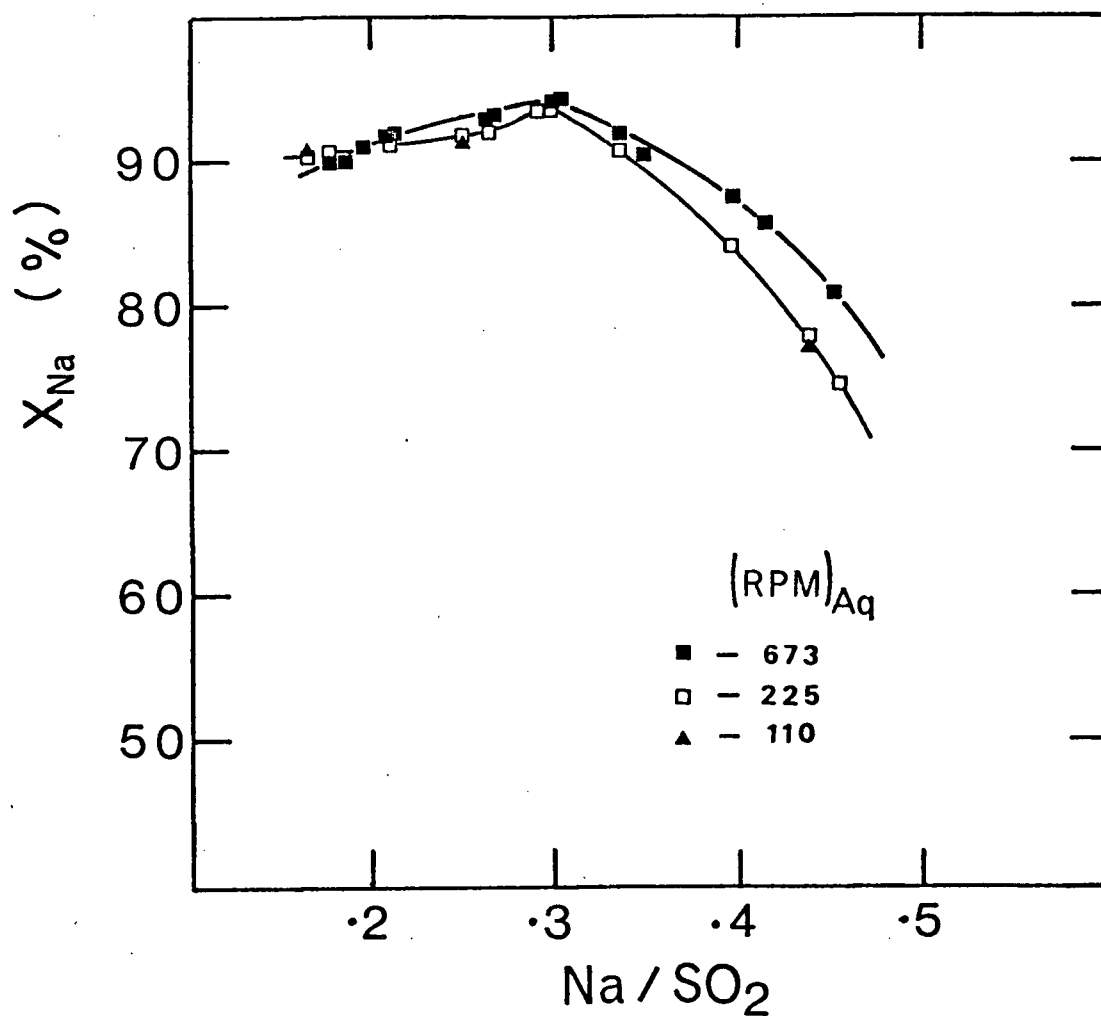


Figure 34 Steady-state conversions of sodium to different products in the CFSTR versus Na/SO₂ ratios entering the CFSTR at different levels of agitation in the aqueous feed. See Tables 5-9 and 13 for the levels of the process variables

Na/SO₂ ratios <0.29, the steady-state conversion of sodium to different products in the reactor (X_{Na}) does not change appreciably, however, at Na/SO₂ ratios >0.29, the steady-state X_{Na} values increase significantly with increase in the level of agitation.

4. Flow rate of aqueous sulfur dioxide solution, i.e. residence time in the aqueous phase

The effect of variation in the flow rate of the aqueous sulfur dioxide solution on the steady-state $C_{S_2O_4}$, Y_{SO_2} , Y_{Na} , CONNA and X_{Na} , at various Na/SO₂ ratios entering the reactor, was investigated in the experimental sets: 94-104 (expts. 94, 96, 98, 100, 102 and 104), 65-77 and 95-105. The flow rates of the aqueous solution in these sets were 66 ml/min, 96 ml/min and 198 ml/min respectively. The levels of the other process variables, under the steady-state conditions, have been reported in Tables 14, 6 and 10 respectively. The steady-state $C_{S_2O_4}$, Y_{SO_2} , Y_{Na} , CONNA and X_{Na} , for the sets: 94-104, 65-77 and 95-105, are plotted against the Na/SO₂ ratios entering the reactor in Figures 35, 9 and 36 respectively.

The curves obtained by plotting the steady-state $C_{S_2O_4}$ versus Na/SO₂, Y_{SO_2} versus Na/SO₂, Y_{Na} versus Na/SO₂, CONNA versus Na/SO₂ and X_{Na} versus Na/SO₂ at the three different flow rates of the aqueous sulfur dioxide solution are shown in Figures 37 to 41 respectively.

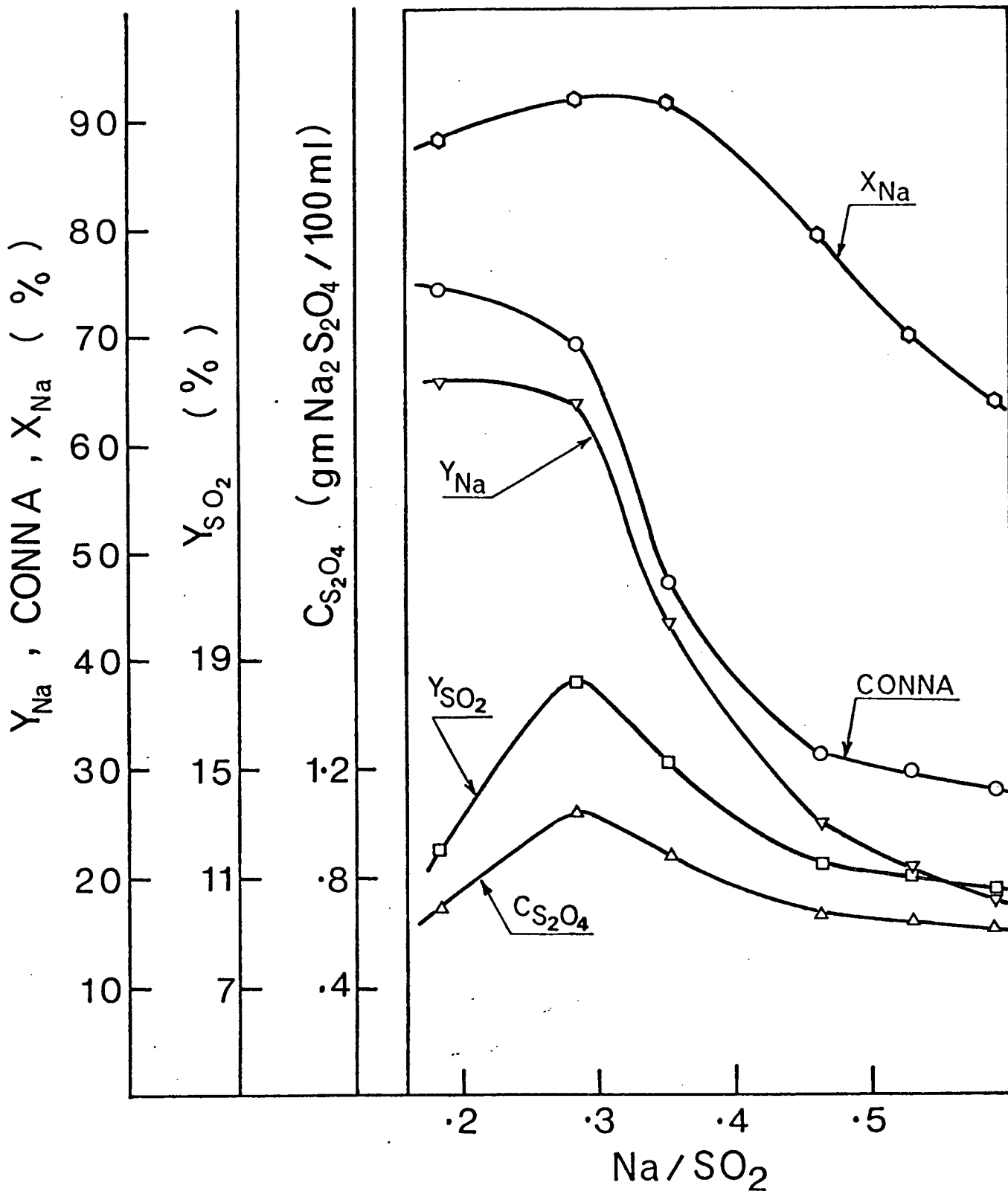


Figure 35 Steady-state values of sodium dithionite concentration and various yields versus Na/SO₂ ratios entering the CFSTR for the experimental set: 94-104. See Table 14 for the levels of the process variables

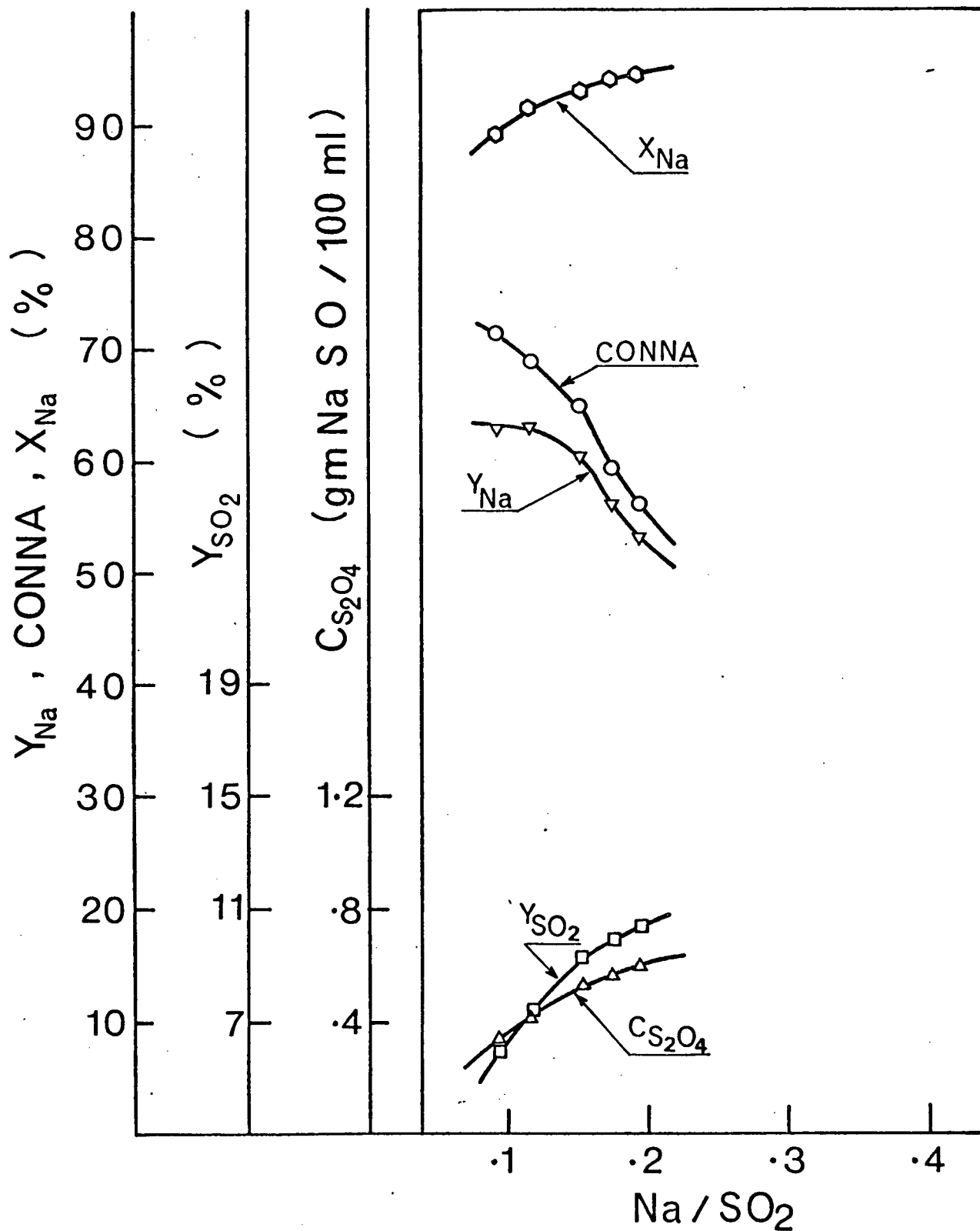


Figure 36 Steady-state values of sodium dithionite concentration and various yields versus Na/SO₂ ratios entering the CFSTR for the experimental set: 95-105. See Table 10 for the levels of the process variables

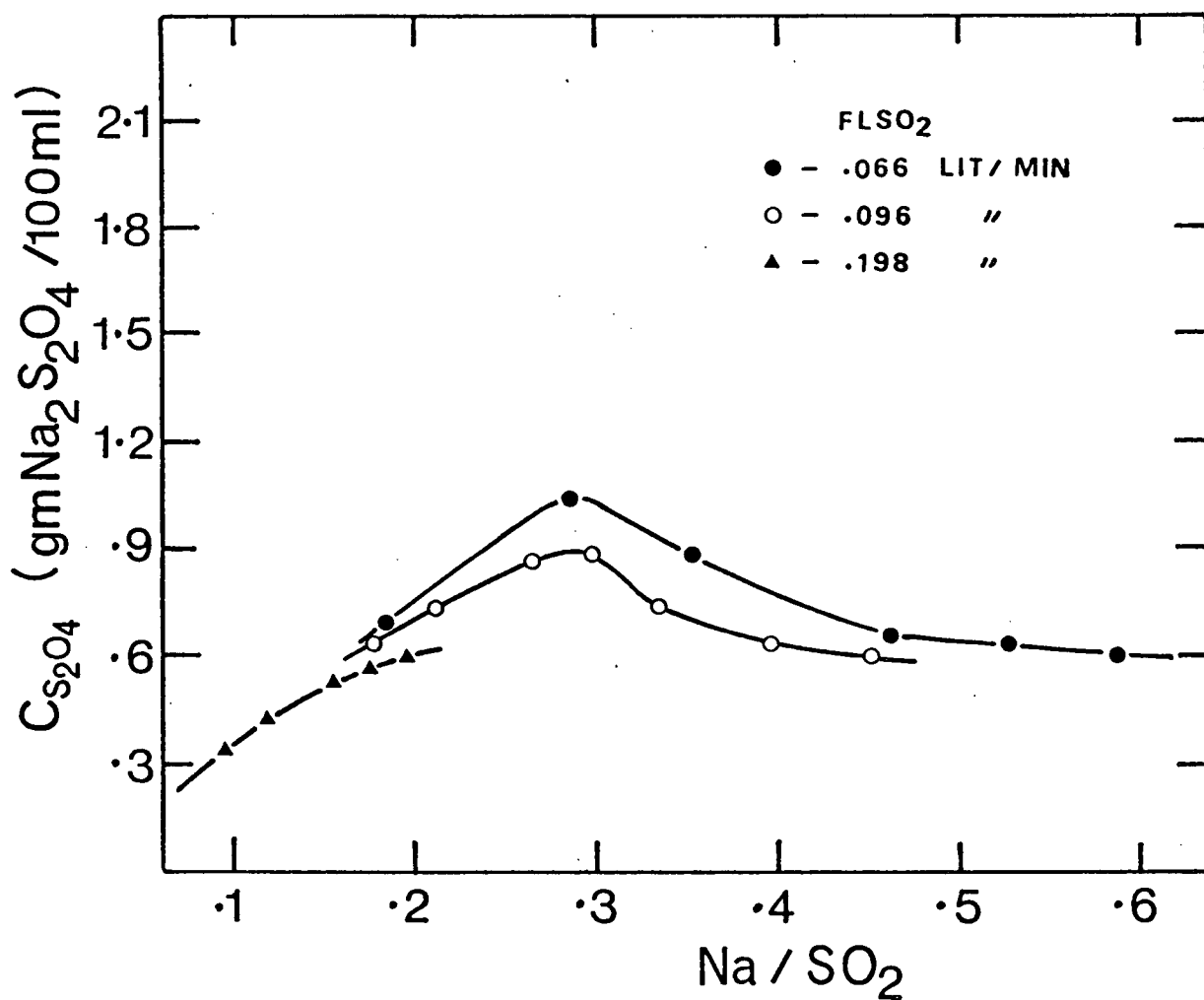


Figure 37 Steady-state sodium dithionite concentrations versus Na/SO₂ ratios entering the CFSTR at different flow rates of the aqueous feed. See Tables 6, 10 and 14 for the levels of the process variables

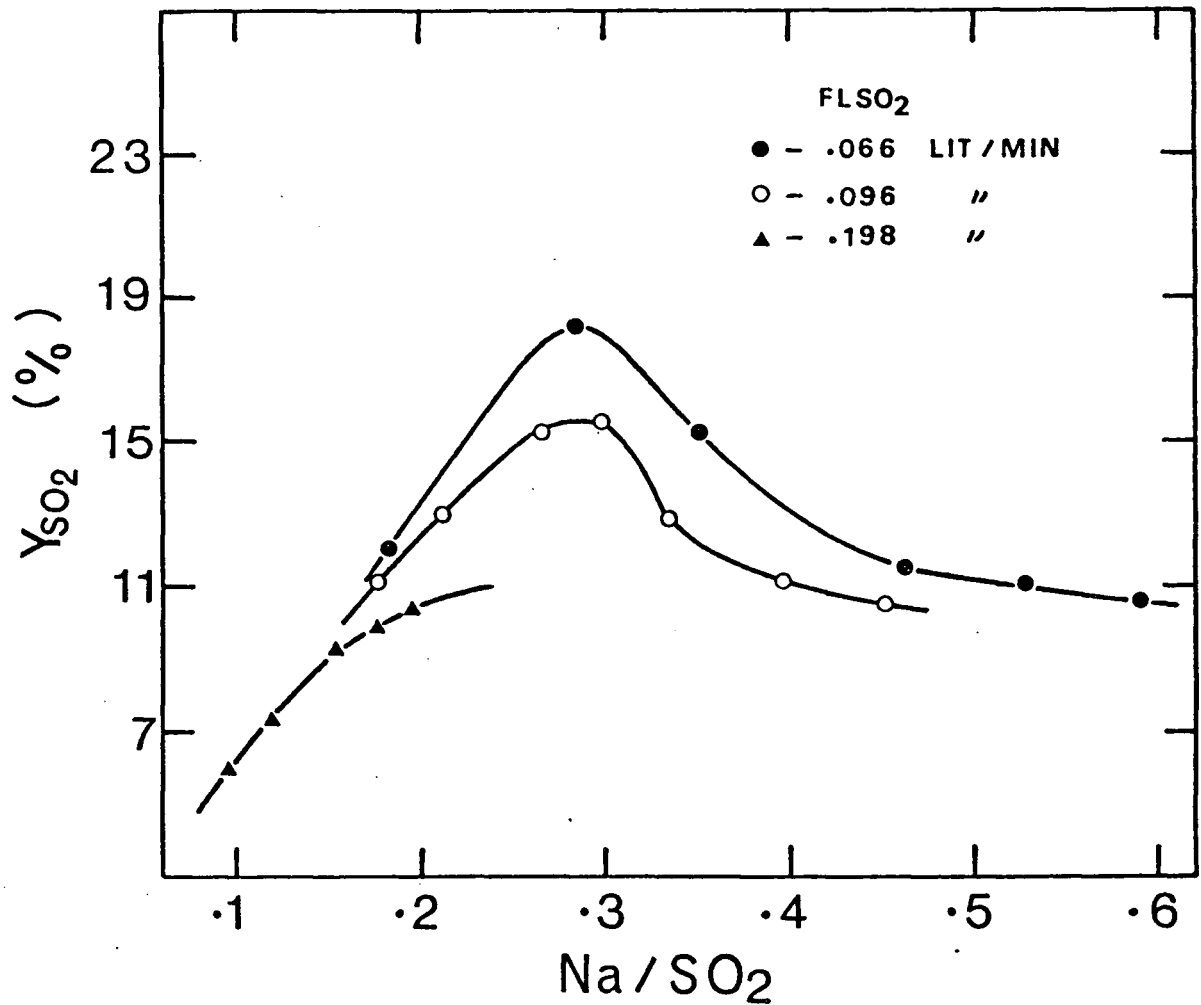


Figure 38 Steady-state yields of sodium dithionite on sulfur dioxide in the aqueous feed versus Na/SO₂ ratios entering the CFSTR at different flow rates of the aqueous feed. See Tables 6, 10 and 14 for the levels of the process variables

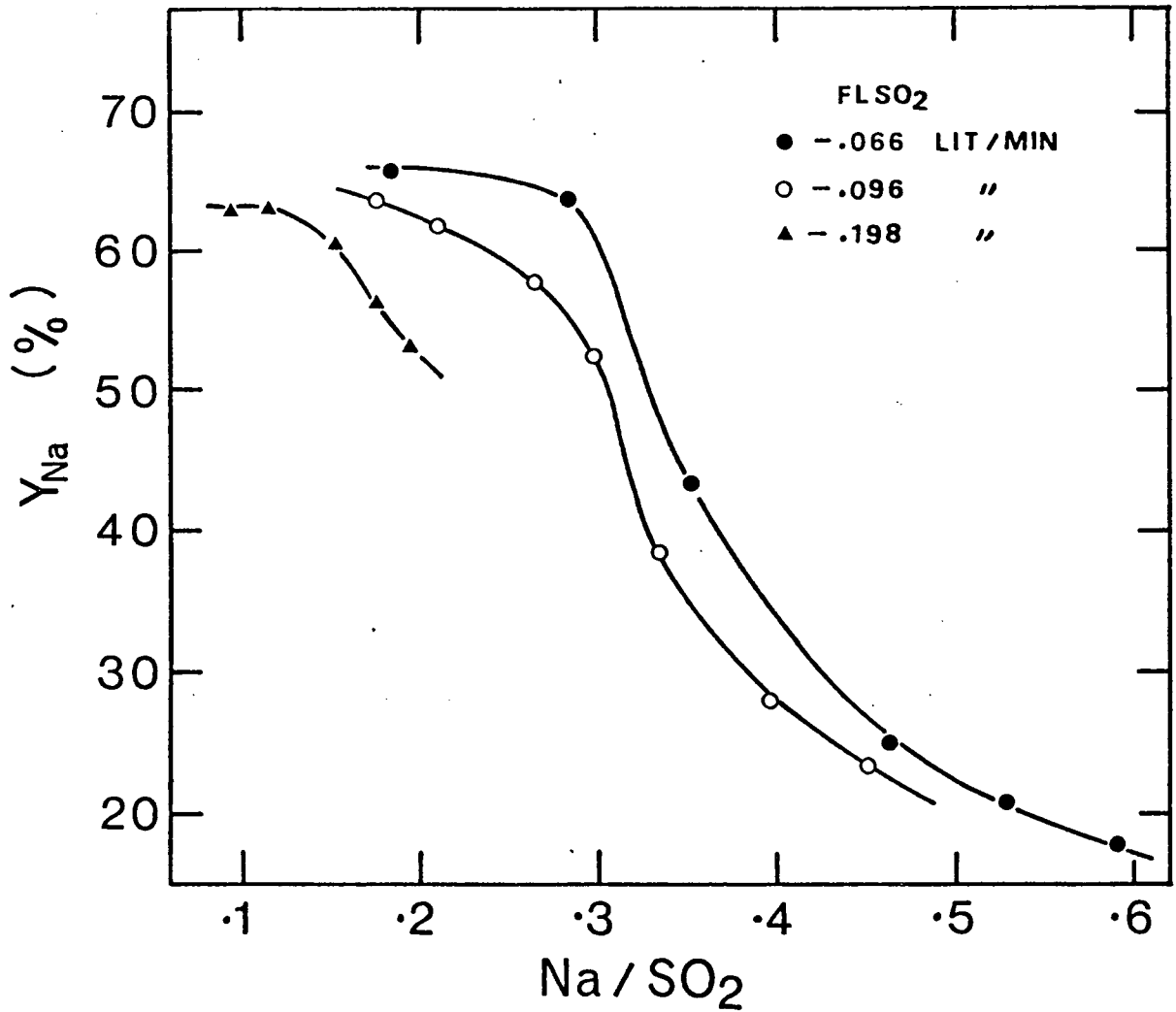


Figure 39 Steady-state yields of sodium dithionite on sodium in the amalgam entering the CFSTR versus Na/SO_2 ratios entering the CFSTR at different flow rates of the aqueous feed. See Tables 6, 10 and 14 for the levels of the process variables

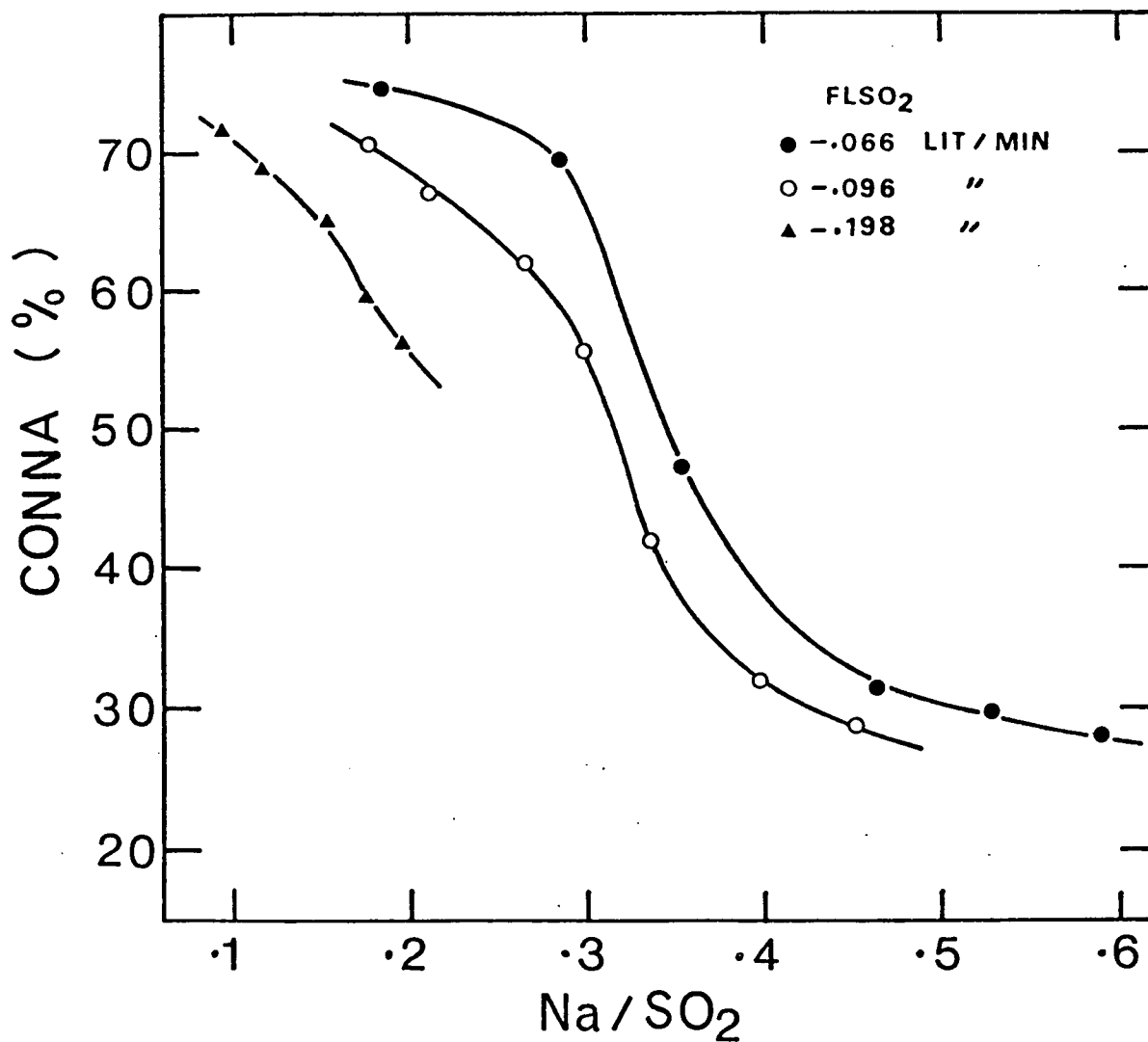


Figure 40 Steady-state yields of sodium dithionite on sodium consumed in the CFSTR versus Na/SO₂ ratios entering the CFSTR at different flow rates of the aqueous feed. See Tables 6, 10 and 14 for the levels of the process variables

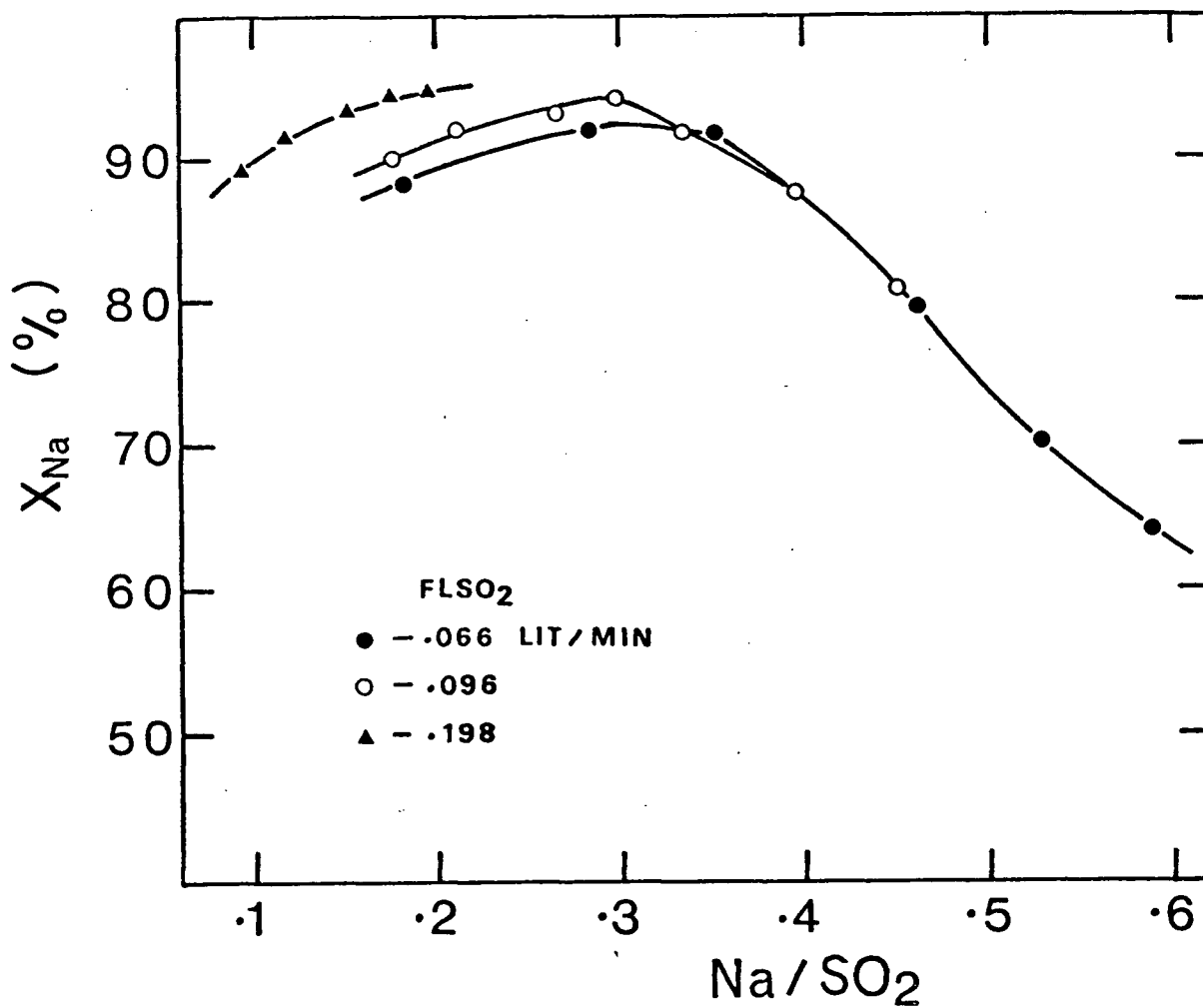


Figure 41 Steady-state conversions of sodium to different products in the CFSTR versus Na/SO_2 ratios entering the CFSTR at different flow rates of the aqueous feed. See Tables 6, 10 and 14 for the levels of the process variables

Figure 37 shows that at all of the values of Na/SO_2 ratio considered, the steady-state concentration of sodium dithionite in the product stream, $C_{\text{S}_2\text{O}_4}$, increases when the flow rate of the aqueous sulfur dioxide solution is decreased (i.e., when the residence time in the aqueous phase is increased). Similar behaviour is observed when the steady-state values of Y_{SO_2} (yields of sodium dithionite on total sulfur dioxide entering the reactor) are plotted against the Na/SO_2 ratios entering the reactor at the three levels of the flow rate (Figure 38).

Figure 39 shows that at low as well as high Na/SO_2 ratios, the percentage of sodium that is converted to sodium dithionite under steady-state conditions, CONNA , increases when the flow rate of the aqueous feed solution is decreased. The trend of the curves obtained by plotting the steady-state yields of sodium dithionite on sodium entering the reactor (Y_{Na}) against the Na/SO_2 ratios at the three levels of the flow rate was similar.

Figure 41 shows that at values of the Na/SO_2 ratio below the steady-state sodium dithionite concentration maximum (i.e., at the Na/SO_2 ratios <0.29), the steady-state conversion of sodium to different products in the reactor (X_{Na}) decreased when the flow rate of the aqueous sulfur dioxide feed was reduced. But at Na/SO_2 ratios >0.29 the steady-state values of X_{Na} did not change appreciably with change in flow rate.

The geometry of the reactor was such that the aqueous sulfur dioxide solution entered the reactor through a 1/4 inch stainless-steel tube, the mouth of which was situated approximately 2 inches above the amalgam surface. Therefore, it was suspected that an increase in the flow rate of the aqueous solution would impart greater turbulence to the amalgam phase. To investigate this a colour tracer was introduced in the inlet aqueous solution. Despite the fact that the propeller was placed directly below the mouth of the tube which brought the aqueous solution to the reactor, it was observed that, at the rpm under consideration, the stream of the inlet aqueous solution did not break completely by the mixer and it impinged on the amalgam surface.

5. Interfacial-area/aqueous-volume ratio

To investigate this process variable, the volume of the aqueous phase was not changed from 980 ml. The interfacial area was changed, as mentioned in Section IV.B.1, by opening the bottom flange of the reactor and introducing thin stainless-steel discs with variable diameter annular holes.

In the experimental sets: 65-77, 122-134 (expts. 122, 125, 128, 131 and 134) and 123-135 (expts. 123, 129, 132 and 135) the area of the interface was 76.8 cm^2 , 24.2 cm^2 and 9.35 cm^2 respectively. These areas corresponded to inter-

facial-area/aqueous-volume ratios of $.0784 \text{ cm}^2/\text{cm}^3$, $.0247 \text{ cm}^2/\text{cm}^3$ and $.0095 \text{ cm}^2/\text{cm}^3$ respectively. The levels of the other process variables, under the steady-state conditions are presented in Tables 6, 15 and 16. The steady-state $C_{\text{S}_2\text{O}_4}$, Y_{SO_2} , Y_{Na} , CONNA and X_{Na} , for the sets: 65-77, 122-134 and 123-135, are plotted against the Na/SO₂ ratios entering the reactor in Figures 9, 42 and 43 respectively.

The curves obtained by plotting the steady-state $C_{\text{S}_2\text{O}_4}$ versus Na/SO₂, Y_{SO_2} versus Na/SO₂, Y_{Na} versus Na/SO₂, CONNA versus Na/SO₂ and X_{Na} versus Na/SO₂ at the three interfacial-area/aqueous-volume ratios are shown in Figures 44 to 48 respectively.

Figures 44 to 48 show that, at a fixed Na/SO₂ ratio entering the reactor, when the interfacial-area/aqueous-volume ratio increases, the values of steady-state $C_{\text{S}_2\text{O}_4}$, Y_{SO_2} , Y_{Na} , CONNA and X_{Na} also increase.

Figure 49 shows that when the values of steady-state concentration of sodium dithionite in the product stream ($C_{\text{S}_2\text{O}_4}$) or the yield of sodium dithionite on sulfur dioxide entering the reactor (Y_{SO_2}) are plotted against the interfacial-area/aqueous-volume ratios, at different Na/SO₂ ratios, straight line relationships are not obtained.

One of the major problems in investigating the process variable under consideration was the following. Every time a stainless-steel disc was forced into position to change the interfacial-area/aqueous-volume ratio, it

TABLE 15

LEVELS OF THE PROCESS VARIABLES IN SET: 122-134

Range of the Changed Variable	VALUES OF THE FIXED VARIABLES						
	STSO ₂	(RPM) _{Aq}	FLSO ₂	FLHG	(A/V) _{Aq}	TEMP	pH
.0488 - .1238	.658 -.664	673	.096	47.5	.0247	17	5.7 - 5.95

TABLE 16

LEVELS OF THE PROCESS VARIABLES IN SET: 123-135

Range of the Changed Variable	VALUES OF THE FIXED VARIABLES						
	STSO ₂	(RPM) _{Aq}	FLSO ₂	FLHG	(A/V) _{Aq}	TEMP	pH
.0488 - .0879	.658 -.664	673	.096	47.5	.0095	17	5.65 - 5.8

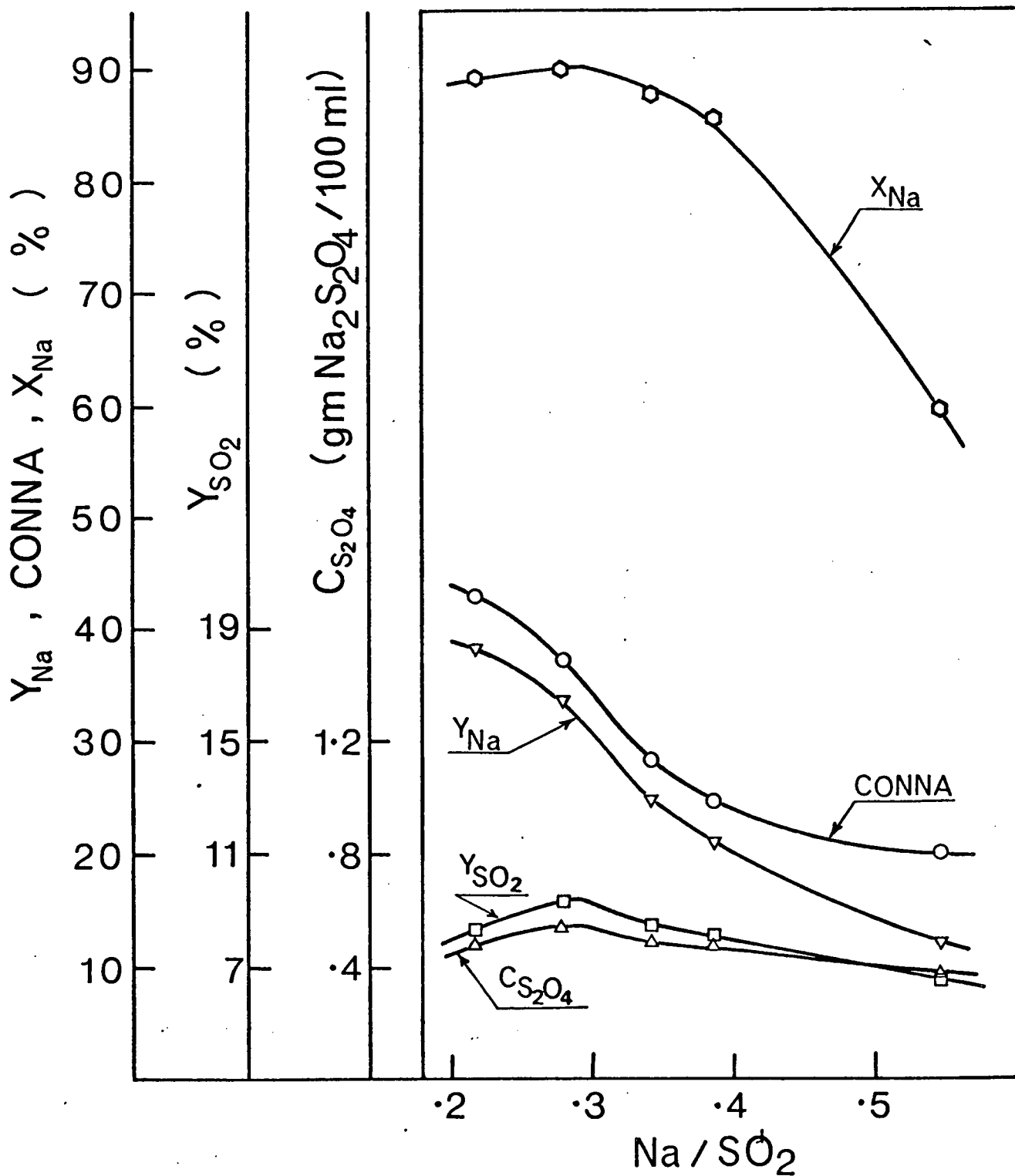


Figure 42 Steady-state values of sodium dithionite concentration and various yields versus Na/SO₂ ratios entering the CFSTR for the experimental set: 122-134. See Table 15 for the levels of the process variables

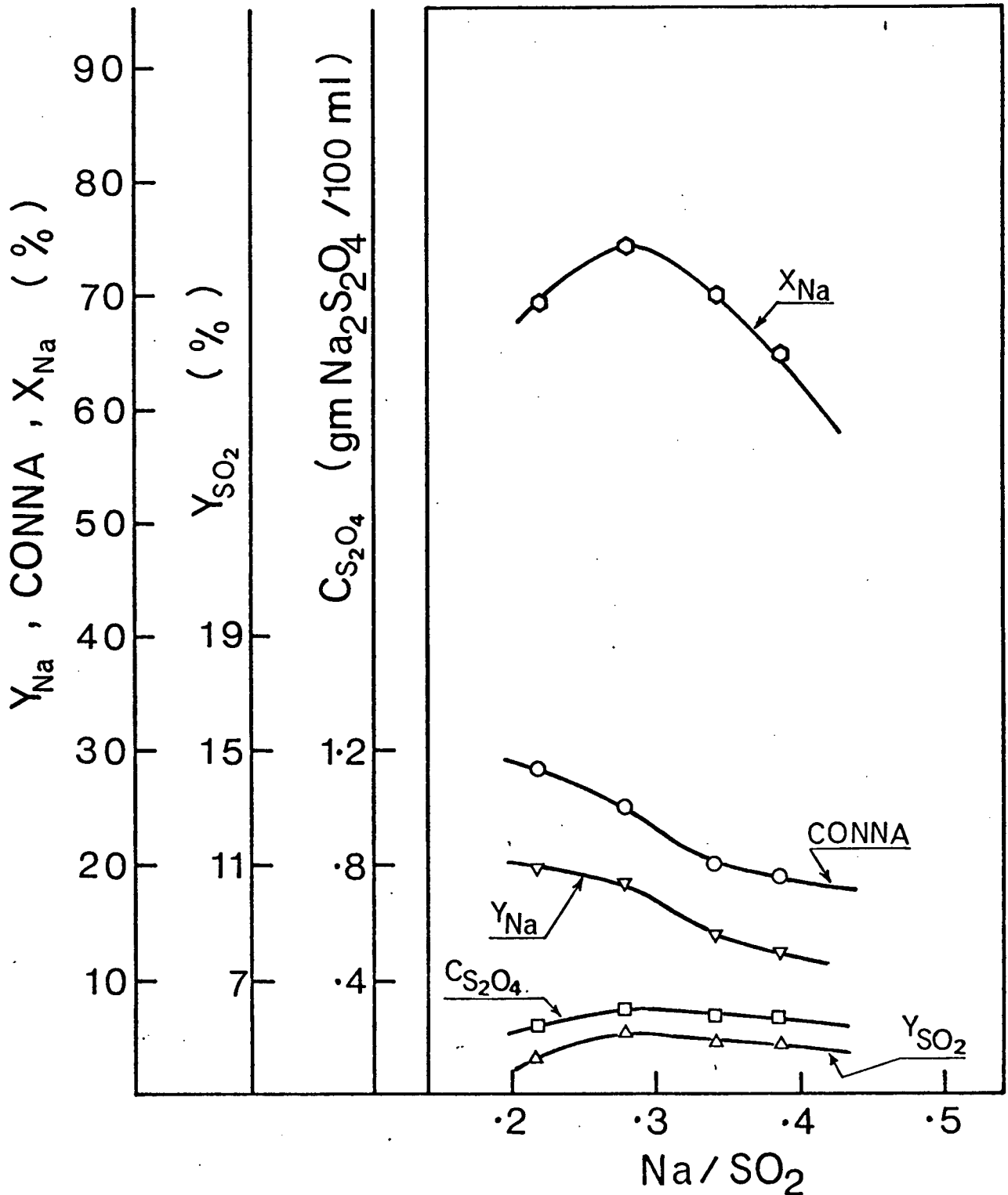


Figure 43 Steady-state values of sodium dithionite concentration and various yields versus Na/SO₂ ratios entering the CFSTR for the experimental set: 123-135. See Table 16 for the levels of the process variables

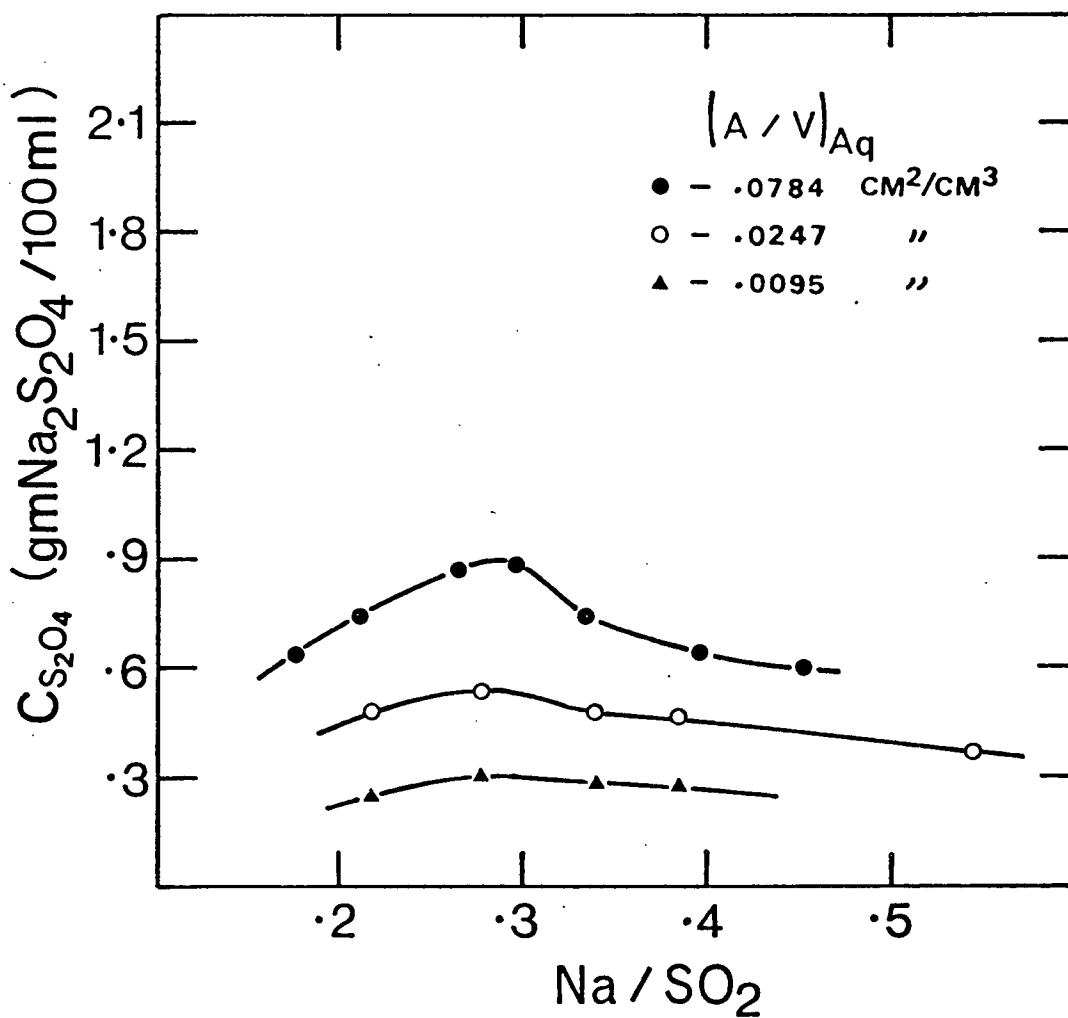


Figure 44 Steady-state sodium dithionite concentrations versus Na/SO₂ ratios entering the CFSTR at different values of interfacial-area/aqueous-volume ratio. See Tables 6, 15 and 16 for the levels of the process variables

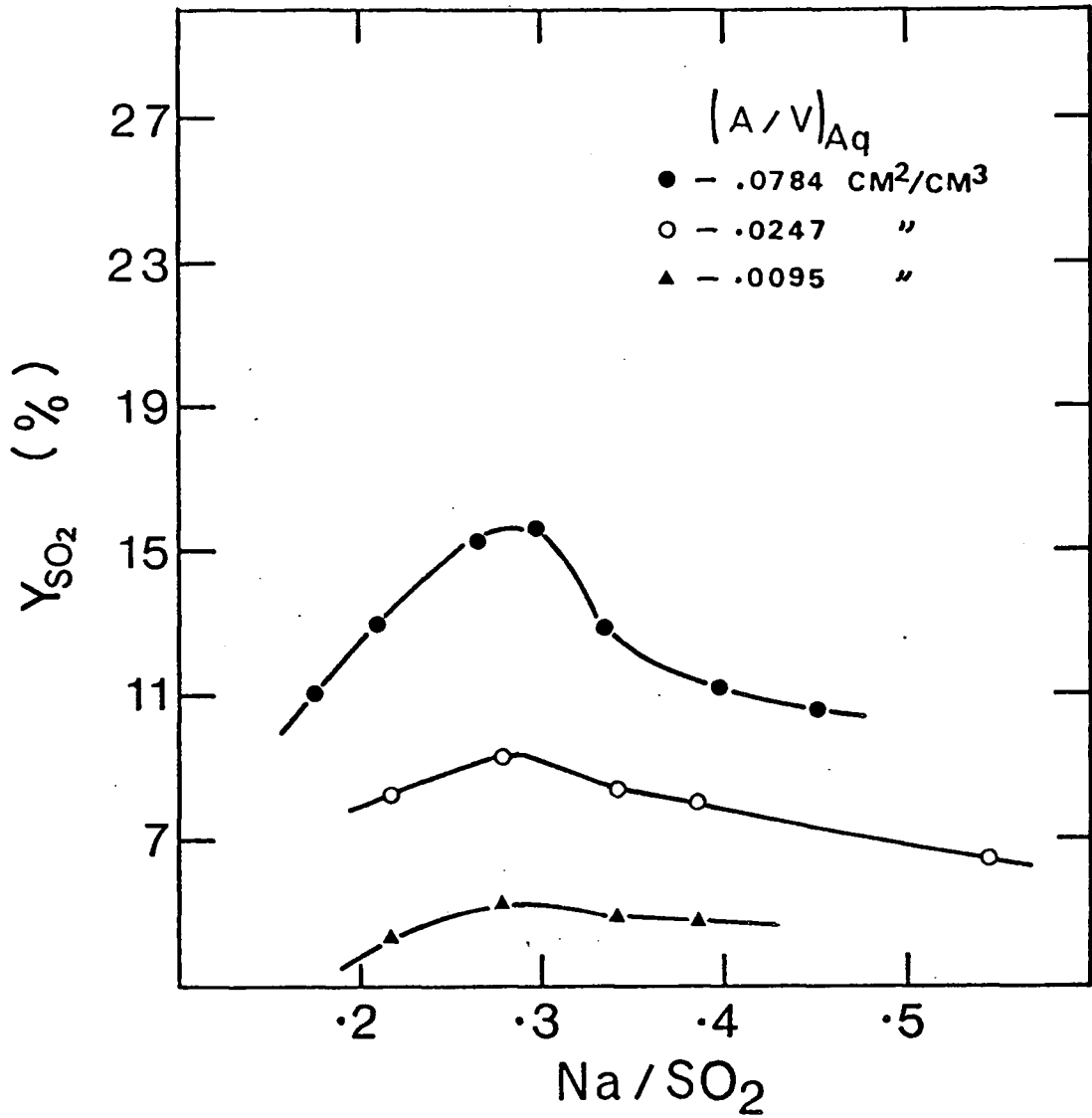


Figure 45 Steady-state yields of sodium dithionite on sulfur dioxide in the aqueous feed versus Na/SO_2 ratios entering the CFSTR at different values of interfacial-area/aqueous-volume ratio. See Tables 6, 15 and 16 for the levels of the process variables

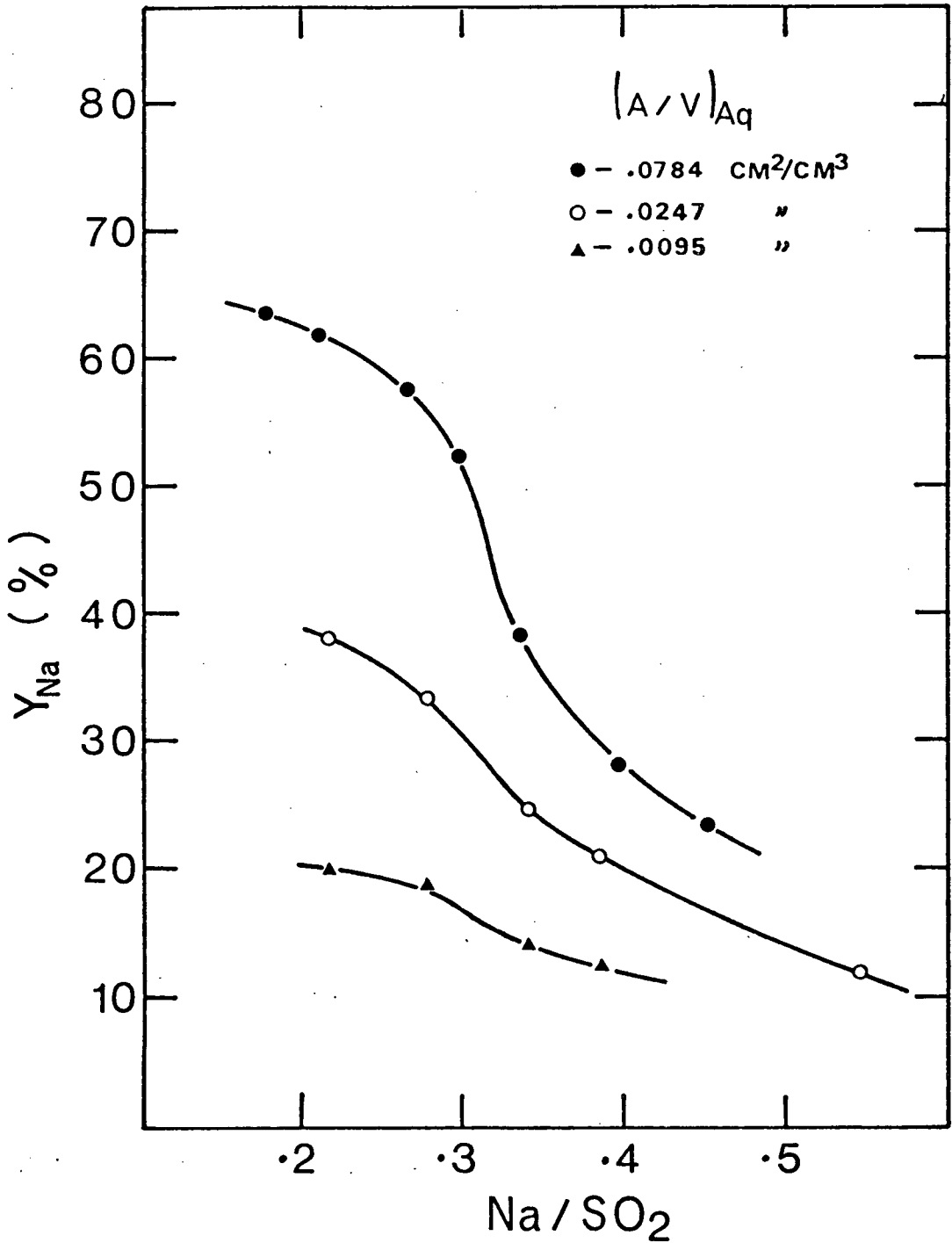


Figure 46 Steady-state yields of sodium dithionite on sodium in the amalgam entering the CFSTR versus Na/SO_2 ratios entering the CFSTR at different values of interfacial-area/aqueous-volume ratio. See Tables 6, 15 and 16 for the levels of the process variables

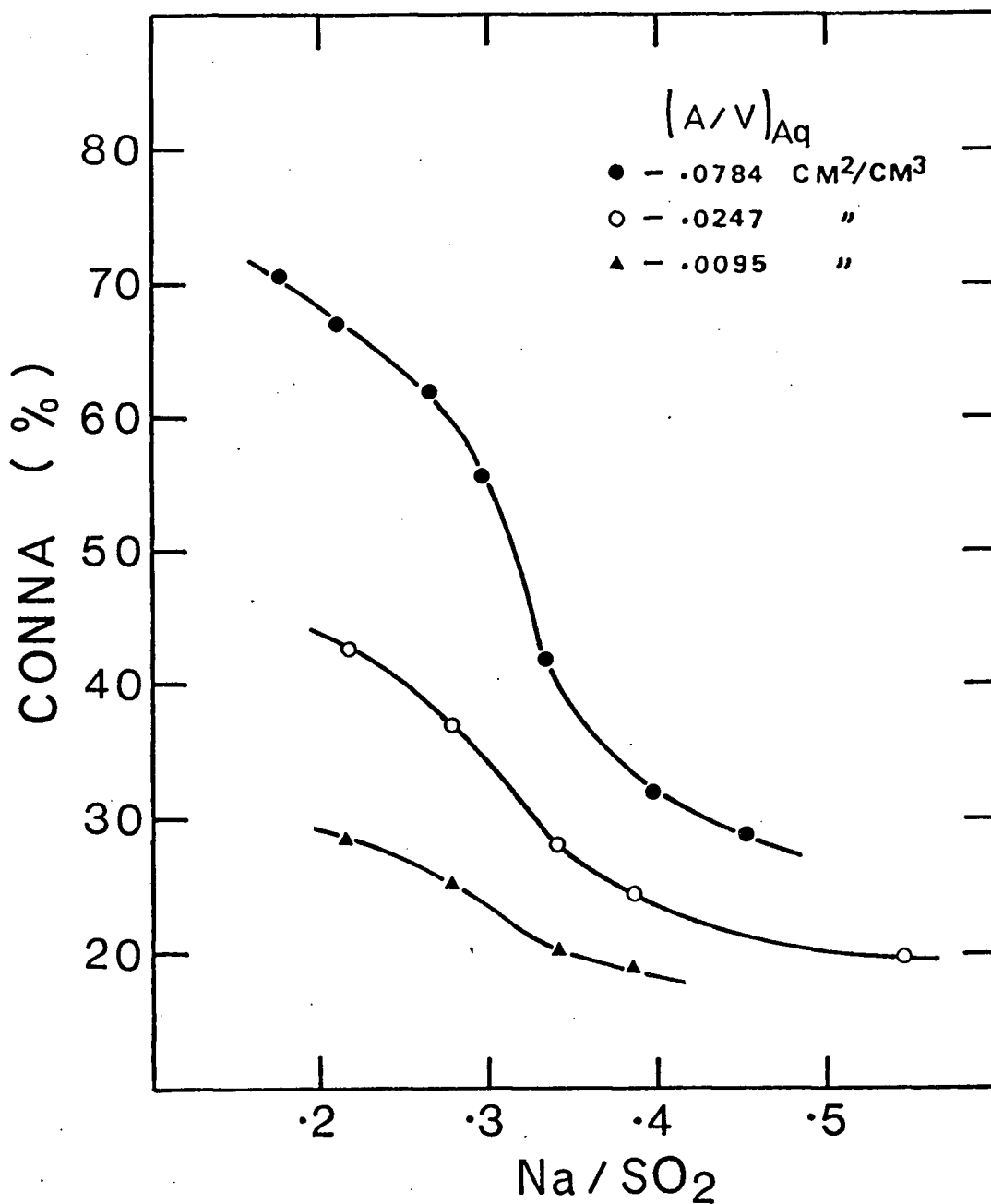


Figure 47 Steady-state yields of sodium dithionite on sodium consumed in the CFSTR versus Na/SO₂ ratios entering the CFSTR at different values of interfacial-area/aqueous-volume ratio. See Tables 6, 15 and 16 for the levels of the process variables

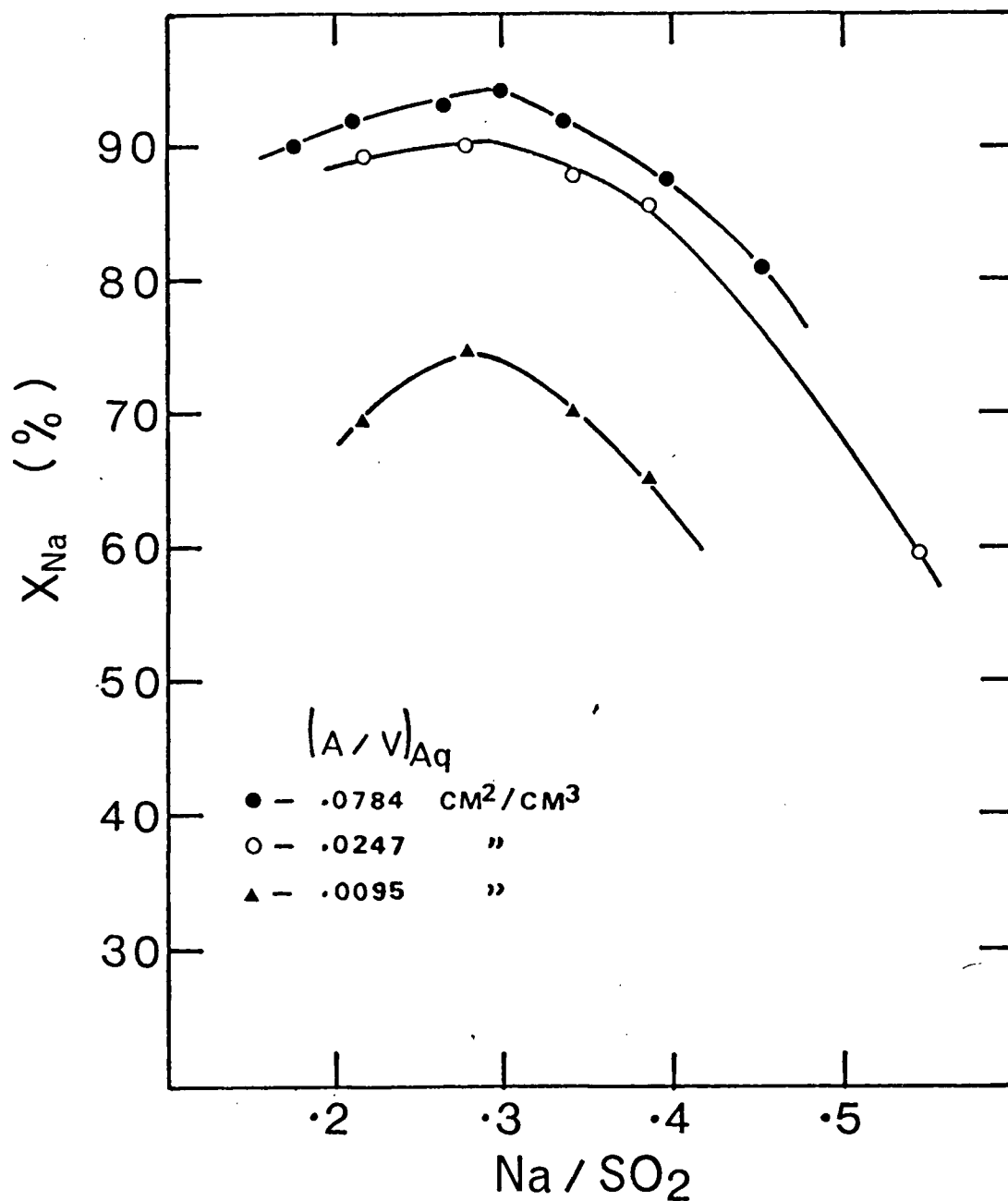


Figure 48 Steady-state conversions of sodium to different products in the CFSTR versus Na/SO₂ ratios entering the CFSTR at different values of interfacial-area/aqueous-volume ratio. See Tables 6, 15 and 16 for the levels of the process variables

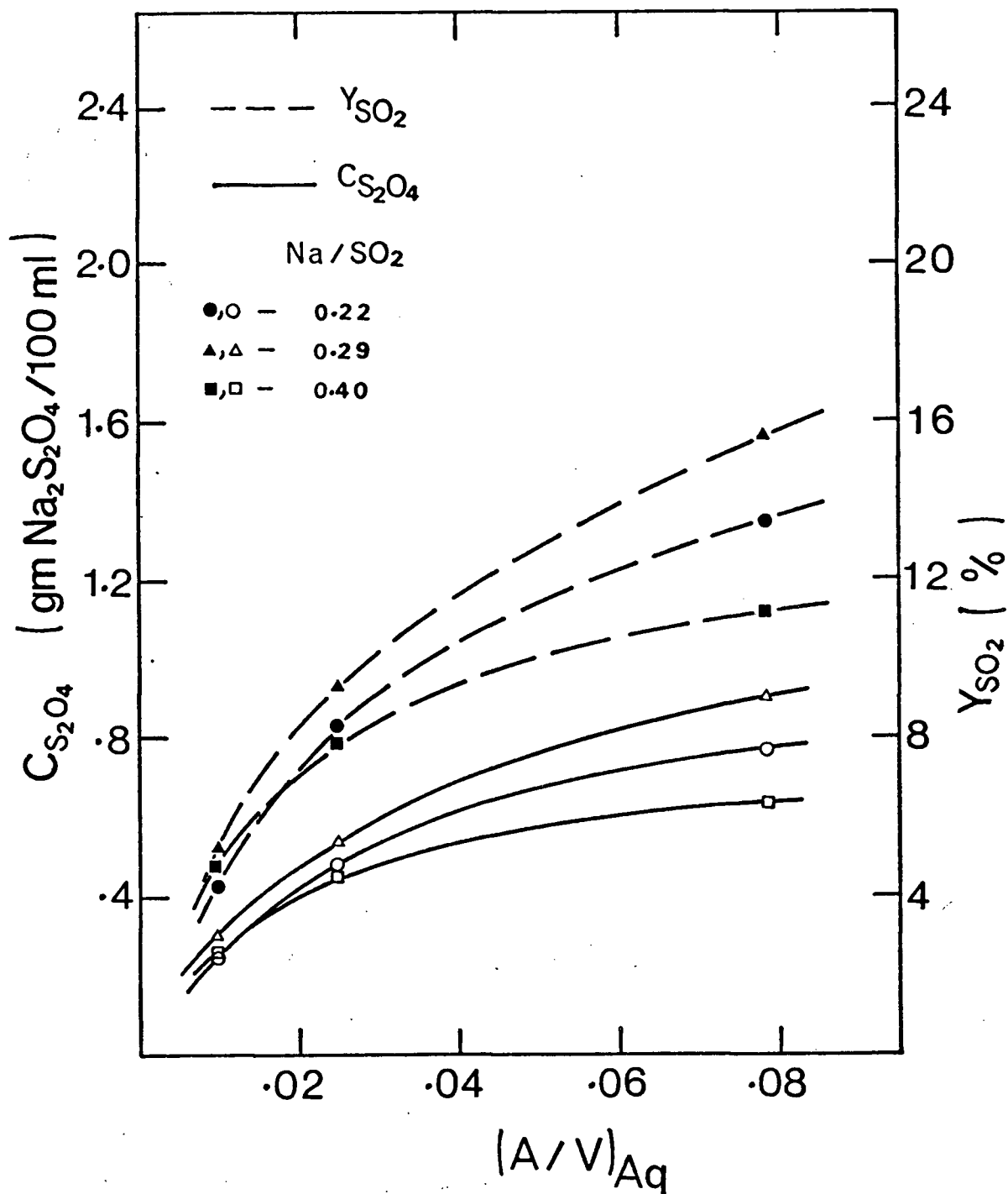


Figure 49 Steady-state values of sodium dithionite concentration and yield of sodium dithionite on sulfur dioxide in the aqueous feed versus interfacial-area/aqueous-volume ratios at different Na/SO_2 ratios entering the CFSTR. See Tables 6, 15 and 16 for the levels of the process variables

was found difficult to position it exactly horizontal. In other words, the interfacial-area/aqueous-volume ratio reported may have been less than the actual interfacial-area/aqueous-volume ratio. This problem could be avoided by using separate reactors with different interfacial-area/aqueous-volume ratios. However, this was not done in the present investigation.

6. Temperature of the aqueous phase

The experimental sets: 106-118 (expts. 106, 109, 112, 115 and 118), 65-77 and 110-113 (expts. 110 and 113) were performed to investigate the effect of variation in the temperature of the aqueous phase on the steady-state yields of sodium dithionite based on the sulfur dioxide entering the reactor (Y_{SO_2}) and on the sodium consumed in the reactor (CONNA).

The steady-state temperature of the aqueous phase in the reactor, for the sets: 106-118, 65-77 and 110-113, was 13°C, 17°C and 27°C respectively. Lower temperatures could not be obtained due to the exothermic nature of the reactions. The levels of the process variables, under the steady-state conditions are presented in Tables 17, 6 and 18.

The steady-state Y_{SO_2} and CONNA values are plotted against the Na/SO₂ ratios entering the reactor at the three temperatures of the aqueous phase. These curves are shown

TABLE 17

LEVELS OF THE PROCESS VARIABLES IN SET: 106-118

Range of the Changed Variable	VALUES OF THE FIXED VARIABLES						
CHGF	STSO ₂	(RPM) _{Aq}	FLSO ₂	FLHG	(A/V) _{Aq}	TEMP	pH
.0372 - .0951	.653 -.660	673	.096	47.5	.0784	13	5.55 - 6.0

TABLE 18

LEVELS OF THE PROCESS VARIABLES IN SET: 110-113

Range of the Changed Variable	VALUES OF THE FIXED VARIABLES						
CHGF	STSO ₂	(RPM) _{Aq}	FLSO ₂	FLHG	(A/V) _{Aq}	TEMP	pH
.0372 - .0646	.653 -.654	673	.096	47.5	.0784	27	5.7 - 5.9

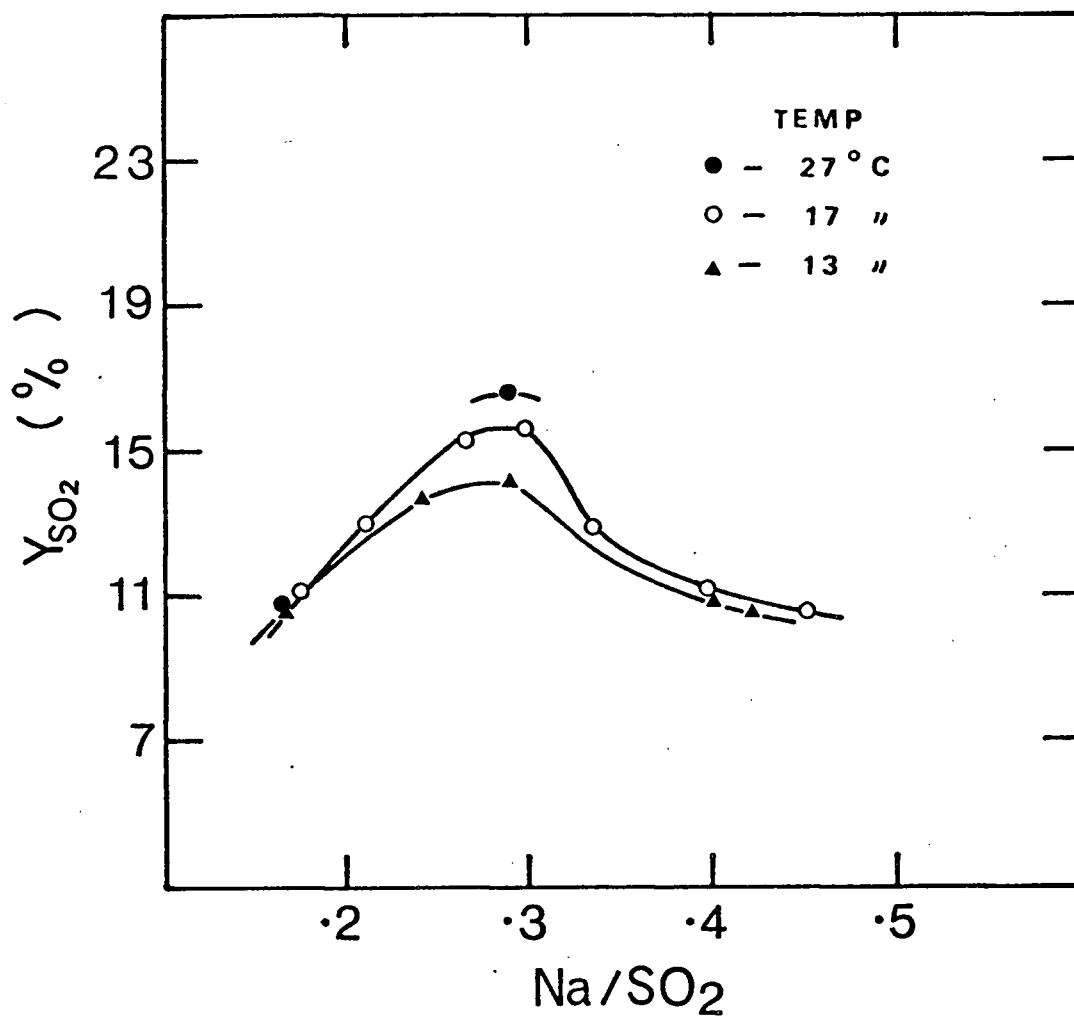


Figure 50 Steady-state yields of sodium dithionite on sulfur dioxide in the aqueous feed versus Na/SO₂ ratios entering the CFSTR at different steady-state temperatures of the aqueous phase. See Tables 6, 17 and 18 for the levels of the process variables

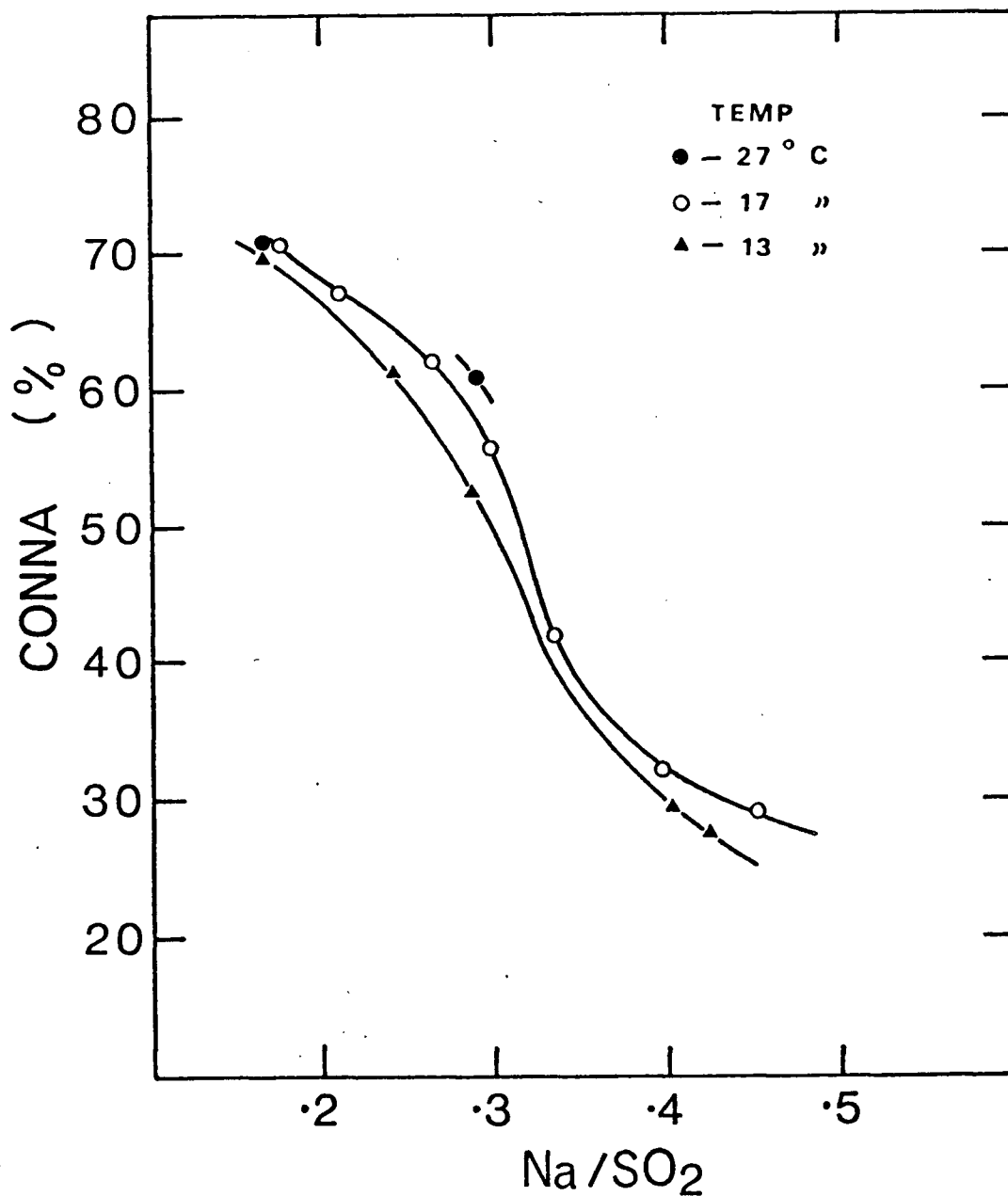


Figure 51 Steady-state yields of sodium dithionite on sodium consumed in the CFSTR versus Na/SO₂ ratios entering the CFSTR at different steady-state temperatures of the aqueous phase. See Tables 6, 17 and 18 for the levels of the process variables

in Figures 50 and 51 respectively. No curves are drawn for the set: 110-113 because there are only two experimental runs in this set.

Figure 50 shows that for different experimental sets (carried out at different temperatures), the maximum in the steady-state Y_{SO_2} versus Na/SO_2 curves is obtained at a Na/SO_2 ratio of 0.29. This figure also shows that there may be an optimum temperature at every Na/SO_2 ratio entering the reactor, above which the steady-state Y_{SO_2} would decrease.

7. pH of the aqueous phase

For all experimental runs discussed in the previous sections, the steady-state pH of the aqueous phase was in the recommended range (Section II.B.) of 5 to 6. To investigate the effect of a variation in the pH, some exploratory experimental runs (expts. 1 to 11) were performed where the pH of the aqueous phase was in the range 0.8 to 2.0. Various combinations of the other process variables were used in these experimental runs. In all these cases, the yields of sodium dithionite on sulfur dioxide entering the reactor were very small.

8. Flow rate of fresh amalgam, i.e. residence time in the amalgam phase

This process variable was not investigated systematically for the reasons outlined in the Section V.B.

However, a few experimental runs (expts. 5 to 11) were performed which gave interesting results.

When the flow rate of the fresh amalgam was increased such that the Na/SO₂ ratio entering the reactor was very high (greater than 1), a white precipitate of sulfur was obtained. It was noted that for none of the experiments was the pH of the aqueous phase less than 0.8.

CHAPTER VI

DISCUSSION

A. Model for the Reacting System in the Proposed Process

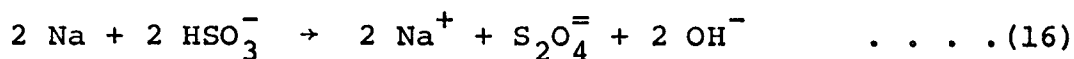
1. Development of the model

It was mentioned in Chapter III that Ketelaar (44) and Gerritsen (30) proposed models for the reacting system sodium-mercury amalgam and aqueous sulfur dioxide. According to Ketelaar's model, the overall rate of sodium dithionite formation is controlled by the rate of sodium mass-transfer to the amalgam-aqueous solution interface. Gerritsen's model does not take into consideration the heterogeneous decomposition of the dithionite formed at the interface and assumes a very simplified expression for the rate of the homogeneous decomposition of dithionite (i.e. rate is a function of the concentration of sodium dithionite in the bulk). Both these models were found inadequate to describe the results presented (Chapter V).

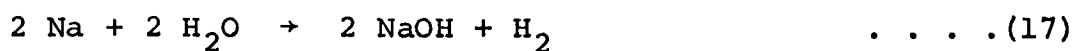
A model for the reacting system at a steady-state pH of 5 to 6 is developed on the basis of the experimental results obtained in this work and the information available in the literature. In the formulation of this model it was found necessary to consider the mass-transfer of different

reacting species in the amalgam and aqueous phases along with the following chemical reactions:

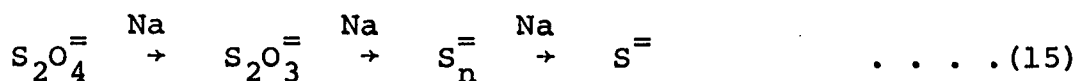
- The sodium dithionite formation reaction



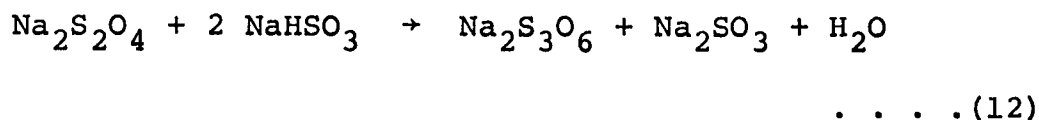
- The water reaction



- The heterogeneous decomposition of sodium dithionite



- The homogeneous decomposition of sodium dithionite



The oxidation of sodium dithionite was eliminated by providing an inert atmosphere of N_2 in the reactor system.

The experimental results indicate that the production of sodium dithionite in the amalgam process depends primarily upon the Na/SO_2 ratio entering the reactor which is related to the Na/SO_2 ratio in the reacting system. The former was controlled in the present investigation and will be called 'Na/SO₂ ratio' henceforth.

In all CFSTR experimental sets, where the concentration of sulfur dioxide in the feed solution was about 0.65 molar, the steady-state concentration of sodium dithionite ($C_{S_2O_4}$), yield of sodium dithionite on sulfur dioxide entering the reactor (Y_{SO_2}) and conversion of sodium to different products in the reactor (X_{Na}) show a maximum at a Na/SO₂ ratio of about 0.29. However, this ratio changes when the concentration of sulfur dioxide in the feed solution changes as shown in Figures 22, 25 and 28. The shift in maxima is probably due to the fact that these quantities are plotted against the Na/SO₂ ratios entering the reactor and not against the Na/SO₂ ratios in the bulk of the two phases. In any event, Figure 24 shows that if the molarity of sulfur dioxide in the aqueous feed solution is known, the concentration of sodium in the amalgam entering the reactor (therefore the Na/SO₂ ratio entering the reactor) at which maximum steady-state $C_{S_2O_4}$, Y_{SO_2} and X_{Na} are obtained, can be estimated. Further, the Na/SO₂ ratio of about 0.29 is not a magic number and it will change, for instance, if the level of turbulence in the amalgam phase is changed.

At values of the Na/SO₂ ratio below the steady-state $C_{S_2O_4}$ maximum, for all experimental sets, the consumption rate of sodium to produce sodium dithionite and other products is directly proportional to the Na/SO₂ ratio or to the concentration of sodium in fresh amalgam. For a typical set

this is shown in Figures 11 and 12 respectively. This result implies that the overall rate of $S_2O_4^{=}$ formation is limited by sodium mass-transfer rate to the interface in the range of Na/SO₂ ratios under consideration.

At values of the Na/SO₂ ratio above the steady-state sodium dithionite concentration maximum, for all experimental sets, the rate of sodium consumption is no longer a linear function of the Na/SO₂ ratio (Figure 11) or concentration of sodium in amalgam (Figure 12). This observation indicates that the mass-transfer of sodium to the interface is no longer the limiting step in the dithionite formation process in this Na/SO₂ ratio range.

The conclusions reached above are supported by evidence presented below which, in some cases, also indicates that at values of Na/SO₂ ratio above the steady-state $C_{S_2O_4}$ maximum, the mass-transfer rate of bisulfite ions in the aqueous phase controls the rate of dithionite formation.

(a) Figure 34 shows that the steady-state conversion of sodium to different products in the reactor (X_{Na}) above a Na/SO₂ ratio of 0.29 is increased significantly by increased stirring in the aqueous phase while at Na/SO₂ ratios below 0.29 the change is insignificant. Figure 30 shows that the rate of dithionite production above a Na/SO₂ ratio of 0.29 increased to a greater extent by increased agitation in the aqueous phase than at values of the Na/SO₂ ratio

below 0.29. These results would be expected if the sodium mass-transfer rate controlled the dithionite formation at values of Na/SO₂ ratio below 0.29 and if mass-transfer rate of bisulfite ions controlled at Na/SO₂ ratios greater than 0.29.

(b) Figures 14 to 17 show that at values of Na/SO₂ ratio above the steady-state C_{S₂O₄} maxima, the unsteady-state concentration profiles of sodium dithionite in the product stream and sodium in the outlet-amalgam (spent amalgam) show maxima and minima respectively. However such maxima and minima are not observed at Na/SO₂ ratios below the steady-state C_{S₂O₄} maxima.

It was discussed in Section II.F. that when sulfur dioxide gas is dissolved in water, depending on the pH of the solution, it can exist in the form of molecular sulfur dioxide, bisulfite ions or sulfite ions. Assuming unit activity coefficients for the different ionic and molecular species that exist when sulfur dioxide gas is dissolved in water, it was shown that most of the sulfur dioxide is available as bisulfite ions at a pH of about 4.5. Above this pH the concentration of sulfite ions increases and the concentration of bisulfite ions decreases. Sulfite ions, as mentioned in the previous sections, can not be reduced by sodium dissolved in mercury to give dithionite.

When an experimental run starts, the rate of sodium dithionite formation increases, thus increasing the concentration of dithionite in the product stream. Starting with the aqueous feed solution at pH = 3 to 3.5 and the system at unsteady-state the pH of the aqueous phase in the CFSTR increases and then attains a steady-state value in the range 5 to 6. At Na/SO₂ ratios above the steady-state C_{S₂O₄} maximum, as the pH of the aqueous phase increases above 4.5, the bulk concentration of the bisulfite ions in the reactor decreases. This decreases the rate of sodium dithionite formation, thus lowering the concentration of sodium dithionite in the product stream. As the same bulk concentration of the bisulfite ions is not available for dithionite formation, the concentration of sodium in the spent amalgam increases and then attains a steady-state value. These maxima and minima are not seen at Na/SO₂ ratios below the steady-state C_{S₂O₄} maxima because the rate of the sodium dithionite formation is controlled by the rate of mass-transfer of sodium from the bulk of the amalgam to the interface and at all times there are sufficient bisulfite ions present at the interface for the reaction.

Further confirmation of the explanation given above is obtained from Figures 18 and 19. These figures show that for the experimental run 65 a maximum and a minimum are observed in the curves obtained by plotting the concentration

of sodium dithionite in the product stream against time and the concentration of sodium in spent amalgam against time respectively. This experiment was done at a Na/SO₂ ratio above 0.29 and the pH of the aqueous phase increased from 3.53 to 6.0. On the other hand the unsteady-state concentration profiles for the experimental runs 71 and 77 do not show any maxima or minima. These experiments were also done at values of Na/SO₂ ratio above 0.29, but the pH of the aqueous phase was fixed at about 5.9 under the unsteady-state and steady-state conditions.

(c) Figure 22 shows that throughout the range of Na/SO₂ ratios investigated, when the concentration of sulfur dioxide in the feed solution increases at a fixed Na/SO₂ ratio, the rate of sodium dithionite formation increases. Figure 28 shows that in the range of relatively low Na/SO₂ ratios, when the concentration of sulfur dioxide is increased at a fixed Na/SO₂ ratio, the steady-state conversion of sodium to different products in the reactor (X_{Na}) does not change significantly. However, in the range of high Na/SO₂ ratios, the steady-state X_{Na} increases with molarity of sulfur dioxide at a fixed Na/SO₂ ratio. This indicates that at low Na/SO₂ ratios although the chemical reaction rates of the sodium consuming reactions may increase, the rate of sodium consumption is still limited by the rate of mass-transfer of sodium to the interface. This is not true at high Na/SO₂ ratios.

(d) Figure 41 shows that the steady-state conversion of sodium to different products in the reactor (X_{Na}) above a Na/SO₂ ratio of 0.29 is not changed significantly by increasing the flow rate of the aqueous feed solution (shortening the residence time in the aqueous phase). Similar behaviour is expected at Na/SO₂ ratios below 0.29 if the rate of sodium mass-transfer to the interface limits the rate of sodium consumption. However, Figure 41 shows that the steady-state X_{Na} increases with increase in the flow rate of the aqueous solution in this range of Na/SO₂ ratios. This observation is consistent with the above-mentioned conclusions as explained below.

During the experiments outlined in Section V.E.4., it was observed that an increase in the flow rate of the aqueous solution increases the level of turbulence in the amalgam phase. At low Na/SO₂ ratios, where the rate of sodium consumption is limited by the rate of mass-transfer of sodium from the bulk of the amalgam phase to the interface, increased turbulence in the amalgam phase would increase the rate of mass-transfer of sodium. At a fixed Na/SO₂ ratio (for values of Na/SO₂ ratio below 0.29), this increased sodium mass-transfer increases the steady-state X_{Na} value. At values of Na/SO₂ ratios above 0.29, the steady-state conversion of sodium to different products in the reactor (X_{Na}) does not increase because the rate of

sodium consumption is not controlled by the rate of mass-transfer of sodium to the interface.

The nature of the response curves obtained during the study and shown in Chapter V is not only affected by the sodium mass-transfer and bisulfite mass-transfer but is also strongly influenced by the chemical reactions taking place. Some of these reactions are listed at the start of this chapter (equations 16, 17, 15, 11 and 12). The relative importance of these reactions at different Na/SO₂ ratios is discussed below.

(i) Na/SO₂ ratios below the steady-state C_{S₂O₄} maximum

Figures 12 and 13 show that at very low concentrations of sodium in mercury (or the Na/SO₂ ratios) no sodium is consumed. However, as the Na/SO₂ ratio entering the reactor is increased, the rate of sodium consumption increases linearly. This is understandable because for all reactions of sodium-mercury amalgam with aqueous solutions, the oxidation potential of sodium at the mercury/water interface determines whether the reaction will take place. At very small concentrations of sodium in mercury, the oxidation potential of sodium is not sufficient to initiate a reaction. As the Na/SO₂ ratio is increased, the concentration of sodium in amalgam required to initiate different sodium-consuming reactions is reached.

It was concluded above that, in the region under consideration, the rate of sodium consumption is limited by the sodium mass-transfer rate to the interface. If it is assumed that only the sodium dithionite formation reaction takes place in this region then all of the sodium consumed by the aqueous phase would be used to give sodium dithionite. Under those conditions, the rate of sodium dithionite formation would increase proportionately with an increase in the rate of sodium consumption (therefore, with an increase in the Na/SO₂ ratio). If the above assumption were true and the values of steady-state yield of sodium dithionite on sodium consumed in the reactor (CONNA) were plotted against the Na/SO₂ ratios, a straight line with zero slope (CONNA = 100) would be expected.

However, this is not the case as shown in Figure 9. This figure shows the steady-state yield of sodium dithionite on sodium consumed (CONNA) for a typical set of experimental runs. It is proposed that the steady-state CONNA is less than 100 per cent due to the homogeneous decomposition of the dithionite in the bulk of the aqueous phase and the heterogeneous decomposition of the dithionite, produced at the interface, by the sodium transferred there. The rate of sodium consumption by the water reaction, under steady-state conditions, is expected to be negligible in the range of Na/SO₂ ratios below the steady-state C_{S₂O₄} maximum. The

information available in the literature (Section II.G.2.) shows that the water reaction takes place at the interface but its rate, in the pH range 4 to 10, is not limited by the mass-transfer rate of sodium to the interface; this rate is controlled by the rate of chemical reaction at the interface.

On the basis of the batch experiments and the information available in the literature (Section II.G.3.a.) homogeneous decomposition of sodium dithionite takes place as given by equations (11) and (12). The empirical expression for the rate of this decomposition has been outlined by Spencer (102).

$$r_{\text{homo}} = k_c [\text{S}_2\text{O}_4^{=}]^1 [\text{HSO}_3^-]^1 [\text{SO}_3^{=}]^0 [\text{H}^+]^x [\text{S}_2\text{O}_3^{=}]^y \dots (13)$$

From the experimental results it is concluded that, in the range of Na/SO₂ ratios under consideration, essentially all of the sodium transferred to the interface is consumed by the sodium dithionite formation reaction and the heterogeneous decomposition of dithionite. The results discussed below (α and β) imply that although the rate of sodium consumption by these two reactions is limited by the sodium mass-transfer rate to the interface, the product distribution depends on their relative reaction rates.

(α) Figures 25 and 27 show that in the region under consideration, when the concentration of sulfur dioxide in the aqueous feed solution is increased at a fixed Na/SO₂ ratio, the steady-state yields of sodium dithionite on sulfur dioxide (Y_{SO_2}) and on sodium consumed in the reactor (CONNA) increase, but the steady-state conversion of sodium in the reactor (X_{Na}) does not change significantly as shown in Figure 29. These results indicate that at a fixed Na/SO₂ ratio, an increase in the concentration of sulfur dioxide in the aqueous feed causes a greater increase in the rate of the sodium dithionite formation reaction than in the rate of the heterogeneous decomposition of the dithionite.

(β) Figures 31 and 33 show that below a Na/SO₂ of about 0.29, the steady-state Y_{SO_2} and CONNA increase at a fixed Na/SO₂ ratio with an increase in the level of agitation in the aqueous phase. However, the increase in the steady-state X_{Na} at that Na/SO₂ ratio is negligible as shown in Figure 35. These results indicate that in the region under consideration, an increase in the level of agitation in the aqueous phase at a fixed Na/SO₂ ratio increases the rate of sodium dithionite formation more than the rate of the heterogeneous decomposition of the dithionite.

(γ) For a typical experimental set the rate of the sodium dithionite formation reaction increases with increasing Na/SO₂ ratios because in the region under consideration

the rate depends on the sodium mass-transfer rate to the interface. The rate of the homogeneous decomposition of dithionite also increases because the concentrations of the $S_2O_4^{=}$ ions and the $S_2O_3^{=}$ ions increase. However, it is doubtful that the homogeneous decomposition of the dithionite alone would cause such a decrease in the steady-state CONNA with increasing Na/SO₂ ratio as shown in Figure 9.

(ii) Na/SO₂ ratios above the steady-state $C_{S_2O_4}$ maximum

It was concluded earlier that in this region, the rate of sodium consumption is not limited by the sodium mass-transfer rate to the interface. Further, it was concluded that the rate of the sodium dithionite formation reaction is limited by bisulfite mass-transfer to the interface. In other words, for an experimental set where the concentration of sulfur dioxide in the aqueous feed is fixed, the rate of the sodium dithionite formation reaction increases to a maximum value with increasing Na/SO₂ ratios.

An equation for the rate of homogeneous decomposition of the dithionite was given by Spencer (equation 13). This rate probably increases as the Na/SO₂ ratio is increased above the value corresponding to a maximum steady-state concentration of sodium dithionite in the product stream. The increase in the rate would be due to increase in the concentration of $S_2O_3^{=}$ ions which are a product of the homogeneous and heterogeneous decomposition reactions. As the Na/SO₂

ratio is further increased the rate of homogeneous decomposition is expected to attain its maximum value because the concentration of dithionite in the bulk of the aqueous phase decreases. This is indicated by the gradual levelling off of the steady-state $C_{S_2O_4}$ versus Na/SO_2 curves at high values of the Na/SO_2 ratio for all of the experimental sets.

The occurrence of the heterogeneous decomposition of the dithionite, at least at very high values of the Na/SO_2 ratio, is indicated by the results presented in sections V.A.3. and V.E.8. (in conjunction with Section V.A.2.).

For none of the experimental runs outlined in Section V.E.8. was the pH of the aqueous phase less than 0.8, so the sulfur could not have formed due to the auto-decomposition of sodium dithionite (see Section V.A.2.). Most probably, the sulfur was formed by the oxidation of the sulfide ions by the sulfur dioxide present in the aqueous phase. These sulfide ions were formed by the heterogeneous decomposition of sodium dithionite at the interface (equation 3). In view of the occurrence of this reaction at Na/SO_2 ratios below the steady-state $C_{S_2O_4}$ maximum and at very high Na/SO_2 ratios, it is logical to assume its presence in the intermediate range of Na/SO_2 ratios. The experimental results tend to support this. For a typical experimental set, Figure 9 shows that the steady-state $C_{S_2O_4}$ decreases sharply when the Na/SO_2 ratio is increased above 0.29 and then tends to level off. It is unlikely that the sharp fall

in the steady-state concentration of sodium dithionite in the product stream ($C_{S_2O_4}$) is caused by the homogeneous decomposition of the dithionite alone. These results also imply that the rate of heterogeneous decomposition of the dithionite, immediately above Na/SO₂ ratio of about 0.29, increases with an increase in the Na/SO₂ ratio. This can happen if the rate of this reaction is limited by the rate of chemical reaction at the interface. However, at very high Na/SO₂ ratios the steady-state $C_{S_2O_4}$ versus Na/SO₂ ratio curve tends to level off implying that the rate of the heterogeneous decomposition also attains its maximum value. This suggests that the rate of this reaction at very high Na/SO₂ ratios is controlled by the removal rate of the $S_2O_4^{=}$ ions from the interface.

The following discussion indicates that at values of Na/SO₂ ratios above the steady-state $C_{S_2O_4}$ maximum, the interfacial concentration of sodium in mercury required to initiate the water reaction is reached.

(α) Figure 9 shows that the steady-state yield of sodium dithionite on sodium consumed in the reactor (CONNA) falls very sharply at Na/SO₂ ratios above 0.29; the fall is gradual at very high Na/SO₂ ratios. The sharp fall in the steady-state CONNA is observed because the rate of the sodium dithionite formation reaction does not change with an increase in the Na/SO₂ ratio but the rate of the water

reaction and the rates of the heterogeneous and homogeneous decomposition of the dithionite increase. Thus, an increasing proportion of the sodium transferred to the interface is used up by the water reaction and the heterogeneous decomposition of the dithionite. The decrease in the steady-state CONNA is more gradual at very high Na/SO₂ ratios because the rates of the heterogeneous and homogeneous decomposition reactions depend upon S₂O₄⁼ concentration and hence do not increase indefinitely.

(β) The curve obtained by plotting the rate of sodium consumption against the concentration of sodium in the fresh amalgam (CHGF) for an experimental set shows that at very high values of CHGF (or Na/SO₂ ratio) the rate of sodium consumption increases gradually with an increase in CHGF. The general nature of this curve, in the region under consideration, is similar to that expected for the water reaction as outlined by Dunning and Kilpatrick (20) [Section II.G.2.].

2. The model

At fixed levels of all the other process variables, when the concentration of sodium in the amalgam entering the reactor increases (the Na/SO₂ ratio increases at a fixed conc. of SO₂ in the feed), the steady-state concentration of sodium dithionite in the reactor passes through a

maximum. The processes occurring in the reactor, at a steady-state pH of 5 to 6 and in the inert atmosphere of N_2 , may be described as follows:

(a) Na/SO_2 ratios below the steady-state $C_{S_2O_4}$ maximum

At very small concentrations of sodium in mercury (or low Na/SO_2 ratios), the oxidation potential of sodium is not sufficient to initiate any reaction. As the Na/SO_2 ratio entering the reactor is increased, the threshold concentration of sodium in mercury required to initiate the sodium dithionite formation reaction is reached. Once the dithionite ions start forming at the interface, their heterogeneous and homogeneous decomposition also start.

In the region under consideration the sodium dithionite formation reaction and the heterogeneous decomposition of the dithionite are the important sodium consuming reactions. The rate of sodium consumption by these reactions is limited by the sodium mass-transfer rate to the interface, however, the product distribution depends on their relative reaction rates.

As the Na/SO_2 ratio increases towards the value corresponding to maximum steady-state sodium dithionite concentration ($C_{S_2O_4}$), the rate of mass-transfer of sodium to the interface increases which in turn increases the rates of the sodium dithionite formation reaction and the hetero-

geneous decomposition of the dithionite. The rate of homogeneous decomposition of dithionite also increases [see equation 13 by Spencer (102)]. However, the increase in the rate of sodium dithionite formation is greater than the increase in the rate of its decomposition.

(b) Na/SO_2 ratios above the steady-state $\text{C}_{\text{S}_2\text{O}_4}$ maximum

When the Na/SO_2 ratio is increased above the value corresponding to the steady-state $\text{C}_{\text{S}_2\text{O}_4}$ maximum, the concentration of sodium in the amalgam interface increases and the threshold concentration of sodium in the mercury required to initiate the water reaction is reached. Therefore, the sodium transferred to the interface is consumed by the sodium dithionite formation reaction, the heterogeneous decomposition of the dithionite and the water reaction. However, in the region under consideration the rate of sodium consumption by these reactions is not limited by the sodium mass-transfer rate to the interface.

The rate of the sodium dithionite formation reaction is limited by the rate of mass-transfer of bisulfite ions to the interface. This rate does not change with increasing Na/SO_2 ratio.

The rate of the heterogeneous decomposition of sodium dithionite is controlled by the rate of chemical reaction at the interface and this rate increases with increasing Na/SO_2 ratio. At very high values of Na/SO_2 ratio the rate

of this reaction becomes controlled by the removal rate of the $S_2O_4^{=}$ ions from the interface and tends to attain its maximum value.

The rate of sodium consumption by the water reaction is controlled by the rate of chemical reaction at the interface. This rate can be given by the empirical expression (equation 10) derived by Dunning and Kilpatrick (20). The rate increases with increasing Na/SO₂ ratio.

The rate of homogeneous decomposition of the dithionite may be given by Spencer's (102) expression shown in equation 13. This rate increases with increasing Na/SO₂ ratio. However, at very high values of the Na/SO₂ ratio the rate of homogeneous decomposition tends to attain a maximum value.

B. Conditions for Improving The Yields of Sodium Dithionite In The Proposed Process

It was mentioned in Chapter I that for the proposed process the steady-state yields of sodium dithionite on sulfur dioxide entering the reactor (Y_{SO_2}) and on sodium consumed in a single pass (CONNA) must be economical. The experimental results show that the conditions for the highest yield on sulfur dioxide are different from the

conditions for the highest yield on sodium consumed. Therefore, the relative costs of the reacting chemicals must be considered.

Figure 10 shows the variation of steady-state CONNA and Y_{SO_2} as a function of the concentration of sodium in fresh amalgam for a typical set of experimental runs where all the other process variables were kept fixed. This figure demonstrates that, for such an experimental set, the highest steady-state CONNA is obtained at a concentration of sodium in the amalgam where the steady-state Y_{SO_2} is relatively small.

Figures 25 and 27 show that at a fixed Na/SO₂ ratio entering the reactor, the steady-state yields on sulfur dioxide in the feed and on sodium consumed in a single pass increase with an increase in the concentration of sulfur dioxide in the feed. At a fixed Na/SO₂ ratio, there may, however, be an optimum concentration of sulfur dioxide in the aqueous feed solution above which the steady-state Y_{SO_2} would decrease. There may be such an optimum concentration of sulfur dioxide for the steady-state CONNA also. These concentrations could not be determined in the present investigation because an aqueous sulfur dioxide solution whose concentration is substantially greater than 1.30 molar would require pressurization of the reactor system.

Figure 24 shows that when the concentration of sulfur dioxide in the aqueous feed is increased, the concentration

of sodium in the fresh amalgam at which maximum steady-state Y_{SO_2} is obtained in a set of experimental runs (critical CHGF) also increases. The critical concentration of sodium in fresh amalgam for the experimental set performed at 1.30 molar sulfur dioxide in the feed was about 0.1439 per cent. The results show that the steady-state Y_{SO_2} and CONNA under these conditions are higher than the steady-state values of these quantities, under critical conditions, at 0.65 molar or 0.4 molar sulfur dioxide. The critical CHGF would increase with a further increase in the molarity of sulfur dioxide in the aqueous feed and the steady-state Y_{SO_2} and CONNA may also increase. These concentrations of sodium in fresh amalgam are well outside the limits recommended for the sodium amalgam: $SO_2 - NaHSO_3/Na_2SO_3$ buffer process (Section II.B.) by previous investigators. This is understandable, because the previous workers were primarily interested in the yield of sodium dithionite on sodium consumed.

Figures 31 and 33 show that an increase in the level of agitation in the aqueous phase increases the desired yields. The increase in the steady-state Y_{SO_2} was found to be greater at values of Na/ SO_2 ratio above the steady-state Y_{SO_2} maximum. For the reasons given in Section V.E.3. the effect of agitation in the aqueous phase could not be investigated exclusively at propeller speeds above 700 rpm.

Figures 38 and 40 show the variation in the values of steady-state Y_{SO_2} and CONNA as a function of the flow rates of the aqueous solution. The recommendation by previous investigators that the residence time of the aqueous solution in the reactor should be as short as possible (Section II.B) does not seem to be correct. The model based on the experimental results suggests that there would be an optimum residence time in the aqueous phase at different Na/SO₂ ratios below which the steady-state Y_{SO_2} and CONNA may decrease.

Figures 45 and 47 show that at a fixed Na/SO₂ ratio entering the reactor, the steady-state yields of sodium dithionite on sulfur dioxide in the feed (Y_{SO_2}) and on sodium consumed in the reactor (CONNA) increase with an increase in the interfacial-area/aqueous-volume ratio. Figure 49 shows that at different Na/SO₂ ratios investigated this relationship is nonlinear. The decrease in the steady-state CONNA values with a decrease in the interfacial-area/aqueous-volume ratio, at a fixed Na/SO₂ ratio was unexpected. This was probably caused by the manner in which the experiments were conducted. The discs which were introduced to decrease the interfacial-area/aqueous-volume ratio were of a finite thickness. When they were introduced, the level of turbulence in the aqueous phase at the interface, where the sodium consuming reactions take place, decreased. That

probably decreased the rate of sodium dithionite formation/ rate of the heterogeneous decomposition ratio.

Figures 50 and 51 shows that at certain Na/SO₂ ratios entering the reactor an increase in temperature increases the steady-state Y_{SO₂} and CONNA. The experimental results suggest that there may be optimum temperatures at every Na/SO₂ ratio above which the steady-state Y_{SO₂} and CONNA will decrease.

For most of the experimental runs done in this investigation, the steady-state pH of the aqueous phase was in the range 5 to 6. This range has been recommended by previous investigators (Section II.B). Few experimental runs that were done at very low pH values (0.8 to 2.0) gave very poor yeilds. When the pH is lowered, the rates of the homogeneous decomposition of the dithionite and the water reaction increase. The rate of the sodium dithionite formation reaction is also expected to increase with limited pH decrease because the effective diffusivity of sulfur dioxide solutions in the aqueous phase would increase as would the concentration of bisulfite ions.

The model for the reacting system based on the experimental results suggests that at values of the Na/SO₂ ratio where the rate of sodium consumption is limited by the sodium mass-transfer rate, the steady-state Y_{SO₂} and CONNA would increase with an increase in the agitation in the amalgam phase. This information may be of a special

interest from the point of view of selecting the operating conditions for the proposed process. It was mentioned earlier that at relatively low Na/SO₂ ratios, in the region under consideration, the steady-state CONNA is high but the steady-state Y_{SO₂} is low. Considering the fact that both of these yields affect the cost of the product, it may be advantageous to increase the level of agitation in the amalgam phase at relatively low Na/SO₂ ratios.

At fixed levels of all the other process variables if the flow rate of the amalgam is increased, the effect on the yields would be the same as if the Na/SO₂ ratio and the agitation in the amalgam phase had been increased.

C. Economic Feasibility of the Proposed Process

Experimental run 44 was chosen for costing. For this run, under the steady-state conditions, the concentration of sodium dithionite in the product stream,

$$C_{S_2O_4} = 2.3 \text{ gms Na}_2S_2O_4/100 \text{ ml}$$

the yield of sodium dithionite on the total sulfur dioxide entering the reactor,

$$Y_{SO_2} = 20.4\%$$

the yield of sodium dithionite on the sodium consumed in the reactor,

$$CONNA = 67\%$$

the yield of sodium dithionite on sodium entering the reactor with the fresh amalgam

$$Y_{Na} = 63\%$$

the conversion of sodium from the amalgam to different products in the reactor,

$$X_{Na} = 95.1 \%$$

The levels of the process variables are presented in the Table 19.

TABLE 19

LEVELS OF THE PROCESS VARIABLES FOR THE RUN 44

CHGF (%)	StSO ₂ (moles) (lit)	(RPM) _{Aq} (rpm)	FLSO ₂ (lit) (min)	FLHG (ml) (min)	(A/V) _{Aq} ($\frac{\text{cm}^2}{\text{cm}^3}$)	TEMP (°C)	pH
.1439	1.297	673	.096	47.5	.0784	17	5.75

BASIS: 100 lb moles of total sulfur dioxide in the aqueous feed.

The overall sodium dithionite formation is:



For every 100 lb moles of the total sulfur dioxide in the feed, 20.4 lb moles are converted to give sodium dithionite.

By stoichiometry, 20.4 lb moles of the sulfur dioxide give = $1/2 \times 20.4 = 10.2$ lb moles of $\text{Na}_2\text{S}_2\text{O}_4$. Further 10.2

lb moles of $\text{Na}_2\text{S}_2\text{O}_4$ contains = $2 \times 10.2 = 20.4$ lb atoms

of sodium. The yield of sodium dithionite on sodium consumed = 67 per cent.

•• Total sodium consumed to give 10.2 lb moles of sodium

$$\text{dithionite} = \frac{20.4}{0.67} = 30.45 \text{ lb atoms.}$$

It was shown in Chapter I that, the cost of sodium in the amalgam $\approx 5\text{¢}/\text{lb}$, and the cost of SO_2 gas $\approx 1.5\text{¢}/\text{lb}$

•• The chemical cost of sodium dithionite

$$= \frac{100 \times 64 \times 1.5 + 30.45 \times 23 \times 5}{10.2 \times 174}$$

$$= 7.4\text{¢}/\text{lb of sodium dithionite}$$

The chemical cost of the dithionite ions produced by the

$$\text{proposed process} = 7.4 \times \frac{174}{128}$$

$$\approx 10\text{¢}/\text{lb } \text{S}_2\text{O}_4^=$$

A small correction could be made for the cost of caustic soda used to adjust the pH of the aqueous sulfur dioxide solution.

The actual cost of sodium dithionite produced by the proposed process would be higher because it would also include the capital and operating costs. However, this cost can be reduced by increasing the yields of $\text{Na}_2\text{S}_2\text{O}_4$ on sulfur dioxide entering the reactor and on sodium consumed in the reactor which can be accomplished by changing the levels of certain process variables as discussed in the last section.

By comparison, zinc dithionite produced from zinc dust at 19¢/lb and sulfur dioxide at 1.5¢/lb, assuming 100% yields on both zinc and sulfur dioxide, gives dithionite at a cost of about 11¢/lb of $\text{S}_2\text{O}_4^{=}$ ions for chemicals alone. The actual cost of ZnS_2O_4 produced in pulp mills, considering lower yields, capital and operating costs, is approximately 16¢/lb of $\text{S}_2\text{O}_4^{=}$ ions.

Thus, it seems economically feasible for a pulp mill to change from zinc dithionite produced *in situ* to sodium dithionite produced by the proposed process without involving extra cost. Additional advantages of the proposed process are that it can run in conjunction with Castner-Kellner type cells and does not discharge zinc ions to the effluent receiving waters.

D. Reactor for the Proposed Process

The bench-scale experiments provide information on the type of reactor which would be suitable for the proposed process. The chosen reactor should be such that it would be possible to have large interfacial-area/aqueous-volume ratio, high level of agitation in the aqueous and amalgam phases and high concentration of sulfur dioxide in the aqueous feed solution.

The reactor used in the present investigation (CFSTR) has the advantages that it does not allow much entrainment of mercury in the product stream and permits fairly good control of the variables such as concentration of sodium in the feed-amalgam, flow rates of the sulfur dioxide solution and the amalgam, temperature and pH. It can be improved by redesigning it so that it has larger interfacial-area/ aqueous-volume ratio. The level of agitation in the amalgam phase can be increased by providing a stirrer and baffles in that phase and the concentration of sulfur dioxide in the aqueous feed can be increased by pressurizing the reactor system.

CHAPTER VII

CONCLUSIONS

1. It is possible to produce sodium dithionite as a relatively dilute (approximately 1-2%) water solution from sodium-mercury amalgam and sulfur dioxide in a simple "once-through" reactor [proposed process]. This solution could be used directly for the brightening of groundwood pulp.
2. The proposed process to produce sodium dithionite can economically compete with the manufacture of zinc dithionite *in situ*.
3. The reactor chosen for the proposed process should be such that it would be possible to have large interfacial-area/aqueous-volume ratio, high level of agitation in the aqueous and amalgam phases and high concentration of sulfur dioxide in the aqueous feed solution. Further, it should permit good control of the variables such as concentration of sodium in the feed-amalgam, the flow rates of the sulfur dioxide solution and the amalgam, temperature and pH.
4. The models suggested by Ketelaar (44) and Gerritsen (30) are inadequate to explain the experimental results

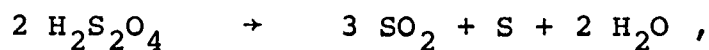
obtained in this investigation. To formulate a model for the reacting system sodium-mercury amalgam and aqueous sulfur dioxide, at a steady-state pH of about 5 to 6 and in the inert atmosphere of N_2 , it is necessary to consider mass-transfer of the reacting species in the amalgam and aqueous phases along with the chemical reactions such as the sodium dithionite formation reaction, the homogeneous and heterogeneous decomposition of the dithionite and the water reaction.

5. The production of sodium dithionite in the proposed sodium amalgam process depends primarily upon the Na/SO_2 ratios entering the reactor. At fixed levels of all the other process variables, when the concentration of sodium in the amalgam entering the reactor increases (the Na/SO_2 ratio entering the reactor increases at a fixed concentration of sulfur dioxide in the aqueous feed solution), the steady-state values of the concentration of sodium dithionite in the reactor, the yield of sodium dithionite on sulfur dioxide in the aqueous feed and the conversion of sodium to different products in the reactor pass through a maximum. The steady-state values of the yield of sodium dithionite on sodium entering with the mercury and on sodium consumed in the reactor decrease with increasing Na/SO_2 ratio.

6. At Na/SO_2 ratios below the steady-state sodium dithionite concentration maximum, the rate of sodium consumption is limited by the sodium mass-transfer rate to the interface. At Na/SO_2 ratios above the steady-state sodium dithionite concentration maximum, the rate of sodium consumption is not limited by the sodium mass-transfer rate to the interface.
7. At Na/SO_2 ratios below the steady-state sodium dithionite concentration maximum, the rate of the sodium dithionite formation reaction is controlled by the rate of sodium mass-transfer to the interface, but at Na/SO_2 ratios above the steady-state sodium dithionite concentration maximum, the rate of the sodium dithionite formation reaction is controlled by the mass-transfer rate of bisulfite ions to the interface.
8. When the steady-state pH of the aqueous phase in the reactor is between 5 to 6, the proportion of sodium consumed by the water reaction is small at Na/SO_2 ratios below the steady-state sodium dithionite concentration maximum.
9. At Na/SO_2 ratios below the steady-state sodium dithionite concentration maximum, the rate of the heterogeneous decomposition of the dithionite is limited by the sodium mass-transfer rate to the interface. At Na/SO_2 ratios

above the steady-state sodium dithionite concentration maximum, this rate is controlled by the chemical reaction at the interface. However, at very high Na/SO₂ ratios the rate of this reaction is controlled by the removal rate of the dithionite ions from the interface.

10. The auto-decomposition of the dithionite according to the equation,



in the pH range 0.8 to 6 is negligibly small under the conditions of the present investigation.

CHAPTER VIII

RECOMMENDATIONS FOR FURTHER WORK

1. The reactor used in the present investigation (CFSTR) should be redesigned or another type of reactor should be chosen according to the guidelines given in the discussion (Chapter VI). Then the proposed process should be optimized at a pilot-scale.
2. Further studies should be conducted to elucidate the processes in the reactor at lower values of pH (pH below 4).
3. The mercury content of the product stream should be determined to see if the product meets the pollution standards. If not, then the process should be modified along the lines suggested in Chapter 2.
4. If possible, the kinetics of the sodium dithionite formation reaction and the heterogeneous decomposition of the dithionite should be investigated separately.
5. The effect of variation in the concentration of electrolytes used in the proposed process on the rate of the water reaction should be investigated.

6. A quantitative expression should be determined for the rate of homogeneous decomposition of the dithionite. It would be of special interest to know how this rate is quantitatively affected by change in the concentration of $S_2O_3^{=}$ ions.
7. The mean activity coefficients of the ionic species and activity coefficients of molecular species present in the $SO_2 - H_2O$ system should be determined at high concentrations of SO_2 gas in water (.5 to 2 molar).

CHAPTER IX

NOMENCLATURE

Symbol	Explanation	Typical Units
a	Activity of the indicated species in equations (1), (2), and (3)	gm moles/liter
A	Surface area of interface	cm ²
(A/V) _{Aq}	Interfacial-area/aqueous-volume ratio	cm ² /cm ³
CHGF	Concentration of sodium in fresh amalgam	$\frac{\text{gm Na}}{100 \text{ gm amalgam}}$
CHGS	Concentration of sodium in spent amalgam	$\frac{\text{gm Na}}{100 \text{ gm amalgam}}$
C _{Na}	Concentration of sodium in amalgam	$\frac{\text{gm moles}}{\text{liter}}$
CONNA	Yield of sodium dithionite on sodium consumed	%
C _{S₂O₄}	Concentration of sodium dithionite in the product stream	gm/100 ml
D	Diffusion coefficient	cm ² /sec
E°	Standard oxidation potential on hydrogen scale at 25°C	volts
E _{1/2}	Half-wave potential (reduction potential)	volts
ECONNA	The 95 per cent confidence limits of CONNA	
EX _{Na}	The 95 per cent confidence limits of X _{Na}	
EY _{Na}	The 95 per cent confidence limits of Y _{Na}	
EY _{SO₂}	The 95 per cent confidence limits of Y _{SO₂}	

Symbol	Explanation	Typical Units
f	Activity coefficient of the indicated species in equations (1), (2), and (3)	
FLHG	Flow rate of sodium-mercury amalgam	ml/min
FLSO ₂	Flow rate of aqueous sulfur dioxide solution	liter/min
ΔH°	Heat of formation of sodium dithionite at 25°C	Kcal/gm moles
k _o	Reaction rate constant for the oxidation of sodium dithionite	$\left(\frac{\text{g moles}}{\text{liter}}\right)^{-\frac{1}{2}}(\text{sec})^{-1}$
k _c	Reaction rate constant for the homogeneous decomposition of sodium dithionite in equation (13)	
k _{water}	Reaction rate constant for the water reaction in equation (10)	
K ₁	Thermodynamic ionization constant for the first dissociation of SO ₂ ·H ₂ O in equation (2)	
K ₂	Thermodynamic ionization constant for the second dissociation of SO ₂ ·H ₂ O in equation (3)	
K _{hs}	Thermodynamic equilibrium constant for SO ₂ ·H ₂ O system in equation (1)	$\frac{\text{gm moles}}{\text{lit atm}}$
M	The Na/SO ₂ ratio for a set of experimental runs at which maximum steady-state C _{S₂O₄} is obtained	
Na/SO ₂	Ratio of sodium to sulfur dioxide entering the reactor	
pH	pH of the aqueous phase	$-\log \frac{(\text{gm ions of H}^+)}{\text{liter}}$
P _{SO₂}	Pressure of sulfur dioxide gas	atm

Symbol	Explanation	Typical Units
r_{homo}	Rate of homogeneous decomposition of sodium dithionite	$\frac{\text{gm moles}}{\text{cm}^3 \text{ min}}$
$r_{\text{oxidation}}$	Rate of oxidation of sodium dithionite	$\frac{\text{gm moles}}{\text{liter sec}}$
$(\text{RPM})_{\text{Aq}}$	Speed of the marine propeller	rev/min
STRUB	Weight of sodium dithionite which would discolour 5 ml of a standard Rubine-R solution	gms
STSO_2	Concentration of total sulfur dioxide in the aqueous feed solution	$\frac{\text{gm moles}}{\text{liter}}$
TEMP	Temperature of the aqueous phase	$^{\circ}\text{C}$
V	Volume of the aqueous phase	cm^3
VDITHI	Volume of the product stream required to discolour 5 ml of a standard Rubine-R solution	ml
x	Variable exponent in the rate equation (13)	%
X_{Na}	Conversion of sodium from the amalgam to different products in the reactor	%
y	Exponent in the rate equation (13)	
Y_{Na}	Yield of sodium dithionite on sodium entering the reactor	%
Y_{SO_2}	Yield of sodium dithionite on sulfur dioxide entering the reactor	%

BIBLIOGRAPHY

1. Anderson, J.S. and Saddington, K., J. Chem. Soc., 381 (1949).
2. Anon., Chem. Eng., p. 146, Aug. (1952).
3. Astarita, G., "Mass-transfer With Chemical Reaction," Elsevier Publishing Co., New York (1967).
4. Bain, E.C. and Withrow, J.R., J. Phys. Chem., 25, 535 (1921).
5. Baly, E.C.C. and Bailey, R.A., J. Chem. Soc., 121, 1813 (1922).
6. Bassett, H. and Durrant, R.G., J. Chem. Soc., 2, 1401 (1927).
7. Bent, H.E., J. Phys. Chem., 37, 431 (1933).
8. BIOS Report 271 (PB 22049).
9. BIOS Report 422 (PB 34027).
10. BIOS Final Report 1373 (1947).
11. Briamacombe, J.K., Graves, A.D. and Inman, D., Chem. Eng. Sci., 25, 1817 (1970).
12. Brönsted, J.N. and Kane, N.L.R., J. Am. Chem. Soc., 53, 3624 (1931).
13. Chappell, N., Soc. of Dyers and Colourists J., 37, 206 (1921).
14. Chassain, Y. and Ostertag, H., Compt. Rend., 242, 1732 (1956).
15. Cholette, A. and Cloutier, L., Can. J. Chem. Eng., 37, 105 (1959).
16. CRC Handbook of Chemistry and Physics, 51st Ed., 1970-71, p. F-23.

17. Crespi Gherzi, R.A., de Venturini, N.C. and de Alvarez, J.S., An.Asoc. Quim. Arg., 40, 1, 3A90 (1952).
18. Dijs, T., Dissertation (Delft), 1950.
19. Dijs, T., Hoogland, J.G. and Waterman, H.I., Chemistry and Industry, No. 44, 1073 (1952).
20. Dunning, W.G. and Kilpatrick, M., J. Phys. Chem., 42, 215 (1938).
21. Elbs, K. and Becker, K., Zeit. Electrochemie, No. 21, 361 (1904).
22. Eriksen, T.E., Chem. Eng. Sci., 22, 727 (1967).
23. Ibid., 24, 273 (1969).
24. Falk, M. and Giguere, P.A., Can. J. Chem., 35, 1195 (1957).
25. Ibid., 36, 1121 (1958).
26. FIAT Final Report No. 818 (PB40351), June 25, 1946.
27. Fletcher, F.A. and Kilpatrick, M., J. Phys. Chem., 42, 113 (1938).
28. Gardiner, W.C., Chem. Eng., 54, 11, 108 (1947).
29. Garrett, C.S., J. Chem. Soc., 107, 1324 (1915).
30. Gerritsen, D.J., Dechema Monograph, 26, 279 (1956).
31. Getman, F.H., J. Phys. Chem., 30, 266 (1926).
32. Gossman, B., Coll. Czechoslov. Chem. Commun., 2, 185 (1930).
33. Groothius, H. and Kramers, H., Chem. Eng. Sci. 4, 17 (1955).
34. Hogg, R.D., B.A.Sc. Thesis, The University of British Columbia, Canada, 1965.
35. Hohn, H., Research, 3, No. 1, 16 (1950).
36. Ibid., 3, No. 9, 407 (1950).
37. Hynes, H.B.N., "The Biology of Polluted Waters," Liverpool University Press, 1960.

38. Ingruber, O.V. and Kopanidis, J., Pulp and Paper Mag. of Canada, 68, No. 6, T-258 (1967).
39. Jellinek, K., Zeit. Electrochemie, No. 17, p. 157, p. 245 (1911).
40. Jellinek, K. and Jellinek, E., Physik. Chem., 93, 325 (1919).
41. Johnson, G., B.A.Sc. Thesis, The University of British Columbia, Canada, 1972.
42. Jones, L.H. and McLaren, E., J. Chem. Phys., 28, 995 (1958).
43. Jouan, R., J. Chim. Physique, 56, 327 (1959).
44. Ketelaar, J.A.A., Chemie - Ing. - Techn., 35, No. 5, 372 (1963).
45. King, C.V. and Braverman, M.M., J. Am. Chem. Soc., 54, 1744 (1932).
46. Klein, L., "River Pollution," Vol. II - Causes and Effects, Butterworth Inc., Washington, D.C., 1962.
47. Kolthoff, I.M. and Belcher, R., "Volumetric Analysis," Vol. III - Titration Methods: oxidation-reduction reactions, Interscience Publishers Inc., New York (1957).
48. Kolthoff, I.M. and Miller, C.S., J. Am. Chem. Soc., 63, 2818 (1941).
49. Kui-Shih Chia and Ung-Ping Wang, Annual meeting of Chinese Chemical Soc. at Chaiyi, Sept. 27 (1959).
50. Lakshminarayanaiah, N., "Transport Phenomena in Membranes," Academic Press, New York (1969).
51. Latimer, W.M., "Oxidation Potentials," 2nd Ed., Prentice-Hall, New York (1952).
52. Laura Creangă, Rev. Chim. (Bucharest), 9, 219 (1958).
53. Lister, M.W. and Gravie, R.C., Can. J. Chem., 37, 1567 (1959).
54. Lynn, S., Ph.D. Thesis, California Inst. of Tech., 1954.

55. Lynn, S., Straatemeier, J.R. and Kramer, H., Chem. Eng. Sci., 4, 49 (1955).
56. MacMullin, R.B., Chem. Inds., 61, 41 (1947).
57. MacMullin, R.B., Chem. Eng. Prog., 46, No. 9, 440 (1950).
58. Maey, E., Zeit. f. Phys. Chem., 29, 119 (1899).
59. Maros, L., Koros, E., Feher, I. and Schulek, E., Magyar Kem. Folyoirat, 65, 58 (1959).
60. Marshak, E.M., Khim. Nauka i Prom., 2, 524 (1957).
61. McGlynn, A. and Brown, O.W., J. Phys. Chem., 33, 1165 (1929).
62. Meret, R.G., "Brightening and Bleaching of Mechanical Pulp," MacMillan, Bloedel and Powell River Ltd., Research Division, Powell River, B.C., Canada, 1966.
63. Meyer, J., z. anorg. chem., 34, 43 (1903).
64. Nicolai, H.W., Chimie und Industrie, 73, 1149 (1955).
65. Oil Paint and Drug Reporter, Sept. 29, 1969.
66. Olmstead, J.L., "Sodium Hydrosulfite," Hooker Chemical Corp., Aug. 10, 1964.
67. Oloman, C. and Austin, R., Pulp and Paper Mag. of Canada, T529 (1969).
68. Oloman, C., J. Electrochem. Soc., 117, No. 12, 1604 (1970).
69. Patel, C.C. and Rao, M.R.A., Proc. Natl. Inst. Sci., India, 15, 127 (1949).
70. Ibid., 19, 231 (1953).
71. Patel, C.C. and Rao, M.R.A., Bull. India. Sect. Electrochemical Soc., 8, 37 (1959).
72. Peaceman, D.W., Sc. D. Thesis, Chem. Eng., M.I.T., 1951.

73. Pratt, L.A., Chem. and Met. Eng., 31, 11 (1924).
74. Prestat, G., Industrie Chim. belg., 20, spec. No. II, 600 (1955).
75. Rabinowitsch, M. and Fokin, A.S., Z. Electrochem., 36, 839 (1930).
76. Ranshaw, N., Chemical Age, 41, 359 (1939).
77. Ratkowsky, D.A. and McCarthy, J.L., J. Phys. Chem., 66, 516 (1962).
78. Riegel, E.R., "Industrial Chemistry," Reinhold Publishing Corp., New York (1962).
79. Rindich, N.A., Nauk. Povidomlennya, Kiiiv Univ., No. 1, 45 (1956).
80. Rinker, R.G., Gordon, T.P., Mason, D.M., Sakaida, R.R. and Corcoran, W.H., Am. Doc. Inst., Washington 25, D.C., Document 6104 (1959).
81. Rinker, R.G., Gordon, T.P., Mason, D.M., Sakaida, R.R. and Corcoran, W.H., J. Phys. Chem., 64, 573 (1960).
82. Rinker, R.G., Lynn, S., Mason, D.M. and Corcoran, W.H., Ind. Eng. Chem. (Fundamentals), 4, 282 (1965).
83. Rinker, R.G. and Lynn, S., I. & E.C. Product Research and Development, 8, No. 4, 338 (1969).
84. Rushton, J.H., Chem. Eng. Prog., 47, No. 9, 485 (1951).
85. Ibid., 48, No. 1, 33 (1952).
86. Ibid., 48, No. 2, 95 (1952).
87. Rushton, J.H. and Oldshue, J.Y., Chem. Eng. Prog., 49, No. 4, 161 (1953).
88. Ibid., 49, No. 5, 267 (1953).
89. Rougeot, L., Compt. Rend., 222, 1497 (1946).
90. Schmidt, F., Ann. d. Physik, 39, 1108 (1912).
91. Scholder, R. and Denk, G., z. anorg. allgem. chem., 222, 48 (1935).

92. Schüller, A., zeit. anorg. chem., 40, 385 (1904).
93. Scott, W.D., Ph.D. Thesis, University of Washington, Seattle, U.S.A., 1964.
94. Scribner, A.K., Am. Dyestuff Reporter, p. 185, March (1933).
95. Shaede, E.A. and Walker, D.C., Chem. Soc., London, Sp. Publ. No. 22, 277 (1967).
96. Shaeffer, K. and Koehler, W., z. anorg. u. allgem. chem., 104, 212 (1918).
97. Shanahan, C.E.A. and Cooke, F., J. Appl. Chem., 7, 645 (1957).
98. Shreve, R.N., "Chemical Process Industries," 3rd Ed., McGraw-Hill Book Co., New York (1967).
99. Simon, A. and Waldmann, K., z. anorg. allg. chem., 281, 113 (1955).
100. Ibid., 283, 359 (1956).
101. Ibid., 284, 36 (1956).
102. Spencer, M.S., Trans. of the Faraday Soc., 63, No. 10, 2510 (1967).
103. Sterbacek, Z. and Tausk, P., "Mixing in the Chemical Industry," Pergamon Press Ltd., New York (1965).
104. Swift, E.H., "A System of Chemical Analysis (Qualitative and Semiquantitative) for the Common Elements," Prentice-Hall Inc., New York (1946).
105. Toor, H.L. and Chiang, S.H., Chem. Eng. Sci., 11, 344 (1959).
106. Tyminski, A., Pulp and Paper Mag. of Canada, 68, No. 6, T-258 (1967).
107. Vanstone, E., Trans. Faraday Soc., 7, 42 (1911).
108. Vanstone, E., Chem. News, 103, p. 181, p. 198, p. 207 (1911).
109. Vanstone, E., J. Chem. Soc., 105, 2617 (1914).

110. Vogel, A.I., "A Text-book of Qualitative Inorganic Analysis," 3rd Ed., John Wiley & Sons, New York, (1961).
111. Wang, Jui-Chung, Ph.D. Thesis, The University of Texas, U.S.A., 1963.
112. Withrow, J.R., J. Phys. Chem., 20, 528 (1916).
113. Witney, R.P. and Vivian, J.E., Chem. Eng. Prog., 45, 322 (1949).
114. Wood, P.J., Am. Dyestuff Reporter, p. 443, June 17 (1957).
115. Wright, R., J. Chem. Soc., 105, 669 (1914).
116. Yost, D.M. and Russell, H., "Systematic Inorganic Chemistry," Prentice-Hall, New York (1944).
117. Yuferev, R.F. and Malushin, P.U., J. Chem. Ind. (Moscow), 7, 553 (1930).
118. Yui, N., Tokyo Inst. Phys. Chem. Res. Bull., 19, 1229 (1940).
119. "Zinc Hydrosulfite," Bulletin 407 J, Virginia Chemicals, U.S.A.
120. Zjiwotinsky, Masjowetz, Fokin, Ukrain. Khem. Zhur, 6, 205 (1931).
121. Ibid., 6, 212 (1931).

PATENTS

122. British P. 25,870 (1910).
123. British P. 11,010 (1913).
124. British P. 700,042 (1953).
125. British P. 763,278 (1956).
126. British P. 786,212 (1957).
127. British P. 916,866 (1963).
128. British P. 1,148,248 (1969).

129. D.R.P. 431,254 (1925).
130. D.R.P. 671,883 (1933).
131. D.R.P. 641,673 (1935).
132. D.R.P. 666,184 (1936).
133. D.R.P. 864,935 (1953).
134. D.R.P. 900,336 (1953).
135. French P. 806,126 (1936).
136. French P. 819,947 (1937).
137. French P. 1,064,998 (1954).
138. French P. 1,065,064 (1954).
139. French P. 1,363,064 (1964).
140. Ger. Offen. 1,036,228 (1958).
141. Ger. Offen. 2,000,877 (1970).
142. Holl. P. 45,450 (1938).
143. Holl. P. 46,832 (1939).
144. Holl. P. 47,030 (1939).
145. Italian P. 489,137 (1954).
146. Japan P. 7,016,327 (1970).
147. U.S.P. 2,193,323 (1940).
148. U.S.P. 2,226,576 (1940).
149. U.S.P. 2,938,771 (1960).
150. U.S.P. 3,226,185 (1965).
151. U.S.P. 3,411,875 (1968).
152. U.S.P. 2,010,651 (1969).

APPENDIX A

EQUIPMENT SPECIFICATION

1. pH measurement

The specifications of the instruments used for continuous pH recording were as follows:

pH electrode; Sargent-Welch S-30072-15

Thermocompensator; Sargent-Welch S-30115-03

pH meter; Sargent-Welch Model PBL S-30009

pH recorder; Sargent-Welch Model SRG

pH recorder chart; Sargent Welch S-72166

2. Digital temperature recording

All electronic instruments used for recording the temperature of the different streams were purchased from United Systems Corporation, Dayton, Ohio, U.S.A. Their specifications were as follows:

Digital clock - 661

Scanner - 635

Digital millivolt meter - 451

Multiplexer - 642

Printer system - 611/620D

BCD cable connecting digital clock to multiplexer 4378-6

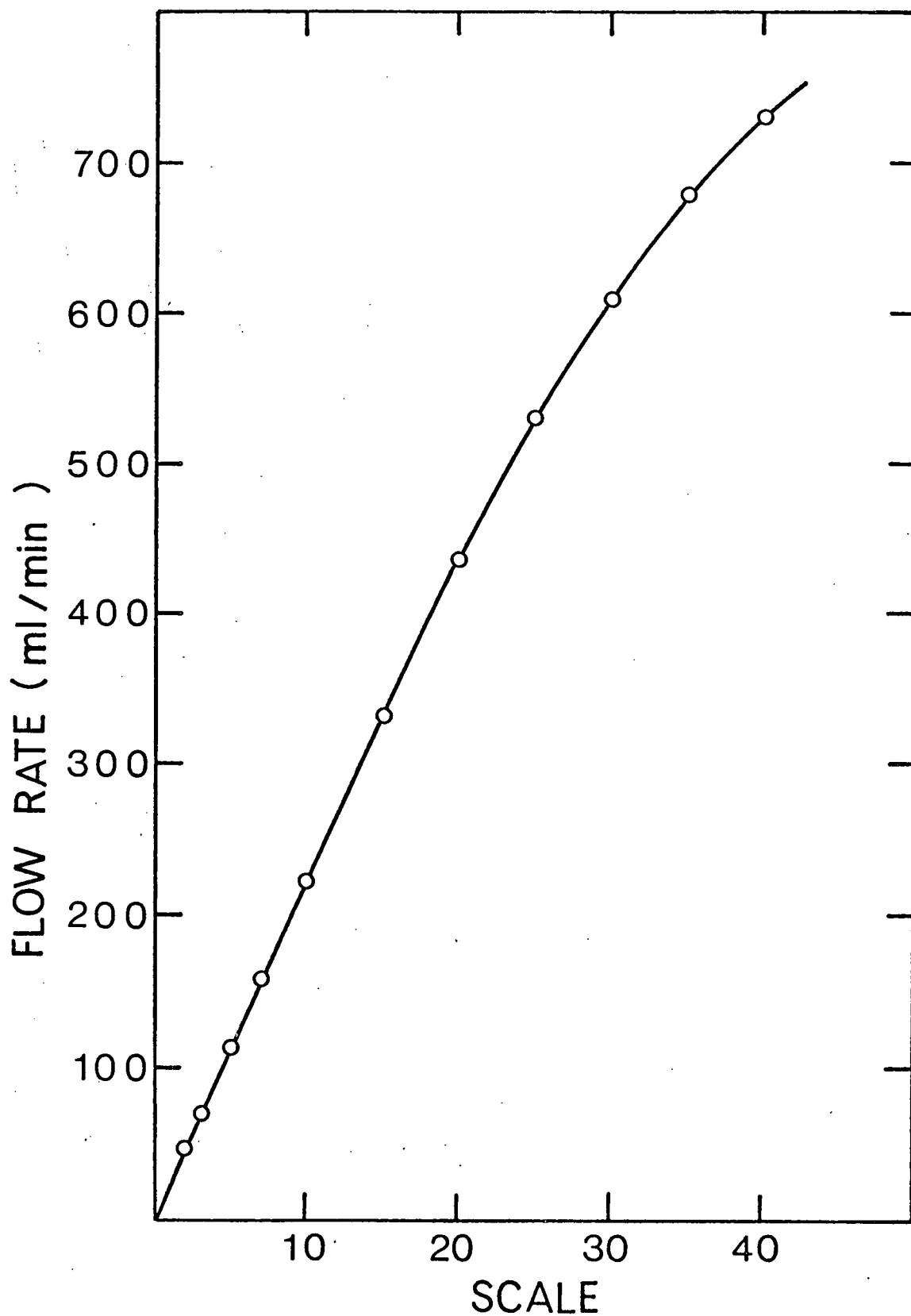
BCD cable connecting scanner to multiplexer 4837-6

BCD cable connecting digital millivolt meter to printer system
4378-20

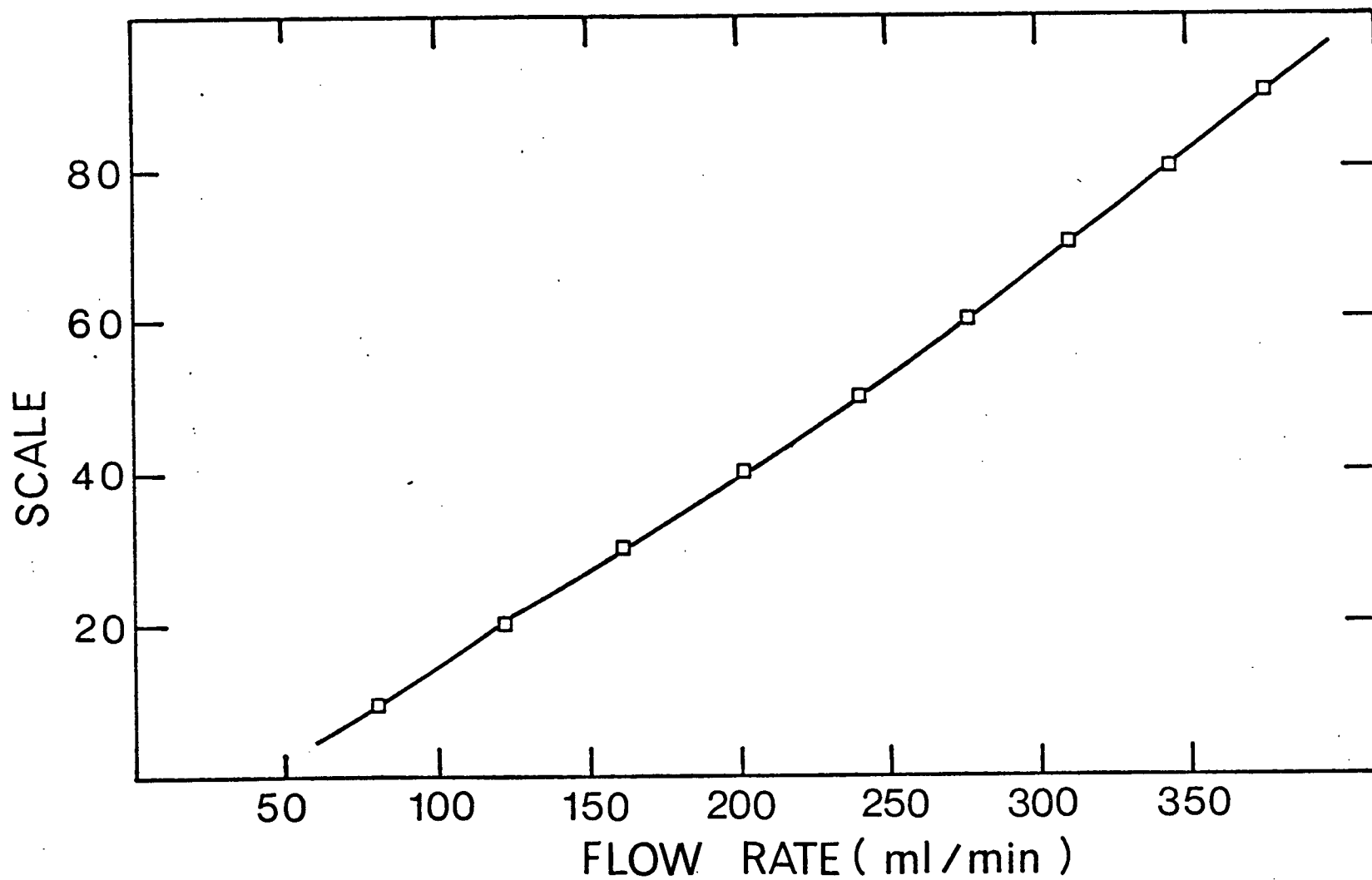
BCD cable connecting multiplexer to printer system 9054-20.

3. Calibration curves

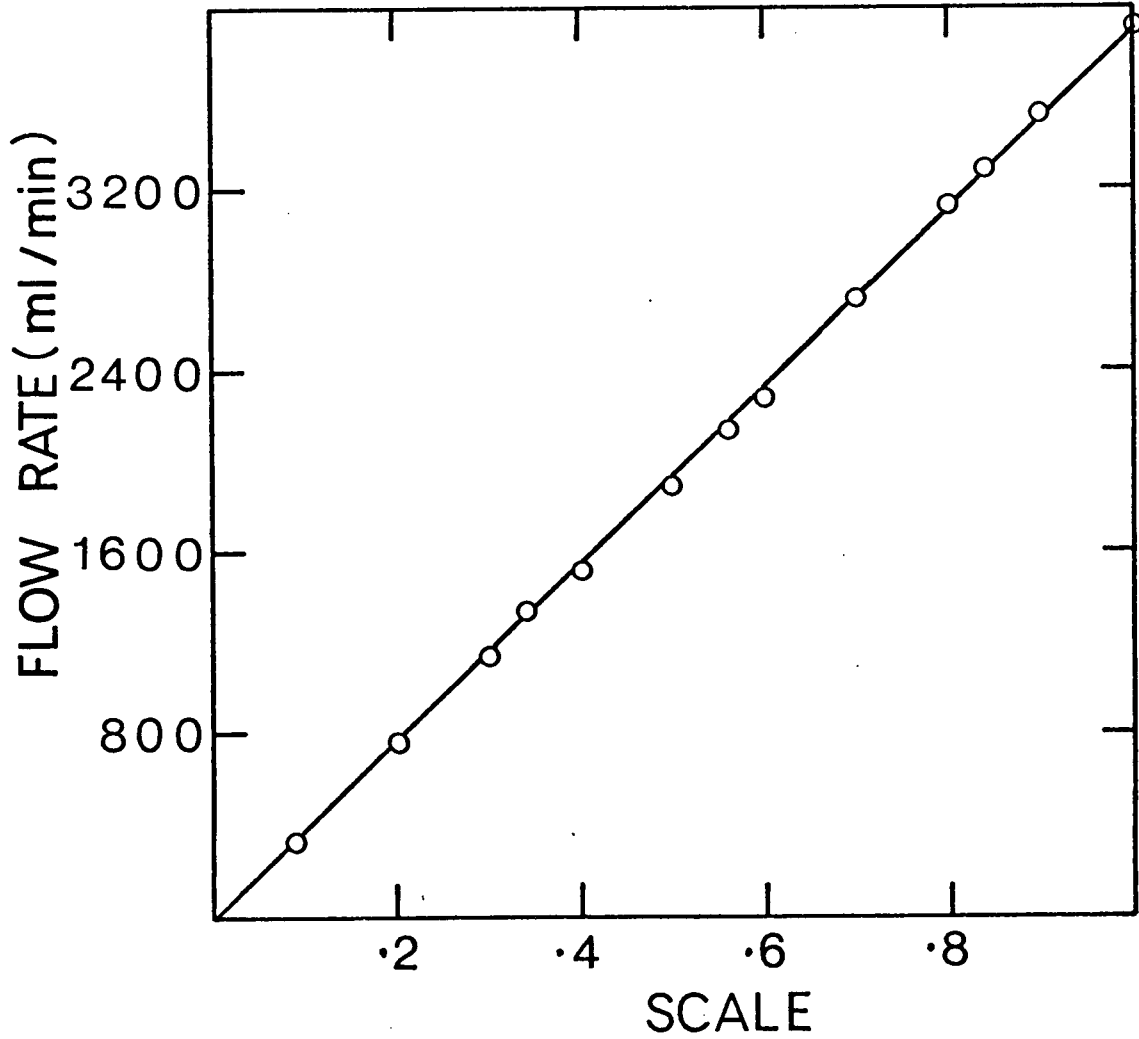
The calibration curves mentioned in Section IV.C. are shown in Figures A-I to A-V.



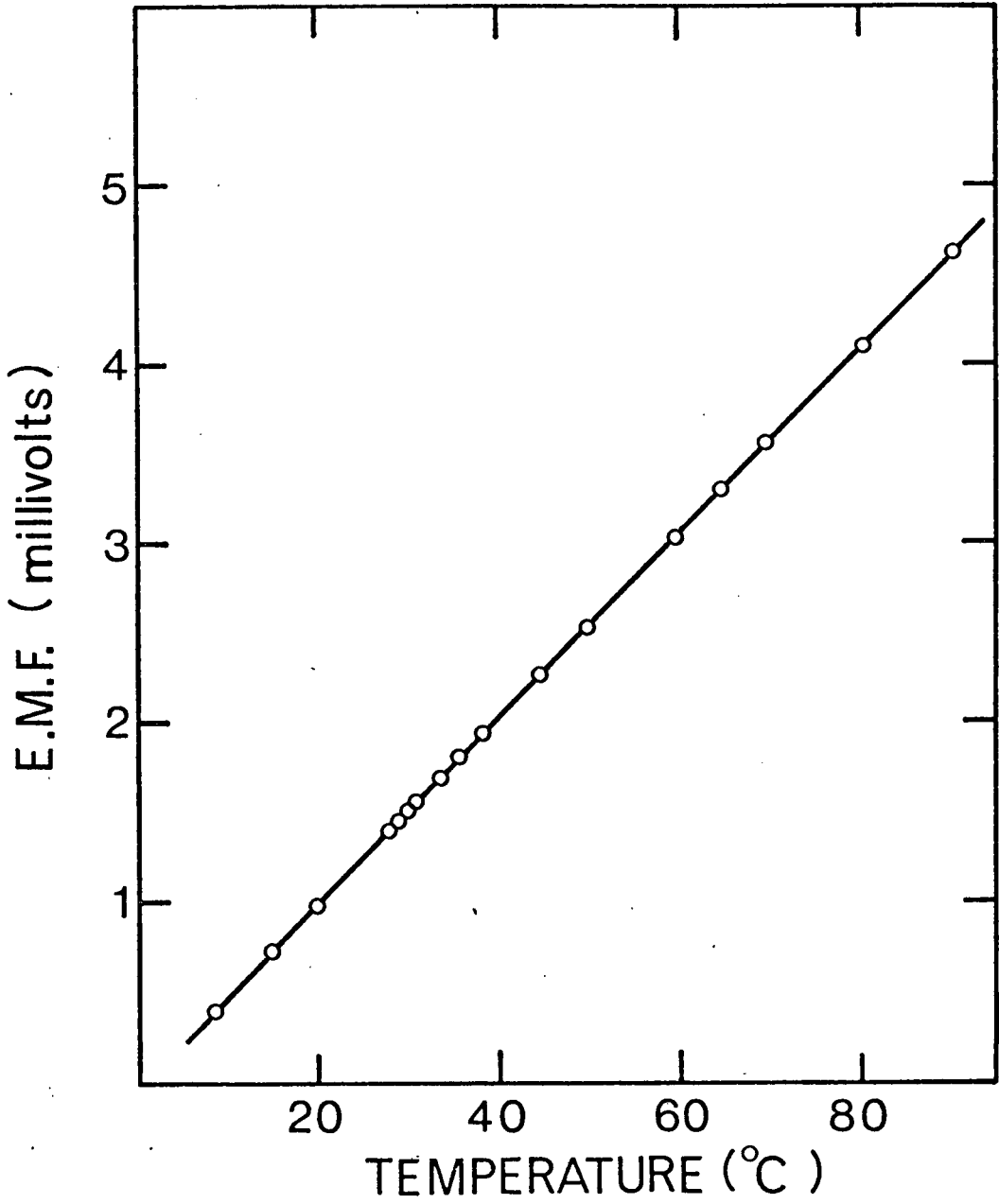
A-I Flow rate of mercury pumped by Moyno pump versus micrometer setting on Graham transmission



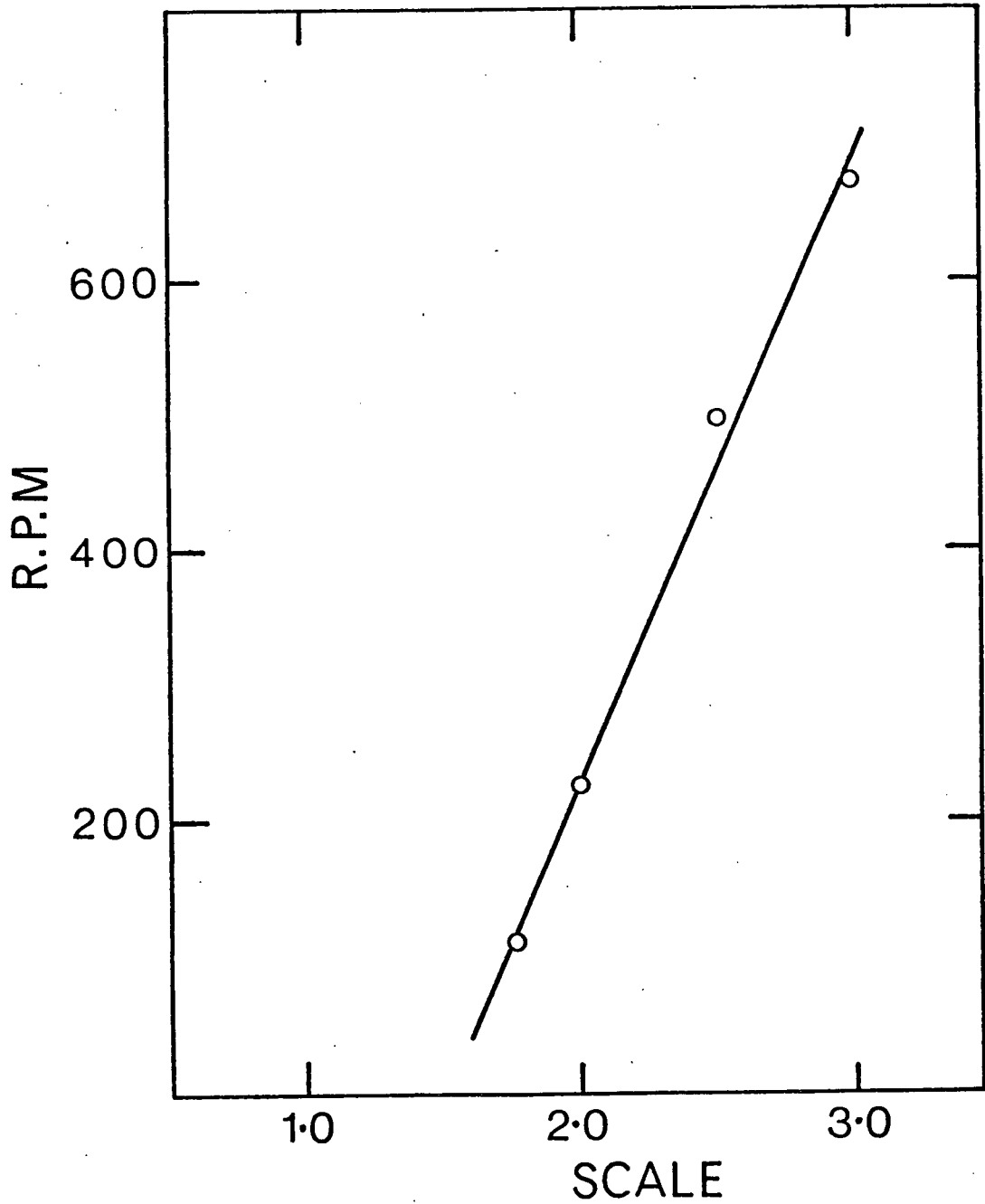
A-II Flow rate of aqueous sulfur dioxide versus reading on the rotameter scale



A-III Flow rate of cooling water versus reading on the rotameter scale



A-IV Millivolt output of iron-constantan thermocouples versus temperature °C



A-V RPM of the propeller versus micrometer setting on the thyatron controller for the variable speed drive (Heller motor)

APPENDIX B

STATISTICAL EVALUATION OF ACCURACY AND PRECISION

1. Error of a measurement process

Eisenhart,¹ Ku² and Murphy³ have described the meaning of certain terms such as "precision" and "accuracy" which specify the error of a measurement process.³

Strictly speaking, the actual error of a reported value, that is, the magnitude and sign of its deviation from the truth, is usually not ascertainable. Limits to this error, however, can usually be inferred, with some risk of being incorrect, from the precision of the measurement process by which the reported value was obtained, and from reasonable limits to the possible bias (or systematic error) of the measurement process.

Precision of a measurement process refers to the closeness of successive independent measurements of a single magnitude. The measurements are generated by repeated applications of the process under specified conditions. The accuracy is determined by the closeness to the true value

-
1. Eisenhart, C., Science, Vol. 160, p. 1201, June (1968).
 2. Ku, H.H., Measurements and Data, p. 72, July-August (1968).
 3. Murphy, R.B., Material Research and Standards, p. 264, April (1961).

of such measurements. Thus, if the bias, or systematic error, of a measurement process is known, its accuracy can be specified.

Precision and accuracy are inherent characteristics of the measurement process employed and not of the particular end result obtained. It is important to note that a measurement process may be extremely precise and at the same time not very accurate. Precision, in statistical language, is some times called "imprecision."

Since imprecision and systematic error are distinctly different components of the uncertainty of a reported value, and are subject to different treatments and interpretation in usage, two numerics respectively expressing the imprecision and bounds to the systematic error of the measurement process should be given along with the measured quantity, whenever both of these errors are factors requiring consideration. According to Eisenhart¹ four distinct cases need to be recognized, viz.,

- (a) both systematic error and imprecision negligible, in relation to the requirements of the intended and likely use of results;
 - (b) systematic error not negligible, imprecision negligible;
 - (c) neither systematic error nor imprecision negligible;
- and

- (d) systematic error negligible, imprecision not negligible.

Eisenhart discussed and outlined the recommended practices on the expression of uncertainties in the above-mentioned cases.

2. Evaluation of accuracy

It has been mentioned in the last section that the bias or systematic error of a measurement process is a measure of its accuracy. The systematic error may be due to uncertainty in constants, uncertainty in calibrated values or bias in the method of computation.

The following devices may yield some information regarding the presence of systematic error in a measurement process.

- (a) Measurement of a quantity whose true value is known.
- (b) Comparison with other measurement processes.
- (c) Comparison with modifications of the given measurement process.

The evaluation of systematic error of a measurement process has been discussed in great detail by Youden.⁴ In short,

(i) Systematic error can be estimated experimentally if the true value of the measured quantity is known.

4. Youden, W.J., Material Research and Standards, p. 268, April (1961).

(ii) Systematic error can be estimated from experience or by judgment.

(iii) Systematic error can be estimated by a number of elemental systematic errors in the measurement process if they are known.

The mode of specifying limits of systematic error (or accuracy) has been well-described by Ku² and Eisenhart¹.

3. Evaluation of precision (or imprecision)

In any investigation, it is necessary to know how well the particular measured value is likely to agree with other values that the same measurement process might have provided in this instance, or might yield on remeasurement of the same magnitude on another occasion. Such information is provided by the estimated standard error of the reported value, which measures (or is an index of) the characteristic disagreement of repeated determinations of the same quantity by the same method and, thus, serves to indicate the precision of the reported value (more correctly, precision of the measurement process in reporting the measured value).

In the following example the precision of a measurement process (or test method) "within a laboratory" has been considered and an expression for its statistical estimate, standard error, has been derived.

Suppose that a given measurement were repeated 10 times. It is called set 1, and $n_1 = 10$. From this set of 10 values, the sample mean, \bar{x}_1 , and the sample estimate of the population variance, s_1^2 , can be calculated by using the following equations⁵

$$\bar{x} = \frac{\sum_{j=1}^n x_j}{n} \quad \dots \dots (B-1)$$

$$s^2 = \frac{\sum_{j=1}^n (x_j - \bar{x})^2}{n - 1} \quad \dots \dots (B-2)$$

Therefore,

$$\bar{x}_1 = \frac{\sum_{j=1}^{10} x_{1j}}{10} \quad \dots \dots (B-3)$$

$$s_1^2 = \frac{\sum_{j=1}^{10} (x_{1j} - \bar{x}_1)^2}{(10 - 1)} \quad \dots \dots (B-4)$$

These quantities are estimates of the population mean, μ , and population variance σ^2 . If a second set of 10 measurements of the same quantity were made, the values of \bar{x}_2 and

5. Mickley, H.S.; Sherwood, T.K. and Reed, C.E., "Applied Mathematics in Chemical Engineering," 2nd Ed., McGraw-Hill Book Co. Inc. (New York), 1957.

s_2^2 , calculated from the second set of 10 values, would be expected to differ from the first set and from the population values. If it is supposed that a large number of sets, each of 10 measurements, were obtained, a new set comprising the sample means $\bar{x}_1, \bar{x}_2, \dots, \bar{x}_k$ could be generated. This set of means would exhibit some very important characteristics. If the grand mean, \bar{x}_m , is calculated

$$\bar{x}_m = \frac{\sum_{i=1}^k \bar{x}_i}{k} \quad \dots \dots (B-5)$$

(where k represents the number of sets), it will be found that \bar{x}_m is a better estimate of the population mean, μ , than individual \bar{x}_i 's. Further, on the average, the deviation of \bar{x}_i from \bar{x}_m will be less than the deviation of a single term, x_{ij} , from the mean of the i th set, \bar{x}_i . The sample estimate of the variance of the set of means

$$s_m^2 = \frac{\sum_{i=1}^k (\bar{x}_i - \bar{x}_m)^2}{k-1} \quad \dots \dots (B-6)$$

will be smaller than the sample estimate of the population variance, s_i^2 . It is also found that the frequency distribution of the sample means, \bar{x}_i , about the population mean, μ , is essentially normal, even though the population frequency distribution may be non-normal! When these findings are

treated analytically, it is found that the sample variance of the mean, s_m^2 , may be estimated from the variance calculated from a single set:

$$s_m^2 \approx \frac{s^2}{n} \quad (B-7)$$

In equation (B-7), s^2 is the sample estimate of the population variance calculated from a single set of measurements, n is the number of measurements in the single set, and s_m^2 is the estimated variance of the set of means. The square root of the estimated variance of the set of means, s_m , is called standard deviation of the mean or standard error. The standard error is usually denoted by s_m .

It is desired to determine the limits within which the true population mean, μ , will fall 95 times out of 100 termed the "95 per cent confidence limits on μ " (sufficient for most engineering investigations). Student's 't' statistics could be used for small sample sizes. For the case discussed above

$$t_{n-1, \alpha=.05} = \frac{\bar{x} - \mu}{s_m} = \frac{\bar{x} - \mu}{\frac{s}{\sqrt{n}}} \quad (B-8)$$

∴ 95 per cent confidence limits on μ are

$$\bar{x} - t_{n-1, \alpha=.05} s_m \leq \mu \leq \bar{x} + t_{n-1, \alpha=.05} s_m \quad \dots (B-9)$$

4. Propagation of random error

Most often an investigator comes across a situation where the precisions (more correctly, precisions in the measurement processes) of several directly measured quantities are known and it is desired to estimate the precision (precision in the measurement process) of any function of these quantities.

To illustrate propagation of random error, it is assumed that a quantity z is calculated from directly measured values of several quantities P_i by means of a mathematical relation which can be represented formally by

$$z = f (P_1, P_2, P_3, \dots, P_i) \quad \dots (B-10)$$

In a very general case, each measurement P is made m times under supposedly identical conditions. The action of random errors results in a series of values of P_1 : $P_{11}, P_{12}, P_{13}, \dots, P_{1m_1}$ which form the P_1 set and a corresponding set forming the P_2 set, etc. It is then desired to estimate the best value of z , variance of z and standard error of z (standard deviation of mean of z).

If the errors in the P's are normally distributed and the variances of P's are small, then the best value of z will be given by the following expression:^{5,6}

$$\bar{z} = f(\bar{P}_1, \bar{P}_2, \bar{P}_3, \dots, \bar{P}_i) \quad \dots \dots (B-11)$$

where \bar{P} is the mean of a series of values in the set P.

If the errors in P's are independent and not too large, the variance of z is given by the following expression:⁵⁻⁸

$$\sigma_z^2 = \left(\frac{\partial z}{\partial P_1}\right)^2 \sigma_{P_1}^2 + \left(\frac{\partial z}{\partial P_2}\right)^2 \sigma_{P_2}^2 + \dots + \left(\frac{\partial z}{\partial P_i}\right)^2 \sigma_{P_i}^2 \quad \dots (B-12)$$

The partial derivative $\frac{\partial z}{\partial P_i}$ is evaluated numerically at the mean value of each set: \bar{P}_1, \bar{P}_2 , etc. It is important to note that validity of equation (B-12) is not dependent upon any

-
6. Parratt, L.G. "Probability and Experimental Errors in Science," Chapter 3, John Wiley and Sons, N.Y. (1961).
 7. Ratkowsky, D.A. "Notes on Statistical Techniques," ChE 453/81, October 14, 1965, Dept. of Chem. Eng., U.B.C., Canada.
 8. Bannett, C.A. and Franklin, N.L. "Statistical Analysis in Chemistry and the Chemical Industry," John Wiley and Sons, N.Y. (1957).

assumption concerning a normal error frequency distribution. Only two conditions are required. First, that no correlation exist between the ΔP_{im_i} terms ($P_{1m_1} - \bar{P}_1 = \Delta P_{1m_1}$; $P_{2m_2} - \bar{P}_2 = \Delta P_{2m_2}$, etc.), an assumption frequently termed "the assumption of statistical independence." Secondly, the errors in the P's must not be too large. On the other hand, the usual methods of relating variance to probability do involve the assumption of a normal frequency distribution.

For the mathematical expression (B-10), the standard deviation of mean of z (standard error of z), σ_{z_m} , can be written as follows:⁶

$$\sigma_{z_m}^2 = \left(\frac{\partial z}{\partial \bar{P}_1}\right)^2 \frac{\sigma_{P_1}^2}{m_1} + \left(\frac{\partial z}{\partial \bar{P}_2}\right)^2 \frac{\sigma_{P_2}^2}{m_2} + \dots + \left(\frac{\partial z}{\partial \bar{P}_i}\right)^2 \frac{\sigma_{P_i}^2}{m_i}$$

. . . . (B-13)

Knowing the standard error of z, the 95 per cent confidence limits of the population mean of z can be estimated by using equation (B-9). One major problem involved in the use of equation (B-9) is that 't' statistics with known degrees of freedom are used for estimating the confidence limits. It may seem difficult to estimate the degrees of freedom of z in the case in point. However, if $P_1, P_2, P_3, \dots, P_i$ are independent, considering different combinations of measurements in different sets, z will have very large

number of degrees of freedom. Under these conditions 't' distribution would approach the 'N' (normal) distribution. Hence the 95 per cent confidence limits on the population mean of z can be estimated by

$$\bar{z} - N_{\alpha=.05} s_{z_m} \leq \bar{z} \leq \bar{z} + N_{\alpha=.05} s_{z_m} \quad (B-14)$$

where,

\bar{z} = best estimate of population mean, \bar{z}

s_{z_m} = estimated standard deviation of the mean of z

$N_{\alpha=.05} = 1.96$ [From normal probability table].

Practical application of equation (B-12) and (B-13) for a function like (B-11) depends upon one's ability to determine $\sigma_{P_1}^2, \sigma_{P_2}^2, \dots, \sigma_{P_i}^2$ from experimental data, or to make an *a priori* estimate of them.

If it is experimentally possible to have estimates (from random samples) of the variances (by equation (B-2)) and variances of the mean (by equation (B-7)) of $P_1, P_2, P_3, \dots, P_i$ etc., then 95 per cent confidence limits on the population mean of z can be estimated by equations (B-13) and (B-14)

In the absence of an experimental random sample, it is possible to get an *a priori* estimate of the variance (or its square root, the standard deviation) from a consideration of the maximum range of random error expected

using a particular measurement method.⁷ It is known from elementary statistics that practically all (actually 99.73 per cent) of the area under the curve of the normal distribution is contained within ± 3 standard-deviations of the population mean of a variable P_i . Considering $\pm 3\sigma_{P_i}$ to be synonymous with the range of the variable P_i , then one merely needs to know or to be able to estimate the range to obtain a reasonable estimate of the standard deviation of the variable P_i .

Sometimes the value of a particular quantity obtained from an instrument or measuring device remains very constant, but the limiting factor to precision of reading is the smallest scale division available on the instrument. If a temperature measurement made with a thermometer is considered in which the smallest division is 1°C , then it seems reasonable to assume that the maximum error range obtainable (due to human reading error alone) is about 1°C (or $\pm 0.5^\circ\text{C}$). Thus an *a priori* estimate of standard deviation of temperature measurement would be $0.5/3 = .167$. Of course, the range may be considerably greater than 1°C , due to large fluctuations or instabilities in the temperature. In that case, one would once again require experimentation in order to obtain an estimate of the variance. The above discussion only applies to steady readings where the smallest scale division imposes a limiting factor on the precision of the reading. Once again

if one considers the problem where

$$z = f (P_1, P_2, P_3 \dots, P_i) ,$$

the standard deviation of z , s_z , can be estimated by equation (B-12) using *a priori* estimates of σ_{P_1} , σ_{P_2} \dots , σ_{P_i} . Also, the 95 per cent confidence limits on the population mean of z can be estimated.⁷

$$z - N_{\alpha=.05} s_z \leq \bar{z} \leq z + N_{\alpha=.05} s_z \quad (B-15)$$

The '95 per cent confidence limits' estimated by equation (B-15) are broader than those calculated by equation (B-14).

APPENDIX C

SODIUM-MERCURY AMALGAM

1. Purity of the chemicals in preparing amalgam

(a) Mercury

Technical grade mercury, obtained from various sources, was thoroughly washed and then distilled in a mercury still available in the laboratory. It was assumed that after distillation the mercury was 100 per cent pure.

(b) Sodium metal

Reagent grade sodium of the following assay was purchased from Canlab Supplies Ltd. (Toronto).

Chloride (Cl)	0.0015%
Nitrogen (N)	0.003%
Phosphate (PO ₄)	0.0005%
Sulfate (SO ₄)	0.002%
Heavy metals (as Pb)	0.0005%
Iron (Fe)	0.001%

(c) Paraffin oil

White, heavy (Saybolt viscosity 335/350), laboratory grade paraffin oil was purchased from Fisher Scientific Co. (Montreal).

2. Problems encountered in preparation of amalgam

(a) Heat of solution

When sodium was dissolved in mercury, a large quantity of heat was liberated. Therefore, small pieces of sodium metal were slowly added to the mercury to promote controlled amalgamation.

(b) Black precipitate in amalgam preparation

When sodium was dissolved in mercury (kept under a thin layer of paraffin oil), a finely divided black precipitate was obtained which could be easily separated from the amalgam by mechanical means.

This finely divided black precipitate was identified as mercury (formed by the reduction of HgO by sodium) which did not dissolve in the bulk of the amalgam because of a coating of paraffin oil on the droplets. Due to this problem it was difficult to make an amalgam of a known sodium-concentration starting with known quantities of mercury and sodium.

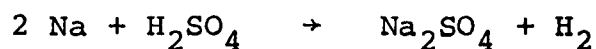
(c) Disposal of small pieces of sodium and its oxide

The layer of oxide, on the surface of sodium metal, was removed by scraping the surface of the metal with a knife under a layer of paraffin oil. The most effective way to dispose of tiny pieces of sodium and scrapings of the oxide was to dissolve them in a solution of iso-propanol and benzene (2:3 V/V).

3. Calculation of sodium content in an amalgam sample

- (a) Normality of the standard NaOH solution, $N_{\text{NaOH}} = 0.1\text{N}$
- (b) Normality of the standard H_2SO_4 solution, $N_{\text{H}_2\text{SO}_4} = 0.1\text{N}$
- (c) Weight of the Erlenmeyer + 100 ml distilled water,
 $W_1 = 275.3$ gms
- (d) Weight of the Erlenmeyer + 100 ml distilled water
 + approximately 2.5 ml amalgam sample, $W_2 = 305.3$ gms
- (e) Weight of the amalgam sample, $W_{\text{AML}} = W_2 - W_1 = 30$ gms
- (f) Volume of $N_{\text{H}_2\text{SO}_4}$ sulfuric acid added to the Erlenmeyer,
 $V''_{\text{H}_2\text{SO}_4} = 0.025$ liter
- (g) Volume of N_{NaOH} sodium hydroxide used to titrate the
 excess of sulfuric acid, $V''_{\text{NaOH}} = 0.020$ liter.

Sodium dissolved in mercury reacts with sulfuric acid according to the following reaction



By stoichiometry, the weight per cent of sodium in the amalgam sample, NAPT, can be given by the following expression.

$$\text{NAPT} = \frac{2300}{W_{\text{AML}}} (V''_{\text{H}_2\text{SO}_4} N_{\text{H}_2\text{SO}_4} - V''_{\text{NaOH}} N_{\text{NaOH}}) \dots (\text{C-1})$$

For the above-mentioned example,

$$\text{NAPT} = \frac{2300}{30} (0.025 \times 0.1 - 0.020 \times 0.1)$$

$$= 0.03833 \text{ gms of sodium/100 gms of the amalgam.}$$

4. Estimation of the precision of the analytical procedure

The following steps were involved in the determination of weight per cent of sodium in amalgam by the proposed analytical procedure.

- (a) Standardization of an aqueous sodium hydroxide solution by potassium hydrogen phthalate^{1,2}

V_{NaOH} liters of N_{NaOH} sodium hydroxide solution was titrated with W_{PHP} gms of potassium hydrogen phthalate dissolved in approximately 200 ml of distilled water.

$$\therefore N_{\text{NaOH}} = \frac{W_{\text{PHP}}}{204.22 V_{\text{NaOH}}} \quad \dots \text{(C-2)}$$

- (b) Standardization of a sulfuric acid solution by the standardized sodium hydroxide solution

1. Swift, E.H., "A system of chemical analysis (qualitative and semiquantitative) for the common element." Prentice-Hall Inc., New York, (1946).
2. Vogel, A.I., "A text-book of qualitative inorganic analysis." 3rd Ed. John Wiley and Sons, New York, 1961.

$V'_{H_2SO_4}$ liters of $N_{H_2SO_4}$ sulfuric acid was titrated with V'_{NaOH} liters of N_{NaOH} sodium hydroxide solution.

$$\therefore N_{H_2SO_4} = \frac{N_{NaOH} V'_{NaOH}}{V'_{H_2SO_4}} \quad \dots (C-3)$$

(c) Sodium-mercury amalgam sample weighed

W_{AML} gms of an amalgam sample was weighed under a layer of distilled water using a Mettler balance.

(d) Addition of standard sulfuric acid solution to the amalgam sample

$V''_{H_2SO_4}$ liters of the $N_{H_2SO_4}$ sulfuric acid was pipetted into the flask containing the amalgam sample.

(e) Excess sulfuric acid back-titrated with the standard sodium hydroxide solution

Sulfuric acid solution that did not react with sodium in the amalgam was titrated with V''_{NaOH} liters of N_{NaOH} sodium hydroxide solution.

As mentioned in Appendix C.3, the weight per cent of sodium in the amalgam can be given by the following expression.

$$NAPT = \frac{2300}{W_{AML}} (V''_{H_2SO_4} N_{H_2SO_4} - V''_{NaOH} N_{NaOH}) \quad (C-1)$$

The measured values of the different quantities involved in the above mentioned steps ((a) to (e)) and the range of random errors associated with them have been presented in Table C-I.

Standard deviations (and hence, the variances) of W_{AML} , $V''_{\text{H}_2\text{SO}_4}$ and V''_{NaOH} were estimated from the total range of the random errors in these quantities by the method outlined in Appendix B.4. The results are shown in the Table C-I.

Standard deviations (and hence, the variances) of the different measured quantities in the equations (C-2) and (C-3), viz.

W_{PHP} , V_{NaOH} , V'_{NaOH} and $V'_{\text{H}_2\text{SO}_4}$ were also estimated from the knowledge of the total range of the random errors in these quantities (Table C-I). The values and the estimates of variances of N_{NaOH} and $N_{\text{H}_2\text{SO}_4}$ were calculated as follows:

(i) Value and variance of N_{NaOH}

Using equation (C-2),

$$N_{\text{NaOH}} = \frac{W_{\text{PHP}}}{204.22 V_{\text{NaOH}}} = \frac{0.6127}{204.22 \times 0.03} = 0.10$$

Using equation (B-12),

$$\begin{aligned} \sigma_{N_{\text{NaOH}}}^2 &= \left(\frac{\partial N_{\text{NaOH}}}{\partial W_{\text{PHP}}} \right)^2 \sigma_{W_{\text{PHP}}}^2 + \left(\frac{\partial N_{\text{NaOH}}}{\partial V_{\text{NaOH}}} \right)^2 \sigma_{V_{\text{NaOH}}}^2 \\ &= 31.229 \times 10^{-10} \end{aligned}$$

TABLE C-I

MEASURED VALUES, RANGE OF RANDOM ERRORS AND VARIANCES OF DIFFERENT QUANTITIES

Variable	Explanation	Measured Value	Measured To	$\sigma = \frac{1}{3} \frac{\text{range}}{2}$	σ^2
W_{PHP}	Weight of potassium hydrogen phthalate taken to standardize N_{NaOH}	.6127 gm	$\pm .0001$ gm	3.3×10^{-5}	1.09×10^{-9}
V_{NaOH}	Volume of N_{NaOH} titrated with p.h.p.	.030 lit	$\pm .00005$ lit	1.67×10^{-5}	2.79×10^{-10}
V'_{NaOH}	Volume of N_{NaOH} taken to standardize $N_{\text{H}_2\text{SO}_4}$.025 lit	$\approx \pm 0$ lit (pipetted)	0	0
$V'_{\text{H}_2\text{SO}_4}$	Volume of $N_{\text{H}_2\text{SO}_4}$ titrated with V'_{NaOH} volume of N_{NaOH}	.025 lit	$\pm .00005$ lit	1.67×10^{-5}	2.79×10^{-10}
W_{AML}	Weight of amalgam sample taken for analysis	30 gm	$\pm .05$ gm	1.67×10^{-2}	2.79×10^{-4}
$V''_{\text{H}_2\text{SO}_4}$	Volume of $N_{\text{H}_2\text{SO}_4}$ added to the amalgam sample	.025 lit	$\approx \pm 0$ lit (pipetted)	0	0
V''_{NaOH}	Volume of N_{NaOH} used in back titration of the acid				
	Amalgam No I	.0248 lit	$\pm .00005$ lit	1.67×10^{-5}	2.79×10^{-10}
	Amalgam No II	.0200 lit	$\pm .00005$ lit	1.67×10^{-5}	2.79×10^{-10}
	Amalgam No III	.005 lit	$\pm .00005$ lit	1.67×10^{-5}	2.79×10^{-10}

(ii) Value and variance of $N_{H_2SO_4}$

By equation (C-3),

$$N_{H_2SO_4} = \frac{N_{NaOH} V'_{NaOH}}{V'_{H_2SO_4}} = \frac{0.1 \times 0.025}{0.025} = 0.10$$

Using equation (B-12),

$$\begin{aligned} \sigma_{N_{H_2SO_4}}^2 &= \left(\frac{\partial N_{H_2SO_4}}{\partial N_{NaOH}} \right)^2 \sigma_{N_{NaOH}}^2 + \left(\frac{\partial N_{H_2SO_4}}{\partial V'_{NaOH}} \right)^2 \sigma_{V'_{NaOH}}^2 \\ &\quad + \left(\frac{\partial N_{H_2SO_4}}{\partial V'_{H_2SO_4}} \right)^2 \sigma_{V'_{H_2SO_4}}^2 \\ &= 75.869 \times 10^{-10} \end{aligned}$$

Knowing the variances of W_{AML} , $V''_{H_2SO_4}$, $N_{H_2SO_4}$, V'_{NaOH} and N_{NaOH} in equation (C-1), the variance of NAPT was estimated by equation (B-12). The 95 per cent confidence limits on population mean of NAPT were estimated by equation (B-15). Sample calculations have been presented below, where the precision of the analytical procedure in determining the concentration of sodium in three different amalgams was estimated. Amalgam No. I ($V''_{NaOH} = 0.0248$ liter)

By equation (C-1),

$$\begin{aligned} \text{NAPT} &= \frac{2300}{30} (0.025 \times 0.1 - 0.0248 \times 0.1) \\ &= 0.00153 \end{aligned}$$

Using equation (B-12),

$$\begin{aligned} \sigma_{\text{NAPT}}^2 &= \left(\frac{\partial \text{NAPT}}{\partial W_{\text{AML}}} \right)^2 \sigma_{W_{\text{AML}}}^2 + \left(\frac{\partial \text{NAPT}}{\partial V''_{\text{H}_2\text{SO}_4}} \right)^2 \sigma_{V''_{\text{H}_2\text{SO}_4}}^2 + \left(\frac{\partial \text{NAPT}}{\partial N_{\text{H}_2\text{SO}_4}} \right)^2 \times \\ &\quad \sigma_{N_{\text{H}_2\text{SO}_4}}^2 + \left(\frac{\partial \text{NAPT}}{\partial V''_{\text{NaOH}}} \right)^2 \sigma_{V''_{\text{NaOH}}}^2 + \left(\frac{\partial \text{NAPT}}{\partial N_{\text{NaOH}}} \right)^2 \sigma_{N_{\text{NaOH}}}^2 \\ &= 5.5561 \times 10^{-8} \end{aligned}$$

$$\therefore \sigma_{\text{NAPT}} = 0.0002357$$

The 95 per cent confidence limits on the population mean of NAPT (By equation (B-15))

$$= 0.00153 \pm 1.96 (0.0002357)$$

$$= 0.0015 \pm 0.0005$$

∴ Percentage precision $\approx \pm 33\%$.

Similar calculations were made for Amalgam No. II and No. III.

Amalgam No II ($V''_{\text{NaOH}} = 0.0200$ liter)

$$\text{NAPT} = 0.03833$$

$$\sigma_{\text{NAPT}}^2 = 5.2068 \times 10^{-8}$$

$$\sigma_{\text{NAPT}} = 0.0002282$$

The 95 per cent confidence limits on the population
mean of NAPT

$$= 0.03833 \pm 1.96 (0.0002282)$$

$$= 0.0383 \pm 0.0005$$

∴ Percentage precision $\approx \pm 1.3\%$.

Amalgam No. III ($V''_{\text{NaOH}} = 0.005$ liter)

$$\text{NAPT} = 0.15333$$

$$\sigma_{\text{NAPT}}^2 = 5.2018 \times 10^{-8}$$

$$\sigma_{\text{NAPT}} = 0.0002281$$

The 95 per cent confidence limits on the population
mean of NAPT

$$= 0.15333 \pm 1.96 (0.0002281)$$

$$= 0.1533 \pm 0.0005$$

∴ Percentage precision $\approx \pm 0.33\%$

APPENDIX D

AQUEOUS SOLUTION OF SULFUR DIOXIDE

1. Purity of the chemicals in preparing aqueous sulfur dioxide solution

(a) Sulfur dioxide gas

A C.I.L. sulfur dioxide tank was used as a source of SO_2 gas.

(b) Water

Freshly distilled water was used for making the aqueous solution of sulfur dioxide.

(c) Sodium hydroxide

Fisher certified ACS sodium hydroxide pellets were used for pH adjustment. Their composition was as follows:

Assay (NaOH)	not less than 97%
Sodium carbonate (Na_2CO_3)	0.5%
Chloride (Cl)	0.005%
Nitrogen compounds (as N)	0.001%
Phosphate (PO_4)	0.001%
Sulfate (SO_4)	0.003%
Ammonium hydroxide ppt	0.02%
Heavy metals (as Ag)	0.002%

Iron (Fe)	0.001%
Nickel (Ni)	0.001%
Potassium (K)	0.02%
Copper (Cu)	0.001%

2. Calculation of the total sulfur dioxide concentration in an aqueous solution sample

(a) Normality of the standard iodine solution, $N_I = 0.1N$

(b) Normality of the standard sodium thiosulfate solution,

$$N_{S_2O_3} = 0.1N$$

(c) Volume of N_I iodine solution taken in the Erlenmeyer flask, $V_1 = 0.075$ liter

(d) Volume of the aqueous sulfur dioxide solution sample, injected into the iodine solution, $V_{SO_2} = 0.005$ liter

(e) Volume of the $N_{S_2O_3}$ sodium thiosulfate solution required to titrate unreacted iodine in the Erlenmeyer flask, $V_2 = 0.0095$ liter.

••• Molarity of total sulfur dioxide in the aqueous

$$\text{solution} = \frac{1}{2V_{SO_2}} (N_I V_1 - N_{S_2O_3} V_2)$$

$$= \frac{1}{2 \times 0.005} (0.1 \times 0.075 - 0.1 \times 0.0095)$$

$$= 0.655 \text{ molar}$$

3. Estimation of the precision of the analytical procedure

The calculation method was similar to that used in estimating the precision of the analytical procedure for evaluating the concentration of sodium in the amalgam. The following steps were involved in determining the concentration of total sulfur dioxide in an aqueous solution by iodometric analysis as performed in our laboratory.

(a) Preparation of a standard potassium dichromate solution (primary standard)

W_{PDC} gms of pure anhydrous potassium dichromate was dissolved in V_{water} liter of distilled water.

$$\therefore N_{\text{Cr}_2\text{O}_7} = \frac{W_{\text{PDC}}}{49.035 V_{\text{water}}} \quad \dots \dots (D-1)$$

(b) Standardization of a sodium thiosulfate solution by the standard potassium dichromate solution

$V'_{\text{S}_2\text{O}_3}$ liters of a $N_{\text{S}_2\text{O}_3}$ sodium thiosulfate solution was titrated with $V_{\text{Cr}_2\text{O}_7}$ liters of the $N_{\text{Cr}_2\text{O}_7}$ potassium dichromate solution.

$$\therefore N_{\text{S}_2\text{O}_3} = \frac{N_{\text{Cr}_2\text{O}_7} V_{\text{Cr}_2\text{O}_7}}{V'_{\text{S}_2\text{O}_3}} \quad \dots \dots (D-2)$$

(c) Standardization of an iodine solution with the standard sodium thiosulfate solution

V_I liters of N_I iodine solution was titrated with $V_{S_2O_3}$ liters of $N_{S_2O_3}$ sodium thiosulfate solution.

$$\therefore N_I = \frac{N_{S_2O_3} V_{S_2O_3}}{V_I} \quad \dots (D-3)$$

(d) Excess of N_I iodine solution taken in an Erlenmeyer flask

V_1 liters of the N_I iodine solution was taken in an Erlenmeyer flask and was diluted with distilled water to get a sharp end point. The volume V_1 was dependent on the concentration of sulfur dioxide in the fixed-volume sample to be tested.

(e) Injection of the sulfur dioxide sample

V_{SO_2} liters of the sulfur dioxide solution was taken by a hypodermic syringe and was injected into the contents in the Erlenmeyer.

(f) Back-titration of excess iodine

The unreacted iodine was titrated with V_2 liters of $N_{S_2O_3}$ sodium thiosulfate solution.

On the basis of the steps (a) to (f), the molarity of total sulfur dioxide could be given by the following expression:

$$\text{Molarity} = \frac{1}{2 V_{\text{S}_2\text{O}_3}} (N_{\text{I}} V_1 - N_{\text{S}_2\text{O}_3} V_2) \quad \dots \dots \dots (\text{D-4})$$

Substituting the values of N_{I} and $N_{\text{S}_2\text{O}_3}$ from the equations (D-3) and (D-2) respectively,

$$\text{Molarity} = \frac{1}{98.07} \left(\frac{W_{\text{PDC}} V_{\text{Cr}_2\text{O}_7}}{V'_{\text{S}_2\text{O}_3} V_3 V_{\text{water}}} \right) \left(\frac{V_1 V_{\text{S}_2\text{O}_3}}{V_{\text{I}}} - V_2 \right) \quad \dots \dots \dots (\text{D-5})$$

Knowing the variances of the different quantities in the equation (D-5), the 95 per cent confidence limits on the population mean of molarity were estimated.

APPENDIX E

SODIUM DITHIONITE IN THE PRODUCT STREAM

1. Details of the analytical procedures and sample calculations

(a) The iodine formaldehyde method

(i) Detailed description of the iodine-formaldehyde method

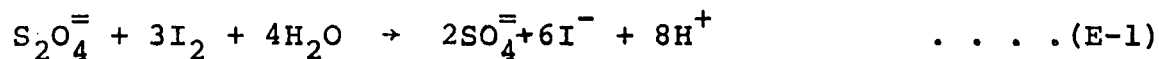
Two equal-volume (≈ 5 ml) samples of the product stream that contained primarily $S_2O_4^{=}$, $S_2O_3^{=}$ and HSO_3^- were taken using a hypodermic syringe. These samples (Sample I and Sample II) were analysed by the iodine-formaldehyde method in the following three parts. It is obvious that the amount of reagents used in different parts of the analytical procedure would depend on the concentrations of $S_2O_4^{=}$, $S_2O_3^{=}$ and HSO_3^- in the sample. Hence, the values given below are only approximate.

Part A - Determination of dithionite + thiosulfate + bisulfite:

[α] A known volume (≈ 50 ml) of a standard ($\approx 0.1N$) iodine solution was taken in an Erlenmeyer flask and diluted to about 200 ml with oxygen-free distilled water.

[β] A 5 ml sample (Sample I) of the product stream was injected under the diluted iodine solution. Iodine oxidizes

$S_2O_4^{=}$, $S_2O_3^{=}$ and HSO_3^- present in the sample as follows:



[γ] Excess iodine was back-titrated with a standard ($\approx 0.1N$) solution of sodium thiosulfate using starch-solution as an indicator.

The amount of iodine consumed by the sample in Part A gave the amount of $(S_2O_4^{=} + S_2O_3^{=} + HSO_3^-)$ in Sample I.

Part B - Determination of dithionite + thiosulfate:

[α] Approximately 25 ml of a formaldehyde solution (35 ml of 37 per cent HCHO: 50 ml of H_2O) at about $pH = 9$ was taken in an Erlenmeyer flask. It was diluted with oxygen-free distilled water (by bubbling N_2 through freshly distilled water). A drop of phenolphthalein was added which turned the colour of the solution pink.

[β] A 5 ml sample (Sample II) of the product stream was injected under the diluted formaldehyde solution. If the pink colour of the solution disappeared, some NaOH solution was immediately added. The sulfoxylate formation took place as follows.

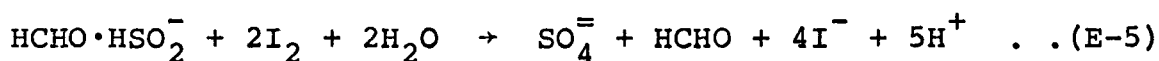


Any bisulfite (or sulfite) present in the sample was also tied down as formaldehyde bisulfite.

[γ] The flask was stoppered and allowed to stand for about 20 minutes during which time the reaction (E-4) completed.

[δ] The solution was acidified (till the pink colour disappeared) by 20 per cent acetic acid solution in water.

[ε] A known volume of a standard ($\approx 0.1\text{N}$) iodine solution was added to the contents in the Erlenmeyer. Provided there was an excess of iodine, formaldehyde sulfoxylate and thiosulfate present in the system were oxidized as follows:



Both reactions took place in acidic medium

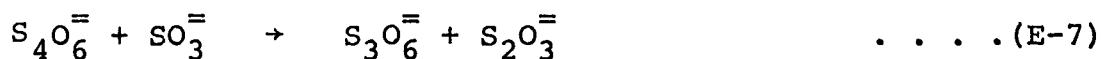
[ζ] Excess iodine was back-titrated with a standard ($\approx 0.1\text{N}$) solution of thiosulfate using starch-solution as an indicator.

The amount of iodine consumed by

HCHO \cdot HSO₂⁻ and S₂O₃⁼ gave the amount of (S₂O₄⁼ + S₂O₃⁼) in Sample II.

Part C - Determination of thiosulfate:

[α] After the end-point had been reached in Part A, approximately 30 ml of a 5 per cent sodium sulfite heptahydrate solution was added to the contents of the Erlenmeyer. The following reaction took place.



[β] The optimum pH range, within which the reaction was quantitative in five minutes, was 5.5 to 9.5. So a drop of phenolphthalein was added and a normal solution of sodium hydroxide was added until the solution turned pink. It was allowed to stand for five minutes.

[γ] Approximately 5 ml of the formaldehyde solution was added to bind excess sulfite.

[δ] The contents in the flask were acidified with 10 ml of 20 per cent acetic acid.

[ϵ] Thiosulfate generated due to reaction (E-7) was titrated with a standard (\approx 0.1N) solution of iodine using a starch-solution as an indicator.

The iodine consumed in Part C corresponds to 1/2 (thiosulfate present in Sample I + thiosulfate added in Part A).

(ii) Sample calculations for the iodine-formaldehyde method

At steady-state, during experimental run 23, two samples of 5 ml were taken by a hypodermic syringe.

Normality of sodium thiosulfate solution used for analysis = 0.1N

Normality of iodine solution used for analysis = .099N

Data obtained in Part A:

Volume of 0.099N iodine taken = 60.0 ml

Volume of sample = 5 ml

Volume of 0.1N $\text{Na}_2\text{S}_2\text{O}_3$ used in back-titration = 18.9 ml

Data obtained in Part B:

Volume of sample dissolved in formaldehyde = 5 ml

Volume of 0.099N iodine taken = 20.0 ml

Volume of 0.1N $\text{Na}_2\text{S}_2\text{O}_3$ used in back-titration = 16.55 ml

Data obtained in Part C:

After adding 30 ml of 5 per cent sodium sulfite heptahydrate,

Volume of .099N iodine used in the titration = 9.75 ml

On the basis of the above mentioned data,

$\text{S}_2\text{O}_4^{=}$ + $\text{S}_2\text{O}_3^{=}$ + $\text{SO}_3^{=}$ consumed (by oxidation in Part A)

$$= (60.0 - \frac{18.9 \times 0.1}{.099}) \text{ml of } .099\text{N Iodine}$$

$$= 40.91 \text{ ml of } .099\text{N Iodine}$$

$\text{S}_2\text{O}_3^=$ in Sample I + $\text{S}_2\text{O}_3^=$ added in Part A

$$\equiv 2 \times 9.75 = 19.50 \text{ ml of } .099\text{N Iodine}$$

$\text{S}_2\text{O}_3^=$ added in Part A

$$\equiv \frac{18.9 \times 0.1}{.099} = 19.09 \text{ ml of } .099\text{N Iodine}$$

Therefore,

$\text{S}_2\text{O}_3^=$ in a 5 ml sample of product stream

$$\equiv 19.50 - 19.09 = 0.41 \text{ ml of } .099\text{N Iodine}$$

$\text{Na}_2\text{S}_2\text{O}_3$ in the product stream

$$= \frac{0.41 \times .099}{1000} = .00004059 \frac{\text{gm moles } \text{Na}_2\text{S}_2\text{O}_3}{5 \text{ ml}}$$

$\text{S}_2\text{O}_4^= + \text{S}_2\text{O}_3^=$ in Sample II consumed

$$= 20 - \frac{16.55 \times 0.1}{.099}$$

$$= 3.283 \text{ ml of } .099\text{N Iodine}$$

$\therefore \text{Na}_2\text{S}_2\text{O}_4$ in the product stream

$$= \frac{(3.283 - 0.41) \times .099}{4 \times 1000} = .0000716 \frac{\text{gm moles Na}_2\text{S}_2\text{O}_4}{5 \text{ ml}}$$

∴ Concentration of $\text{Na}_2\text{S}_2\text{O}_4$ in the product stream

$$= .0000716 \times 174 \times 20 = \frac{.249 \text{ gms Na}_2\text{S}_2\text{O}_4}{100 \text{ ml}}$$

NaHSO_3 in the product stream

$$= \frac{(40.91 - 2.893 \times \frac{6}{4} - 0.41) \cdot 099}{2 \times 1000}$$

$$= .0017899 \frac{\text{gm moles NaHSO}_3}{5 \text{ ml sample}}$$

∴ Total SO_2 in 5 ml of the product stream,

$$\text{SO}_2 \text{ from Na}_2\text{S}_2\text{O}_4 = 2 \times .0000716 = .0001432 \text{ gm moles}$$

$$\text{SO}_2 \text{ from Na}_2\text{S}_2\text{O}_3 = 2 \times .00004059 = .0000812 \text{ gm moles}$$

$$\text{SO}_2 \text{ from NaHSO}_3 = .0017899 = .0017899 \text{ gm moles}$$

$$\text{Total} = .0020143 \text{ gm moles}$$

The concentration of 'total' SO_2 going into the reactor was checked by iodometry. The concentration of sulfur dioxide in aqueous solution entering the reactor was .400 molar

∴ 5 ml of the sulfur dioxide solution entering the reactor

contained .002 moles of SO_2 which compares well with the SO_2 in the product stream.

(b) The Rubine-R method

(i) Detailed description of the Rubine-R method

A standard solution of Rubine-R dye for dithionite analytical purposes was purchased from Virginia Chemicals, Portsmouth, Va., U.S.A. This dye solution was re-standardized before use in the laboratory.

Five ml of a standard (N_{RR}) solution of Rubine-R was pipetted into an Erlenmeyer flask. The dye solution was diluted with approximately 150 ml of oxygen-free distilled water. The Erlenmeyer flask with its contents was flushed with a stream of N_2 gas and then it was stoppered with a rubber bung. Samples of product stream were drawn into a burette from the reactor, periodically, during an experimental run. These samples were titrated with the bright red dye solution, with vigorous agitation, to an amber end-point. Throughout the titration, the burette and the Erlenmeyer flask were kept under N_2 atmosphere.

During the course of experiments, it was observed that at low pH (about pH = 1.0), the colour changed from bright red to colourless very sharply at the end-point. Hence, approximately 2 ml of concentrated sulfuric acid

was added to the diluted Rubine-R before titrating it with dithionite in the product stream. It was observed that the addition of sulfuric acid to the Rubine-R solution did not have any significant effect on the results.

If V_p liters of the product stream were titrated with V_{RR} liters of N_{RR} Rubine-R solution.

∴ the concentration of $\text{Na}_2\text{S}_2\text{O}_4$ in the product stream

$$= \frac{87.0526 V_{RR} N_{RR}}{10 V_p} \frac{\text{gms Na}_2\text{S}_2\text{O}_4}{100 \text{ ml}} \dots (E-8)$$

The use of the Rubine-R method depends on accurate standardization of the dye solution. Rubine-R solution was standardized with a standard solution of $\text{Ti}_2(\text{SO}_4)_3$. Preparation and standardization of $\text{Ti}_2(\text{SO}_4)_3$ solution and standardization of Rubine-R with $\text{Ti}_2(\text{SO}_4)_3$ solution have been discussed below.

[α] Preparation of $\text{Ti}_2(\text{SO}_4)_3$ solution

A 20 per cent standardized solution of $\text{Ti}_2(\text{SO}_4)_3$ was purchased from La Motte Chemical Products CO., Chestertown, Maryland, U.S.A. According to manufacturer's specification, the solution was prepared for chemical tests and was free of sulfides (commercial titanous sulfate solution sometimes contains sulfides which can be eliminated as hydrogen sulfide on boiling). One hundred ml of the concentrated

solution was diluted to one liter by oxygen-free distilled water. The solution was kept under an atmosphere of oxygen-free carbon dioxide gas (CO_2 was scrubbed through a solution that contained one part of $\text{Na}_2\text{S}_2\text{O}_4$, two parts of NaHCO_3 and 20 parts H_2O).

[β] Standardization of $\text{Ti}_2(\text{SO}_4)_3$ Solution

$\text{Ti}_2(\text{SO}_4)_3$ solution is unstable at high temperatures, in presence of oxygen and when exposed to direct sunlight. The following text-book methods were used to standardize diluted $\text{Ti}_2(\text{SO}_4)_3$ solution before its use in the laboratory.

- The ferric ammonium sulfate method¹
- The potassium dichromate method¹
- The iron content determination method²

The results obtained by these three methods were comparable and reproducible. Only potassium dichromate method has been described here, briefly, for it is a very accurate and precise method. Information on the other methods can be obtained from the literature cited.

-
1. Vogel, A.I., "A text-book of qualitative inorganic analysis," 3rd Ed. John Wiley and Sons, New York, 1961.
 2. Pierson, R.H. and Gantz, E. St. Clair., Analytical Chemistry, 26, No. 11, 1809 (1954).

The potassium dichromate method:

If very accurate results are desired or if the normality of ferric ammonium sulfate solution is not exactly known, the standardization of $Ti_2(SO_4)_3$ solution can be carried out with 0.1N potassium dichromate solution using the approximately 0.1N ferric ammonium sulfate solution as an intermediary.

Into a 250 ml flask, 25.0 ml of primary standard 0.1N potassium dichromate and 20 ml of dilute sulfuric acid (2:5 W/W) were placed, oxygen-free carbon dioxide was passed to displace air and the stream of gas was maintained during the titration. Forty ml of the titanous sulfate solution was added to the contents in the flask. The liquids were mixed by swirling the flask gently and the excess titanous solution was titrated with 0.1N ferric ammonium sulfate solution. When the dark colour due to the titanous salt had nearly disappeared, 10 ml of 10 per cent ammonium thiocyanate solution was added and the addition of ferric ammonium sulfate solution was continued until a red or pink colouration was obtained which was permanent for at least one minute. In the same way 40.0 ml of the titanous sulfate solution was titrated with 0.1N ferric ammonium sulfate solution but the addition of 0.1N potassium dichromate solution was omitted. From the results obtained, the exact normality of the ferric ammonium sulfate solution and the

normality of titanous sulfate solution was calculated.

The method of calculation has been described below.

If,

N_T = Normality of $Ti_2(SO_4)_3$ solution

N_{Fe} = Normality of ferric ammonium sulfate solution

$N_{Cr_2O_7}$ = Normality of potassium dichromate solution

V_T = Volume of $Ti_2(SO_4)_3$ solution taken in the flask during the first titration where potassium dichromate solution was added

$V_{Cr_2O_7}$ = Volume of potassium dichromate solution taken in the first titration

V_{Fe} = Volume of ferric ammonium sulfate solution used in the first titration

V'_T = Volume of $Ti_2(SO_4)_3$ solution taken in the flask during the second titration where no potassium dichromate solution was added

V'_{Fe} = Volume of ferric ammonium sulfate solution used in the second titration

∴ during first titration,

$$V_T N_T - V_{Cr_2O_7} N_{Cr_2O_7} = V_{Fe} N_{Fe} \quad \dots (E-9)$$

and during second titration,

$$V_T' N_T = V_{Fe}' N_{Fe} \quad \dots (E-10)$$

From equations (E-9) and (E-10),

$$N_T = \frac{V_{Cr_2O_7} N_{Cr_2O_7}}{V_T - \frac{V_T' V_{Fe}}{V_{Fe}'}} \quad \dots (E-11)$$

[γ] Standardization of Rubine-R solution by standard $Ti_2(SO_4)_3$ solution³

Twenty five ml of Rubine-R dye solution was pipetted into a 300 ml Erlenmeyer flask. To this was added, 25 ml of distilled water, 5 ml of 10 per cent Na_2CO_3 solution, 50 ml of methanol and 25 ml of 25 per cent sodium tartarate solution. The contents in the Erlenmeyer flask were boiled gently for five minutes while sweeping with oxygen-free CO_2 and were titrated hot with the standard solution of $Ti_2(SO_4)_3$. The colour change at the end-point was from pink to amber and was quite sharp.

3. Wood, P.J., Am. Dyestuff Reporter, 443, June 17 (1957).

If,

N_{RR} = Normality of Rubine-R solution

N_T = Normality of $Ti_2(SO_4)_3$ solution

V_{RR} = Volume of the Rubine-R solution taken in the flask

V_T'' = Volume of $Ti_2(SO_4)_3$ solution used in the titration

$$\therefore N_{RR} = \frac{V_T'' N_T}{V_{RR}} \quad \dots \dots (E-12)$$

(ii) Sample calculations for the Rubine-R method

[α] Standardization of $Ti_2(SO_4)_3$ solution by potassium dichromate solution:

The following data was obtained for the parameters in equation (E-11)

$N_{Cr_2O_7}$ = 0.10204

V_T = 0.020 liter

$V_{Cr_2O_7}$ = 0.010 liter

V_{Fe} = 0.0112 liter

V_T' = 0.010 liter

V_{Fe}' = 0.1055 liter

Using equation (E-11),

$$N_T = \frac{V_{Cr_2O_7} N_{Cr_2O_7}}{V_T - \frac{V_T' V_{Fe}}{V_{Fe}'}} = \frac{0.010 \times 0.10204}{0.020 - \frac{0.010 \times 0.0112}{0.01055}}$$

$$= 0.10874N$$

[β] Standardization of the Rubine-R solution by $Ti_2(SO_4)_3$ solution

The following data was obtained for the parameters in equation (E-12)

$$N_T = 0.10874N$$

$$V_{RR} = 0.010 \text{ liter}$$

$$V_T'' = 0.0106 \text{ liter}$$

Using equation (V. 12),

$$N_{RR} = \frac{V_T'' N_T}{V_{RR}} = \frac{0.0106 \times 0.10874}{0.010} = 0.11526N$$

[γ] Concentration of sodium dithionite in the product stream

During the experimental run 23, under steady-state conditions, the values of the parameters in equation (E-8) were as follows:

$$\begin{aligned}
 V_{RR} &= 0.005 \text{ liter} \\
 N_{RR} &= 0.11526N \\
 V_P &= 0.01828 \text{ liter}
 \end{aligned}$$

∴ Using equation (E-8),

The concentration of $\text{Na}_2\text{S}_2\text{O}_4$ in the product stream

$$\begin{aligned}
 &= \frac{87.0526 V_{RR} N_{RR}}{10 V_P} \\
 &= \frac{87.0526 \times 0.005 \times 0.11526}{10 \times 0.01828} \\
 &= 0.2744 \frac{\text{gms Na}_2\text{S}_2\text{O}_4}{100 \text{ ml of the product stream}}
 \end{aligned}$$

2. Estimation of the precision of the Rubine-R method

In this section various steps involved in determining the concentration of $\text{Na}_2\text{S}_2\text{O}_4$ in a sample, from the product stream of the reactor, by the Rubine-R method have been outlined. The method of error calculation was indicated in connection with the analysis of an amalgam sample (Appendix C). For brevity, the calculations have not been attached. The different steps were:

- (a) Preparation of a standard solution of iodine.
- (b) Standardization of a sodium thiosulfate solution by the standard iodine solution.
- (c) Standardization of a potassium dichromate solution by the standard solution of sodium thiosulfate.
- (d) Standardization of a titanous sulfate solution by the standard solution of the potassium dichromate.
- (e) Standardization of a Rubine-R solution by the standard solution of titanous sulfate.
- (f) Titration of a product stream sample, containing sodium dithionite, with a known volume of the standard solution of Rubine-R.

APPENDIX F

DATA PROCESSING

1. Mathematical expressions for calculating $C_{S_2O_4}$, Y_{SO_2} , Y_{Na} , CONNA, X_{Na} , Na/SO₂, rate of sodium consumption, and sample calculations.

(a) Mathematical expressions

Mathematical expressions to calculate these quantities were derived from their definitions and the results have been included. The symbols used in these expressions have been explained in Chapter IX. It was assumed that the density of an amalgam did not change significantly in the range of temperatures used for the present investigation. Therefore, the density of amalgam was calculated by the following expression (Section II.E.4):

Density of the amalgam (gm/ml)

$$= 13.55 - 0.9986 \times (\text{gms of sodium}/100 \text{ gms of the amalgam})$$

- (i) Concentration of sodium dithionite in the product stream,

$$\begin{aligned}
 C_{S_2O_4} &= \frac{(\text{gms of sodium dithionite})}{(100 \text{ ml of the product stream})} \\
 &= \frac{100 \times \text{STRUB}}{\text{VDITHI}} \quad \dots (F-1)
 \end{aligned}$$

(ii) Yield of sodium dithionite on total sulfur dioxide entering the reactor (%),

$$Y_{SO_2} = \frac{(\text{gm molar conc. of Na}_2\text{S}_2\text{O}_4 \text{ in product}) \times 2 \times 100}{(\text{gm molar conc. of total SO}_2 \text{ in aqueous feed})}$$

$$= \frac{2 \times 10^5 \times \text{STRUB}}{174.1052 \times \text{STSO}_2 \times \text{VDITHI}} \quad \dots \dots \text{(F-2)}$$

(iii) Yield of sodium dithionite on sodium entering the reactor with the fresh amalgam (%),

$$Y_{Na} = \frac{(\text{gm moles of Na}_2\text{S}_2\text{O}_4 \text{ in product/min}) \times 2 \times 100}{(\text{gm moles of Na entering with fresh amalgam/min})}$$

$$= \frac{46 \times 10^7 \times \text{FLSO}_2 \times \text{STRUB}}{174.1052 \times \text{VDITHI} \times \text{FLHG} \times \text{CHGF} \times (13.55 - 0.9986 \times \text{CHGF})}$$

(iv) Yield of sodium dithionite on sodium consumed in the reactor (%),

$$\text{CONNA} = \frac{(\text{gm moles of Na}_2\text{S}_2\text{O}_4 \text{ in product/min}) \times 2 \times 100}{\left(\begin{array}{l} \text{gm moles of Na entering with fresh amalgam/min} \\ - \text{gm moles of Na leaving with spent amalgam/min} \end{array} \right)}$$

$$\text{CONNA} = \left(\frac{46 \times 10^5 \times \text{FLSO}_2 \times \text{STRUB}}{174.1052 \times \text{VDITHI} \times \text{FLHG} \times (\text{CHGF} - \text{CHGS})} \right) \times \left(\frac{(100 - \text{CHGS})}{(13.55 - 0.9986 \times \text{CHGF})} \right) \dots \dots \dots (\text{F-4})$$

(v) Conversion of sodium from the amalgam to different products in the reactor (%),

$$X_{\text{Na}} = \frac{\left(\begin{array}{l} \text{gm moles of Na entering with fresh amalgam/min} \\ - \text{gm moles of Na leaving with spent amalgam/min} \end{array} \right) \times 100}{(\text{gm moles of Na entering with fresh amalgam/min})}$$

$$= 100 \times \left(1 - \frac{(100/\text{CHGF} - 1)}{(100/\text{CHGS} - 1)} \right) \dots \dots \dots (\text{F-5})$$

(vi) Na/SO₂ ratio entering the reactor,

$$= \frac{(\text{gm moles of Na entering with fresh amalgam/min})}{-(\text{gm moles of Na leaving with spent amalgam/min})}$$

$$= \frac{\text{FLHG} \times \text{CHGF} \times (13.55 - 0.9986 \times \text{CHGF})}{2300 \times \text{STSO}_2 \times \text{FLSO}_2} \dots \dots \dots (\text{F-6})$$

(vii) Rate of sodium consumption in the reactor,

$$= (\text{gm moles of Na entering with fresh amalgam/min}) \\ - (\text{gm moles of Na leaving with spent amalgam/min})$$

$$= \left(\frac{\text{FLHG} \times (13.55 - 0.9986 \times \text{CHGF})}{2300} \right) \\ \times \left(\text{CHGF} - \frac{(100 - \text{CHGF})}{(100 - \text{CHGS})} \times \text{CHGS} \right) \dots (F-7)$$

(b) Sample Calculations

Experimental run 54 was considered for the sample calculations. The process variables were fixed at the following levels:

CHGF	=	.04029%
STSO ₂	=	.6425 gm moles/liter
(RPM) _{Aq}	=	673 rpm
FLSO ₂	=	.0955 liters/min
FLHG	=	47.5 ml/min
(A/V) _{Aq}	=	.0784 cm ² /cm ³
TEMP	=	17°C
pH	=	5.6

Under the steady state conditions,

$$\text{CHGS} = .00407\%$$

$$\text{VDITHI} = 7.40 \text{ ml}$$

$$\text{STRUB} = .049397 \text{ gms of Na}_2\text{S}_2\text{O}_4$$

- (i) Steady-state concentration of sodium dithionite in the product stream

Using equation (F-1),

$$C_{\text{S}_2\text{O}_4} = \frac{100 \times \text{STRUB}}{\text{VDITHI}} = \frac{100 \times .049397}{7.40} = .66753 \frac{\text{gms}}{100 \text{ ml}}$$

- (ii) Steady-state yield of sodium dithionite on total sulfur dioxide entering the reactor (%)

Using equation (F-2),

$$Y_{\text{SO}_2} = \frac{2 \times 10^5 \times .049397}{174.1052 \times .6425 \times 7.40} = 11.935\%$$

- (iii) Steady-state yield of sodium dithionite on sodium entering the reactor with fresh amalgam (%)

Using equation (F-3),

$$Y_{\text{Na}} = \frac{46 \times 10^7 \times .0955 \times .049397}{174.1052 \times 7.40 \times 47.5 \times .04029 \times (13.55 - 0.9986 \times .04029)}$$

$$= 65.145\%$$

(iv) Steady-state yield of sodium dithionite on sodium consumed in the reactor (%)

Using the equation (F-4),

$$\text{CONNA} = \left(\frac{46 \times 10^5 \times .0955 \times .049397}{174.1052 \times 7.40 \times 47.5 \times (.04029 - .00407)} \right)$$

$$\times \left(\frac{(100 - .00407)}{(13.55 - 0.9986 \times .04029)} \right)$$

$$= 72.462\%$$

(v) Steady-state conversion of sodium from the amalgam to different products in the reactor (%)

Using equation (F-5),

$$X_{\text{Na}} = 100 \times \left(1 - \frac{(100/.04029) - 1}{(100/.00407) - 1} \right) = 89.902\%$$

(vi) Na/SO₂ ratio entering the reactor

Using equation (F-6),

$$\begin{aligned} \text{Na/SO}_2 &= \frac{47.5 \times .04029 \times (13.55 - 0.9986 \times .04029)}{2300 \times .6425 \times .0955} \\ &= .18320 \end{aligned}$$

(vii) Rate of sodium consumption

Using equation (F-7),

$$\begin{aligned} \text{Rate} &= \left(\frac{47.5 \times (13.55 - 0.9986 \times .04029)}{2300} \right) \\ &\quad \times \left(.04029 - \frac{(100 - .04029)}{(100 - .00407)} \times .00407 \right) \\ &= .010106 \text{ gm moles/min} \end{aligned}$$

2. The 95 per cent confidence limits of the steady-state $C_{S_2O_4}$, Y_{SO_2} , Y_{Na} , CONNA, X_{Na} , Na/SO₂ and rate of sodium consumption for an experimental run.

To estimate the 95 per cent confidence limits of the steady-state $C_{S_2O_4}$, Y_{SO_2} , Y_{Na} , CONNA and X_{Na} for an experimental run, it was necessary to know the values and the variances

of the parameters used in equations (F-1) to (F-7). The data taken during experimental run 54 was used for the sample calculations.

(a) Value and variance of STRUB

The normality of the Rubine-R solution used for the analysis of sodium dithionite in the product stream was determined by the method outlined in the Section E.1.b. The normality of the Rubine-R solution used in the experimental run 54 was, $N_{RR} = .1134885N$.

The variance of the normality of the Rubine-R solution was estimated by the method of propagation of random error. The steps involved have been outlined in the Appendix E (steps a to e Section E.2). The variance of the normality of the Rubine-R solution was estimated to be, $\sigma_{N_{RR}}^2 = .856884 \times 10^{-7}$ (\therefore 95 per cent confidence limits of $N_{RR} = \pm .0006$).

STRUB = gms of $Na_2S_2O_4$ which would discolour 5 ml of
.1134885N Rubine-R solution

$$= 87.0526 \times .005 \times .1134885$$

$$= .0493973 \text{ gms of } Na_2S_2O_4$$

Neglecting any error involved in pipetting the 5 ml of Rubine-R solution, the variance of STRUB was estimated to be, $\sigma_{STRUB}^2 = .16236 \times 10^{-7}$ (\therefore 95 per cent confidence limits of STRUB = $\pm .0003$).

(b) Value and variance of VDITHI

Volume of the product stream, at steady-state, required to discolour 5 ml of 0.1134885N Rubine-R solution, VDITHI, was 7.40 ml.

The variance of VDITHI was estimated by knowing the maximum range of random error expected in using a 50 ml burette.

$$\therefore \sigma_{VDITHI}^2 = \left(\frac{.05}{3}\right)^2 = 2.7889 \times 10^{-4}$$

(\therefore 95 per cent confidence limits of VDITHI = $\pm .03$).

(c) Value and variance of STSO₂

The method to calculate STSO₂ and $\sigma_{STSO_2}^2$ has been outlined in Appendix D. Knowing the values and the variances of the parameters in equation (D-5), the value and the variance of STSO₂ were calculated.

$$STSO_2 = 0.6425 \text{ molar}$$

$$\sigma_{STSO_2}^2 = .327441 \times 10^{-5}$$

(\therefore 95 per cent confidence limits of STSO₂ = $\pm .004$).

(d) Value and Variance of $FLSO_2$

The flow rate of the aqueous sulfur dioxide solution, $FLSO_2$, was determined by measuring the volume of the aqueous solution that flowed into a graduated cylinder in a fixed length of time. This procedure was repeated several times and the mean flow rate, $FLSO_2$, was found to be .0955 liters/min. The variance of $FLSO_2$, $\sigma_{FLSO_2}^2$, was estimated by equation (B-2).

$$\sigma_{FLSO_2}^2 = .11758 \times 10^{-5}$$

(∴ 95 per cent confidence limits of $FLSO_2 = \pm .002$).

(e) Value and variance of FLHG

The flow rate of pure mercury, FLHG, was determined by measuring the volume of the mercury that collected in a graduated cylinder in a fixed length of time. This procedure was repeated several times and the following results were obtained.

$$FLHG = 47.5 \text{ ml/min}$$

$$\sigma_{FLHG}^2 = .188695$$

(∴ 95 per cent confidence limits of FLHG = ± 0.8).

(f) Values and variances of CHGF and CHGS

The values of CHGF and CHGS were calculated by the method indicated in Appendix C. Knowing the variances of different measured quantities in the mathematical expression to calculate CHGF or CHGS (equation C-1, Appendix C), the variances of CHGF and CHGS were calculated by the method of propagation of random error. The following results were obtained

$$\begin{aligned} \text{CHGF} &= .04029\% \\ \sigma_{\text{CHGF}}^2 &= .63426 \times 10^{-7} \end{aligned}$$

(••• 95 per cent confidence limits of CHGF = $\pm .0005$).

$$\begin{aligned} \text{CHGS} &= .00407\% \\ \sigma_{\text{CHGS}}^2 &= .82510 \times 10^{-7} \end{aligned}$$

(••• 95 per cent confidence limits of CHGS = $\pm .0005$).

Knowing the values and the variances of the parameters mentioned above, the variances of $C_{\text{S}_2\text{O}_4}$, Y_{SO_2} , Y_{Na} , CONNA, X_{Na} , Na/SO₂ and rate of sodium consumption were estimated by the method of propagation of random error. The 95 per cent confidence limits of these quantities were estimated by using equation (B-15) (Appendix B). The results were as follows:

$$C_{S_2O_4} = .668 \pm .005 \quad (\cdot \cdot \cdot \text{Percentage error} \approx .75\%)$$

$$Y_{SO_2} = 11.9 \pm .1 \quad (\cdot \cdot \cdot \text{Percentage error} \approx .84\%)$$

$$Y_{Na} = 65 \pm 2 \quad (\cdot \cdot \cdot \text{Percentage error} \approx 3.1\%)$$

$$CONNA = 72 \pm 3 \quad (\cdot \cdot \cdot \text{Percentage error} \approx 4.2\%)$$

$$X_{Na} = 90 \pm 1 \quad (\cdot \cdot \cdot \text{Percentage error} \approx 1.1\%)$$

$$Na/SO_2 = .183 \pm .006 \quad (\cdot \cdot \cdot \text{Percentage error} \approx 3.3\%)$$

Rate of sodium consumption

$$= .0101 \pm .0003 \quad (\cdot \cdot \cdot \text{Percentage error} \approx 3\%)$$

It is interesting to note that despite a large error in determining CHGS ($\approx 12\%$), the error in CONNA and X_{Na} is relatively small.

3. Experimental data and results

Tables F-I to F-XIV show the steady-state values of the process variables and other quantities which were used to calculate the steady-state values of Na/SO_2 , rate of sodium consumption, $C_{S_2O_4}$, Y_{SO_2} , Y_{Na} , CONNA and X_{Na} . The results and the 95 per cent confidence limits of Y_{SO_2} , Y_{Na} , CONNA and X_{Na} are also presented.

Tables F-XV to F-XXXII show the unsteady-state results for runs in the experimental sets: 42-46, 23-28 and 65-77.

TABLE F-I

STEADY-STATE DATA AND RESULTS FOR EXPERIMENTAL SET 47-57 (Expts. 47, 50, 52, 53, 54, 55 and 57)

(RPM)_{Aq} = 673; FLSO₂ = .0955; FLHG = 47.5; (A/V)_{Aq} = .0784; TEMP = 17; STRUB = .049397

RUN	CHGF	CHGS	STSO ₂	pH	VDITHI	Na/SO ₂	C _{S₂O₄}	Y _{SO₂} ±EY _{SO₂}	Y _{Na} ±EY _{Na}	CONNA ±ECONNA	X _{Na} ±EX _{Na}
47	.09322	.01347	.65500	5.75	7.700	.414	.642	11.3 ±.1	27.2 ±.8	32 ±1	85.6 ±.5
50	.04573	.00383	.64500	5.80	6.650	.207	.743	13.2 ±.1	64 ±2	70 ±2	92 ±1
52	.04257	.00384	.63950	5.60	7.520	.194	.657	11.8 ±.1	61 ±2	67 ±2	91 ±1
53	.07735	.00762	.64775	6.0	7.158	.348	.690	12.2 ±.1	35 ±1	39 ±1	90.2 ±.7
54	.04029	.00407	.64250	5.60	7.400	.183	.668	11.9 ±.1	65 ±2	72 ±3	90 ±1
55	.05776	.00399	.63900	5.80	5.770	.264	.856	15.4 ±.1	58 ±2	63 ±2	93.1 ±.9
57	.06854	.00391	.65625	5.95	5.60	.304	.882	15.4 ±.1	51 ±2	54 ±2	94.3 ±.7

TABLE F-II

STEADY-STATE DATA AND RESULTS FOR EXPERIMENTAL SET 65-77 (Expts. 65, 67, 69, 71, 73, 75 and 77)

(RPM)_{Aq} = 673; FL_{SO₂} = .0955; FLHG = 47.5; (A/V)_{Aq} = .0784; TEMP = 17; STRUB = .049397

RUN	CHGF	CHGS	STSO ₂	pH	VDITHI	RATE OF Na CONSUMPTION*	Na/SO ₂	C _{S₂O₄}	Y _{SO₂} ±EY _{SO₂}	Y _{Na} ±EY _{Na}	CONNA ±ECONNA	X _{Na} ±EX _{Na}
65	.10104	.01932	.65125	6.00	8.250	.0227	.451	.599	10.56 ±.09	23.4 ±.7	28.9 ±.9	80.9 ±.5
67	.06626	.00387	.65000	5.95	5.600	.0174	.297	.882	15.6 ±.1	52 ±2	56 ±2	94.2 ±.8
69	.04677	.00374	.65050	5.65	6.733	.0120	.210	.734	13.0 ±.1	62 ±2	67 ±2	92 ±1
71	.07542	.00609	.65800	5.95	6.717	.0193	.334	.735	12.8 ±.1	38 ±1	42 ±1	91.9 ±.5
73	.05914	.00414	.65300	5.80	5.700	.0153	.264	.867	15.2 ±.1	58 ±2	62 ±2	93.0 ±.9
75	.03921	.00391	.65075	5.40	7.795	.0098	.176	.634	11.2 ±.1	64 ±2	71 ±3	90 ±1
77	.08920	.01104	.65550	5.70	7.770	.0217	.396	.636	11.1 ±.1	28.1 ±.8	32 ±1	87.6 ±.6

* gm moles/min

TABLE F-III

STEADY-STATE DATA AND RESULTS FOR EXPERIMENTAL SET 66-76 (Expts. 66, 68, 70, 72, 74 and 76)

 $(RPM)_{Aq} = 225$; $FLSO_2 = .0955$; $FLHG = 47.5$; $(A/V)_{Aq} = .0784$; $TEMP = 17$; $STRUB = .049397$

RUN	CHGF	CHGS	STSO ₂	pH	VDITHI	Na/SO ₂	C _{S₂O₄}	Y _{SO₂} ±EY _{SO₂}	Y _{Na} ±EY _{Na}	CONNA ±ECONNA	X _{Na} ±EX _{Na}
66	.06626	.00421	.6500	5.95	6.120	.297	.807	14.3 ±.1	48 ±1	51 ±2	93.7 ±.7
68	.04677	.00415	.65050	5.65	7.237	.210	.683	12.1 ±.1	57 ±2	63 ±2	91 ±1
70	.07542	.00703	.65800	5.90	7.450	.334	.663	11.6 ±.1	35 ±1	38 ±1	90.7 ±.5
72	.05914	.00471	.65300	5.75	6.237	.264	.792	13.9 ±.1	53 ±2	57 ±2	92.0 ±.9
74	.03921	.00361	.65075	5.35	8.400	.176	.588	10.38 ±.09	59 ±2	65 ±2	91 ±1
76	.08920	.01437	.65550	5.75	9.330	.396	.529	9.28 ±.08	23.4 ±.7	27.9 ±.8	83.9 ±.5

TABLE F-IV

STEADY-STATE DATA AND RESULTS FOR EXPERIMENTAL SET 62-63 (Expts. 62 and 63)

 $(RPM)_{Aq} = 225$; $FLSO_2 = .0955$; $FLHG = 47.5$; $(A/V)_{Aq} = .0784$; $TEMP = 17$; $STRUB = .049397$

RUN	CHGF	CHGS	STSO ₂	pH	VDITHI	Na/SO ₂	C _{S₂O₄}	Y _{SO₂} ±EY _{SO₂}	Y _{Na} ±EY _{Na}	CONNA ±ECONNA	X _{Na} ±EX _{Na}
62	.10116	.02563	.64550	6.15	9.750	.456	.507	9.02 ±.07	19.8 ±.6	26.5 ±.8	74.7 ±.5
63	.06352	.00413	.6390	5.70	6.210	.290	.795	14.3 ±.1	49 ±1	53 ±2	93.5 ±.7

TABLE F-V

STEADY-STATE DATA AND RESULTS FOR EXPERIMENTAL SET 87-91 (Expts. 87, 89 and 91)

 $(RPM)_{Aq} = 225$; $FLSO_2 = .0955$; $FLHG = 47.5$; $(A/V)_{Aq} = .0784$; $TEMP = 17$; $STRUB = .047495$

RUN	CHGF	CHGS	STSO ₂	pH	VDITHI	Na/SO ₂	C _{S₂O₄}	Y _{SO₂} ±EY _{SO₂}	Y _{Na} ±EY _{Na}	CONNA ±ECONNA	X _{Na} ±EX _{Na}
87	.05605	.00472	.65800	5.75	6.172	.249	.770	13.4 ±.1	54 ±2	59 ±2	92 ±1
89	.09863	.02162	.65450	5.85	9.064	.438	.524	9.2 ±.1	21.0 ±.6	26.9 ±.8	78.1 ±.5
91	.03723	.00360	.65800	5.35	8.38	.165	.567	9.9 ±.1	60 ±2	66 ±2	90 ±1

TABLE F-VI

STEADY-STATE DATA AND RESULTS FOR EXPERIMENTAL SET 95-105 (Expts. 95, 97, 99, 103 and 105)

 $(RPM)_{Aq} = 673$; $FLSO_2 = .198$; $FLHG = 47.5$; $(A/V)_{Aq} = .0784$; $TEMP = 17$; $STRUB = .047495$

RUN	CHGF	CHGS	STSO ₂	pH	VDITHI	RATE OF Na CONSUMPTION*	Na/SO ₂	C _{S₂O₄}	Y _{SO₂} ±EY _{SO₂}	Y _{Na} ±EY _{Na}	CONNA ±ECONNA	X _{Na} ±EX _{Na}
95	.04387	.00533	.65700	5.20	14.040	.0108	.094	.338	5.92 ±.06	63 ±2	72 ±2	88 ±1
97	.09119	.00487	.65800	5.65	8.010	.0240	.195	.593	10.4 ±.1	53 ±1	56 ±1	94.7 ±.6
99	.08184	.00467	.65700	5.60	8.450	.0215	.175	.562	9.8 ±.1	56 ±1	60 ±1	94.3 ±.6
103	.05460	.00455	.66000	5.40	11.267	.0140	.116	.422	7.34 ±.08	63 ±1	69 ±2	92 ±1
105	.07107	.00487	.65300	5.65	9.017	.0184	.153	.527	9.3 ±.1	61 ±1	65 ±2	93.2 ±.8

* gm moles/min

TABLE F-VII

STEADY-STATE DATA AND RESULTS FOR EXPERIMENTAL SET 23-28 (Expts. 23, 24, 25, 26, 27 and 28)

 $(RPM)_{Aq} = 673$; $FLSC_2 = .0955$; $FLHG = 47.5$; $(A/V)_{Aq} = .0784$; $TEMP = 17$; $STRUB = .050169$

RUN	CHGF	CHGS	STSO ₂	pH	VDITHI	RATE OF Na CONSUMPTION*	Na/SO ₂	C _{S₂O₄}	Y _{SO₂} ±EY _{SO₂}	Y _{Na} ±EY _{Na}	CONNA ±ECONNA	X _{Na} ±EX _{Na}
23	.01725	.00176	.39996	5.20	18.283	.0043	.126	.274	7.88 ±.08	62 ±3	70 ±4	90 ±4
24	.03765	.00376	.40300	5.70	14.200	.0095	.273	.353	10.1 ±.1	36.9 ±1	41 ±1	90 ±1
25	.05444	.01243	.39898	5.90	19.100	.0117	.398	.263	7.56 ±.08	19.0 ±.6	24.6 ±.9	77 ±1
26	.04712	.00688	.39924	5.70	17.000	.0112	.345	.295	8.49 ±.09	24.6 ±.8	29 ±1	85 ±1
27	.03027	.00268	.39700	5.40	13.100	.0077	.223	.383	11.1 ±.1	50 ±2	55 ±2	91 ±2
28	.02428	.00239	.39949	5.30	14.850	.0061	.178	.338	9.7 ±.1	55 ±2	61 ±3	90 ±2

* gm mles/min

TABLE F-VIII

STEADY-STATE DATA AND RESULTS FOR EXPERIMENTAL SET 42-46 (Expts. 42, 43, 44, 45 and 46)

 $(RPM)_{Aq} = 673$; $FLSO_2 = .0955$; $FLHG = 47.5$; $(A/V)_{Aq} = .0784$; $TEMP = 17$; $STRUB = .098795$

RUN	CHGF	CHGS	STSO ₂	pH	VDITHI	RATE OF Na CONSUMPTION*	Na/SO ₂	C _{S₂O₄}	Y _{SO₂} ±EY _{SO₂}	Y _{Na} ±EY _{Na}	CONNA ±ECONNA	X _{Na} ±EX _{Na}
42	.06561	.00542	1.3100	5.00	7.119	.0168	.146	1.39	12.2 ±.1	83 ±2	91 ±3	91.7 ±.7
43	.10344	.00678	1.3000	5.50	5.217	.0268	.231	1.89	16.7 ±.2	72 ±2	77 ±2	93.5 ±.5
44	.14386	.00708	1.2970	5.75	4.300	.0379	.322	2.30	20.4 ±.2	63 ±2	67 ±2	95.1 ±.3
45	.21265	.03749	1.2875	5.00	6.400	.0483	.476	1.54	13.8 ±.1	28.9 ±.9	35 ±1	82.4 ±.2
46	.18438	.01515	1.2638	5.70	5.600	.0467	.422	1.76	16.0 ±.2	38 ±1	41 ±1	91.8 ±.2

* gm moles/min

TABLE F-IX

STEADY-STATE DATA AND RESULTS FOR EXPERIMENTAL SET 86-90 (Expts. 86, 88 and 90)

 $(RPM)_{Aq} = 110$; $FLSO_2 = .0955$; $FLHG = 47.5$; $(A/V)_{Aq} = .0784$; $TEMP = 17$; $STRUB = .047495$

RUN	CHGF	CHGS	STSO ₂	pH	VDITHI	Na/SO ₂	C _{S₂O₄}	Y _{SO₂} ±EY _{SO₂}	Y _{Na} ±EY _{Na}	CONNA ±ECONNA	X _{Na} ±EX _{Na}
86	.05605	.00494	.65800	5.75	6.394	.249	.743	13.0 ±.1	52 ±2	57 ±2	91 ±1
88	.09863	.02232	.65450	5.80	9.467	.438	.502	8.81 ±.09	20.1 ±.6	26.0 ±.8	77.4 ±.5
90	.03723	.00353	.65800	5.35	8.590	.165	.553	9.7 ±.1	58 ±2	64 ±2	91 ±1

TABLE F-X

STEADY-STATE DATA AND RESULTS FOR EXPERIMENTAL SET 94-104 (Expts. 94, 96, 100, 102 and 104)

 $(RPM)_{Aq} = 673$; $FLSO_2 = .0656$; $FLHG = 47.5$; $(A/V)_{Aq} = .0784$; $TEMP = 17$; $STRUB = .047495$

RUN	CHGF	CHGS	STSO ₂	pH	VDITHI	Na/SO ₂	C _{S₂O₄}	Y _{SO₂} ±EY _{SO₂}	Y _{Na} ±EY _{Na}	CONNA ±ECONNA	X _{Na} ±EX _{Na}
94	.04387	.00351	.65700	5.95	4.580	.284	1.037	18.1 ±.2	64 ±2	69 ±2	92 ±1
96	.09119	.03275	.65800	6.10	7.850	.587	.605	10.6 ±.1	18.0 ±.5	28.1 ±.9	64 ±.5
98	.08184	.02440	.65700	6.10	7.502	.528	.633	11.1 ±.1	21.0 ±.6	29.9 ±.9	70.2 ±.6
100	.02801	.00324	.65150	5.75	6.945	.183	.684	12.1 ±.1	66 ±2	74 ±3	88 ±2
102	.05460	.00449	.66000	6.10	5.420	.351	.876	15.3 ±.2	43 ±1	47 ±2	92 ±1
104	.07107	.01469	.65300	6.10	7.270	.462	.653	11.5 ±.1	24.9 ±.7	31 ±1	79.3 ±.8

TABLE F-XI

STEADY-STATE DATA AND RESULTS FOR EXPERIMENTAL SET 122-134 (Expts. 122, 125, 128, 131 and 134)

 $(RPM)_{Aq} = 673$; $FLSO_2 = .0955$; $FLHG = 47.5$; $(A/V)_{Aq} = .0247$; $TEMP = 17$; $STRUB = .047495$

RUN	CHGF	CHGS	STSO ₂	pH	VDITHI	Na/SO ₂	C _{S₂O₄}	Y _{SO₂} ±EY _{SO₂}	Y _{Na} ±EY _{Na}	CONNA ±ECONNA	X _{Na} ±EX _{Na}
122	.06283	.00629	.66000	5.70	8.930	.278	.532	9.3 ±.1	33 ±1	37 ±1	90 ±1
125	.12382	.05016	.66064	5.90	12.793	.544	.371	6.46 ±.07	11.9 ±.4	19.9 ±.6	59.5 ±.4
128	.04884	.00527	.65802	5.70	10.038	.217	.473	8.26 ±.09	38 ±1	43 ±1	89 ±1
131	.07673	.00942	.65628	5.95	9.900	.341	.480	8.40 ±.09	24.7 ±.8	28.1 ±.9	87.7 ±.7
134	.08789	.01267	.66400	5.80	10.160	.385	.467	8.09 ±.08	21.0 ±.6	24.5 ±.7	85.6 ±.6

TABLE F-XII

STEADY-STATE DATA AND RESULTS FOR EXPERIMENTAL SET 123-135 (Expts. 123, 129, 132 and 135)

 $(RPM)_{Aq} = 673$; $FLSO_2 = .0955$; $FLHG = 47.5$; $(A/V)_{Aq} = .0095$; $TEMP = 17$; $STRUB = .047495$

RUN	CHGF	CHGS	STSO ₂	pH	VDITHI	Na/SO ₂	C _{S₂O₄}	Y _{SO₂} ±EY _{SO₂}	Y _{Na} ±EY _{Na}	CONNA ±ECONNA	X _{Na} ±EX _{Na}
123	.06283	.01603	.66000	5.65	15.897	.278	.299	5.20 ±.04	18.8 ±.4	25.2 ±.7	74.5 ±.9
129	.04884	.01494	.65802	5.65	19.350	.217	.245	4.29 ±.04	19.8 ±.6	28 ±1	69 ±1
132	.07673	.02303	.65628	5.80	17.275	.341	.275	4.81 ±.05	14.1 ±.4	20.2 ±.7	70.0 ±.7
135	.08789	.03064	.66400	5.65	17.100	.385	.278	4.81 ±.05	12.5 ±.4	19.1 ±.6	65.2 ±.6

TABLE F-XIII

STEADY-STATE DATA AND RESULTS FOR EXPERIMENTAL SET 106-118 (Expts. 106, 109, 112, 115 and 118)

$(RPM)_{Aq} = 673$; $FLSO_2 = .0955$; $FLHG = 47.5$; $(A/V)_{Aq} = .0784$; $TEMP = 13$; $STRUB = .047495$

RUN	CHGF	CHGS	STSO ₂	pH	VDITHI	Na/SO ₂	C _{S₂O₄}	Y _{SO₂} ±EY _{SO₂}	CONNA ±ECONNA
106	.08996	.00742	.65300	6.00	7.740	.401	.614	10.8 ±.1	29.3 ±.9
109	.06455	.00421	.65350	5.80	5.198	.288	.803	14.1 ±.2	52 ± 2
112	.03715	.00344	.65250	5.55	7.947	.166	.598	10.5 ±.1	70 ± 3
115	.05455	.00431	.65950	5.80	6.073	.241	.782	13.6 ±.2	61 ± 2
118	.09505	.00875	.65471	6.00	7.932	.422	.599	10.5 ±.1	27.4 ±.9

TABLE F-XIV

STEADY-STATE DATA AND RESULTS FOR EXPERIMENTAL SET 110-113 (Expts. 110 and 113)

 $(RPM)_{Aq} = 673$; $FLSO_2 = .0955$; $FLHG = 47.5$; $(A/V)_{Aq} = .0784$; $TEMP = 27$; $STRUB = .047495$

RUN	CHGF	CHGS	STSO ₂	pH	VDITHI	Na/SO ₂	C _{S₂O₄}	Y _{SO₂} ±EY _{SO₂}	CONNA ±ECONNA
110	.06455	.00354	.65350	5.90	5.037	.288	.943	16.6 ±.2	61 ±2
113	.03715	.00357	.65250	5.70	7.850	.166	.605	10.7 ±.1	71 ±3

TABLE XV

UNSTEADY-STATE RESULTS FOR EXPERIMENTAL RUN 42

Initial pH = 3.4; Final pH = 5.0; CHGF = .06561

TIME (min)	10.4	14.3	17.5	21.5	24.4	30.0	35.0	39.5	44.0	51.6	54.0	57.5	61.1	63.8	66.6	69.6	71.4	73.8
C _{S₂O₄}	.915	1.040	1.116	1.198	1.235	1.283	1.291	1.300	1.309	1.392	1.372	1.411	1.392	1.382	1.392	1.353	1.372	1.392
TIME (min)	4.5	7.5	12.0	19.0	29.0	34.0	41.0	68.0	73.0									
CHGS	.00560	.00593	.00524	.00545	.00503	.00550	.00558	.00506	.00449									

TABLE XVI

UNSTEADY-STATE RESULTS FOR EXPERIMENTAL RUN 43

Initial pH = 3.3; Final pH = 5.5; CHGF = .10344

TIME (min)	9.7	13.7	16.9	21.3	27.2	30.8	34.7	37.3	41.8	44.8	49.4	52.0	56.0	58.4				
C _{S₂O₄}	1.176	1.432	1.544	1.689	1.780	1.830	1.864	1.864	1.882	1.918	1.900	1.900	1.882	1.882				
TIME (min)	3.1	8.5	11.5	18.5	23.0	29.0	33.0	46.5	54.0	59.5								
CHGS	.00888	.00649	.00630	.00673	.00685	.00634	.00697	.00666	.00702	.00688								

TABLE XVII

UNSTEADY-STATE RESULTS FOR EXPERIMENTAL RUN 44

Initial pH = 3.3; Final pH = 5.75; CHGF = .14386

TIME (min)	6.5	9.8	14.3	16.6	22.0	25.0	28.8	32.8	37.5	41.4	65.2	67.6	74.5
C _{S₂O₄}	1.326	1.620	1.976	2.058	2.171	2.195	2.245	2.271	2.271	2.298	2.298	2.298	2.298
TIME (min)	4.5	7.8	11.3	18.0	27.0	52.0	57.0	63.0	71.0				
CHGS	.00754	.00712	.00707	.00705	.00717	.00720	.00697	.00715	.00689				

TABLE XVIII

UNSTEADY-STATE RESULTS FOR EXPERIMENTAL RUN 45

Initial pH = 3.15; Final pH = 5.0; CHGF = .21265

TIME (min)	8.4	11.6	14.9	20.4	23.3	27.9	31.5	35.4	40.9	45.5	49.5	51.9	55.5
C _{S₂O₄}	1.718	1.918	2.016	1.882	1.813	1.689	1.633	1.620	1.556	1.556	1.544	1.544	1.544
TIME (min)	2.5	7.0	10.5	16.3	22.0	25.3	29.5	33.3	37.5	47.0	61.5		
CHGS	.04245	.00802	.00777	.01504	.02939	.03519	.03608	.03698	.03735	.03850	.03664		

TABLE XIX

UNSTEADY-STATE RESULTS FOR EXPERIMENTAL RUN 46

Initial pH = 3.0; Final pH = 5.7; CHGF = .18438

TIME (min)	6.2	10.8	15.8	18.3	21.8	25.2	28.7	32.3	36.8	40.1	43.1	46.4	48.9	51.6	54.8	57.3	60.0	62.5	65.3	67.8	70.3
C _{S₂O₄}	1.259	1.900	2.148	2.195	2.245	2.171	2.102	1.976	1.956	1.882	1.882	1.830	1.830	1.813	1.749	1.796	1.780	1.780	1.749	1.764	1.764
TIME (min)	3.0	8.5	14.3	20.2	24.0	27.0	33.8	39.0	45.0	53.0	63.5										
CHGS	.02508	.00776	.00717	.00915	.01070	.01166	.01348	.01384	.01468	.01616	.01462										

TABLE XX

UNSTEADY-STATE RESULTS FOR EXPERIMENTAL RUN 23

Initial pH = 4.0; Final pH 5.2; CHGF = .01725

TIME (min)	4.5	7.4	13.2	23.6	27.2	30.6	32.7	34.5	41.7	46.6	52.5	54.7	57.1	60.9	65.5	68.9					
C _{S₂O₄}	.148	.181	.216	.255	.263	.265	.267	.273	.268	.274	.276	.271	.278	.271	.276	.274					
TIME (min)	8.8	13.8	30.0	45.0	50.0	73.0	74.0														
CHGS	.00174	.00176	.00178	.00170	.00200	.00206	.00150														

TABLE XXI

UNSTEADY-STATE RESULTS FOR EXPERIMENTAL RUN 24

Initial pH = 4.2; Final pH = 5.7; CHGF = .03765

TIME (min)	7.7	11.5	15.7	19.8	32.9	39.5	52.8	57.5	61.1	63.9	66.7	68.4
$C_{S_2O_4}$.261	.320	.364	.369	.364	.366	.356	.353	.353	.353	.344	.353
TIME (min)	10.0	15.4	24.8	35.0	41.0	49.3	60.9					
CHGS	.00220	.00300	.00370	.00370	.00400	.00400	.00376					

TABLE XXII

UNSTEADY-STATE RESULTS FOR EXPERIMENTAL RUN 25

Initial pH = 4.1; Final pH = 5.9; CHGF = .05444

TIME (min)	6.8	10.3	14.2	18.9	22.3	29.0	37.0	72.4	77.0	80.0	84.0
$C_{S_2O_4}$.215	.261	.282	.282	.280	.267	.263	.261	.263	.263	.263
TIME (min)	8.4	11.8	20.2	26.8	59.5	70.2	78.0	84.0			
CHGS	.00487	.00618	.01081	.01157	.01243	.01306	.01243	.01243			

TABLE XXIII

UNSTEADY-STATE RESULTS FOR EXPERIMENTAL RUN 26

Initial pH = 4.1; Final pH = 5.7; CHGF = .04712

TIME (min)	9.7	12.7	16.6	19.9	23.3	28.3	35.0	39.3	42.5	47.9	53.0	55.9	60.5
C _{S₂O₄}	.282	.326	.330	.330	.328	.318	.302	.299	.295	.297	.293	.295	.295
TIME (min)	6.5	16.0	23.0	37.0	45.0	50.0	58.0	63.0	64.0				
CHGS	.00334	.00400	.00601	.00718	.00737	.00672	.00668	.00677	.00657				

TABLE XXIV

UNSTEADY-STATE RESULTS FOR EXPERIMENTAL RUN 27

Initial pH = 4.0; Final pH = 5.4; CHGF = .03027

TIME (min)	8.0	12.9	16.9	19.8	26.0	29.0	33.2	37.3	41.6	46.9	50.6	55.5
C _{S₂O₄}	.237	.295	.337	.344	.366	.380	.383	.380	.382	.386	.382	.386
TIME (min)	5.1	10.8	22.0	35.1	48.4	52.0	56.8					
CHGS	.00325	.00185	.00234	.00232	.00292	.00298	.00283					

TABLE XXV

UNSTEADY-STATE RESULTS FOR EXPERIMENTAL RUN 28

Initial pH = 3.9; Final pH = 5.3; CHGF = .02428

TIME (min)	9.7	13.7	16.9	21.7	24.9	33.8	40.6	45.2	47.9	51.3	54.3	61.1	64.7	67.5
C _{S₂O₄}	.227	.270	.287	.304	.312	.322	.326	.330	.330	.333	.335	.339	.337	.338
TIME (min)	7.3	19.0	35.5	49.5	55.8	62.9	66.6							
CHGS	.00248	.00281	.00187	.00248	.00232	.00239	.00238							

TABLE XXVI

UNSTEADY-STATE RESULTS FOR EXPERIMENTAL RUN 65

Initial pH = 3.53; Final pH = 6.0; CHGF = .10104

TIME (min)	9.8	14.0	20.0	27.5	34.7	44.7	54.7	61.3	65.0	68.0	71.0
C _{S₂O₄}	.602	.650	.642	.602	.599	.595	.606	.606	.599	.599	.595
TIME (min)	6.6	11.6	18.0	33.1	47.0	56.4	68.0				
CHGS	.00869	.00769	.01456	.01945	.01903	.01922	.01960				

TABLE XXVII

UNSTEADY-STATE RESULTS FOR EXPERIMENTAL RUN 67

Initial pH = 3.38; Final pH = 5.95; CHGF = .06626

TIME (min)	8.3	13.5	19.8	26.3	32.2	41.7	46.7	51.7	55.3
$C_{S_2O_4}$.561	.721	.817	.867	.882	.882	.882	.882	.882
TIME (min)	6.3	11.8	17.8	24.0	29.0	40.0	44.0	50.2	53.8
CHGS	.00436	.00386	.00358	.00343	.00361	.00377	.00393	.00405	.00374

TABLE XXVIII

UNSTEADY-STATE RESULTS FOR EXPERIMENTAL RUN 69

Initial pH = 3.35; Final pH = 5.65; CHGF = .04677

TIME (min)	8.6	13.7	20.9	27.1	33.1	39.4	45.3	48.5	52.0	57.3	60.8	63.5	66.3
$C_{S_2O_4}$.447	.567	.643	.696	.707	.716	.716	.726	.726	.734	.732	.737	.732
TIME (min)	6.7	12.1	18.9	25.1	31.5	36.7	43.3	50.2	55.7	68.4			
CHGS	.00421	.00383	.00348	.00388	.00388	.00399	.00368	.00358	.00373	.00364			

TABLE XXIX

UNSTEADY-STATE RESULTS FOR EXPERIMENTAL RUN 71

Initial pH = 5.88; Final pH = 5.95; CHGF = .07542

TIME (min)	5.3	8.3	14.0	19.3	25.3	31.8	34.6	38.4	46.0	49.8	53.6
C _{S₂O₄}	.706	.721	.726	.721	.726	.737	.732	.737	.737	.732	.737
TIME (min)	3.7	10.3	17.1	23.5	30.2	36.8	44.1	51.8			
CHGS	.00554	.00615	.00614	.00599	.00615	.00610	.00605	.00610			

TABLE XXX

UNSTEADY-STATE RESULTS FOR EXPERIMENTAL RUN 73

Initial pH = 5.75; Final pH = 5.8; CHGF = .05914

TIME (min)	9.1	15.3	21.3	30.0	35.4	41.0	45.5	53.0	58.5
C _{S₂O₄}	.844	.849	.867	.867	.867	.867	.867	.867	.867
TIME (min)	5.3	11.9	18.2	23.8	32.3	37.8	42.3		
CHGS	.00429	.00454	.00464	.00414	.00422	.00408	.00412		

TABLE XXXI

UNSTEADY-STATE RESULTS FOR EXPERIMENTAL RUN 75

Initial pH = 5.35; Final pH = 5.4; CHGF = .03921

TIME (min)	4.5	10.3	14.6	20.2	24.7	32.5	37.6	44.0	49.2	51.6
C _{S₂O₄}	.587	.613	.618	.625	.633	.633	.632	.633	.637	.633
TIME (min)	7.8	12.9	17.3	27.1	35.2	40.8				
CHGS	.00391	.00399	.00394	.00387	.00392	.00386				

TABLE XXXII

UNSTEADY-STATE RESULTS FOR EXPERIMENTAL RUN 77

Initial pH = 5.76; Final pH = 5.7; CHGF = .08920

TIME (min)	8.5	14.3	19.7	24.8	32.8	40.8	44.9	52.3	55.0
C _{S₂O₄}	.608	.629	.633	.629	.625	.633	.635	.642	.633
TIME (min)	11.1	17.7	22.1	30.7	39.0	43.1	48.8	55.0	
CHGS	.00976	.01074	.01094	.01167	.01113	.01094	.01121	.01087	